Product Safety and Quality Engineering
Manuel Löwer und Nadine Schlüter (Hrsg.)

3

Design and evaluation of holistically sustainable mobility systems

Baris Can

PRODUKT SICHERHEIT QUALITÄT

BERGISCHE UNIVERSITÄT WUPPERTAL

BERGISCHE
UNIVERSITÄT
WUPPERTAL

Design and evaluation of holistically sustainable mobility systems

Dissertation
zur Erlangung eines Doktorgrades

in der
Fakultät für Maschinenbau und Sicherheitstechnik
der
Bergischen Universität Wuppertal

vorgelegt von
Baris Can

Wuppertal 2022

Product Safety and Quality Engineering – Band 3
Baris Can
Design and evaluation of holistically sustainable mobility systems
Herausgeber: Manuel Löwer und Nadine Schlüter,
Bergische Universität Wuppertal,
Fachgebiet Produktsicherheit und Qualität,
Gaußstraße 20, 42119 Wuppertal
Umschlaggestaltung: Franz Wieck

Zugl.: Wuppertal, Univ., Diss. 2022
DOI: https://doi.org/10.25926/BUW/0-139
URN: https://nbn-resolving.org/urn:nbn:de:hbz:468-2-1390

Die Deutsche Nationalbibliothek verzeichnet diese Publikation
in der Deutschen Nationalbibliografie; detaillierte bibliografische
Daten sind im Internet über http://dnb.dnb.de abrufbar.

Vorwort und Danksagung

Die Ergebnisse, Meinungen und Schlüsse der im Rahmen der veröffentlichten Doktorarbeit sind allein die des Doktoranden.

The results, opinions and conclusions of the doctoral research published within the framework of the thesis are solely those of the doctoral student.

Diese Arbeit entstand im Rahmen meiner Tätigkeit als Doktorand in der Abteilung Mobility Systems and Powertrain Solutions der Group Innovation der Volkswagen AG. An dieser Stelle möchte ich mich bei allen Personen bedanken, die mich während der Promotionszeit unterstützt und somit zum Gelingen der Dissertation beigetragen haben.

Mein besonderer Dank gilt Herrn Professor Dr.-Ing. Manuel Löwer, Leiter des Lehrstuhls für Produktsicherheit und Qualität an der Bergischen Universität Wuppertal, für die Betreuung der Dissertation sowie für die vielen Anregungen und Diskussionen. Die zahlreichen Gespräche auf intellektueller und persönlicher Ebene werden mir immer als bereichernder und konstruktiver Austausch in Erinnerung bleiben. Weiterhin bedanke ich mich bei Professor Hyunjune Yim, PhD der Hongik University in Seoul für die Übernahme der Rolle des Zweitgutachter.

Danken möchte ich auch meinen Vorgesetzten und allen Kollegen der Abteilung Mobility Systems and Powertrain Solutions der Group Innovation der Volkswagen AG, die mich durch die gute Zusammenarbeit, die Beantwortung fachlicher Fragen, in konstruktiven Diskussionen sowie ihre Hilfsbereitschaft unterstützt haben. Mein besonderer Dank gilt dabei meinen Betreuern seitens der Volkswagen AG, Dr.-Ing. Oliver Ludwig und Dr.-Ing. Hendrik Schröder, die mir mit zahlreichen Anregungen, Ideen und ihrem Wissen zur Seite standen. Mithilfe der insbesondere vielen fachlichen und regelmäßigen Diskussionen konnte ich die Probleme in meiner Arbeit lösen.

Außerdem möchte ich mich bei meiner Familie herzlich für den stets bedingungslosen Rückhalt bedanken. Allen meinen Freunden danke ich für die Ausdauer, Ruhe und Geduld, womit sie mir stets zur Seite standen. Abschließend bedanke ich mich ganz besonders bei meiner Freundin Büsra für die Unterstützung, das Verständnis und die vielen motivierenden Worte während der gesamten Promotionsdauer.

Baris Can

Kurzfassung

Der Verkehrssektor spielt eine wichtige Rolle bei der Einhaltung der ehrgeizigen Klimaschutzziele des Pariser Klimaabkommens und wird daher von den Regierungen hinsichtlich der CO_{2eq} Emissionen stark reguliert. Aufgrund der daten- und rechenzeitintensiven Modelle hat sich die wissenschaftliche Arbeit in diesem Bereich bisher meist auf Teilaspekte des skizzierten Themas konzentriert. So wird die Antriebsstrangauslegung und -optimierung meist für einzelne Fahrzeuge im Privatbesitz durchgeführt. In dieser Arbeit wird eine Methode zur ganzheitlichen Gestaltung und Bewertung von nachhaltigen Mobilitätssystemen vorgestellt. Diese Methode kombiniert eine agentenbasierte Mobilitätssimulation mit den Ergebnissen einer Antriebssimulation, einer Lebenszyklusanalyse und einem Kostenmodell in einem multidisziplinären Ansatz. Mit Hilfe dieser Methode werden die CO_{2eq} Emissionen, die Mobilitätskosten aus Kunden- und Investitionssicht sowie der Energiebedarf der Mobilität für ein gesamtes Mobilitätssystem berechnet. In diesem Zusammenhang können auch Dekarbonisierungsstrategien modelliert und analysiert werden. Mit der kombinierten Methodik ist es möglich, verschiedene Parameter des Mobilitätssystems in einer theoretischen Analyse zu optimieren, wie zum Beispiel das Antriebsportfolio. Die Beobachtungen zeigen, dass mit diesem Ansatz verschiedene Parameter des Mobilitätssystems optimiert und Potenziale identifiziert werden können.

Schlagwörter: Mobilitätssimulation, Antriebsstrangsimulation, Life-Cycle-Assessment, nachhaltige Mobilitätssysteme

Abstract

The transport sector plays an important role in meeting the ambitious climate change targets of the Paris Climate Agreement and is therefore heavily regulated by governments in terms of CO_{2eq} emissions. Due to the data and computational time intensive models, scientific work in this area has mostly focused on partial aspects of the outlined topic. For example, powertrain design and optimization is mostly performed for individual privately owned vehicles. In this thesis, a method for holistic design and evaluation of sustainable mobility systems is presented. This method combines an agent-based mobility simulation with the results of a powertrain simulation, a life cycle analysis and a cost model in a multidisciplinary approach. This method is used to calculate CO_{2eq} emissions, mobility costs from a customer and investment perspective, and mobility energy demand for an entire mobility system. In this context, decarbonization strategies can also be modeled and analyzed. With the combined methodology, it is possible to optimize different parameters of the mobility system in a theoretical analysis, such as the powertrain portfolio. Observations show that this approach can be used to optimize various parameters of the mobility system and identify potentials.

Keywords: Mobility simulation, powertrain simulation, life-cycle-assessment, sustainable mobility systems

Abbreviations

ALCA – Attributional LCA

AWD – All Wheel Drive

BEV – Battery Electric Vehicle

CDT – Crowding Distance

CLCA – Consequential LCA

DoE – Design of Experiments

DRT – Demand Responsive Transport

FCEV – Fuel Cell Electric Vehicles

GA – Genetic Algorithms

GDP – Gross Domestic Product

ICE – Internal Combustion Engine

ICEV – Internal Combustion Engine Vehicle

LCA – Life Cycle Assessment

LCI - Life Cycle Inventory

LCIA - Life Cycle Inventory Assessment

NEDC – New European Driving Cycle

OSM – OpenStreetMap

PHEV – Plug-In Hybrid Electric Vehicle

SOC – State of Charge

T2W – Tank-to-Wheel

V2G – Vehicle-to-Grid

WLTC – The Worldwide Harmonized Light Vehicles Test Cycle

W2T – Well-to-Tank

W2W – Well-to-Wheel

Table of Content

List of Figures

List of Tables

1 Introduction

1.1 Motivation and problem statement

The transport sector plays an important role in complying with the ambitious climate protection targets of the Paris Climate Agreement and is therefore highly regulated by the governments with regard to CO_{2eq} emissions. Regional solutions have emerged from the commitment of the climate agreement and are being implemented. In Germany, for example, the transport sector was the third largest contributor to greenhouse gas emissions, with a share of 19% in 2019 [Bundesministerium für Umwelt 2019]. On European level, the European Commission agreed on the Green Deal with the goal of achieving net zero greenhouse gas emissions by 2050. This means an 80-95% reduction in emissions by 2050 compared to 1990 [Bothe et al. 2020] and additional compensation through reforestation or carbon capturing and storage. Identifying effective ecologically, economically and sociologically reasonable pathways to achieve net-zero emissions in the transport sector can only be achieved by holistic approaches, due to the complexity and interactions. Such a holistic approach needs to incorporate human behavior, sector coupling, vehicles and powertrains, transportation modes, energy sources, and infrastructure. Due to data and computation time intensive models, scientific work in this field has so far mostly focused on partial aspects of the outlined topic. For example, powertrain design and optimization is mostly performed for single vehicles in private ownership. Mobility simulations for fleet vehicles often neglect essential aspects of driving energy consumption or the detailed mapping of charging processes. And in sustainability assessment, there are severe limitations in terms of system boundaries and extrapolated dynamics such as concerning future energy chains. Methods already exist for performing life-cycle-assessment (LCA) of individual vehicles. However, these are mostly considered separately from the systems. I.e., the vehicle with its production process and an assumed constant use phase is considered and evaluated. While the underlying assumptions are valid for most internal combustion engine vehicles, the electrification and digitalization of mobility create new opportunities that also need to be considered. Electric vehicles can be used while parking, e.g. due to their electrical storage, but also after the actual life phase, there are possible further second-uses for different components such as the battery or the e-motors. When limited to a specific stage of the life cycle, such as the use phase of a vehicle, the balance of emission sources and savings for a given component might be over- or underestimated, compared to a holistic view. This brief example illustrates that the narrow sector-specific, geographical and temporal perspective only gives a limited view on overall emissions. This can lead to incorrect assessments of the effectiveness of measures in the vehicle and beyond, and subsequently to misleading decisions. Additionally, emission balances and savings have to be put into perspective with economic feasibility and sociological reasonability. To get a meaningful statement about the real impact of the vehicles, a holistic view beyond the system boundaries of a vehicle and vehicle lifetime has to be performed.

1.2 Goal of this study

Therefore, this thesis presents a method for holistic design and assessment of sustainable mobility systems. This method combines an agent-based mobility simulation with the results of a powertrain simulation, a life cycle analysis and a cost model in a multi-disciplinary approach. With the help of this method, CO_{2eq} emissions, mobility costs from the customer's and investment point of view as well as mobility energy demand are calculated for a whole mobility system. In this context, decarbonization strategies can be modeled and analyzed. The focused actuators of the mobility system include power-train types, vehicle and mobility concepts, such as autonomous driving robotaxis, new technologies, such as smart-charging, that can be applied in parallel as well as the time course of the emissions. In addition, political measures, such as driving bans in inner cities, can be implemented and evaluated. The scientific claim of this work extends in the environment of novel mobility concepts over simulation-based powertrain design including requirements analysis, and extended life-cycle-assessment approaches, being combined in a holistic system optimization approach. Furthermore, methods for the forecast of key-values such as CO_{2eq} emissions are derived and the calculation time is optimized by analyzing system parameters as well as downscaling and simplifying of the mobility system.

1.3 Structure of the work

The thesis is structured as follows. In chapter 2, the state of the art is presented. Here, the relevant topics of agent-based mobility simulation, powertrain simulation, life cycle analysis and the combination of the individual methods are considered in more detail. The chapter concludes with a critical examination of the considered sources, as well as a target picture of the method developed here. Chapter 3 describes the derived need for action in this thesis. In chapter 4 the new holistic method is described. The following chapters deal with the individual modules of the method. Chapter 5 describes the agent-based mobility simulation and its integration into the method. In chapter 6, the powertrain simulation as well as the evaluation of the mobility forms of the mobility system are presented. Chapter 7 presents the extended life cycle analysis. Chapter 8 describes the cost calculation. In addition, the method is integrated in an optimization procedure, which is described in Chapter 9. In Chapter 10, a sensitivity analysis is performed to analyze the robustness of the method and to identify sensitivities. In the next step presented in chapter 11, the method is applied to the Berlin region as an example and the method is validated. Here, two optimization scenarios are carried out. In chapter 12 a critical discussion of the results of this thesis and the fulfillment of the target picture is performed. Finally, the summary and the outlook are presented in chapter 13.

2 State of the art

The achievement of developing a method for holistic mobility system analysis and optimization requires the application and combination of methods from very different disciplines, which are the agent-based mobility simulation, powertrain simulation as well as the life-cycle-assessment. In the following, an overview of these methods and the relevant state of the art is given.

2.1 Agent-based modeling and mobility simulation

For the simulation in general, it is necessary to make an abstraction of the real world complexity. A middle course must be found that on the one hand takes into account as many aspects as possible and on the other hand remains feasible in terms of parameter set, computation times and analysis of results. Different approaches to traffic simulation models are [Herdt 2005]:

- Microscopic: Observation of individual vehicles or agents
- Mesoscopic: Mixture of macroscopy and microscopy
- Macroscopic: Observation of the dynamics of vehicle collectives

The goal of this thesis is to analyze the mobility behaviors and emission sources of discrete individuals. Thus, it is necessary to use micro- to mesoscopic models. Here in particular, agent-based models are used to calculate the dynamic behavior in a mobility system. In this field MATSim (Multi Agent Transport Simulation) is an open-source tool used in a wide range of scientific mobility related work. For a detailed description of MATSim, the reader is referred to [Horni et al. 2016].

Typical use cases for the mobility simulation are in the field of city planning or the impact analysis of mobility concepts. In [Querini et al. 2014] an approach with reference to this thesis is described. Here the potential environmental benefits of policies aiming at promoting the deployment of electric vehicles and car use in Luxembourg and neighboring France is evaluated. This study points out that agent based modeling allows to obtain a holistic life cycle inventory that includes all the variability of the car characteristics and uses. In [Bishoff et al. 2019] the impact of a largescale electrification of vehicles in long-distance trips is evaluated by combining an agent-based long distance transport model of Sweden with a detailed model of energy consumption and battery charging. Energy consumption and charging schemes are simulated for different types of vehicles and chargers. In a first application, vehicle traffic is assumed fully electrified. Results demonstrate that the daily estimate for energy consumption equals approximately 40% of the current Swedish electricity consumption. These studies show that a combination of agent-based models with different methods such as a LCA or powertrain simulation is possible and feasible and enables the analysis of mobility systems.

Various approaches are known for generating input data for mobility simulations, concerning traffic demand, traffic networks, and schedules, differing in the level of detail and necessary sources. For example in [Hörl et al. 2020] a methodology is proposed for an open-source and modular framework for population synthesis in the context of agent-based traffic simulation. The framework establishes a clear path from raw data to the final scenario. In [Horni et al. 2016] the necessary input data generation such as plans for agents from statistical data and surveys or network from e.g. OpenStreetMap is described. [Ziemke et al. 2019] describe how a scenario can be generated for the Berlin metropolitan area exclusively on the basis of open data and fully synthetic traffic demand. Since MATSim is used as a tool for the mobility simulation in this thesis, the fundamentals of agent-based modeling and the mobility simulation in MATSim are be described in the following.

2.1.1 Agent-based modeling

From the formulated objective of holistically optimizing mobility systems, it can be deduced that the mobility behavior of individuals must be considered in detail. The focus on individual mobility behaviors determines which forms of mobility are used in particular, to what extend and with which vehicles. The need for analyzing individuals leads to the application of agent based mobility simulation. Agent-based models can represent complex systems and interactions within the system. In contrary to the agent-based approach, aggregated four-step models are used traditionally to evaluate new policies or infrastructure investments in the modeling of transportation. The four-step process for traffic modeling consists of the trip generation, the trip distribution, the modal split and the route assignment. This approach is based on matrices, which include time-dependent route information [Ortúzar et al. 2011]. While this approach is suitable for applications in for example city planning, there are certain restrictions compared to agent-based modeling. Here a traffic flow analysis summarizes the target variables such as travel distance and mean velocity of the mobility simulation for a region, so that no statements can be made at individuals level. Thus, four-step models fail to capture the interactions between individual persons, their decisions and behavior. These interactions are especially important, when it comes to find such as the right powertrain technologies, vehicles or mobility concepts. In addition, new mobility solutions such as ridesharing, ride pooling or micro-mobility as well as their operational challenges cannot be modeled suitably [Hörl et al. 2020]. Furthermore, modeling larger mobility systems with a larger person group leads to a larger number of different activities, transport modes as well as different times of the day. Using the four-step approach, this results in a large number of matrices and unfeasible computation times.

Contrary to this approach, agent-based models enable to analyze the mobility system on the individual level including their mobility behavior, decisions and interaction. Thus it becomes possible to analyze new mobility concepts. Agent-based modeling can be more efficient in large or suburban context, because the large number of matrices with only a handful of trips is replaced by a list of individual agents. Furthermore agent-based modeling helps to maintain physical constraints, because every event happens in an ordered time-flow [Horni et al. 2016]. Therefore agent-based modeling for traffic simulation is applied in this thesis and is described in detail in the following chapters.

2.1.2 Fundamentals of mobility simulation in MATSim

For the agent-based simulation part of the methodological approach, MATSim (Multi-Agent-Transport-Simulation) is chosen. The input data for generating the scenarios in the mobility simulation is typically derived from different sources. These sources are, for example, census data for modeling the population in the form of synthetic agents, mobility surveys for modeling the activity plans of the agents, and OpenStreetMap data for modeling the region including road infrastructure, charging infrastructure, and points of interest. In MATSim, a co-evolutionary algorithm is used. Here, the agents' predetermined plans are optimized throughout the day in terms of activities, travel times, or routes. Each agent tries to optimize its own plan until an equilibrium on system level is reached, where the agents cannot optimize their plans any further. The idea of this equilibrium is based on the Nash equilibrium. The Nash equilibrium defines the solution of a non-cooperative game involving two or more players. Here, it is assumed that each player knows the equilibrium strategies of the other players, and each player can only change their own strategy [Osborne et al. 1994]. The Nash equilibrium is reached when no player can increase their own expected payoff by changing their strategy while the other players keep theirs unchanged as well as each player has chosen a plan. In MATSim it is possible to consider different travel modes such as cars, public transport, bicycles or also new mobility concepts such as robotaxis and analyze how individuals use these travel modes on a daily basis. The mode choice depends on scoring functions, which is explained in the next chapters. After performing a mobility simulation, a realistic mobility behavior of the region under consideration can be generated and stored for further analysis and the design and evaluation of the mobility system. The process of the agent-based mobility simulation in generating the realistic mobility behavior is shown in Figure 1.

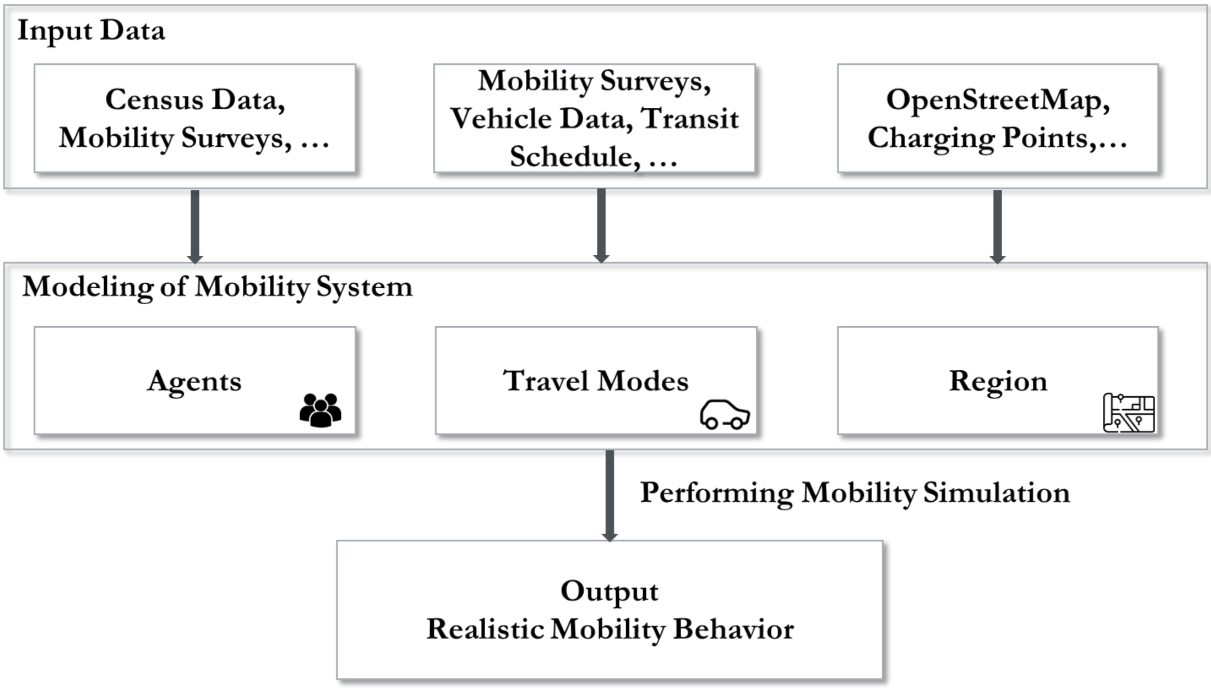

Figure 1: Sequence of the agent-based mobility simulation in MATSim

2.1.3 Level of modeling

Traditionally, meso and macro simulations are used in transportation planning due to the data available, such as road traffic counts or commuter matrices, and the lack of computing power. This has changed over time with continuously increasing computing time. With this development, the issues and data basis in traffic planning have become more complex and detailed, such as the use of GPS technology for detailed analysis of the behavior of individual road users [Wolf et al. 2004]. Currently, microsimulation of traffic demand is becoming more and more important. The main reasons for this are the more varied output options, from aggregate statistical analysis to detailed information about individuals in a scenario, as well as explicitly modeling the decision-making process of each individual. This is important because mobility is generated by individuals, not vehicles [Balmer et al. 2008].

For daily planning, a real person has to make many different decisions. The person has for example to decide where to perform a certain activity, which transport mode or combination of modes to use to get from one place to the next, in which order and at what time to perform activities and with whom to plan certain activities together. In addition, there are numerous of other decisions to be made. Some of these are spontaneous and short-term and typically arise due to unforeseen circumstances. Other decisions require a long lead time and careful planning. Another important factor is that many decisions induce other decision-making processes. Therefore, it is extremely important to consider the entire planning horizon of a person to model transportation behavior and to implement this in a simulation model. These decisions lead to an interaction between individuals, which has an effect on the decision making of the individuals itself [Balmer et al. 2008]. In MATSim, exactly this is implemented and described in the following.

2.1.4 Event based modeling

The mobility simulation in MATSim creates events as a form of documentation. Each event contains the time, type and variable additional attributes. There are different types of events such as agent starts or ends of an activity. During the mobility simulation millions of events occur. Subsequently the events can be analyzed. The event sequences depend on the used transport mode. These are described in appendix A.1 in detail.

While events are the output of the mobility simulation, plans are needed as an input to perform a mobility simulation. Plans include the activity chain of an agent during the day, such as going to work at 8 am, then going to the gym at 4 pm. Events and plans often do not match, due to assumptions for example for the travel times in the plans that might be wrong and not achievable as well as unforeseen interactions between agents. Furthermore, the same plan can create different events when executed multiple times, because the activities of other agents can change and this results in different interactions between agents [Rieser 2019]. Events are processed by an event manager in MATSim, which distributes the events for further processing to different handlers depending on their type. The event reader reads all the events from an output file created during the mobility simulation and passes the data one after another to the events manager. Here, all handlers are tracked and all events distributed accordingly. For example, one handler could count the number of vehicles passing a link over the day [Horni et al. 2016].

2.1.5 Queue model

Networks in MATSim, such as the road network, consist of nodes and connecting links. The links are modeled as queues. Interactions only happen at the start or the end of the queue. In MATSim the mobility simulation "QSim" is implemented [Horni et al. 2016]. In QSim all interactions take place at the end of the link. With that, cars can only depart or arrive at the end of a link as well as that public transport stops can only be served when the busses or trains are at the end of a link. The links are unidirectional. To model a bidirectional road two links are needed. This can lead to u-turns, that vehicles need to make to reach a certain link [Rieser 2019].

Figure 2 shows the flow capacity of the links. By default the inflow-capacity of the links is infinite. The output-capacity is defined and acts as the link's capacity. The reason for this approach is that a defined inflow capacity can lead to traffic jams up too far downstream, which is not realistic. There are options to enable kinematic waves to mitigate the missing inflow capacity. The links have different attributes such as free speed in meters per second, length in meters, capacity in vehicles per hour and the transport mode allowed on them such as cars. MATSim has integrated tools to convert OpenStreetMap data to network data including the needed capacity factors and attributes for all links [Horni et al. 2018].

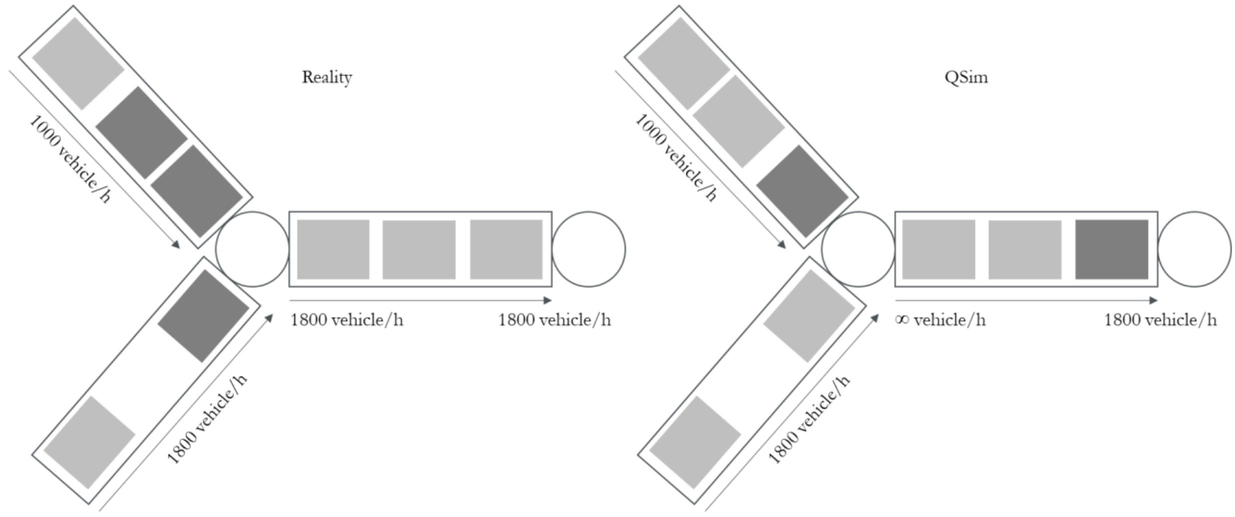

Figure 2: Flow capacity of the links based on [Rieser 2019]

The nodes in the network represent intersections, but with no extent. QSim moves vehicles from the upstream link to the down-stream link for each incoming link if the two following criteria are fulfilled. There needs to be a vehicle in the upstream link that can leave the link and there needs to be free capacity in the downstream link. The order in which links are simulated in each time frame is randomized but weighted with a function in dependence of the link's flow capacity. A higher flow capacity leads to a higher probability for having their vehicles moved before vehicles from lower capacity links move [Rieser 2019].

2.1.6 MATSim Algorithm – MobSim, Scoring and Replanning

MobSim

Here the MATSim's co-evolutionary algorithm is explained. Figure 3 shows the general design of the "MATSim" simulation system. The first step of the simulation is to read the initial demand. The initial demand includes the description of the infrastructure as well as agents and the configuration of the simulation. The data of the infrastructure is stored in the network and transit data. The data of the agents is stored in the plans file. The configuration of the simulation is stored in the config file. The minimal required data for performing a mobility simulation are the network, plans and the config file. Additional data sets to improve the data quality can be for example public transport data, facility data, road pricings or data about signals and traffic lights. The second step is the execution of the mobility simulation, in which the agents travel and execute their plans. Hereby the different events are created.

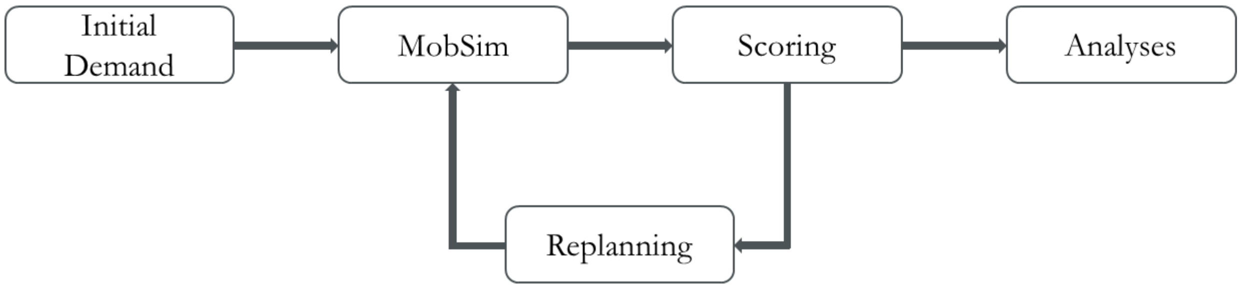

Figure 3: General design of MATSim loop based on [Horni et al. 2016]

Scoring

The evaluation of the executed plans is performed on hands of scoring functions. This happens in the third step of the simulation. The "Charypar-Nagel Utility Function" is implemented in MATSim and is described in the following. The scoring function is divided in different utilities, which all have different impacts on the score. Performing activities have a positive utility, whereas travelling, monetary costs as well as arriving late or leaving early have negative utilities. The score for the plan is the sum of all utilities over a day [Horni et al. 2016].

In equation 1 the scoring function S_{plan} and all the used parameters are explained. The scoring function is calculated by the sum of all activity utilities plus the sum of all travel utilities. The last activity is merged with the first activity to produce an equal number of trips and activities [Horni et al. 2016]:

$$S_{plan} = \sum_{i=0}^{N-1} S_{act,i} + \sum_{i=0}^{N-1} S_{trav,mode,i} \qquad \text{(eq. 1)}$$

- N: Number of activities
- i: Trip i is the trip that follows activity i

The activity utilities $S_{act,i}$ of an activity i are calculated as shown in equation 2:

$$S_{act,i} = \mathrm{S_{dur,i}} + S_{wait,i} + S_{late,ar,i} + S_{early,dp,i} + S_{short,dur,i} \qquad \text{(eq. 2)}$$

- $S_{dur,i}$: Describes the duration spent at an activity. The higher the duration, the higher the score becomes.
- $S_{wait,i}$: Describes the time the agent has to wait until an activity starts, for example if the stores are still closed. The longer the agent needs to wait, the lower the score becomes, therefore this is actually a negative utility.
- $S_{late,ar,i}$: Describes the time the agent arrived late for example to work. The later the agent arrives, the lower the score becomes. This utility function is also negative.
- $S_{early,dp,i}$: Is a penalty for not staying long enough, e.g., if the agent leaves work too early. This is often zero, because good quality of data to measure this penalty is hard to find.
- $S_{short,dur,i}$: Describes a penalty for a too short activity, whereas the shortest possible activity time needs to be defined. Because this data is also hard to quantify, this utility is recommended to be zero.

The negative travel utilities for a leg q is shown in equation 3:

$$S_{trav,i} = \mathrm{C}_{\mathrm{mode,i}} + \mathrm{S}_{\mathrm{trave,mode,i}} + S_{trav,effort,mode,i} + S_{marg,money,i} + S_{transfer,i} \text{ (eq. 3)}$$

- $C_{mode,i}$: Describes a mode-specific constant. This can help to quickly change the modal split in favor of a specific transport mode.
- $S_{trave,mode,i}$: Is the direct marginal utility of time spent traveling.
- $S_{trav,effort,mode,i}$: Is the marginal utility of distance. This describes the effort the agents has to make to travel. For example, traveling by car can be more comfortable than traveling by bike.
- $S_{marg,money,i}$: Describes the cost for the mobility.
- $S_{transfer,i}$: Are penalties for transfers in public transport.

For further details on how to calculate the different utilities see [Horni et al. 2016].

Replanning

In the fourth step, agents can change their plans or create new ones to achieve a higher score. There are different types of replanning strategies. The agents can change their route choice, the departure time and the transport mode. For the transport mode it is possible to change it for the whole plan or for single trips, creating an intermodal mobility. Furthermore, the plan selection method can also be adapted to create a different output. The implemented methods are for example one to pick the plan with the best score, another one to randomly pick a plan or one, which implements a weighted function for the selection and is recommended to use [Horni et al. 2016].

The "ReRoute" strategy calculates a route for each trip in dependence of the transport mode and plan. The different considered transport modes are for example car on network, public transport on a separate network or teleportation. For cars on network a time-dependent least-cost-path algorithm such as the Dijkstra algorithm is used. In newer versions of MATSim an alternative faster routing algorithm called SpeedyALT is used. For public transport routing a variant of Dijkstra's shortest-path algorithm is used. In the newer versions of MATSim the algorithm called "SwissRailRaptor" is used as the default transit router. The travel for teleportation mode is calculated either by using the bee-line distance factor and average speed or by using a scaled freespeed factor [Horni et al. 2016].

The "TimeAllocationMutator" strategy randomly changes the activity end time and can be configured in the config file. The "ModeChoiceMutator" includes three different strategies. The first strategy changes the mode of a single trip in the plan. The second strategy changes the modes of all trips, although different modes for different trips are possible. The last strategy analyses the plan for subtours and assigns modes to all legs in each sub-tour. This allows to create an intermodal mode choice, if it scores well in the agent's plan. Some strategies such as the "TimeAllocationMutator" perform a random mutation while other strategies such as "ReRoute" apply a best-response mutation. Best-response mutations can find good plans faster; however they do not create many variation. In contrast, random mutation can force agents to perform bad plan variations and require more iterations to find good plans. To avoid fluctuations, not every agent should perform replanning in each iteration. To reach an equilibrium at the end, replanning strategies and also the innovation of new plans should be disabled after a certain iteration. Otherwise, this could also lead to agents trying bad plans and creating errors in the simulation [Horni et al. 2016].

These three steps are carried out iteratively, so that each agent can try to optimize its day. This is based on an evolutionary algorithm, where agents have a set of plans, which is by default five. Through replanning, new plans can be added while plans with a low score are removed. In MATSim this algorithm is enhanced by a co-evolutionary algorithm, because the score of the plan depends also on the score of other agents and their interactions. A global optimum is therefore hard to achieve and not realistic. That's why a Nash equilibrium is aimed, where each agent tries to optimize its plan, like in the real world. At the end of the simulation, the events are analyzed. Typical output data are for example the traffic volumes, average speeds, utility changes, emissions and accessibility [Horni et al. 2016].

2.2 Powertrain design

In the field of powertrain simulation, a large number of sources exists that deal with the subject area. Therefore, the scientific literature overview given here is limited to sources with direct reference to this work. With the help of longitudinal dynamic simulation, it is possible to design vehicles and their powertrain for a given requirement profile. The simulation approach in this thesis is based on a methodology for identifying optimal component characteristics of a wide range of higher electrified powertrain architectures, described in [Weiß 2018]. The simulation models used in the methodology focus on computational speed under retention of result quality, allowing the optimization of a large number of parameters. Furthermore, an operational strategy applicable for all considered powertrain architectures is developed for the comparison of different component properties. In addition to the criteria and boundary conditions regarding vehicles with internal combustion engines, other properties that are particularly relevant for electrified powertrains, such as the electric range, are taken into account. Here a quasi-static, map-based approach is used for the powertrain simulation. However, here no forecasts are derived for these properties. In [Schneider 2022] a methodology for analyzing the future technological potentials of vehicle powertrain concepts is presented. This method is based on a database for technology forecasts of powertrain components, which can be integrated in a longitudinal dynamics simulation tool such as in [Weiß 2018]. With the approach of [Schneider 2022] forecasts can be used to generate and scale future maps for powertrain components. In the following the fundamentals of powertrain design is presented.

2.2.1 Fundamentals of powertrain design

This chapter focuses on the fundamentals of the powertrain design. In the first step, the considered powertrain types and powertrain components are described. In the next step the differences between static and dynamic simulation are presented, before describing the simulation framework from [Weiß 2018]. In this work, the four powertrain types Internal Combustion Engine Vehicle (ICEV), Plug-In Hybrid Electric Vehicle (PHEV), Battery Electric Vehicle (BEV), and Fuel Cell Electric Vehicle (FCEV) are considered. For a detailed description of the powertrain types, please refer to the sources [Eckstein 2015], [Blasinski 2008], [Guzella et al. 2013] and [Reif et al. 2012]. The powertrains comprise different components in a specific combination. These can be divided into the three categories of energy storage, energy converters, and energy transformers. Energy storage systems include the battery, hydrogen tank systems, and tanks for liquid and gaseous fuels including e-fuels and biofuels. For a detailed description of the components, please refer to the sources [Reif et al. 2012], [Hofmann 2014], [Birke et al. 2013], [Friedrich et al. 2011], [Fink et al. 2015], [Cluzel et al. 2012], [Huss et al. 2013], [Töpler et al. 2017], and [Kunze et al. 2012]. Energy converters include the internal combustion engine, fuel cell systems, and e-motors. A detailed description of the components is given in the sources [Pischinger 2016], [Reif 2011], [Hofmann 2014], [Eckstein 2015], [Töpler et al. 2017], and [Reif et al. 2012]. Power converters include power electronics (DC/DC converter and pulse inverter) as well as gearboxes. For a detailed description of the components, please refer to the sources [Hofmann 2014], [Reif et al. 2012] and [Steinhilper et al. 2012].

2.2.2 Variants of powertrain simulation

Quasi-static and dynamic simulation

In the context of powertrain simulations, a distinction is made between quasi-static and dynamic approaches. The quasi-static approach is characterized by the fact that the output variable only depends on the input variable at the same time [Lunze 2012]. In quasi-static powertrain simulations, the component losses are determined in discrete time steps. This is often done by interpolation in simulated or measured maps such as in the consumption calculation of vehicles with combustion engines. This approach is characterized by a relatively fast calculation time and is particularly suitable for consumption calculations and optimization of energy management [Guzella et al. 2013].

In dynamic systems, on the other hand, the output variable depends not only on the current value, but on the previous course of the input variable and the system's current state. These systems are often described by differential equations. For example, the battery represents a dynamic system, since its state of charge (SOC) depends on the entire course of the delivered and absorbed power as well as start value [Lunze 2012]. The dynamic powertrain simulations additionally considers high-frequency dynamic and transient processes in the powertrain. This can include, for example dynamic clutch and gearshift processes or the charging behavior of compressors in the combustion engine or in the air path of a fuel cell system. These models can represent the real dynamic behavior of a powertrain much more accurately than the quasi-static models when it comes to for example mechanical or electrical vibrations. Many of these dynamic processes are not relevant for calculating fuel consumption, but they bring a high modeling and calculation effort. This manifests itself in significantly longer simulation times compared to the quasi-static powertrain simulations [Weiß 2018].

Forward and backwards simulation

In the literature, the powertrain simulation approaches are also characterized by the direction of the simulation [Guzella et al. 2013], [Fröberg 2008]. In Figure 4 both approaches are shown with the example of an ICEV. In the forward simulation, the driver is taken into account as a control element for controlling the driving speed to match driving profiles such as the WLTP. The driver model determines the operating point of for example the combustion engine based on the temporal load profile. The driver in this case is a controller with the speed as controlled variable and the pedals and if necessary, gear selection as manipulated variables. The dynamic engine model passes on the effective output torque to the wheels via the torque converter, transmission and differential. Finally, the driving speed is set there. By changing the virtual throttle and brake pedal position, the actual driving speed is approximated in time to the specified driving curve. Mapping the real signal flows with the forward-based approach allows for development of ECU code, among other things. Another advantage of this approach is the consideration of component limits, since performance limitations have a direct effect on the vehicle acceleration and speed [Weiß 2018].

The backwards simulation is a quasi-static simulation. The calculation is performed backwards, starting from the driving profile such as WLTP. From the load profile, vehicle speed and acceleration as well as drive torque and wheel speed are calculated. In case of the ICEV, via the differential, transmission, torque converter and/or clutch modules, the required (effective) output torque and speed of the combustion engine are obtained. All discrete-time output torques and the corresponding speeds determine the operating points of the internal combustion engine and enable the estimation of fuel consumption and other engine-specific variables. The limits of the available system power can be shown but has no influence on the vehicle speed. The backwards simulation offers overall advantages in terms of calculation time, in particular because no controller is required as a driver model [Weiß 2018].

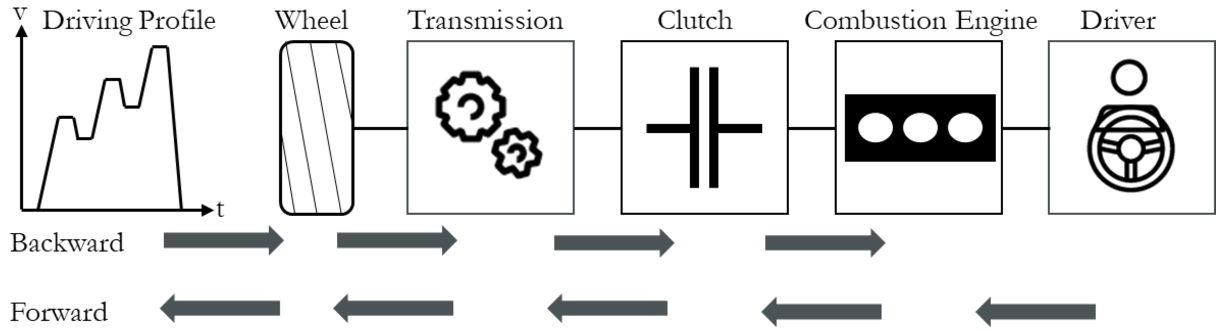

Figure 4: Sequence of forward and backward powertrain simulation with the example of the ICEV based on [Weiß 2018]

2.2.3 Powertrain simulation framework

In this thesis, the modular simulation framework from [Weiß 2018] is used and enhanced to fulfill the formulated goals. The applied simulation framework realizes a quasi-static approach and is able to determine the consumption for given driving profiles as well as the driving performance of all considered powertrain types. The approach comprises, a vehicle and a powertrain model are needed. While the vehicle model allows to calculate the driving resistances, the powertrain model incorporates the losses of the powertrain components and the overall efficiency.

Vehicle model

In the following, the vehicle model and the driving resistances needed for the consumption calculation are described. In the powertrain simulation, the vehicle model is used to convert a velocity and acceleration input and acceleration specifications into the required wheel parameters. These are independent of the rest of the powertrain and can therefore be calculated in a generally valid manner for all architectures if the total weight, the rotating masses and gear ratio is known. Figure 5 shows the individual driving resistances, which consist of rolling resistance, air resistance, climbing resistance and acceleration resistance.

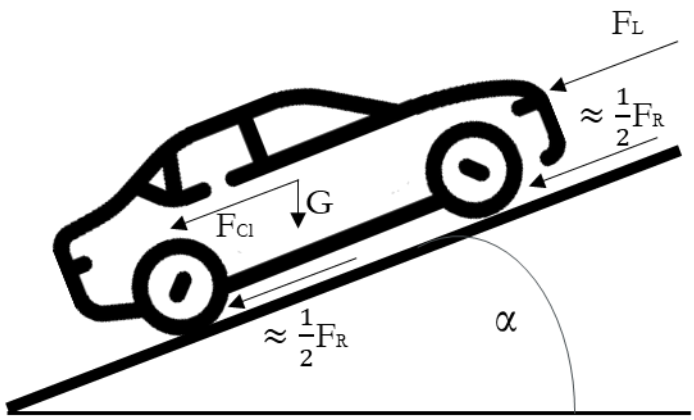

Figure 5: Driving resistance on the vehicle based on [Guzella et al. 2013]

Rolling resistance is a frictional force that occurs when a wheel rolls and contributes to the overall driving resistance. The causes are the friction of the outer surface of the wheel with the ground, such as a road surface. In addition, frictional losses can occur within a tire, which is deformed by the contact pressure. Typically, rolling resistance is considerably higher for wheels that are easily deformed, such as those with rubber tires, than for hard wheels such as steel wheels on railroads. A soft or uneven surface can also significantly increase friction. If, for example, a tire sinks significantly into the subsoil, substantial friction also occurs within the subsoil. The calculation of the total rolling resistance is performed by using the following equation. The rolling resistance coefficient f_R can be assumed to be constant at low speeds but increases significantly at higher speeds. Here in the vehicle model, the coefficient is therefore stored as a speed-dependent characteristic curve [Guzella et al. 2013].

$$F_R = f_R * m_{veh} * g * cos(\alpha) \tag{eq. 4}$$

- F_R: Rolling resistance
- f_R: Rolling resistance coefficient
- m_{veh}: Vehicle mass
- g: Gravity
- α: Climbing gradient

The climbing resistance occurs when the vehicle must overcome a gradient with an angle of α. The climbing resistance is calculated with the following formula [Guzella et al. 2013]:

$$F_{Cl} = m_{veh} * g * sin(\alpha) \tag{eq. 5}$$

- F_{Cl}: Climbing resistance
- m_{veh}: Vehicle mass
- g: Gravity
- α: Climbing gradient

When a vehicle is moved through the air, air resistance occurs. The reason is that air is partially entrained by the vehicle and set in motion, with turbulent flows also occurring at higher speeds. This results in a loss of energy that is related to the frictional force that is created. The energy loss is equal to the frictional force multiplied by the distance over which the body is moved. This type of friction is called drag. For a moving vehicle, these aerodynamic forces mean that correspondingly more propulsive power must be applied to maintain speed. In vehicles and other motor vehicles, air resistance is the dominant part of the total driving resistance as long as the driving speed is not too low, e.g., below 30 km/h. At very low speeds rolling resistance dominates.

The air resistance is calculated with the following formula [Paschotta 2020]:

$$F_L = c_W * A * \frac{\rho_L}{2} * v^2 \qquad \text{(eq. 6)}$$

- F_{Cl}: Air resistance
- c_W: Drag coefficient
- ρ_L: Air density
- A: Cross-sectional area
- v: Relative velocity between vehicle and ambient air

The acceleration resistance indicates the force required to accelerate the vehicle against the mass inertia. It consists of translational and rotational components as shown in the following equation. The translator component results from the product of the vehicle acceleration and the vehicle mass and can therefore be calculated directly for a given cycle. The conversion of the total rotatory component into a reduced moment of inertia at the wheel would involve mass inertias of all rotating parts in the powertrain. Because this would prevent the separation of vehicle and powertrain model, only the rotational part of the wheels at this point is considered. The mass moments of inertia of the wheels on front and rear include the inertias of the tires, rims, brakes, cardan shafts and all other rotating components up to the axle differential or wheel. All other of the total mass moment of inertia are considered within the calculation of the specific powertrain [Guzella et al. 2013]:

$$F_A = F_{A,tr} + F_{A,rot} \qquad \text{(eq. 7)}$$

- F_A: Acceleration resistance
- $F_{A,tr}$: Translational part of acceleration resistance
- $F_{A,rot}$: Rotational part of acceleration resistance

The required torque on the wheel to overcome the total driving resistance is calculated with the following equation:

$$M_{wheel} = (F_R + F_{Cl} + F_L + F_A) * \mathrm{r_{wheel}} \qquad \text{(eq. 8)}$$

- M_{wheel}: Required Torque
- r_{wheel}: Dynamic wheel radius

The wheel speed can be derived from the given velocity with the following formula:

$$n_{wheel} = \frac{v}{2 * \pi * r_{wheel}} \qquad \text{(eq. 9)}$$

- n_{wheel}: Wheel speed
- v: Vehicle speed

Driving cycles

For the cycle as a speed progression a driving cycle is used. A driving cycle is an elementary component of vehicle simulation, since it specifies the speed profile including slope to be driven and thus defines wheel torque and speed. Accordingly, the efficiencies and thus the overall consumption are also strongly influenced by the cycle. Within this methodological framework different driving cycles such as the WLTC are analyzed, and further cycles can be implemented. Since the WLTC is mainly used here, it is described in the following [DieselNet 2022].

With the WLTC, the UNECE World Forum for Harmonization of Vehicle Regulations introduced a global standard for measuring emissions, fuel and electric consumption which replaces the regional and national regulations. The Worldwide Harmonized Light Vehicles Test Cycle (WLTC) shows a dynamic behavior and provides for a uniform distribution of speeds, with higher speeds up to the maximum speed of 131 km/h. This is shown in Figure 6. The distribution of accelerations and decelerations is almost symmetrical. The total distance of the profile is more than twice as long as that of the New European Driving Cycle (NEDC), at over 23 km, while the average speed is about 13 km/h higher.

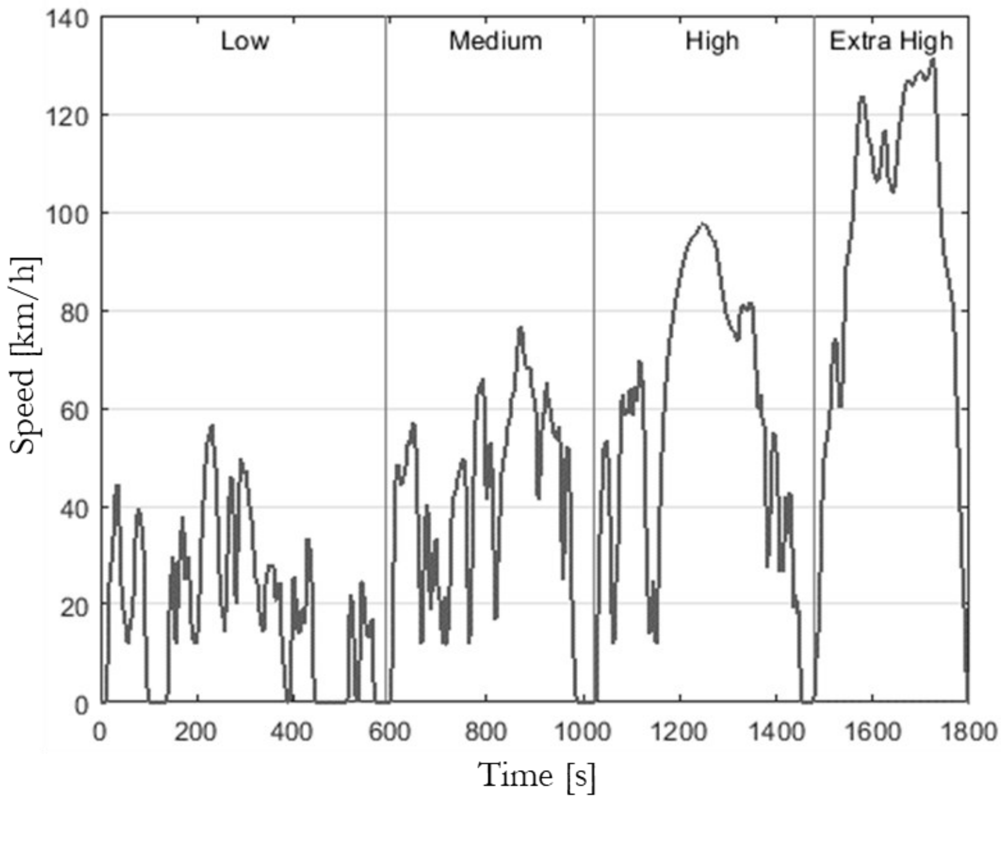

Figure 6: The WLTC drive cycle for Class 3b [DieselNet 2022]

Powertrain model

With the powertrain model, the overall efficiency and all powertrain losses of the powertrain can be calculated. Each powertrain component is implemented as a submodel with defined interfaces. By coupling the mechanical and electrical signals, all required powertrains can thus be implemented without having to create a completely new overall model as shown in Figure 7 with the example of a BEV. For a detailed description of the modeling of the components, please refer to [Weiß 2018]. The control is done by the operation strategy and includes the shift strategy for gear selection as well as the energy management for sensible power or torque sharing and the control of the battery state of charge. Potential consumption savings can be achieved with the right energy management. The operation strategy is applicable to all considered architectures and their dimensions and enables objective comparability. For a detailed description of the implementation of the operating strategy, reference is also made to [Weiß 2018].

Because most dynamic processes have a subordinate influence on the consumption, they are neglected. The neglected processes include, for example, rotational speed oscillations due to elasticity, synchronization processes or the opening and closing of switching elements. Contrary to the dynamic effects, temperature depended processes have a major influence on energy consumption. Nevertheless, these are neglected as well, because a valid consideration requires a huge parameter set and a forward simulation approach. Such a forward simulation is carried out for full-load accelerations considering also the temporal decrease in tractive force because of switching operations, due to the direct influence on the acceleration time [Weiß 2018]. Moreover, a backward-based approach is used, i.e. starting from a speed specification and without a driver model. Here the signal flows in the real vehicle do not need to be modeled and it enables the shortest possible computation time. However, when simulating an acceleration process, the velocity is not known, but represents the result of the maximum acceleration. This results from the maximum system power of the powertrain and can therefore only be calculated forward, i.e. starting from the power sources up to the wheel. Accordingly, the simulation environment offers both options. The backward-based approach is used for the calculation of the consumption for predefined cycles and the forward-based approach for the special case of the full load acceleration. Both approaches are included in the presented simulation framework [Weiß 2018].

Figure 7 shows an example of the architecture of a BEV created from the powertrain component modules. The BEV is designed as a single-shaft vehicle. In the backwards simulation, the wheel status variables from the vehicle model are transferred to the transmission model. First, the appropriate gear is selected in the shift strategy if there is more than one gear, and then the resulting gear ratio is used to calculate the transmission input variables. These are transferred to the e-motor model, which takes over the required torque in accordance with the operating strategy. The electrical power of the e-motor and the power requirement of the auxiliary consumer result in the required battery power. Finally, the energy demand of the battery including losses and the charging efficiency can be calculated.

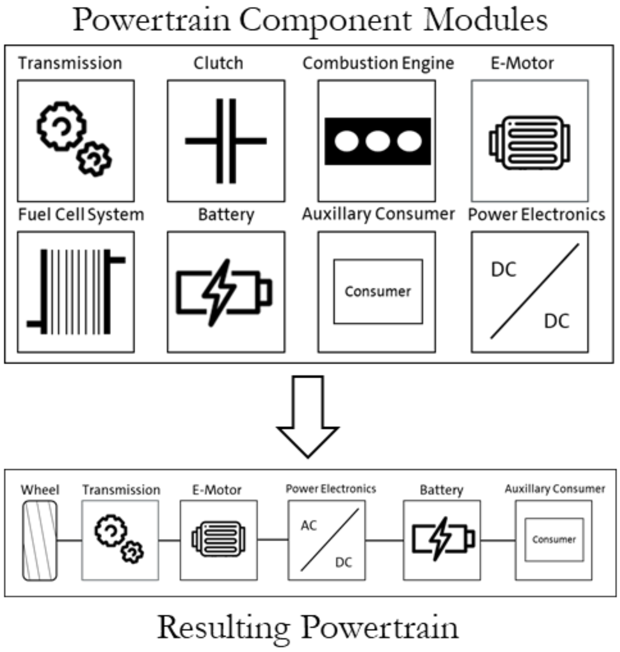

Figure 7: Modular approach of the powertrain design and simulation with an example of a BEV based on [Weiß 2018]

Besides the energy demand, vehicle performance indicators are calculated, including acceleration time and elasticity as well as the achievable maximum speed and climbing ability. These are needed for the design and scaling of the powertrain components. The acceleration time is the minimum time in which the vehicle can accelerate from standstill to a defined speed, for example 100 km/h. The elasticity differs in that, that the acceleration time is specified from a positive starting speed. This is intended to evaluate the power development at higher speeds. The vehicle acceleration is calculated by the serial forward simulation of all components starting with the sources and ending with the wheel. An energy management system to control a driver model is not required for this, as the maximum available torque is required. The influence of a decreasing SOC is taken into account, because this can lead to performance restrictions of the electrical system. One aspect that is additionally modeled in comparison to the backward-based consumption simulation is the contact from the wheel to the road at the limit. Thus, during an acceleration under full load, the maximum force that can be transmitted by friction can be exceeded. In order to prevent this, the maximum transmissible force due to the dynamic axle load displacement is determined and, if it is exceeded, analogously to the traction control, the wheel torque is reduced iteratively until the limit value is reached. For a more detailed description of the vehicle acceleration please refer to [Weiß 2018].

The maximum speed is reached, when the force provided by the powertrain at the wheel is equal to the sum of the air, rolling, and climbing resistance. Accordingly, no further acceleration takes place. It may happen that the maximum speed of a powertrain component is reached before this condition is fulfilled. In this case, the maximum speed is determined by the maximum speed of the powertrain component. Since it is not known in advance in which gear the maximum speed is reached, the calculation must be carried out for different gears. Depending on the powertrain architecture, the powertrain components relevant for the continuous top speed differ. The decisive factors are always the components that permanently provide the power in the respective architecture. In the case of the parallel PHEVs this is due to the limited battery energy content of the battery. In the case of the FCEV, the continuous power of the e-motor and fuel cell limits the mechanical and electrical power available for top speed, and in the case of the BEV, this is the continuous power of the e-motor and the traction battery. The tractive power available is determined by simulating the powertrain from the previously described continuous power-relevant components to the wheel, including all losses. The maximum available torque is always provided by the powertrain components, taking into account the source power [Weiß 2018].

The continuous climbing ability indicates the gradient that a vehicle can climb continuously at a given speed. The calculation of the gradient is based on the driving resistance with the assumption that the acceleration resistance is zero and a defined vehicle speed. To determine the available tractive force at the wheel, the components are considered analogously to the maximum speed, which permanently provide the power in the respective powertrain architecture. In addition, a short-term available climbing ability can be determined with the total released system power [Weiß 2018].

2.2.4 Design and scaling of powertrain components

In this powertrain simulation framework it is possible to scale powertrain components through dimensioning to fulfill requirements placed on the system. The dimensioning describes a certain characteristic of a component. This is made possible by scaling approaches, with which the component properties, e.g. torque-speed curve, mass moment of inertia and power loss map are derived from known reference components of the component library according to the desired dimensioning.

Component modeling can basically be realized in different ways such as map-based or based on simplified analytical relationships. The used modeling approach in this framework is based on the use of characteristic maps. For such a simulation, the quasi-static losses are stored in a map as a function of various input variables and the losses are then calculated by interpolation. Because any stationary effects can be taken into account in the map, the quality of the results is higher compared to the simplified analytical relationships. However, the necessary interpolations also increase the computational effort. Compared to detailed FEM and equivalent circuit models, however, the level of detail is lower. One advantage of the map-based approach is the possibility of presenting the results of these models in the form of characteristic maps. Further advantages of map-based simulation are the possibility to use the measurement results of real components as well as any technology variants without model adaptations and only by replacing the characteristic maps. A challenge is the required scaling of the maps, as it is not practical to store a separate map for each possible dimensioning. Due to the advantages mentioned above, the map-based component modeling is used for the component modeling in the used simulation framework. The maps and curves can represent power losses as well as component boundaries and other properties. For a detailed description of the physical models as well as the associated scaling, please refer to [Weiß 2018].

Powertrain component forecasts

Another important requirement for the holistic methodology is the derivation of forecasts to evaluate mobility systems of the future. In the field of powertrain simulation, [Schneider 2022] has developed a method for the prediction of the development of powertrain component attributes and integration in the powertrain design. The output coincides with the map-based approach of [Weiß 2018] and can therefore be integrated into the presented powertrain simulation framework. The predicted powertrain component attributes depend on the considered component itself, such as the energy density for the battery. Attributes having an essential impact on the results at the vehicle level are focused. Two different main sources are used for the determination of forecasts. The first source is based on a database with internal corporate forecasts. This data comes from experts of different automotive disciplines. The second source is based on literature research of publicly available data such as from scientific publications or feasibility studies ordered by governments. This data is weighted in dependence of actuality of the publication and the used forecast approach in the considered source. Subsequently data fusion methods are used to combine this data. To achieve a consistent technological reference and similar boundary conditions for all used data sources, the data sources are filtered within the database. The sources are filtered with regard to the source type, the time period of the forecasts, the considered technology as well as the system design. Furthermore, the derived forecasts are integrated in the used simulation models to analyze future vehicle concepts [Schneider 2022]. A similar forecast approach is shown in chapter 7 to derive forecasts for CO_{2eq} emissions.

Exemplary scaling of an e-motor

Here a fictional, exemplary scaling of an e-motor is performed to show the processes with the goal to design a new e-motor with a higher power output. In the first step a reference e-motor with known values regarding power, torque, mass and efficiency as well as a characteristic map containing torque over speed with the corresponding efficiencies for the production year of 2020 is taken, as shown in Figure 8 on the left side.

Now an e-motor with a power output of 200 kW in the year 2030 needs to be designed. The power is scaled via the length scaling of the e-motor. The map is scaled using the derived predictions for the year 2030 for the power density and the efficiency at the best point and under full load of the e-motor under consideration. With the help of the new map, the e-motor can be designed with the new power output. In addition to the power, the resulting mass, torque and efficiency of the e-motor is calculated as shown in Figure 8 on the right side. These characteristics are used for the powertrain simulation.

Attributes	2020	2030
Power Density	3.5 kW/kg	4.0 kW/kg
Efficiency in best point	95 %	96 %
Efficiency under full load	90 %	92 %

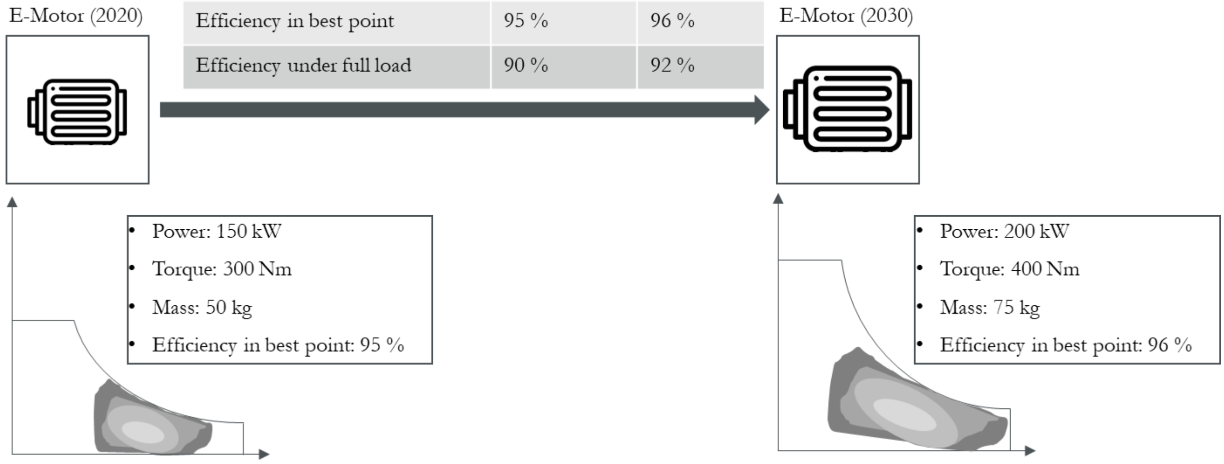

Figure 8: Exemplary scaling of an e-motor including forecasts

2.3 Life-Cycle-Assessment (LCA)

LCA according to DIN ISO 14040/14044 [ISO 14044 2006] is often used in the automotive sector to assess and compare individual vehicles with different powertrain architectures. The clear guidelines of DIN ISO for LCA ensure the comparability of products on the one hand and allow the certification of values for external communication on the other. For example, various automotive-related studies focus on the comparison of battery electric vehicles against conventional vehicles with combustion engines, such as in [Castellani et al. 2017], [Francesco et al. 2018], [Burchart-Korol et al. 2019], [Girardi et al. 2015], [Hawkins et al. 2013]. Due to the high CO2eq emissions impact of traction batteries in electric vehicles, many studies concentrate on the batteries and analyze them in detail, such as [Dai et al. 2019], [Dunn et al. 2014], [Peters et al. 2017]. Specific studies on the recycling phase can be found in [Dunn et al. 2012], [Raugei et al. 2018], [Unterreiner et al. 2016]. In addition, the impacts of the deployment of electric vehicle fleets are investigated in [Lajunen et al. 2020], [Dér et al. 2018] or ride sharing concepts in [Ding et al. 2019]. The environmental impact of measures during and beyond the vehicle use phase is analyzed in the following sources. [Ahmadi et al. 2014], [Bobba et al. 2018], [Faria et al. 2014] and [Reid et al. 2016] analyze the impact of second-life applications. In [Zhao et al. 2015] the impact of vehicle-to-grid applications is evaluated. In [Dér et al. 2018], agent-based mobility simulation is coupled with LCA as a novel approach to evaluate large-scale mobility-related interventions such as electric vehicles.

All sources nominated so far rely on the ISO standard for lifecycle-assessment, which can be regarded representative for the current state-of-the-art. However different problem statements need new methodological approaches to evaluate the impact. For example, in the field of carbon capturing, in [Brandão et al. 2013] six different options for the assessment of temporary carbon storage for a 100-year time horizon are compared. Hereby literature research is performed to find different approaches to calculate the positive impact. In [Steubing et al. 2016] a modular LCA approach is presented, which enables an efficient modeling and comparison of various product life cycles. Here different combinations of life cycle inventories can be analyzed and optimized in the context of scenario analysis. This modular approach is based on interconnected and exchangeable modules, as shown in Figure 9. These modules are user-defined life cycle stages with product input and outputs. For these modules Ecoinvent processes as well as processes modeled by the practitioner can be used. The Ecoinvent database contains processes, that are used to model the vehicles and infrastructure, which include the respective material and energy inputs for production. With this approach, modules have to be carefully combined to avoid double counting and user-defined cutoffs need to be introduced. These studies already show the need of an enhanced LCA approach in order to evaluate new measures to reduce the impact of mobility in terms of emissions. To derive requirements for the enhanced LCA the fundamentals of LCA need to be analyzed. Therefore, in the next chapter the fundamentals of LCA as well as the differentiation of attributional and consequential LCA is described.

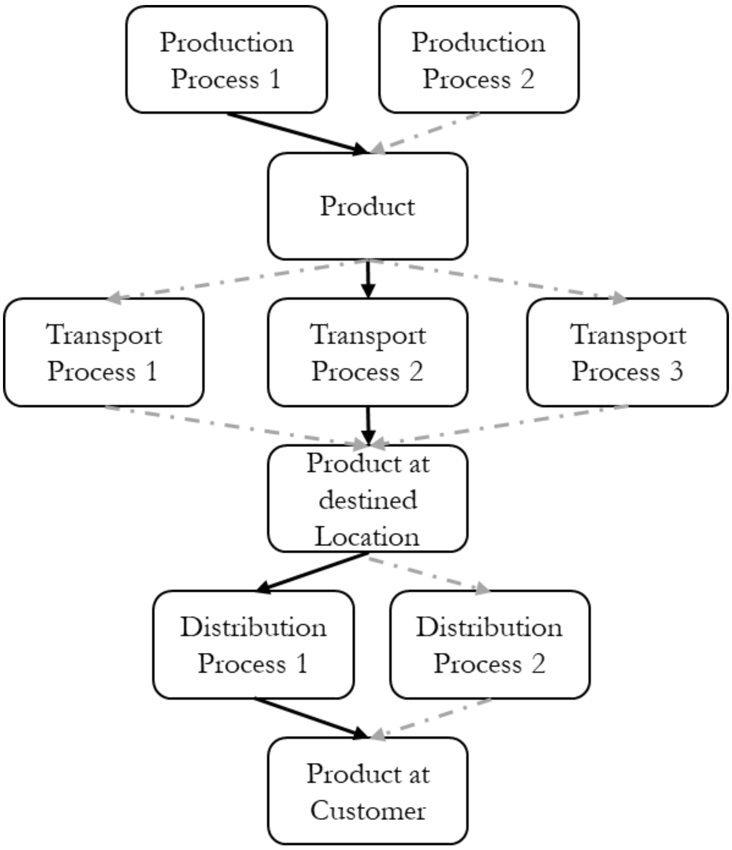

Figure 9: Representation of alternative pathways to produce a product

2.3.1 Fundamentals of life-cycle-assessment

The importance of environmental protection and the possible impacts associated with the manufactured and used products such as vehicles led to the development of methods to better understand and evaluate these impacts. One of the developed methods is the life-cycle-assessment (LCA). The LCA is an internationally standardized and comprehensive method. In this method all relevant emissions, related environmental and health impacts and resource consumption that are associated with any products or services are quantified. Here LCA can support to [ISO 14044 2006]:

- Identify opportunities to optimize products regarding their environmental impact at various points in their life cycle
- Make decisions for strategic planning, priority setting or designing of products and processes
- Select relevant environmental impact indicators including measurement techniques
- Marketing with certification and ecolabeling

In a so-called cradle-to-grave balance, shown in Figure 10, the full life cycle of a product or service is taken into account in the life-cycle-assessment. The different considered life cycle phases are the extraction of resources, production, use, end-of-life including recycling and the disposal of remaining waste. Considering single life cycle phases separately can solve problems in the considered life cycle phase while creating further emissions in the other life cycle phases. Here the LCA helps to avoid this scenario. For example, a battery electric vehicle as solution for the transport sector can reduce emissions in the use-phase, however the emissions in the production phase can increase. Therefore, LCA is a powerful decision support tool helping to make the products and services more sustainable [European Commission 2010].

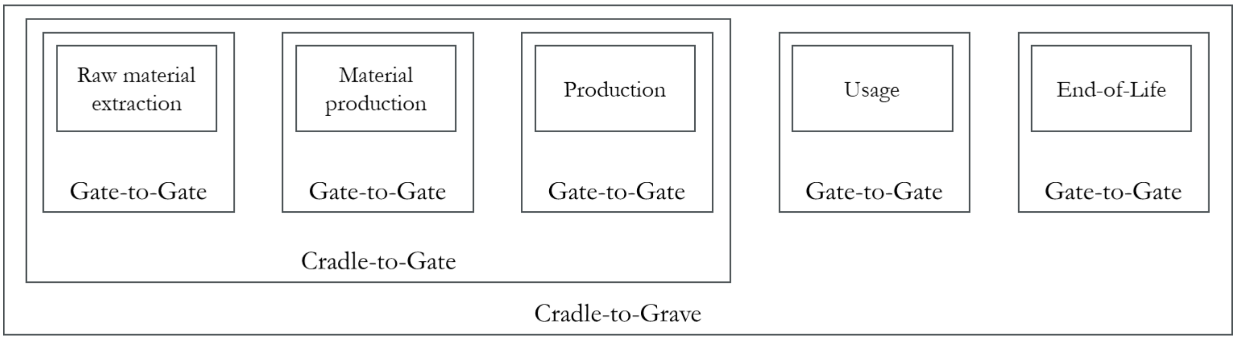

Figure 10: Overview of life cycle phases in cradle-to-grave based on [Schmuck et al. 2010] based on [VDA-Datenerhebungsformat für Ökobilanzen 2003]

The LCA framework is defined in the ISO 14040 and 14044 [ISO 14044 2006] and is described in the following. There are 4 phases in the LCA study, as shown in Figure 11. The first phase is the definition of the goal and scope including the system boundary. Here the level of detail can vary and depends on the subject and the planned use of the study. The following points need to be clearly defined and consistent with the intended application [ISO 14044 2006]:

- The reason for carrying out the study
- The intended audience, which is addressed
- The functions of the product system
- The functional unit

- The system boundary
- The used allocation procedures
- The used life cycle impact assessment (LCIA) methodology and impact factors
- The used interpretation methods, data requirements and quality of data which includes
    - age of data, geographical coverage, technology coverage, precision, completeness, representativeness, consistency, reproducibility, sources of the data, uncertainty of the information, missing data, all assumptions that are made, value choices and optional elements, limitations, type of critical review as well as
- The reference product and system for the comparison

The second phase is the analysis of the life cycle inventory (LCI). This phase includes an inventory of input and output data describing the product. Following steps need to be included in the LCI. The necessary data needs to be collected and the collection process needs to be described. The sources of the data need to be referenced and evaluated regarding their quality. Data for energy, raw material, ancillary and other physical inputs is needed. All calculation procedures including all assumptions need to be documented. The same procedure should be used throughout the study. A sensitivity analysis should be performed to show that life cycle stages, processes or input and output can be excluded due to lack of significance or should be included due to high significance. Allocation should be avoided. If not possible, the allocation should be based on physical relationships. If this is also not possible allocation should be in a way that reflects other relationships between them such as monetary value. It should be clearly described [ISO 14044 2006].

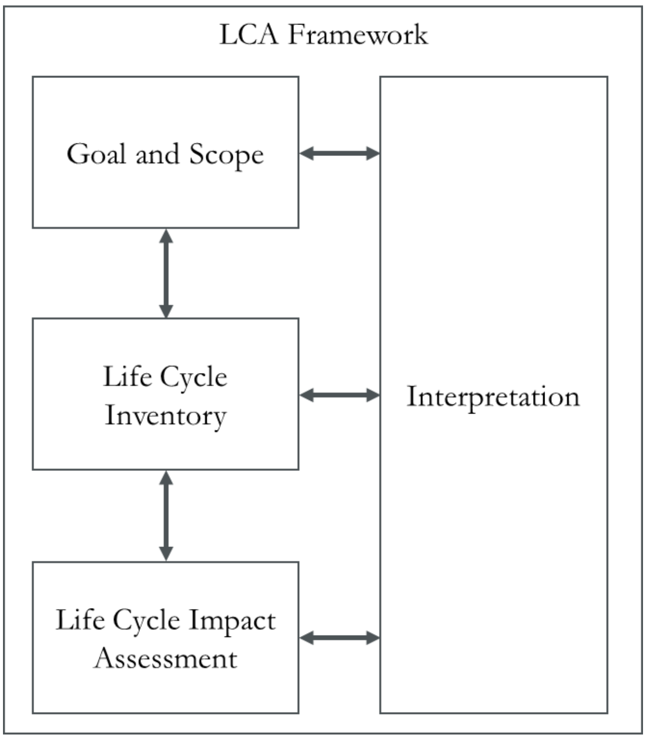

Figure 11: Four phases of the LCA framework based on [Schmuck et al. 2010] based on [VDA-Datenerhebungsformat für Ökobilanzen 2003]

The third phase is the life cycle impact assessment (LCIA). Here the environmental impact indicators are defined, calculated and assessed. The best known assessment methods are CML2001 or ReCiPe. The choice of the method depends on the product and service which is analyzed. The fourth and last phase is the interpretation phase. The results are discussed and used as basis for conclusions, recommendations and decision-making in accordance with the first phase goal and scope definition. Then significant issues are identified. Afterwards an evaluation is performed that considers completeness, sensitivity and consistency checks. In the end conclusions, limitations and recommendations are described [ISO 14044 2006].

2.3.2 Attributional and Consequential LCA

There are two types of LCA described in literature. The attributional LCA and the consequential LCA. The attributional LCA (ALCA) considers products or services at a certain point of time for a given amount of the functional unit and describes the environmentally relevant physical flows to and from its life cycle system. The ALCA is suited for cases where steady state assumptions apply and the system can be described by average data, because the existing market remains unaffected by the studied LCA. The results scale linearly with the functional unit. The ALCA fails, if the LCA is supposed to inform on the consequences of a change in demand for the functional unit underlying a decision process [Baustert et al. 2017].

To overcome these limitations, the consequential LCA (CLCA) was derived. This approach includes the impacts generated by all the systems affected by the change in demand of the functional unit. Additionally, processes affected through market relationships and not through physical ones are also included. The CLCA includes a bigger scope of the system boundary which leads to analyzing the impact of indirect effects, as shown in Figure 12. For example more energy is needed for a product, which leads to additional energy plants and this leads to an increase of the indirect impact [Baustert et al. 2017].

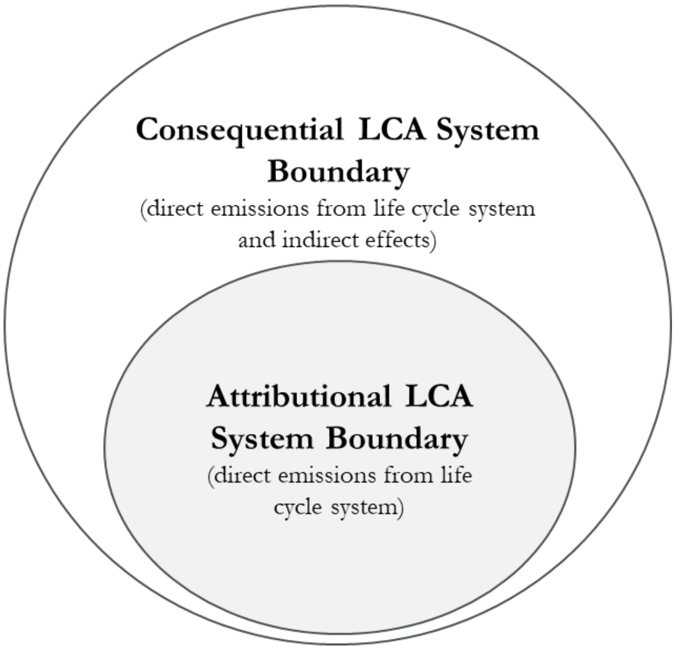

Figure 12: System boundaries of ALCA and CLCA based on [Brander et al. 2009]

Instead of average data, marginal data for the relevant technology is used. Results are no longer linearly dependent on the functional unit due to the expansion of the system, which takes into account indirect effects that occur outside of the attributional LCA of the product made of physical relationships between unit processes. The CLCA is also better suited to evaluate the environmental consequences of decisions [Baustert et al. 2017]. To further enhance the CLCA, it can be coupled with agent-based modeling for a more adequate representation of the complex mobility system. This approach was implemented in the following exemplary studies [Baustert et al. 2017], [Baustert et al. 2019], [Syré et al. 2020], [Querini et al. 2017] and [Göhlich et al. 2020].

The goal of consequential models is to identify the consequences of changes and how activities influence each other and their environment. These models are steady-state, linear, homogeneous models, with each unit process fixed at a specific point in time. It does not include dynamic feedbacks as well as activities far into the future, if the changes take place now [Consequential-LCA 2015]. The CLCA is a suitable approach for the new enhanced LCA described in chapter 7.

2.4 Holistic analysis of mobility systems

In accordance with the previously formulated objective of a holistic analysis of mobility systems, a methodology is developed in [Syré et al. 2020] that combines an agent-based traffic simulation and downstream LCA in one framework. This methodology, in contrast to conventional LCA of single vehicles, allows to analyze potential future strategies at the level of transport systems, such as the comparison of autonomous on-demand mobility and conventional personalized mobility. The approach is adaptable with respect to different input data, LCA databases, simulation data, choice of system boundaries and impact categories. Synthetic vehicles are analyzed in the MATSim "Open Berlin Scenario" and road-specific consumption is calculated. In addition, the base case is compared with three different new scenarios that include measures to reduce environmental impacts. For the LCA, data from the Ecoinvent database is used. Here, processes such as "glider production, passenger car" are taken as a basis and adapted for the new vehicles under investigation.

In [Göhlich et al. 2020] this approach is extended by a longitudinal dynamic simulation to design and evaluate different vehicles and powertrains. Here, a new method for deriving and analyzing strategies for a fully decarbonized urban transportation system is presented, combining a conceptual vehicle design, an agent-based traffic simulation, an operating cost analysis, and a life cycle assessment for a complete urban region. The holistic approach evaluates the technical feasibility, system cost, energy demand, transportation time, and sustainability-related impacts of different decarbonization and charging strategies. In contrast to previous work, the consequences of a transformation to fully decarbonized transportation system scenarios are quantified across all transportation segments, taking into account procurement, operation, and disposal. Vehicle types with different powertrains such as battery electric vehicles (BEV) and fuel cell electric vehicles (FCEV) are compared with internal combustion engine vehicles (ICEV). The vehicle and powertrain design is applied to receive realistic component sizing and consumption data for different applications and traffic segments that are considered in future scenarios. The methodology can be applied to any region and any transport system. The metropolitan region of Berlin is chosen as a demonstration case. MATSim is used as a tool for the agent-based mobility simulation. Ecoinvent is used to perform the LCA, where this step is done in the post-process. Furthermore, a method for estimating the required charging infrastructure for electric vehicles is presented. These two approaches show the feasibility of combining different methodologies in order to model and evaluate holistic mobility systems, which is a goal in this thesis.

2.5 Evaluation of the state of the art

In Figure 13 the most important sources from the literature review are summarized. The relevant disciplines for the method that is derived in this thesis are presented. Here it is examined whether the sub-disciplines have already been addressed by the sources and to what degree. Derived from the state of the art, a target picture for the method is developed. With regard to the state of the art, the four disciplines of agent-based mobility simulation, powertrain simulation, life-cycle assessment, and the combination of the individual disciplines are examined.

In the area of mobility simulation, it is investigated to what extend mobility demand modeling and mobility simulation take place. In [Querini et al. 2014], [Bishoff et al. 2019], [Hört et al. 2020], [Dér et al. 2018], [Syré et al. 2020] and [Göhlich et al. 2020] these topics are addressed, whereas in [Querini et al. 2014] no mobility simulation is performed. Similar to these studies, MATSim is used and integrated into the new methodology here as well. Here, the whole chain of mobility demand modeling up to the evaluation is considered similar to the sources.

In the area of powertrain simulation, requirement analysis and powertrain design, powertrain simulation and powertrain technology forecast are investigated. Powertrain simulation or a simplified characteristic based approach is used in [Querini et al. 2014] and [Dér et al. 2018]. In [Bishoff et al. 2019], a powertrain simulation is performed. In [Göhlich et al. 2020], powertrains are designed and simulated. Especially the powertrain design and simulation of [Weiß 2018] and [Schneider 2022] play a major role for this work, as the tool chain is integrated and extended in the new methodology.

In the area of life-cycle-assessment, the detailed LCA is investigated first. This is used in [Querini et al. 2014], [Dér et al. 2018], [Steubing et al. 2016], [Syré et al. 2020] and [Göhlich et al. 2020] to evaluate sustainability criteria for different products and scenarios. Here, [Steubing et al. 2016] extends the approach to achieve modularity in order to evaluate arbitrary products with one life-cycle inventory. With regard to a holistic evaluation of the mobility system with an integrated optimization, the detailed LCA is not suitable. Therefore, new approaches are pursued for the new method, which are modular and a key-value based approach. This enables the possibility to derive forecast values, which are needed to be able to evaluate future mobility systems.

In the last point, the combination of methods is considered. Here, the first sources show initial approaches, such as [Dér et al. 2018] or [Syré et al. 2020], where an agent-based mobility simulation is combined with a LCA. [Göhlich et al. 2020] extends the approach with a powertrain simulation. In this work, a method is to be developed that combines an agent-based mobility simulation with a powertrain simulation as well as an integrated LCA and additionally offers the option of an optimization. Thus, a degree of novelty is achieved in these research areas.

The following target picture for the methodology is derived from these considerations. For the agent-based mobility simulation, MATSim is to be used in a similar way to the aforementioned sources. MATSim is suitable here because it is an open source tool associated with a large and active community. For the powertrain simulation, the simulation environment of [Weiß 2018] as well as the technology forecasts of [Schneider 2022] will be integrated into the methodology. For the new LCA approach, instead of the detailed LCA, a new key-value oriented approach based on detailed LCAs will be developed. This key-value based approach shall be modular and dynamic and shall allow the derivation of forecasts. The individual methods are to be combined into an overall methodology and, in addition, optimization is to be possible.

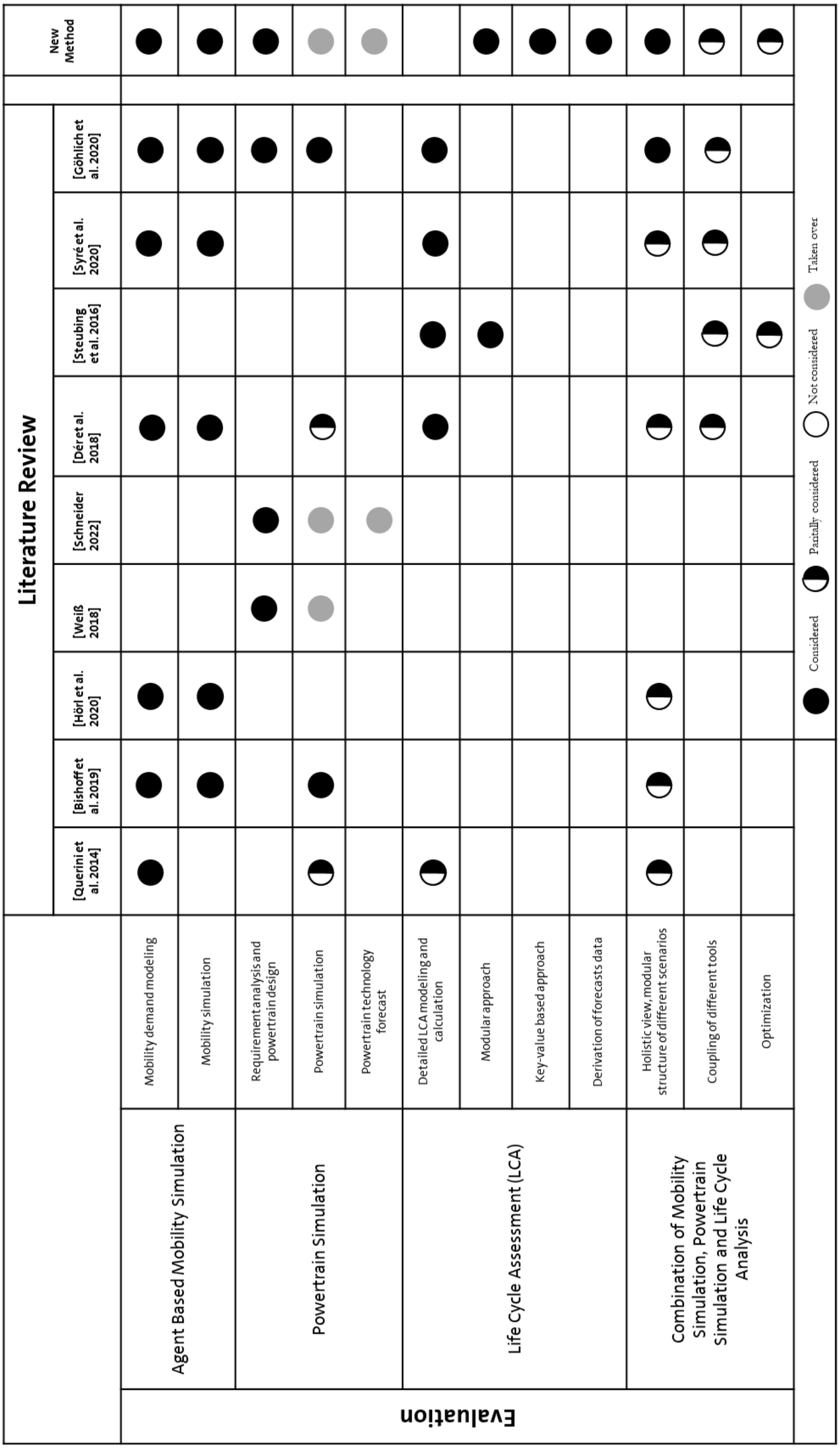

Figure 13: Comparison of the considered scientific approaches and classification of the present work

3 Derived need for action

The goal of this thesis is to derive a method to design and evaluate holistically sustainable mobility systems. As indicated, this purpose requires a combination of an agent-based mobility simulation with the results of a powertrain simulation, a life cycle analysis and a cost model in a multi-disciplinary approach. With regard to these disciplines, that state of the art is integrated where possible and enhanced (or modified) where needed. For the agent-based mobility simulation, MATSim is a suitable tool to describe individual mobility behavior and the overall performance of mobility systems. It is well-known in science and research and the open-source character allows customized, purpose-fitted code. Therefore, MATSim is used here and customized to fit the requirements of the overall method. In the field of powertrain simulations [Weiß 2018] and [Schneider 2022] describe methods that allow powertrain simulations within an optimization environment and predict the properties of future powertrain technologies with reduced computing time. These methods are integrated here and extended concerning the objectives of this work. This includes the overall system design, the component optimization, the operation strategy optimization as well as forecasts for different powertrain components described in [Schneider 2022]. With the help of the method, not only specific vehicles can be optimized, but future vehicles can be designed for different applications, taking into account different types of transport.

As discussed above, the LCA strictly based on the ISO standard 14040/14044 gives a standardized procedure enabling comparability and traceability of the results and certification of published values. However, the standardized procedure restricts the calculation of holistic CO2eq emissions to a static level and dynamic changes within the analyzed system are not taken into account. The required detailed description of processes within the balance envelope also limits the application to the current or a nearby point in time with well-known technology, material and energy flows. Thus an approach needs to be developed, which enables the consideration of dynamic systems including the predictability of a (far) future.

Furthermore, while LCA is commonly used to describe single products, this thesis aims to determine the cumulative environmental impacts of future mobility systems. This includes not only private and public vehicles and their energy requirements, but also the different transport modes as well as the required infrastructure for all transport sectors. A novel approach of a mobility system LCA is shown in [Syré et al. 2020] and [Göhlich et al. 2020] using Ecoinvent datasets and software. This enables a comprehensive analysis of sustainability criteria. However, due to the data-intensive LCA models as well as the increased computation time, this analysis is performed in post-process, as presented in [Göhlich et al. 2020]. Thus, an automatic optimization is not applied. With this thesis an approach is pursued, that allows the integration of the LCA into optimization procedures.

In the following the most important target goals are summed up:

Sub-Target 1:	Development of a modular method framework to evaluate and optimize holistic mobility systems
Sub-Target 2:	Integration of MATSim
Sub-Target 3:	Integration of powertrain simulation
Sub-Target 4:	Development of a new and enhanced LCA
Sub-Target 5:	Combination of individual methods and integration of a fitting optimization approach
Sub-Target 6:	Performing a sensitivity analysis
Sub-Target 7:	Validation of the method

The procedure for achieving the sub-targets is briefly described below.

Sub-Target 1: Development of a modular method framework to evaluate and optimize holistic mobility systems

In order to develop a modular method framework to evaluate and optimize holistic mobility systems the methods of agent-based mobility simulation, powertrain simulation, LCA and cost models need to be analyzed and combined into one single method. Therefore, the single methods are analyzed and interfaces between them are defined.

Sub-Target 2: Integration of MATSim

Integration of MATSim, an agent-based mobility simulation tool into the method framework. Agent-based modeling is needed to evaluate the impact of different measures at person level. For this, an agent-based mobility simulation is used, considering the whole chain from mobility demand modeling to evaluation. The total mobility demand should be taken into account. This means that in addition to private cars, other forms of mobility such as public transport, bicycles or completely new forms of mobility should also be modeled. MATSim is chosen as a tool to corporate the agent-based mobility simulation into the new derived method framework.

Sub-Target 3: Integration of powertrain simulation

Integration of the powertrain simulation into the method framework. Powertrain simulation and technology prediction based on [Weiß 2018] and [Schneider 2022] are integrated into the method. With the help of this method, it is possible to generate and evaluate vehicle portfolios for different scenarios.

These vehicle portfolios include the requirement analysis as well as powertrain design to calculate vehicle and component masses as well as consumptions, that are needed to evaluate the target criteria of the mobility system.

Sub-Target 4: Development of a new and enhanced LCA

A new LCA approach is to be developed and integrated into the method framework. The novel LCA-approach shall fulfill the following requirements:

- Dynamic balance and envelope
- Holistic mobility systems analysis
- Predictability of future scenarios
- Integrability into an optimization loop

In order to achieve this sub-target a modular, key-value based LCA approach is developed. The key-values are researched via a meta-study as well as modelled in detailed LCA-Software such as GaBi, where key-values are derived. This data is then used in combination with data-fusion approaches to prognose future trends of these values to model and evaluate future scenarios.

Sub-Target 5: Combination of individual methods and integration of a fitting optimization approach

The individual methods are to be combined into an overall methodology. A fitting optimization method needs to be integrated into the method framework. Therefore, different optimization approaches are analyzed and a fitting approach is chosen. The method enables the evaluation and optimization of mobility systems holistically with regard to their CO_{2eq} emissions, costs and energy requirements. To make the optimization feasible computation time reduction under retention of simulation quality to allow optimization loops is needed.

Sub-Target 6: Performing a sensitivity analysis

Performing a sensitivity analysis to show correlations between influencing variables and result variables. Here, especially the influence of sample sizes of the region as well as the influence of key-values are analyzed.

Sub-Target 7: Validation of the method

Validation of the method on the basis of a case study. In this thesis the region of Berlin is chosen as an application example. Needed input data for modeling the region of Berlin is researched. Simulation results are compared with researched data. Different optimization scenarios are performed and analyzed.

Summary

The overall process for the design and evaluation of holistically sustainable mobility systems of the formulated sub-targets is shown in Figure 14. The logical sequence consists of seven sub-steps, starting with the development of a modular framework (1), integrating the agent-based mobility simulation in MATSim (2), integration of the powertrain simulation (3), developing and integrating of a new and enhanced LCA approach (4), combining the individual methods (5), performing a sensitivity analysis (6) and validating of the method (7).

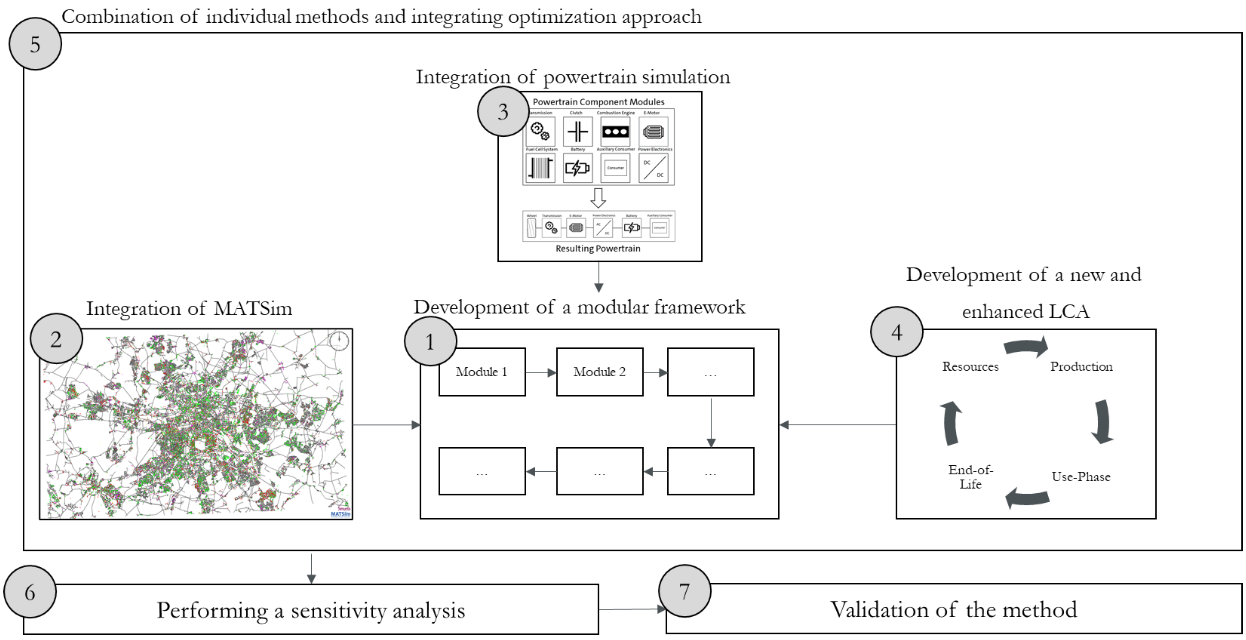

Figure 14: Classification of the formulated sub-target (circles 1-7) in the overall process for the design and evaluation of holistic sustainable mobility systems

4 Methodological approach – Holistic mobility system analysis

For the evaluation of ecologically, economically and sociologically reasonable decarbonization strategies, mobility systems must be considered holistically. Therefore, in the first step the system boundaries need to be defined. Within these system boundaries, the mobility behavior of the population, the different forms of mobility, the different vehicle and powertrain options as well as energy sources and the infrastructure including the charging infrastructure are considered. Subsequently, the entire mobility system is evaluated regarding the target variables.

4.1 Definition of the mobility system

To model a mobility system from a simulation perspective, it is important to define the mobility system in the first step. The mobility system in this work consists of three pillars, describing the mobility demand including person transport, the different travel modes as well as the specific region itself. The mobility demand includes data on mobility behavior, lifestyle, requirements and specific needs of the population. In the travel modes pillar, different forms of private owned and shared mobility as well as public transport and further new travel modes such as micro mobility are modeled. These are then evaluated in terms of emissions, costs and energy demand. These calculations are made in dependence of each agent and their individual behavior. The third pillar of the mobility system is the specific region itself. This pillar includes the mobility specific infrastructure and interfaces to e.g. the energy sector. This incorporates the traffic network where agents and vehicles move as well as charging infrastructure and the region specific energy pathways. The definition of the mobility system is shown in Figure 15. For the holistic approach it is important to consider all these pillars in one methodological framework to design and evaluate different scenarios, which are a compilation of the different use cases of all the participants in the mobility system. This holistic approach is described in the following.

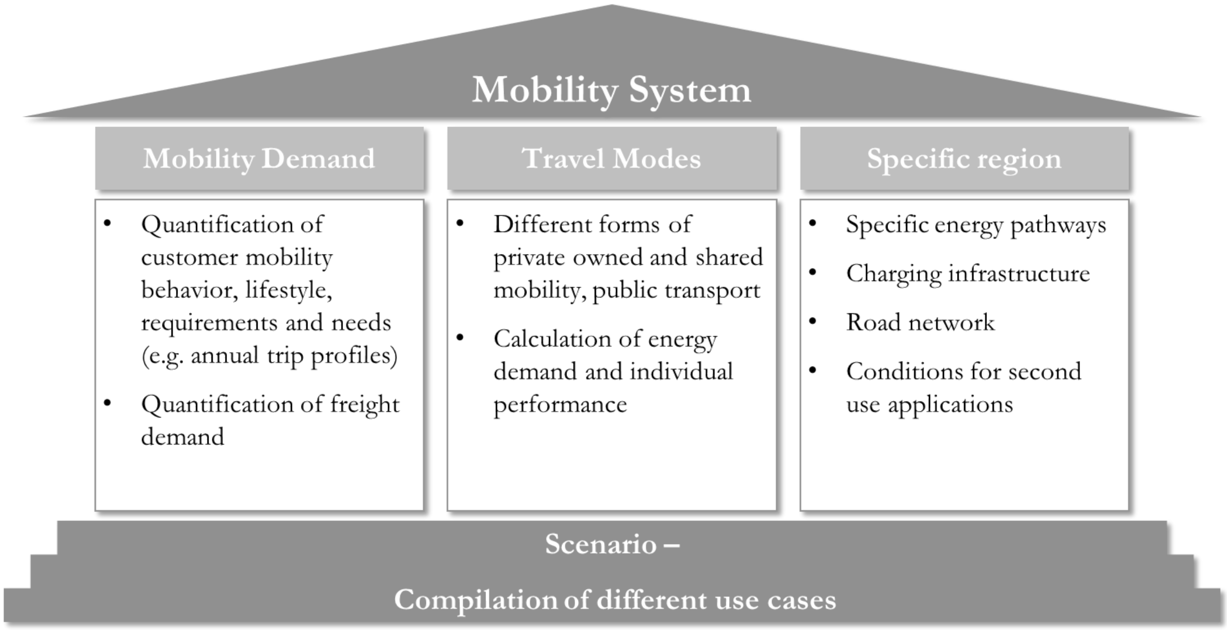

Figure 15: Definition of the mobility system

4.2 Holistic approach

To fulfill the stated requirements, a holistic approach is needed, which consists of a combination of an agent-based mobility simulation with a powertrain simulation as well as LCA and cost models, where the LCA is integrated in the overall methodology. In the beginning of the method the initial mobility system configuration needs to be defined and the parameters need to be set. This includes the input data for the modeling of the considered region as well as the measures for reducing the impact regarding $CO2_{eq}$ emissions. Subsequently the design and evaluation of the mobility system starts. In Figure 16, a process scheme of the pursued holistic method approach is shown. The process to achieve this goal consists of five blocks. In the first block the parameter settings such as the mobility system configuration and input values such as $CO2_{eq}$ key-values are read. In the second block, the simulation of the mobility system takes place. Here, the mobility simulation as well as the simulation and evaluation of the different travel modes is carried out. Subsequently, the analysis takes place in the next block. Here the target variables $CO2_{eq}$ emissions, costs as well as the energy demand are to be analyzed. The fourth block describes the optimization loop, that reconfigures the simulation based on the results. The optimal parameter settings with regard to the defined target criteria are sought. In the last block the results are shown and visualized.

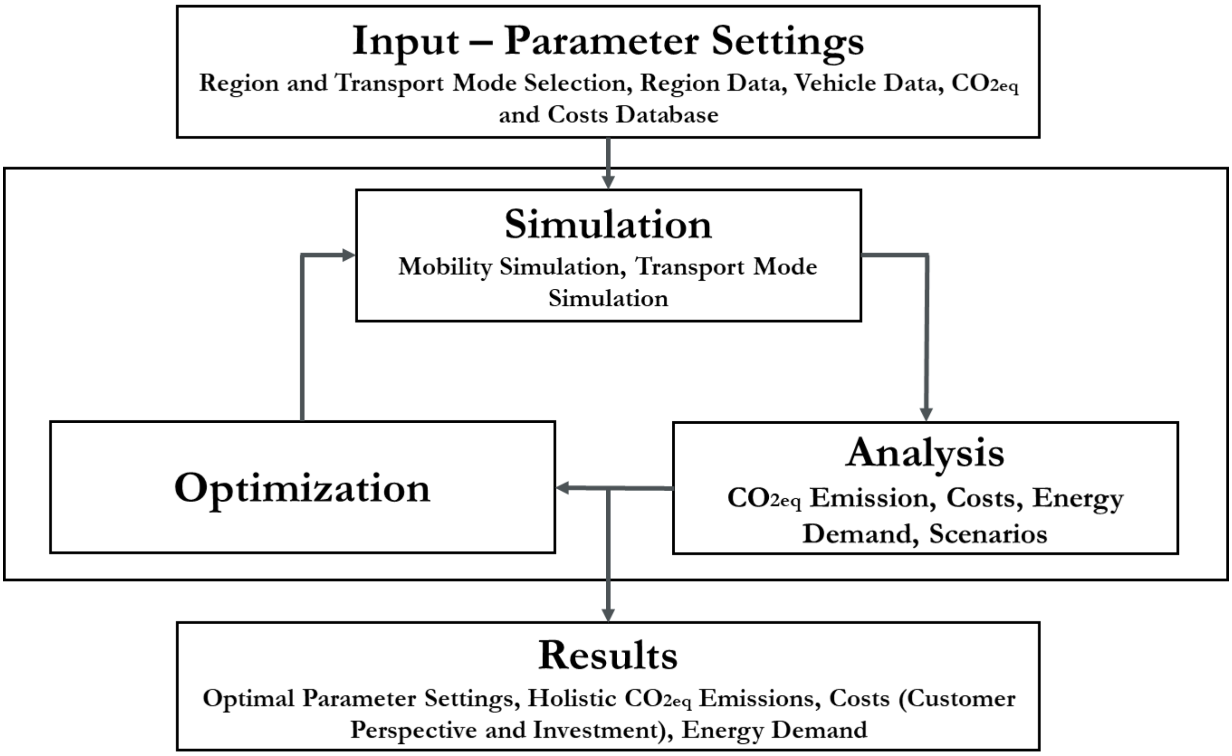

Figure 16: Overview of the method

4.3 Structure of the methodical approach

The simulation is divided in the following steps. As first step, the agent-based mobility simulation is performed. Here the dynamic mobility behavior of the considered region is simulated and evaluated. This is described in detail in chapter 5. In the next step, the different travel modes are evaluated regarding their simulated mobility patterns. For private owned and shared cars, a longitudinal powertrain simulation is performed, which is described in chapter 6. In addition, further travel modes are modeled and analyzed. Here the energy demand calculation is performed. The holistic mobility system is evaluated then regarding sustainability criteria. The enhanced LCA approach, developed for this purpose is described in chapter 7. Additionally, the costs from the customer's perspective are calculated. The cost models are described in chapter 8. Furthermore, the method is extended by an optimizer. Here an optimization of the holistically mobility system can be performed. The optimization method is described in chapter 9. After developing the method, a sensitivity analysis is performed to analyze the influence of different parameters of the mobility systems in Chapter 10. In the next step the method is applied on the region of Berlin. Two optimization scenarios are performed. The results are shown in chapter 11. To quantify the influence of different measures a comparison analysis is performed, in which a referenced scenario is build and compared with different future scenarios. In chapter 12 the critical discussion of this new methodological approach is described.

5 Agent-based modeling and mobility simulation

In this chapter the use of agent-based modeling as well as the integration in the whole method is presented. In the first step the generation of input data for the mobility simulation including the network, facilities and plan for agents is described. In addition, a method for the estimation of the needed infrastructure as well as the evaluation of the mobility system is shown. Subsequently, each step of the process plan for modeling the mobility system in MATSim is run through. This is done using the Berlin region as an example. The Berlin region is particularly well suited, since a good publicly accessible data basis is available and thus the results can be better plausibilized and validated. For this purpose, input data for the modeling of the agents including their plans, the different mobility forms as well as region data for Berlin are researched. Finally, exemplary mobility simulations are carried out with the generated region.

5.1 Generation of input data for the mobility simulation

In the following chapters the generation of needed input data for the mobility simulation in MATSim is described. These include the network and facilities of the region as well as the daily travel- and activity-plans of the synthetic agents. Additionally, the evaluation of the mobility simulation results is described. The methodological approach is described step by step and exemplary applied on the region of Berlin. Nevertheless, the aim of this work is to derive a generally applicable method that can be applied to any region. For this purpose, the method is deliberately designed in a modular way. In the following the single aspects of the methodological approach are described.

5.1.1 Generation of the network

The network in MATSim describes the infrastructure of the considered region including roads for cars, public transport or also pedestrians, facilities and charging infrastructure such as gas stations or charging stations for battery electric vehicles. For the modeling of the network OpenStreetMap (OSM) data is used here. This data can be extracted for example from https://extract.bbbike.org/, https://planet.openstreetmap.org/ or https://download.geofabrik.de/. In the next step the raw OSM data needs to be converted into a MATSim readable format, e.g. by MATSim internal methods. The conversion includes cutting the focus area, selection of needed road types and assigning of MATSim attributes such as link speed and length with road specific defaults. MATSim also expects coordinates to be transformed into an Euclidean coordinate system with meter as unit to calculate distances. In the next step the network is cleaned to remove unconnected parts where agents might get stuck. For a detailed description of the network class please refer to the [MATSim Javadoc 2022].

5.1.2 Generation of the facilities

Activity facilities in MATSim describe the locations of performed agent activities such as homes, work spaces, leisure or errand places on the network. Facility data can also be extracted from OSM data. As there is no MATSim internal method available, custom methods are developed here. In the first step the raw OSM data is searched for all buildings. For all buildings the attributes and coordinates from the corresponding nodes are extracted. Additionally, a coordinate transformation takes place so that the coordinates of the buildings match those of the network. Then the facilities are clustered into the categories home, work, errand and leisure if one of the keywords shown in Table 1 is found in the building's OSM data attributes.

Table 1: Attributes for clustering buildings

Home buildings	"apartments", "bungalow", "cabin", "detached", "dormitory", "farm", "ger", "hotel", "house", "houseboat", "residential", "semide-tached_house", "static_caravan", "terrace", "hut", "shed", "bunker", "building"
Work buildings	"commercial", "industrial", "kiosk", "office", "warehouse", "civic", "fire_station", "government", "hospital", "public_buildings", "public", "university", "barn", "cowshed", "farm_auxiliary", "greenhouse", "sty", "hanger", "digester", "service", "transformer_tower", "water_tower", "construction", "retail", "supermarket", "bakehouse", "kindergarten", "school", "library", "museum", "theatre", "cinema", "restaurant"
Errand buildings	"retail", "supermarket", "bakehouse", "kindergarten", "school", "toilets", "mall"
Leisure buildings	"cathedral", "chapel", "church", "mosque", "religious", "shrine", "syna-gogue", "temple", "conservatory", "stable", "grandstand", "pavilion", "riding_hall", "sports_hall", "stadium", "bridge", "ruins", "library", "mu-seum", "theatre", "cinema", "restaurant"

Here it is important to distinguish that for certain agents a place can be work. For example, a bakery, if an agent is a baker, this agent can go to work, whereas the other agents go there to shop. When generating the activity plans and assigning the locations, this needs to be considered. In this thesis the network and facilities are generated for the region of Berlin. In Figure 17 the raw OSM Map is shown and is converted into a MATSim readable format.

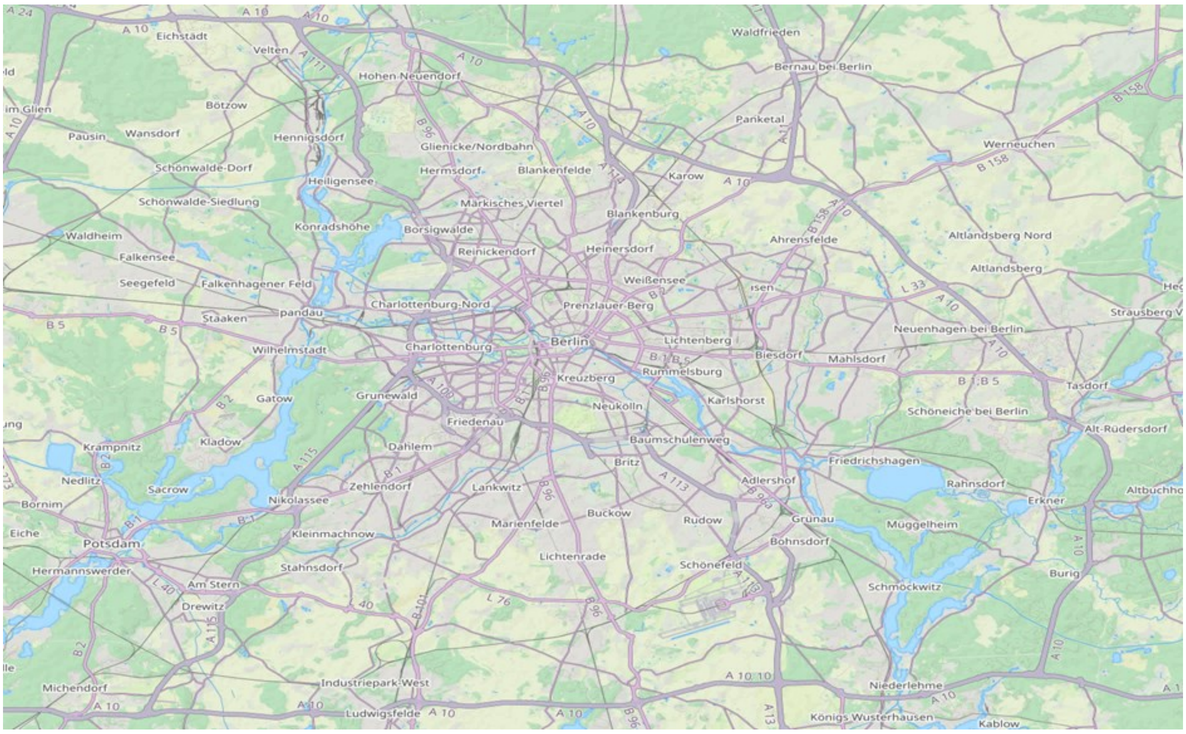

Figure 17: OSM raw data of Berlin extracted from https://extract.bbbike.org/

In Figure 18 the converted map is shown. Here, the roads of the considered region as well as the different facilities can be seen.

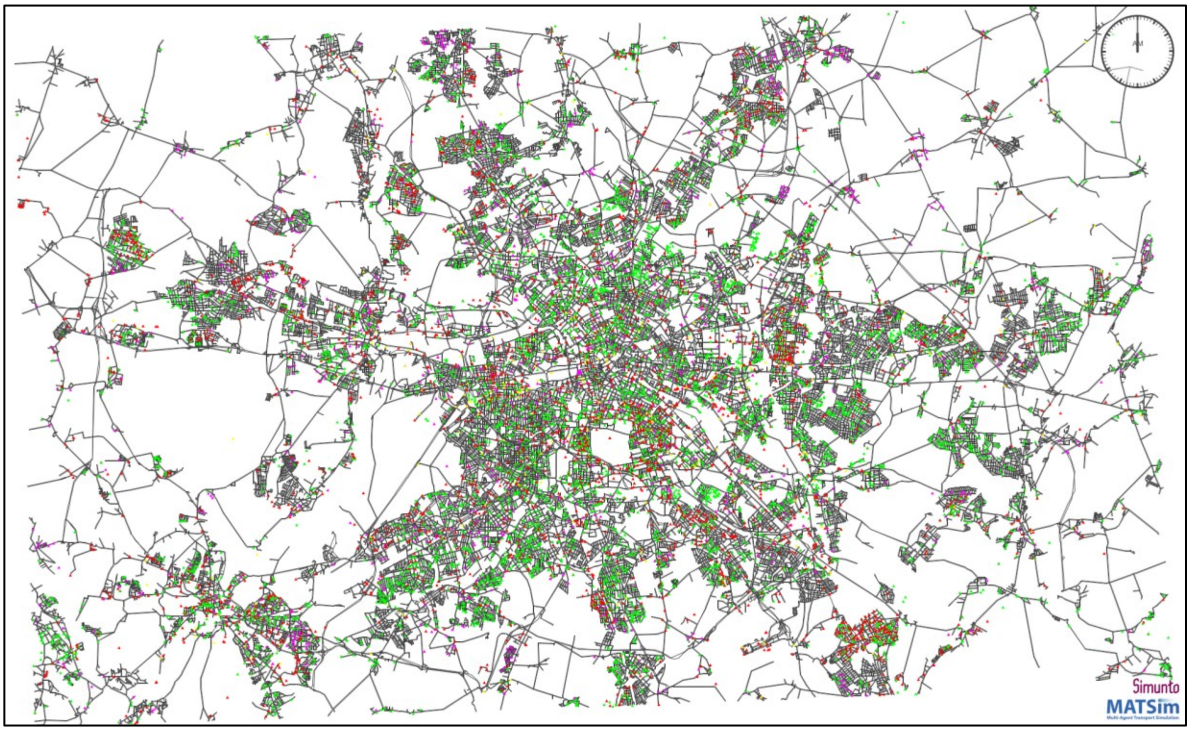

Figure 18: Network, Facilities and Infrastructure of Berlin and surroundings

5.1.3 Generation of additional infrastructure

The infrastructure data, such as charging stations and gas stations can also be extracted from the OSM data similar to the facilities, but the quality of results depends on the considered region. For European regions the charging infrastructure coverage is high, whereas other regions such as the USA have lower coverages. Here it is possible to use other data sources, such as Google. The additional data can then be added here to a complete infrastructure map. In the core MATSim software, ICEVs are considered as default cars. Therefore, battery electric vehicles including their state of charge of the battery and subsequently charging events are not considered in the mobility simulation. However the goal of this thesis is to optimize holistic mobility systems and electrified mobility is one way to achieve goals in terms of sustainable criteria. Thus a simplified approach for estimating the charging infrastructure is developed to calculate the impact of the needed charging infrastructure in dependence of the considered powertrain portfolio and enable a holistic evaluation. In addition, the simplified approach helps to reduce computation time and enables the analysis of various scenarios with different powertrain portfolios. Here the charging infrastructure has no effect on the simulation and is not taken into account. Since no charging events are simulated, the location and density of charging stations, for example, is irrelevant. In reality, there are certainly influences, e.g. on the installation costs. However, the goal of the simplified method is to estimate the impact the needed infrastructure has on the mobility system in terms of CO_{2eq} emissions and costs. This approach is described in the following.

Calculation of necessary charging infrastructure

The minimum necessary number of charging stations is calculated in dependence of the needed energy demand for mobility per day as well as the average provided energy by the charging stations.

$$N_{min} = E_{needed}/E_{avg,chargSt} \qquad \text{(eq. 10)}$$

- N_{min}: Minimum needed number of charging stations
- E_{needed}: Needed energy demand for mobility per day
- $E_{avg,chargSt}$: Average provided energy by a charging station

To estimate the needed energy demand per day the driving profile of each agent as well as the consumption of the used vehicles is needed. The driving profile from each individual agent is a result from the mobility simulation including driven distances and mean velocity on a daily basis over the year. To calculate the consumptions, an internally developed longitudinal dynamic simulation is used to design the vehicles. Here each agent is assigned a vehicle based on statistical data describing the current vehicle portfolio. This simulation is described in chapter 6. For the calculation of the minimum necessary number of charging stations it is important to know the share of agents charging at home as well as the share of agents charging publicly. In [Sperka 2022] it is assumed that today around 90% of electric charging events take place at home and around 10% of electric charging events take place at publicly available charging stations. Here the electric vehicles include BEV and PHEV. For the future it is estimated that around 70% of electric charging events take place at home and 30% of electric charging events take place at public available charging stations. Since in this work new scenarios in the future are analyzed, for the calculation of the necessary charging station, it is assumed that 70% of electric vehicle users charge at home and 30% charge at public available charging stations. The needed energy demand for mobility per day is calculated with the following equation:

$$E_{needed} = share_{public} * E_{day,total} \quad \text{(eq. 11)}$$

- E_{needed}: Needed energy demand for mobility per day
- $share_{public}$: Share of agents charging at public chargers
- $E_{day,total}$: Total energy demand per day

In the next step the average provided energy by the charging stations needs to be calculated. The average provided energy depends on the utilization rate of the charging station describing how long the charging station is used over the day as well as the power output of the charging station. In [Sperka 2022] a utilization rate of 0.9h up to 2h for a day for slow chargers below 22kW power output is stated. For fast chargers a utilization rate of 1.5h up to 4.22h is given. In this work the utilization rate coming from the expectation of the charging industry is used. The expected values lie at 1.72h for slow chargers and 4.22h for fast chargers [Sperka 2022]. Furthermore, in [Sperka 2022] it is assumed that 57% of publicly available chargers are slow chargers with an average power output of 7.7 kW and 43% are fast chargers with an average power output of 130 kW. The same assumption is also made in this work. The average provided energy by the charging stations can be calculated with the following equation. With the assumed values an average energy output of 88 kWh per charger per day is calculated:

$$E_{avg,chSt} = share_{slow} * util_{slow} * P_{slow} + share_{fast} * util_{fast} * P_{fast} \quad \text{(eq. 12)}$$

- $E_{avg,chargSt}$: Average provided energy by a charging station
- $share_{slow,fast}$: Share of slow/fast chargers
- $util_{slow,fast}$: Utilization rate of slow/fast chargers
- $P_{slow,fast}$: Power output of average slow/fast chargers

In the following example the minimum necessary number of charging stations for Berlin with an assumed 100% BEV scenario is calculated. In Berlin there are around 1.2 million vehicles registered [Steinmeyer et al. 2017]. It is assumed that each agent uses a BEV. The vehicle types and segments are assumed equal to the current distributions that are described in [Kraftfahrt-Bundesamt 2022]. With the assumption of 30% of the agents charging at publicly available charging stations, this leads to a needed energy demand of around 3.2 GWh per day. With the calculated average energy output of 88 kWh per charger per day, this leads to around 36500 necessary publicly available charging stations. Overall, with this approach the minimum necessary number of charging stations in dependence of the analyzed powertrain portfolio and calculated energy demand can be calculated.

5.1.4 Generation of a synthetic population

After the region itself including the network, facilities and infrastructure is determined, the regional population can be synthetized. In this work, statistical distributions of the considered attributes are derived from publicly available data, such as OSM data, census data, and mobility surveys. This data is used in an automated process to generate the population and plans. For example, the distribution of the type of mobility used and the age distribution are considered here. The following data of the considered region is collected to model the agents. For each attribute, a statistical distribution is derived. The attributes for the region of Berlin are shown in the appendix A.2:

- Number of inhabitants
- Employment status
- Gender, age and income
- Number of children
- Activity plans of individuals including activity chains and times
- Driven distances
- Modal split for calibration and validation of mobility simulation
- Share of homeowners
- Vehicle requirements such as range, costs, maximal velocity or vehicle type

Generation of activity plans for each agent

In the following the process for the full generation of activity plans of each synthetic agent is described and the data each agent subsequently contains is shown in Figure 19. Here the overview of the stored data of each synthetic agent is shown. Each agent stores information about the following attributes such as employment status, gender, age, income, number of children as well as home ownership. The employment status has an effect on the agent, if he drives to work. The number of children has an effect on the probability if the agent needs to drive the children to the school or kindergarten. Furthermore, for the generation of activity plans data with regard to the number of activities, the performed activity types, starting locations, destinations, which are also defined by the activity types, starting and end times, driven distances as well as used travel mode is stored. This data is assigned to each agent, so that the statistical distributions and assumption fit.

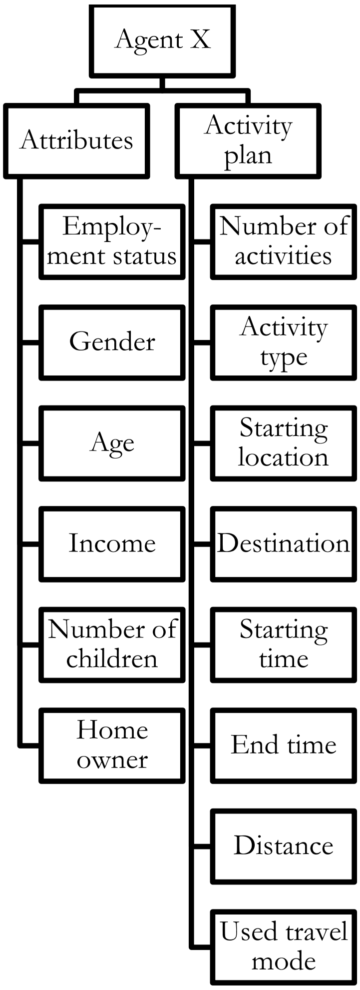

Figure 19: Data model of synthetic agents

The generated facilities indicate the network coordinates, at which agents perform certain activities such as living or working. In addition, the typical distances between two activities are given by the distributions, derived from the collected data of the region. With this information and the agents' activity chains, the individual best fitting distribution of visited locations can be determined. To distribute the agents home locations, the capacity of the facilities is needed to know how many agents fit in one home facility. However, for the estimation of the capacity the z-coordinate of the facilities is needed, but these are missing in the OSM data. In order to ensure a realistic distribution of agents, the population density for the region districts are used. Based on the population density the agents are assigned home locations. Each agent starts at his respective home. In reality, there are also people who do not start the day at home since for example they can work in a nightshift. To reduce complexity, they are neglected here. Subsequently further activities are assigned to each agent depending on probabilities and random functions, which define if this activity is executed, as well as the statistical distributions, as shown in Figure 20 for the region of Berlin. For example, an employed agent will drive to work on work days and an agent with children has a higher probability to drive children to their schools. The number of specific activity trips is limited by the statistical distribution.

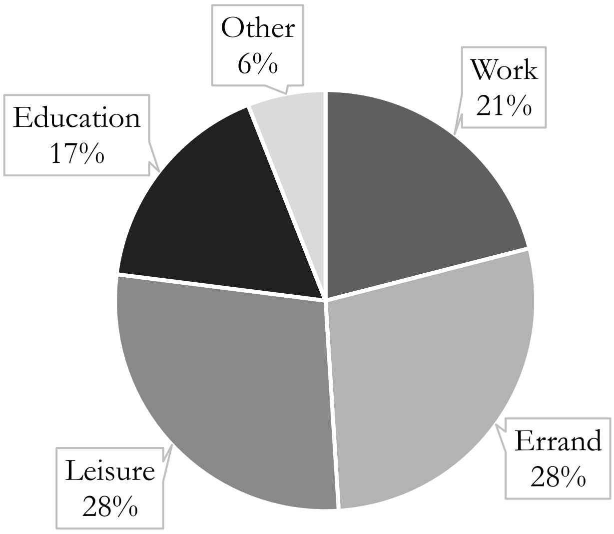

Figure 20: Statistical distribution of activity location over all trips in Berlin [Gerike et al. 2019]

The number of activities in the activity chain are based on statistical distributions, as shown in Figure 21. Here it can be seen that people under 15 years perform in average 3 trips per day. People between the age of 15 and 65 perform in average 3.6 trips per day and people over 65 years perform in average 3.3 trips per day [Gerike et al. 2019].

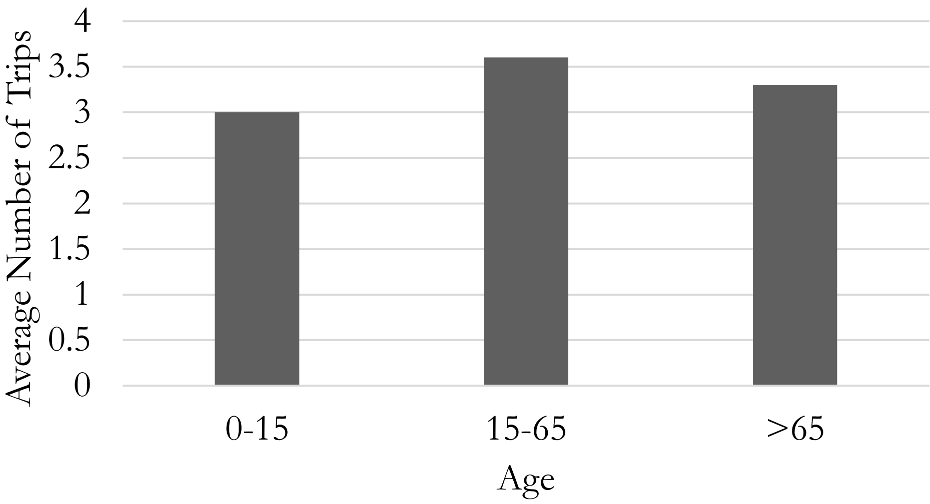

Figure 21: Average number of trips in dependence of the age [Gerike et al. 2019]

The start and end times of the activities are set with a random tolerance time window within defined boundaries. The time frames are detailed in the next steps. Agents start their day depending on the employment status in the morning and usually come back in the evening. The activity plan is based on a modular method, so it is possible to add activities.

This procedure leads to a full activity chain for each agent, which for example looks like in the following for an employed agent, as shown in Figure 22:

- Agent departs from home (H) and drives to work location (W) at 8 am.
- Agent works for 8 hours and leaves work (W) to go shopping (E) for 1 hour.
- After shopping (E) the agent goes to the gym (L) for 1 hour.
- After the gym (L) the agent drives back home (H) and ends the day.
- Therefore, the activity chain for this agent looks like this: H → W → E → L → H
- It is assumed that each agent returns home at the end of the day.
- There can also be agents, who do single trips like H → W → H and agents, who do not leave the house H, due to home office for example.
- The same is done for students and the rest of the population. For the rest of the population it is assumed, that the probability that these agents stay at home is higher.

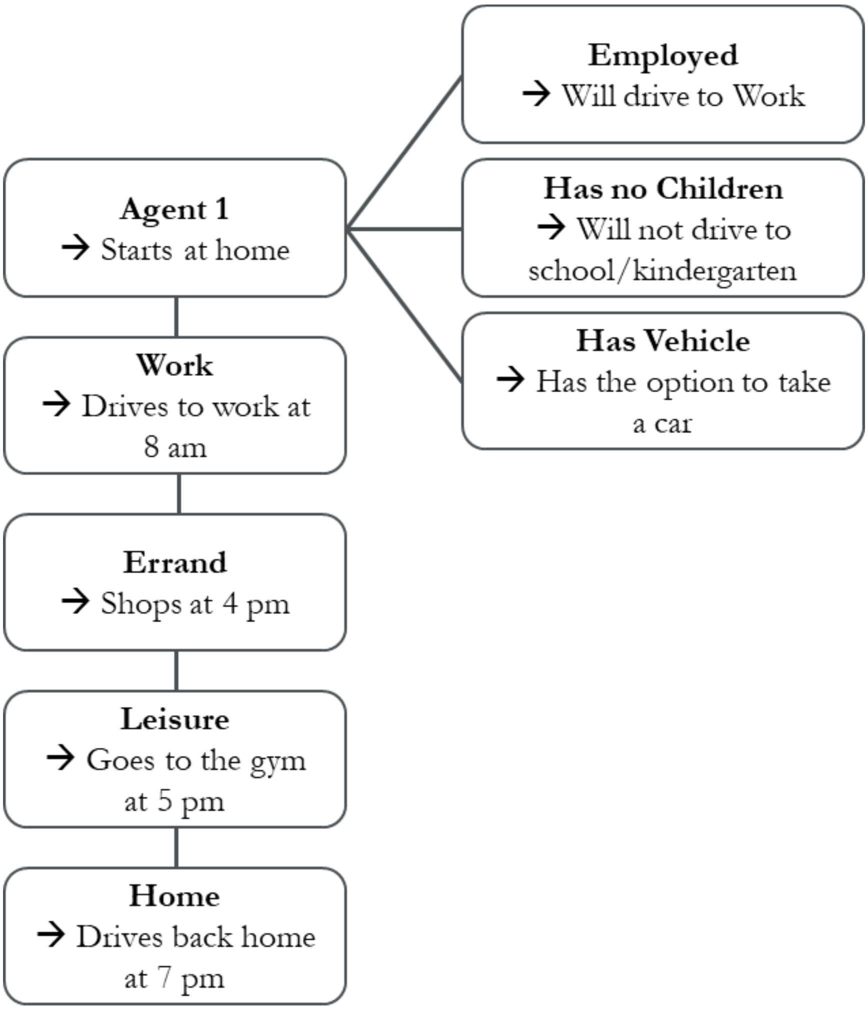

Figure 22: Full activity chain for one exemplary agent

Finding fitting locations to perform activities

In the next step, fitting locations for the activity chain of each agent need to be found. Here the building type must fit the activity of the activity chain of the considered agent and the resulting driven distances must correspond to the average of the driven distances derived from the statistical data. To calculate the driven distances the number of activities is considered. Here the return to the home is also considered. In the first step the daily driven distance of each agent is calculated based on the statistical distribution. Then the average daily driven distances per trip are calculated for each agent. In Figure 23 the average distances per activity type for the region of Berlin is shown.

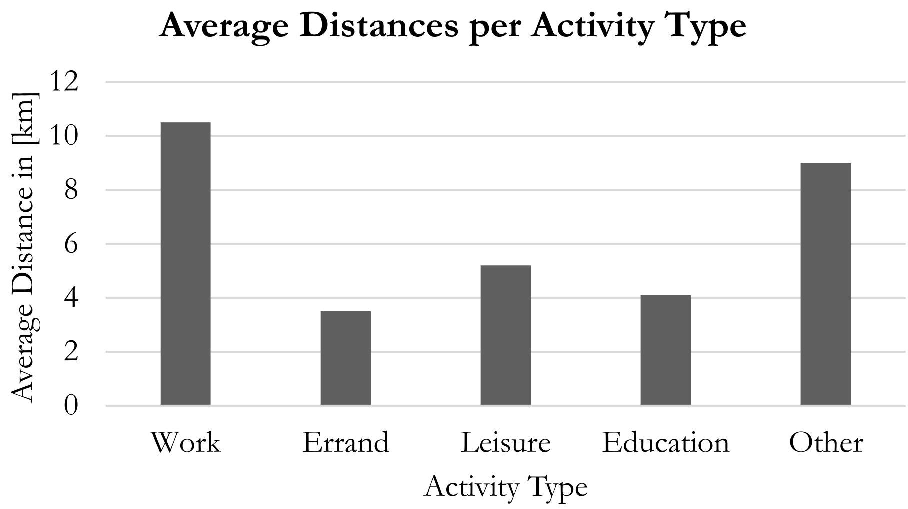

Figure 23: Average driven distances per activity type [Gerike et al. 2019]

Now it is known where the agent lives and how long each trip is in average. Buildings, which fit the activity of the activity chain of each agent can be assigned with premise that these buildings lay in the average driven distance. Different combinations of possible destinations are analyzed and the distances are calculated. The distances can be calculated with the coordinates data coming from OSM. Subsequently the best combination of building locations, which fit the activity chain and the daily driven distances derived from statistical data is assigned to the agent. In Figure 23 the approach is shown by an example. Here an exemplary home location of one agent and the trip distance the agent has to drive to reach the work location is shown. The circle represents the coverage of the trip distance, where a work location can lie. In the next step different work locations are analyzed and the distances are calculated and compared to the coverage. Here it can be seen that work location 2 fits the best and is therefore assigned as the location for the activity in the activity chain.

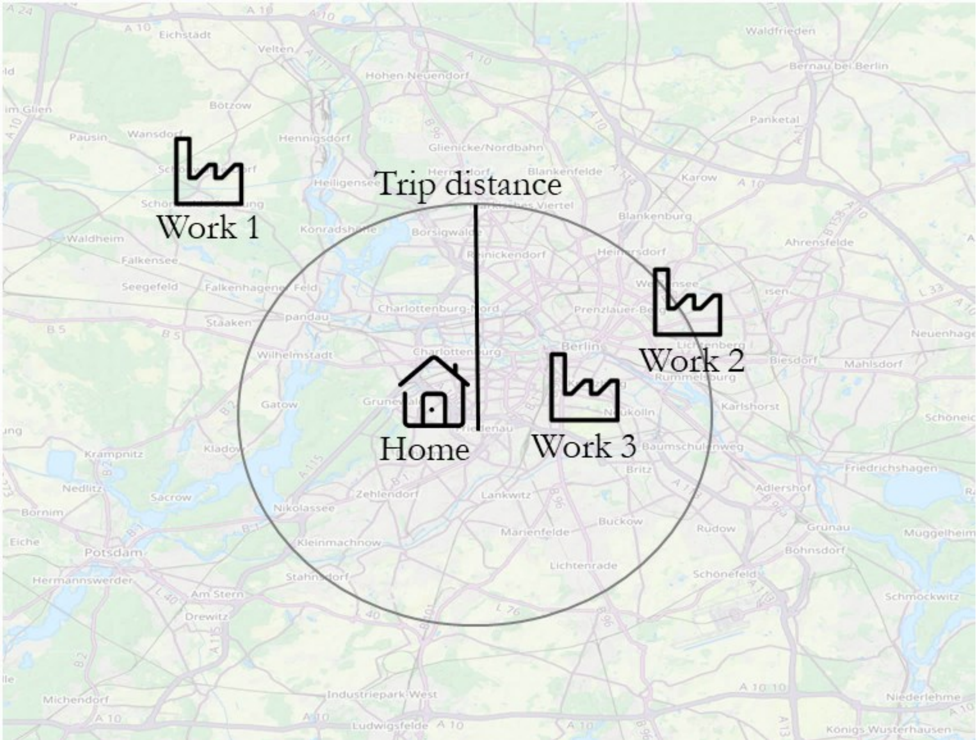

Figure 24: Assigning locations to the activities of the activity chain

Assignment of initial transport modes

Agents choose their transport modes based on the scoring and replanning during the mobility simulation. However, an initial transport mode needs to be assigned to the single trips of each agent. For a sensible initial transport mode distribution, the following approach is chosen. A fitting transport mode is chosen based on driven distance and a random probability of the agent. The longer the average distance of the agent is, the higher the probability, that this agent will choose a car or public transport. On the other side, the shorter the average distance is the higher the probability that this agent will choose to walk or ride a bicycle.

Calculation of travel and corresponding end times

For the activity plans of the agents, the desired starting and end time is needed. As described before, the starting time lies in a defined time slot depending on the employment status of the agent as well as a random function. Here it is assumed that most agents start their day at 7 am with a standard deviation of ±2h, as shown in Figure 25. The travel time is calculated in dependence of the driving distance and the average mean velocity of the assigned travel modes. The assumed values are shown in appendix A.3. With this approach, an estimated arriving time can be calculated, so that during the simulation the agents will realistically reach their destination in the given time. The end times of activities are the sum of the starting times as well as the corresponding travel times.

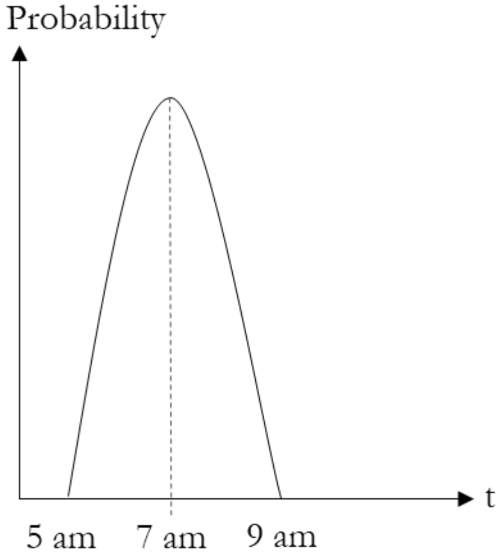

Figure 25: Assumed distribution of starting times

5.1.5 Public transport in MATSim

Public transport summarizes schedule-based traffic modes that move in separate or in the car network, such as subway, train or bus. Public transport can be modeled in different ways in MATSim. In terms of computation time, the fastest approach is to use the so-called teleport mode and define an average speed for the public transport from point to point. This approach neglects access and egress to stations and connectivity between lines with the typical stellar structure. The more detailed approach is to create own networks, transit schedules and transit vehicles to model public transport and its infrastructure. To create these by MATSim internal methods the GTFS data for the region, as well as the OSM file of the region for the network is needed. The General Transit Feed Specification (GTFS) defines a digital interchange format for public transit schedules and associated geographic information such as stop locations. In this thesis, a combination of both approaches is used. The MATSim internal methods are used to create the public transport stations on the network and transit vehicles. Here agents walk to the stations to access the public transport. When entering the public transport, the actual movement is a teleport mode to reduce computation times. In appendix A.1 the event sequences of public transport are shown. In this thesis public transport is considered as a teleport mode.

5.1.6 Modeling of a realistic market behavior

In order to incorporate customer choices in the evaluation of CO_{2eq} emissions and derive an annual CO_{2eq} development for future scenarios that is as realistic as possible, a private vehicle market model is additionally implemented in the holistic methodological approach. Without considering the customers market behavior, the initially assigned vehicles are used for the entire duration considered. Real market behavior as understood here means, that vehicles are exchanged after a certain time and with a certain probability, or travel modes are changed. For this purpose, the vehicle age of the used vehicles is modeled in the first step. Statistical data can be used to model the vehicle age of the respective region under consideration. For Germany, for example, the data from the KBA [Kraftfahrt-Bundesamt 2021] are available. Based on this statistical data, vehicle ages can be assigned to the vehicles.

Subsequently, the mobility system is evaluated annually. Here, the agents have the opportunity to decide annually for new vehicles or new travel modes. The decision tree is shown in Figure 26. Here, the following steps are considered. First, it is checked if the agent owns a vehicle at the time under consideration. If the agent owns a vehicle, a probability for either keeping or selling the vehicle is calculated depending on a random seed as well as the current vehicle age and the usage time of this vehicle. If the agent keeps his vehicle, it is used for another year. After another year, the probability is recalculated. With increasing usage time, vehicle age and income of the agent, the probability that the agent sells or disposes his vehicle increases.

If the agent sells or disposes his vehicle, two paths are formed. One is from the vehicle's perspective. The older the vehicle is, the more likely it is disposed. Otherwise, the vehicle moves to the used market. Here it is assumed that at the beginning of the simulation the used market is empty and includes only the considered region to avoid allocation. The longer the vehicle is on the used market and thus gets older, the more likely it is to be disposed. Second, from the agent's point of view, it is checked, if the agent needs a vehicle. The greater the distance traveled per trip by the agent, the more likely that he needs a vehicle. Otherwise, the agent has the option to change its mobility mode, such as to public transport. If the agent needs a vehicle, he has the option to buy a new vehicle or one from the used market. Here, a probability is determined as a function of income. The higher the agent's income, the more likely he is to buy a new vehicle. Otherwise, a suitable vehicle is fetched from the used market. For all newly added vehicles, whether new or used, a vehicle is assigned analogous to the vehicle assignment shown in chapter 6.3. If there is no suitable vehicle on the used market, a new vehicle is assigned. This process is performed annually for each agent. The realistic market behavior can be enhanced by integrating market predictions about new car sales. These predictions are often made for bigger market segments and regions and can be used to derive predictions for the considered smaller region. However, deriving predictions for smaller regions creates a big uncertainty and leads to allocation, which should be avoided, as described in chapter 2.3. This is not implemented in this thesis.

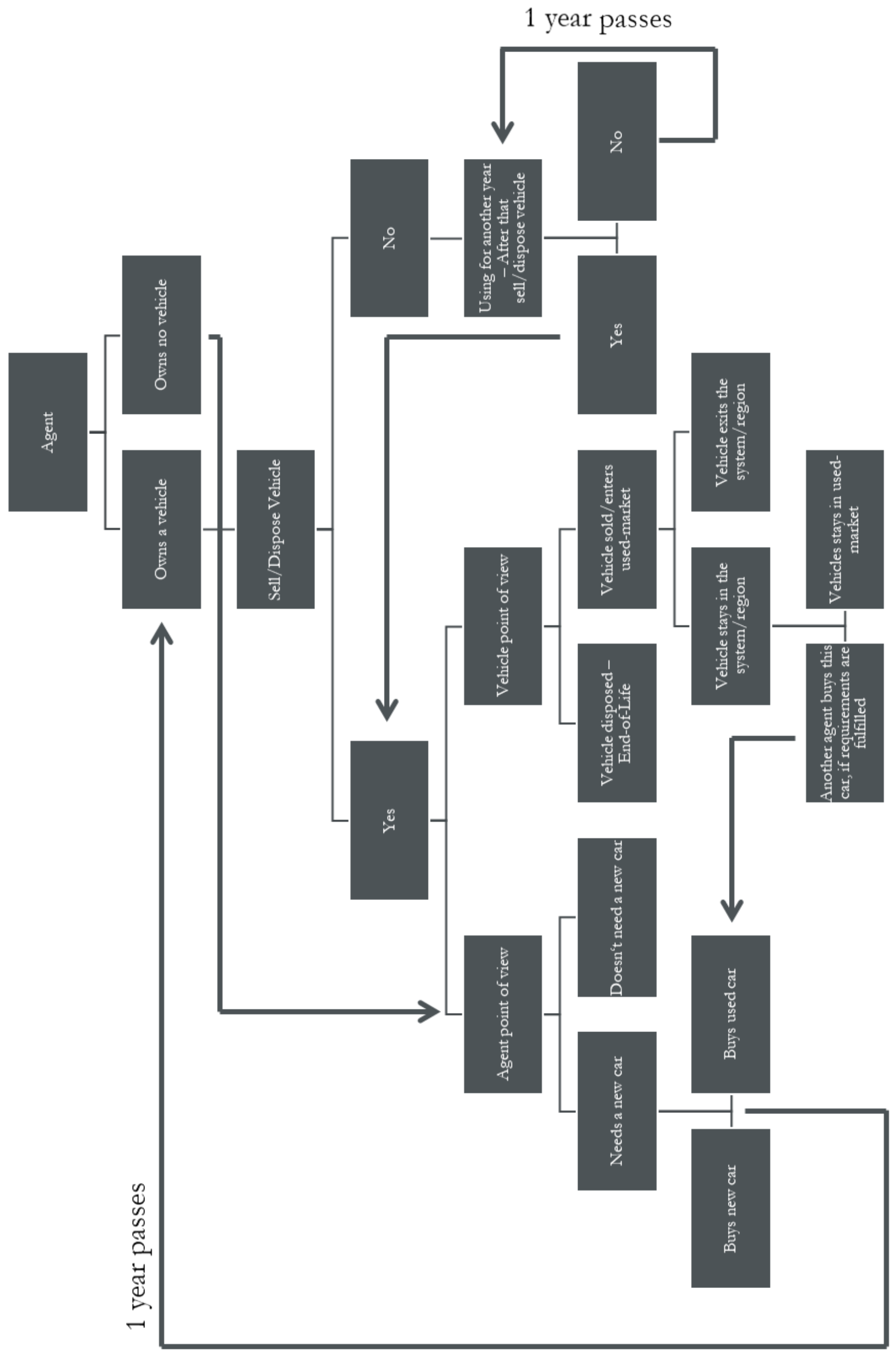

Figure 26: Yearly decision tree of an agent

In the next step, the number of new vehicle registrations is examined. From [Kraftfahrt-Bundesamt 2020], historical data from 2011 up to 2020 are known, as shown in Figure 27. From 2021, the number of new registrations is shown based on the simulation. Overall, it can be seen that the historical data is about 80,000 newly registered passenger cars in Berlin each year. The drop from 2020 onwards can be explained by the pandemic situation. The simulated results are in a similar range with fluctuations from 55000 to 106000 newly registered passenger cars. This is because agents keep younger vehicles with a higher probability and replace older vehicles with a higher probability. This then implies that either younger vehicles or older vehicles predominate in the vehicle portfolio at these points in time.

Overall, it can be seen that the results are within a realistic range and thus a realistic market behavior is sufficiently represented.

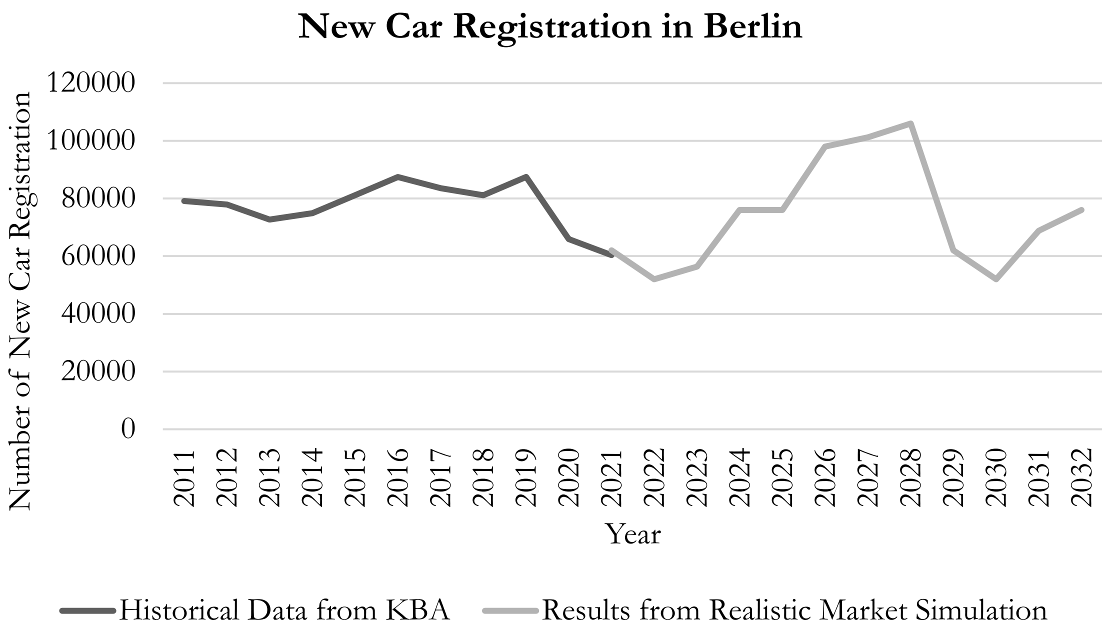

Figure 27: New Car Registration in Berlin based on [Kraftfahrt-Bundesamt 2020]

5.2 Evaluation of the mobility behavior

The results of the mobility simulation in MATSim are saved in a so called events file, that contains all the events that happen during the simulation. These events describe each trip takeoff of the agents. To analyze the event file of MATSim a method is derived with which any event file from the MATSim simulation can be evaluated and translated into trip tables. This enables a modular approach to easily change the considered region and scenario. Each event is then assigned to the corresponding agent. The distances can be calculated with lengths, which are stored in the links in the network.

For the translation of the events, sequences of the considered travel modes need to be defined. In general each travel mode can be analyzed as long as the event sequence is described. In the following the typical MATSim travel modes car, public transport and teleported travel modes are described. For private owned vehicles the event sequences for the agent start with the end of the current activity, for example leaving its home. Then the agent enters his vehicle. In the next event the vehicle enters the corresponding link. While driving, the vehicle leaves the current link and enters the next link until the destination is reached. Another considered travel mode is the public transport. Here the agent ends his current activity and departs from his current location. Then the agent walks to the public transport stop. When arrived, the agent waits for the public transport. Meanwhile the public transport arrives at the stop. The agent interacts with the public transport and enters the vehicle. Afterwards the vehicle departs and drives to the next stop. When the agent reaches his destination, the agent leaves the vehicle and walks to the activity location to perform his activity. Meanwhile the public transport departs for the next stop. If the events of a certain travel mode are not defined, it is possible to model them as teleported travel modes. This is a simplified approach, where the travel mode is mostly defined by its average speed and beeline distance factor, which estimates the actually traveled distances. In the following the event sequence for teleported modes is described. At the beginning the agent ends his current activity, departs and disappears from the network. Then the travel time is estimated with the average speed of the travel mode as well as the distance from the starting location to the destination. As soon as the travel time has been reached, the agent will reappear at his destination and start his activity. These travel modes and further travel modes such as demand responsive transport (DRT) for mobility on demand concepts are described in detail in appendix A.1.

The generated trip tables represent the mobility behavior of the considered region. These trip tables are used as an input for the evaluation of the mobility system. Each agent is analyzed and their mobility behavior is holistically evaluated regarding $CO2_{eq}$ emissions, costs and energy demand. The trip table contains the following data for each agent:

- Agent Id,
- Trip number, distance and time
- Mean velocity
- Transport mode and total waiting time for public transport for the day
- Vehicle Id and type
- Starting location and purpose of trip
- As well as following attributes of the agents:
    - target group, employment status, age, gender, income, homeowner

Calculation of the yearly driven distances of the agents

In MATSim the mobility simulation calculates the daily driven distances of each agent. In [Syré et al. 2020] it is assumed that one MATSim day equals a regular work day and that 0.82 MATSim days equal a weekend day. This value is derived from mobility data. This assumption is also used here to calculate the yearly driven distances for each agent for passenger cars. For all the other travel modes it is assumed that one MATSim day is representative for all days in the week.

$$distance_{year} = distance_{daily} * (5 + 2 * 0.82)\ days * 52\ weeks \qquad \text{(eq. 13)}$$

- $distance_{year}$: Extrapolated yearly driven distance
- $distance_{day}$: Daily driven distance in MATSim

5.3 Critical discussion on the mobility simulation approach

In this work, the goal is to build models with which the mobility system of a given region can be analyzed holistically and new solution approaches can be implemented, analyzed and optimized. For the mobility simulation within the developed method, it is important that the results reach a sufficient quality, are reproducible and that the computation time can be reduced to enable the simulation of many scenarios and optimization.

In this thesis MATSim is used as a tool for the mobility simulation, since it represents the state of the art in mobility simulations and fulfills the stated requirements. The mobility simulation in MATSim is based on statistical data obtained for individual regions or entire countries. Here it is assumed that based on this data representative statements on mobility behavior in the region under consideration can be made. As described in the beginning, the aim of the work is not to realize a 1:1 representation, but to model a realistic representative mobility system of the considered region according to the statistical distributions. With the help of open, statistical data, the population and its mobility behavior can be modeled with sufficient accuracy. By using more detailed simulation approaches such as micro simulations, the overall level of detail can be increased. However, the additional knowledge gained is not commensurate with the huge additional effort required. Furthermore, it is assumed that preferences as well as decision criteria for a travel mode are very similar for nearby regions. For example, if certain data are not available for the Berlin region, these data can be substituted with data for Germany. The region itself can also be modeled sufficiently accurately with, for example, OSM data in MATSim. MATSim enables the modeling of various travel modes as well as their usage. Based on this, comprehensible decisions of the agents can be represented and realistic modal splits can be derived. Subsequently, it becomes possible to make well-founded statements and perform analyses. In addition, the simulations are reproducible by using the same random seed and the computation time can be reduced by for example downsizing the sample size of the considered population. This and further approaches to reduce computation time is discussed in detail in chapter 9. Overall, it can be seen that the requirements are met. Thus it can be said, that with open data realistic scenarios can be created and sufficient and representative statements can be made. In the next step the different travel modes used by the agents need to be designed and evaluated.

6 Transport mode simulation

In this chapter, simulation and evaluation approaches for the different transport modes are described. Since private owned vehicles have a high impact in today's mobility behavior and most policies such as taxes on emissions address private owned mobility, the focus in this work lies on private owned vehicles. Therefore, cars are analyzed with a detailed powertrain simulation. The fundamentals of powertrain design including the simulation approaches, vehicle model, powertrain model, scaling of different components as well as the deriving of forecast data is described in chapter 2.2. Here the powertrain simulation is used to design a vehicle portfolio in dependence of predefined requirement classes. In addition, the key-value based approach and evaluation of further travel modes for a holistic evaluation of the mobility system is shown. In the last step the methodological approach of the assignment of vehicles to each agent is described.

6.1 Design of the vehicle portfolio

As described before, the simulation environment developed by [Weiß 2018] including the methods by [Schneider 2022] are used here as a basis for the powertrain simulation and extended with regard to the objective of this thesis, such as calculating the CO_{2eq} emissions as well as costs, which are described in the next chapters. The mobility simulation indicates the usage of the different mobility forms and their assignment to the individual agents. In the mobility simulation itself, simplified travel mode models are used. For example, the default vehicles are a medium sized 4 seaters. Accordingly, the vehicle proportions are known, which are needed for the travel flow simulation. In order to evaluate the different travel modes in more detail, a post process simulation with the described powertrain simulation framework is performed.

An overriding goal of the holistic method is to enable optimization of the holistic mobility system. Here, the computation time plays a decisive role. An integration of the detailed design and evaluation of the travel modes leads to the fact that the entire chain of simulation methods must be run through when considering different scenarios and thus the computation time increases immensely. Separating the methods into individual modules has the advantage that calculations only have to be performed when changes occur. For example, if the powertrain portfolio is to be optimized for a region under consideration, the mobility behavior can be kept constant in this case, i.e. the mobility simulation only has to be run once, and within the overall methodology only the powertrain simulation is called up. It is also possible to temporarily store results and load them at a suitable point. For example, the powertrain portfolio can be designed and saved so that the powertrain simulation does not need to be called again within the overall methodology. For these reasons, the detailed design and evaluation of the mobility modes within the mobility simulation is not integrated, but deliberately decoupled to allow a modular design and parallelization of the independent calculations in the holistic method approach to reduce computation time. In terms of energy demand, the approach neglects the simulated driving profiles of the vehicles.

In the next step the approach for the design and evaluation of the considered travel modes is described. The powertrain simulation consists of three steps. In the first step the vehicle configuration is read. Values such as production year, vehicle type, powertrain type, and vehicles parameterization are defined here. The complete vehicle parameter list is shown in Table 2. Depending on the configuration, the different powertrain component maps are taken into account and the respective components are scaled. Then the longitudinal dynamics simulation is performed and e.g. the consumptions are calculated. Here it is possible to store the calculated vehicles in a "vehicle portfolio". These calculations can be performed in a pre-process in order to generate and store a vehicle portfolio. The optimizer can then select various vehicles from the vehicle portfolio in the optimization process and assign them to the agents, who use a car as the travel mode, with the aim of optimizing the mobility system regarding the defined target criteria. Here it is assumed that agents who own a vehicle also use their vehicles. Vehicles that are possibly owned but not used are neglected here.

The powertrain simulation incorporates scalable physical models of the different powertrain components. This makes it possible to calculate and evaluate existing vehicles and to design new vehicle concepts. In addition, the technology database from [Schneider 2022] described before, is integrated, with which it is possible to design and analyze future vehicle concepts. To represent a realistic market, 72 vehicles are designed, analyzed and temporarily stored in a vehicle portfolio. The structure of the vehicle portfolio is shown in Figure 28. The vehicle portfolio is divided into the following points:

- Powertrain types: Internal Combustion Engine Vehicle (ICEV), Plug-In Hybrid Electric Vehicle (PHEV), Battery Electric Vehicle (BEV), and Fuel Cell Electric Vehicle (FCEV)
- Vehicle segments: Small (A00 and A0), Compact (A and B), Large (C and D).
- Vehicle types: Flat and SUV
- Requirement classes: Low, Medium and High in terms of electric range, max. speed and acceleration times. A detailed description of the requirement classes can be found in the Appendix A.5.

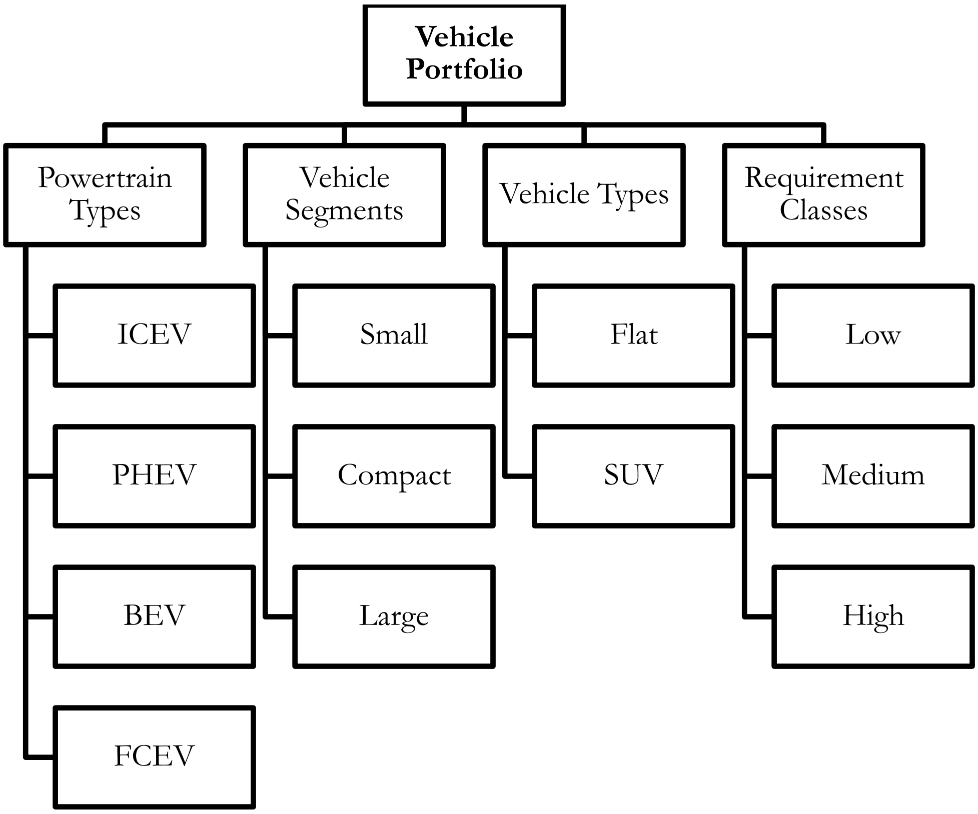

Figure 28: Overview of the vehicle portfolio

With the help of the described portfolio, vehicles are designed for different use cases so that a realistic vehicle fleet can be modeled based on statistical data. This approach leads to a suited compromise between considering the effects of different vehicles in the market and the computational effort during the runtime. Each vehicle is defined by a parameter set. This parameter set is shown in appendix A.6. For an initial parameterization, reference vehicles fitting to the categorized vehicles are researched and assigned. For the compact, flat ICEV a Golf 8 is a representative vehicle. Here the values from the Golf 8 for the shown parameters are researched and assigned to the categorized vehicles. During the simulation, the parameters change in accordance with the requirements and the derived scaled powertrain components fulfilling these requirements. Once the vehicle portfolio is derived, the CO_{2eq} emissions, costs and energy demand in dependence of the considered scenario can be calculated. However, in terms of energy demand, the approach neglects the simulated mobility profiles of the vehicles and uses driving cycles such as the WLTP. This approach is described in detail in the following chapters.

6.1.1 Fit for purpose powertrain components

Once the initial configuration of the vehicles is done, the scaling of the powertrain components starts with regard to defined requirements. For each powertrain type and vehicle segment as well as vehicle type, the following requirements are considered:

- The maximum velocity,
- the maximum electrical velocity of PHEV,
- the acceleration time and
- emission free range

In Appendix A.5, the requirements are described in detail. To fulfill these requirements, the powertrain components are scaled in an iterative process. Here the changing masses of the newly scaled powertrain components are considered in the vehicle model and subsequently in the simulation as well. The system here is overdetermined, leading to the possibility of overreaching certain requirements. For example, the minimal maximum velocity can be overreached to achieve the required maximal acceleration time. While some components are scaled continuously, the battery for example is built from single cells and allows only discrete combinations also regarding the voltage level. Abortion criteria ensure the iteration process to finish in case of oscillations or if no exact matches for the requirement is achieved. For the scaling of the powertrain components to fulfill the requirements, each vehicle in each category needs to be defined. From the configuration it is known what types of powertrain components such as the battery type or e-motor type is used. In the following the rightsizing algorithm for the relevant powertrain components of the considered powertrain types is described.

Battery Electric Vehicle

For battery electric vehicles (BEV) the maximum velocity is achieved through the scaling of the axle transmission ratio, which is calculated with the equation below, whereas a safety factor of 5 km/h is considered to fulfill this requirement. For the e-motor power, the initial parameter settings are used:

$$i_{axle} = \frac{n_{EM}}{\frac{\left(v_{max}+5\frac{km}{h}\right)}{3.6*2*\pi*r_{dyn}}*60} \quad \text{(eq. 14)}$$

- i_{axle}: Axle transmission ratio
- n_{EM}: Maximum revolution speed
- v_{max}: Maximum velocity
- r_{dyn}: Dynamic wheel radius

Once the maximum velocity with newly scaled axle transmission ratio and the initial e-motor power is reached, the e-motor power is scaled to achieve the required acceleration time. This is an iterative process, in which the e-motor is scaled until the requirements are fulfilled. The battery power then needs to be scaled as well to provide the needed e-motor power. The range is achieved through battery capacity. This is also an iterative process. In case of all wheel drive (AWD) the rear e-motor, which is considered to be the main e-motor in this simulation, is adjusted to achieve the required maximum velocity coming from continuous power. The front e-motor is adjusted to achieve the acceleration time.

Fuel Cell Electric Vehicle

For the e-drive of the fuel cell electric vehicles (FCEV) the same approach as for BEVs is used. The maximum velocity is achieved through the axle transmission ratio, which is calculated with equation 14. For the e-motor power the initial parameter settings are used again. The acceleration time is achieved through the power of the e-motor in an iterative process. After fulfilling these requirements, the electric source system consisting of the fuel cell, DCDC converter as well as the battery needs to be adapted in dependence of the newly scaled e-motor. Here the following equations are used to scale the fuel cell system, whereas a safety factor of 2 kW is considered to fulfill this requirement:

$$P_{FC} = P_{EM,continuous} \quad \text{(eq. 15)}$$

$$P_{DCDC} = P_{FC} + 2\ kW \quad \text{(eq. 16)}$$

$$P_{BATT} = \frac{P_{EM,mech}}{\eta} + 2\ kW - P_{FC} \quad \text{(eq. 17)}$$

- P_{FC}: Power of fuel cell
- $P_{EM,continuous}$: Continuous power of e-motor
- $P_{EM,mech}$: Power of e-motor
- P_{DCDC}: Power of DCDC converter
- P_{BATT}: Power of battery
- η: Battery efficiency

The required range is achieved through quantity of hydrogen, which is scaled in an iterative process. In case of AWD the rear e-motor, which is considered here the main e-motor, is adjusted to achieve the required maximum velocity coming from continuous power. The front e-motor is adjusted to achieve the acceleration time. For the battery power the adjusted equation 18 is used, considering the two e-motors:

$$P_{BATT} = \frac{P_{EM,mech,1}+P_{EM,mech,2}}{\eta} + 2\ kW - P_{FC} \quad \text{(eq. 18)}$$

- $P_{EM,mech,1}$: Power of e-motor 1
- $P_{EM,mech,2}$: Power of e-motor 2

Plug-In Hybrid Electric Vehicle

The scaling algorithm for plug-in hybrid electric vehicles (PHEV) is described in the following. The axle transmission ratio is assumed to be constant and defined by the initial parameterization. The maximum velocity is achieved through the engine power in an iterative scaling process. The maximum electrical velocity is achieved through the e-motor in an iterative scaling process. With the engine defined from the maximum velocity, the acceleration time will also be achieved through the power of the e-motor in an iterative scaling process. This makes the system overdetermined and may cause one of the requirements to be exceeded. The emission free, electric range is achieved through the battery capacity in an iterative scaling process. In case of an AWD, a mechanic AWD is assumed and that the powertrain components are scaled the same as for a one-wheel drive. The power in the front axle is then defined by the engine power. The power in the rear axle is defined by the e-motor.

Internal Combustion Engine Vehicle

For internal combustion engine vehicles (ICEV) the scaling algorithm is described in the following. It is assumed that the axle transmission ratio is constant and defined by the initial parameterization. The maximum velocity is achieved through the engine power in an iterative scaling process. The acceleration time is achieved through the power of the combustion engine as well. This makes the system overdetermined and may cause one of the requirements to be exceeded. Same as for the PHEV in case of an AWD it is assumed that the same process as for one wheel drive can be applied, whereby the power of the combustion engine is split on both axles.

6.1.2 Charging behavior

One characteristic feature of a PHEV is the possibility to drive purely electrically as well as purely with an internal combustion engine. Thus, the operating strategy of the PHEV has a major influence on the results. Due to the lower CO_{2eq} emissions in production compared to the BEV and the theoretically possible low emissions in the use phase due to electric operation, there are theoretical CO_{2eq} advantages for a PHEV. Therefore, it is particularly important here to define the recharging behavior precisely and to map it as realistically as possible. In this method, a distinction is made between optimal PHEV operation and realistic PHEV operation. In the optimal PHEV operation, the consumption values determined in the WLTP cycle are used. In the realistic PHEV operation, the procedure is as follows. Every agent with an electric vehicle is assigned a random SOC (state of charge) for the day. The distribution of the SOC is shown in Figure 29. It is assumed that the focus of the distribution is at 50% SOC. Depending on the assigned SOC, the daily driven distances as well as the consumption of the vehicle the actual electric driven distances and subsequently the realistic combined consumption of the PHEV can be calculated. This approach can be further enhanced but is sufficient in the context of this work.

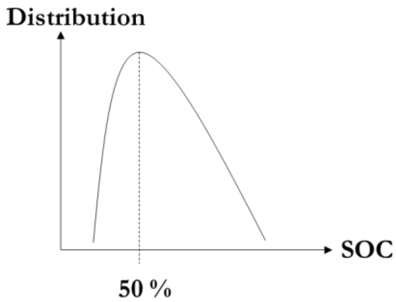

Figure 29: Distribution of average SOC

6.2 Evaluation of further travel modes

For the evaluation of further travel modes such as public transport, bicycles, walking or micro mobility, key-value based models are implemented. These models contain data regarding the maximum velocity, range, number of seats, trunk volume, CO_{2eq} emissions in the production phase as well as use phase, costs per person kilometer and month, investment costs needed for the additional infrastructure and the energy demand. These attributes are presented in Table 2. The required key-values are determined by means of a literature search. Subsequently the total CO_{2eq} emissions, costs as well as energy demand in dependence of the considered scenario can be calculated. In Appendix A.4 the values for the considered additional travel modes are shown.

Table 2: Attributes of further travel modes

Attributes	**Unit**
Max. Velocity	km/h
Range (electric / fossil)	km
Number of seats	-
Trunk volume	l
CO_{2eq} emissions in the production phase	kgCO_{2eq}
CO_{2eq} emissions in the use phase	kgCO_{2eq}
CO_{2eq} emissions in total	kgCO_{2eq}
Costs (per month and pkm)	€/month and €/pkm
Total costs	€
Investment costs for development of pt, charging infrastructure, …	€/component
Energy demand (electric / fossil)	kWh/km

6.3 Initial assignment of vehicles to agents

The initial assignment of vehicles is based on statistical data and the attributes of the agents such as income. In the first step the base scenario is built deploying statistical data, accessed for example from the KBA (Kraftfahrtbundesamt) in the case of Germany [Kraftfahrt-Bundesamt 2022]. For the assignment of specific vehicles, the following assumptions are made. If the agent is driving a car, the agent is assigned a SUV, if the share of SUVs is not exceeded and the income of the agent is higher than 40.000 € per year. Otherwise, the agent is assigned a compact class vehicle, if the share of compact class vehicles is not exceeded and the income of the agents is higher than 20.000 € per year. If none of this is applicable the agent is assigned a small vehicle. This approach leads to a distribution of vehicles best fitting the statistical data and agent attributes. The decision tree of assigning vehicles is shown in Figure 30.

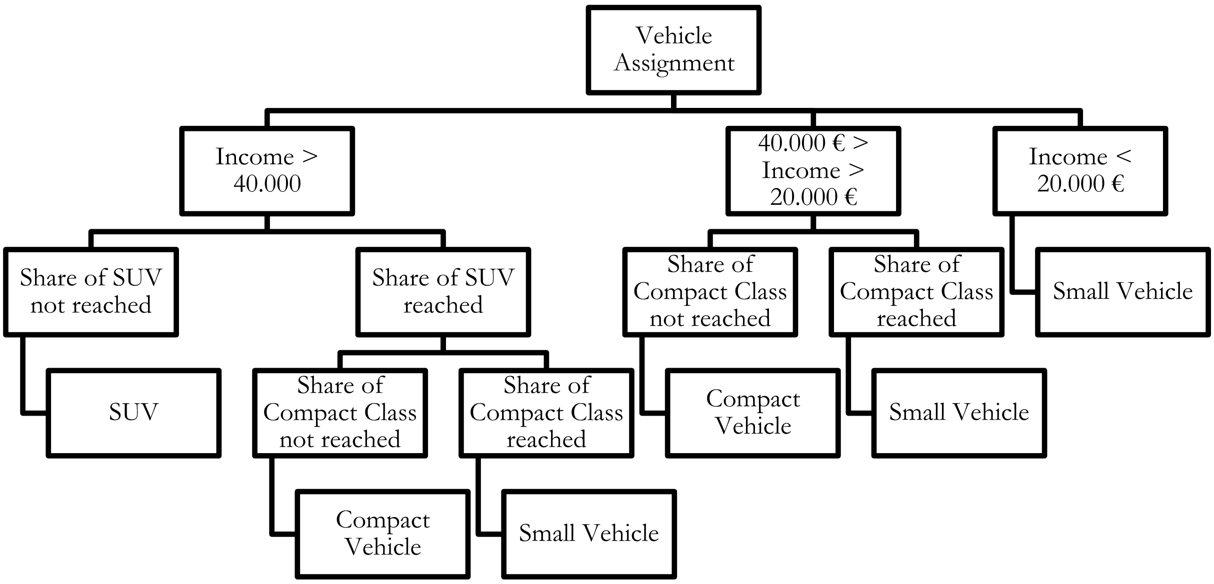

Figure 30: Decision tree of assigning vehicle types

For the optimization it is assumed that the agents most likely take a similar vehicle they had in the base scenario with the changes coming from the optimizer such as a new powertrain. For example, the powertrain portfolio is optimized. Agent 1 is driving a SUV ICEV, which fulfills the requirements of the high requirement class in the base scenario. In the new scenario this agent is assigned a similar vehicle with a different and more CO_{2eq}-, cost- or energy-efficient powertrain. Here the vehicles with the lowest emissions, costs or energy demand are picked from the pre-calculated vehicle portfolio which also fits this agent. In this example it could be a SUV BEV, which fulfills the requirements of the high requirement class and is then assigned to the agent. Alternatively, it is also possible to manually define the share of powertrain types in the powertrain portfolio of the region and to analyze defined scenarios. In the next step the mobility system needs to be evaluated regarding ecological and economic criteria, which is described in the following chapters 7 and 8.

6.4 Analysis of the energy demand

Energy demand for mobility is an important target variable in the mobility system when it comes to optimization. Since renewable energies will not be available in abundance in the foreseeable future, it is important to use them as efficiently as possible and to minimize the energy demand holistically. Therefore, the energy demand for mobility is examined and described in more detail below.

The required energy demand for mobility is calculated using the determined driven distance from the mobility simulation as well as the determined consumptions of the different travel modes of each agent. The focus in this work lies on the energy demand for mobility. The energy demand is presented in kWh, where e.g. fossil fuel consumptions in liter are included and converted into kWh to achieve comparability. For electricity generation, losses during transport and charging are also taken into account. In the following formula the calculation of the total energy demand is shown:

$$E_{mobility} = \sum_{i=1}^{N_{agents}} \sum_{j=1}^{N_{trips,i}} consumption_{i,j} * distance_{i,j} \qquad \text{(eq. 19)}$$

- $E_{mobility}$: Total energy demand for the mobility of people
- N_{agents}: Number of considered agents
- $N_{trips,i}$: Number of trips of considered agents
- $consumption_{i,j}$: Consumption of the used transport mode including losses in kWh/km
- $distance_{i,j}$: Driven distance of considered agents with the used transport mode

The consumption is solely calculated in dependence of the used vehicle and powertrain type. However, the resulting emissions depend on the used energy carriers. The following energy carriers are considered in this work:

- Gasoline and eGasoline produced with renewable energy
- Diesel and eDiesel produced with renewable energy
- CNG and eCNG produced with renewable energy
- Biofuels
- Hydrogen and eHydrogen produced with renewable energy
- Electricity mixes for different regions such as Germany

In the next step the analysis of the CO_{2eq} emissions with the help of the derived enhanced LCA approach is described.

7 Enhanced LCA

In chapter 2.3 the fundamentals as well the differentiation between attributional and consequential LCA is shown. Based on that, in this chapter the suitability of the standardized LCA is investigated regarding the holistic methodological approach. Subsequently, requirements for the LCA are derived. Here it is shown that the standard approach is not suitable. To fill the gaps, in the next step, an enhanced LCA is developed and described.

7.1 Requirements for the LCA

LCA based on ISO 14040/14044 [ISO 14044 2006] is a standardized method, that gives clear guidelines to calculate the environmental impact of very different products or processes. This ensures for example the comparability and the evaluation of improvement measures. However, when it comes to dynamically developing systems, or virtual evaluation of a possible, and therefore uncertain future, LCA is limited. The ISO-based LCA assumes that all premises and assumptions are made at the beginning and remain constant throughout the life of the product under study. However, some input parameters may change over time, such as the electricity mix. One possible approach to model these changes may be to take the average value over the lifetime. This leads to average impacts over the lifetime and the actual impacts in each year cannot be represented. Therefore, dynamic input parameters that can change over time are needed to represent the impacts in each year. In addition, in the LCA based on ISO, the system boundary including the system products must be defined at the beginning. Therefore, the analyzed system and product must be known and defined at the beginning. However, in complex mobility systems, the system-relevant components such as vehicles or infrastructure can change over time, and so can the energy required. This makes it difficult to evaluate future vehicle and mobility concepts, new measures such as vehicle-to-grid (V2G) as well as different scenarios by standardized LCA. Therefore, a dynamic system boundary approach is required for the assessment of the dynamic behavior in mobility systems. Furthermore, random events can occur in mobility systems based on random factors as well as decisions of individual agents which subsequently influence each other. In addition to that, as described in chapter 5, a realistic market behavior is included in which individual agents can change their vehicles each year and therefore generate new emissions. The occurrence of this event is based on a probability function including a random factor. However, for a LCA based on ISO, the analysis must be comprehensible and reproducible.

The first step is to investigate what scope the standardized ISO according to 14040 offers to meet these requirements. In [Consequential-LCA 2015] it is described which methodological freedom in the ISO 14040 exists to perform new approaches within a LCA. Here, it is considered whether the Consequential LCA (CLCA) is compatible with the ISO 14040 collection. In [Consequential-LCA 2015], it is mentioned that requirements for a CLCA are already described, even if it is not clearly separated from an Attributional LCA (ALCA). The ISO 14040 series is part of the general ISO 14000 series, that includes a commitment to continuous improvement as a basic requirement. This also applies to ISO 14040 and is also clear from the introduction to ISO 14040:2006, which states improvement in all listed applications of LCA. It points out, that LCA should help to identify opportunities to improve the environmental performance of products at different points in their life cycle and inform decision makers, e.g. for the purpose of strategic planning in terms of priority setting, product or process design or redesign, selection of relevant environmental performance indicators, or marketing [ISO 14044 2006]. It is also mentioned that decisions in a LCA should preferably be based on natural science. Allocation should be avoided in LCA and scientific principles such as mass balances should generally be used. In addition, it is described that the Life Cycle Inventory is based on material balances between input and output. Allocation procedures should therefore approximate such input-output relationships [ISO 14044 2006]. This is a clear indication that consistent modeling is the only way to keep mass and other balances intact during inventory calculation [Consequential LCA 2015]. In addition, ISO 14040 includes a reference to ISO 14049, which describes a very precise description of a CLCA. In summary, the ISO 14040 series supports a CLCA.

From this consideration of the CLCA it can be concluded that further, scientifically based enhancements of the LCA are possible. It was mentioned at the beginning that a holistic mobility system should be evaluated regarding sustainability criteria and that this system should also be optimized concerning these criteria. Therefore, in the following, an enhanced LCA approach is described, which is tailored to the problem in this work. The following requirements are placed on the method to be able to evaluate mobility systems with regard to $CO2_{eq}$ emissions:

- The method should be based on the ISO 14040/14044, more specifically on the CLCA, to make it possible to analyze a dynamic system behavior with time-dependent variables, which need to be added to the CLCA approach. In addition to the direct emissions, the indirect effects should also be taken into account here.
- Furthermore, this approach should be backwards compatible and can be used to perform a standardized LCA according to the ISO mentioned above by deactivating the dynamic part of the method.
- The LCA should be comprehensible and reproducible.
- It should be a modular approach to be able to map as many scenarios as possible and thus also enable optimization of the holistic system.

- This method needs to be integrated in the holistic approach and the LCA needs to be part of the optimization loop.
- It should be possible to make predictions to also design and analyze future mobility systems. Here a database needs to be built and integrated in the process to fulfill this requirement.
- The focus in this work with respect to sustainability lies on $CO2_{eq}$ emissions but should be extendable to any other parameter.

7.2 Methodological approach

The aim of the extended method is to allow the estimation of the overall and time wise $CO2_{eq}$ emissions in diverse and dynamic systems. More precise, this approach enables the consideration and evaluation of the mobility behavior of the considered region as well as future vehicles and mobility concepts and new measures such as smart charging including forecasts regarding $CO2_{eq}$ emissions. In order to be able to integrate the LCA approach into the holistic evaluation and optimization of mobility systems, a simplified approach is needed without too many compromises in the results quality. Therefore, suitable approaches are analyzed in the following, whereby a key-value based approach including a $CO2_{eq}$ database turns out to be suitable. In addition, the key-value based approach can be built modularly, analogue to the holistic approach, so that key-values for each life cycle stage of each emission source can be derived. This enables the possibility to model any number of scenarios and thus optimize mobility systems.

The derived LCA approach is based on the CLCA according to ISO 14040/14044, which enables the analysis of a dynamic system behavior as described in the mobility simulation. Furthermore, with this approach implemented, it is possible to analyze the system for a given time frame at discrete time points, whereas time-dependent variables are included. By keeping the variables constant and disable dynamic changes in the mobility system it is possible to perform a standardized LCA according to the ISO, making this approach backwards compatible. In order to reconcile the randomness of the mobility simulation, which makes it possible to generate and investigate entirely new scenarios, with the comprehensibility and reproducibility of the LCA, the randomness is defined by a random seed, which allows to comprehend and reproduce the scenarios. To enable the key-value based approach, dynamic time-dependent variables and also derived predictions of future emissions, a $CO2_{eq}$-database is built. This database is based on the work in [Schneider 2022] and [Can 2019]. For all relevant components of the mobility system, key-values are determined through literature research as well as proprietary LCA models in GaBi. These key-values are then stored in a database. The $CO2_{eq}$ database including the prediction methods is described in the following. Additionally, the different possibilities of the calculation of $CO2_{eq}$ emissions are examined and compared in this chapter.

7.2.1 Key-value based LCA approach

In this chapter two approaches to perform a LCA are analyzed. One approach is the detailed LCA approach and the second approach is the key-value based LCA approach. Building a detailed LCA model requires a high effort due to the need of data for the input / output modelling of the considered system. Modeling entire mobility systems strictly on this level is especially difficult since all transport modes, energy paths and infrastructure elements in combination with a dynamic system behavior need to be considered. As described in the literature review, entire mobility systems are often modeled using pre-built processes, e.g. one process for manufacturing a BEV, where these are then scaled by their market volume. To differ between vehicles, the processes can be scaled by their weight. These datasets often use older vehicles as a reference, where the products and processes are well known. The advantage of using detailed processes in LCA software is that a holistic analysis regarding environment criteria can be carried out.

However, the goal of this thesis is to derive a method to optimize holistic mobility systems in terms of economic and ecological criteria. Since detailed LCA models are data and computation time intense, they do not enable optimization. Therefore, the evaluation approach must be simplified to be able to perform optimizations. Another challenge is to get all data at a similar level of quality and detail. In this work, a key-value based approach is chosen instead of the detailed LCA approach that enables the possibility to carry out investigations on component level and to calculate overall CO_{2eq} emissions for different transport modes and vehicle models. The advantages of a key-value based approach are the following:

- Key-value based approaches are simplified approaches. This leads to lower computation times, which enables the integration of the LCA in the optimization loop of holistic mobility systems.
- It is possible to analyze any number of scenarios with different variations such as the impact of different powertrain components on the mobility system.
- The key-values are determined by a literature search and stored in a database. These key-values are often derived from detailed and well understood LCA models. In addition, it is easy to add new data and thus new components of the mobility system as well as other new or proprietary data sources.
- It is possible to make predictions based on statistical data and the usage of regression models. Here a database is built and integrated into the process.
- Missing data can be derived by many means such as literature research, expert knowledge or proprietary LCA models.
- Assumptions and results as well as how the two are related to each other are easier to understand.

But there are also disadvantages of a key-value based approach that need to be noted here:

- In order to simplify the approach and handle the effort of researching key-values and building a sufficient database, the focus is set on a limited set of indicators such as CO_{2eq} emissions. It is assumed though, that the CO_{2eq} emissions are a good first indicator for the optimization of mobility systems regarding ecological criteria.
- Inaccuracies can occur due to the assumption of linear scaling of the key-values.

In the following, the quality of the results is examined using the example of a Volkswagen ID.3. Here, the calculated values with the derived key-value approach are compared with the results from [Volkswagen AG 2021]. The 2020 ID.3 model with 150 kW and a 62 kWh battery capacity is considered. A lifetime mileage of 200.000 km is assumed. Figure 31 shows the CO_{2eq} emissions for the production, use phase and total emissions. It is noticeable that the calculated emissions are smaller overall. This is mainly due to the fact that the emissions in the production phase are calculated in more detail in the report. Processes are taken into account in detail that are not considered in this work, such as the maintenance of individual components or the emissions of many small parts. For the use phase, the electricity mix from the GaBi software, a commercial available LCA software, is chosen. The emissions of this electricity mix amounts to 420 gCO_{2eq}/kWh and is used as a key-value for the use-phase. In the report, a consumption of 15.85 kWh/100km is given. In this case a consumption of 16.4 kWh/100km is calculated with the presented powertrain simulation using maps. As a result, the emissions in the use phase are higher in the simulation.

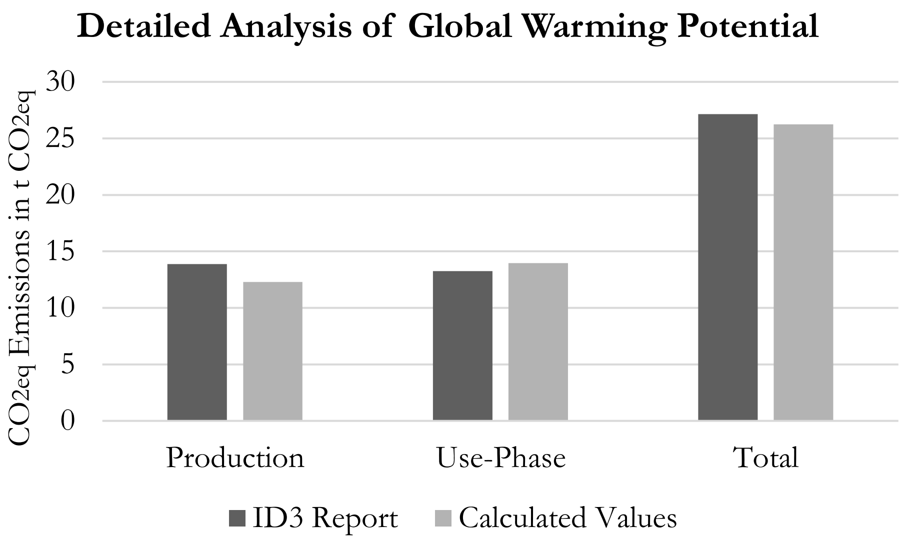

Figure 31: Detailed analysis of global warming potential of the ID.3

The production emissions are examined in detail in Figure 32. This shows that the emissions of the main components, e-motor and battery, almost equal the emissions from the report. However, differences arise when looking at the body and the rest of the vehicle. Here, the calculated emissions are lower than the emissions reported [Volkswagen AG 2021]. This is mainly due to the fact that the rest of the vehicle is considered in more detail in the report. In addition to the body, many small parts are taken into account, which are neglected in this work.

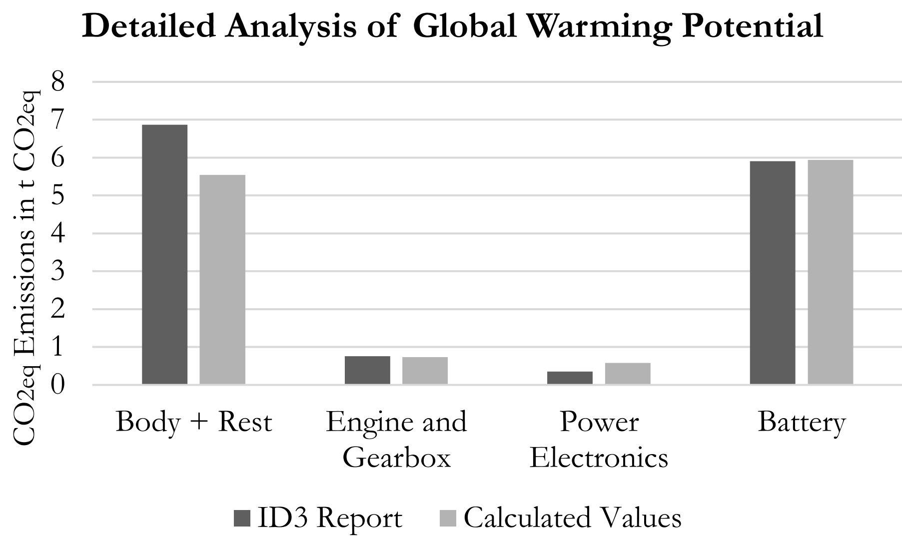

Figure 32: Detailed analysis of global warming potential of the ID.3 of the production phase

Overall, a very good quality of results can be achieved with the key-value based approach. Despite the known disadvantages the key-value approach is the right decision in order to fulfill the requirements in objective of this thesis. Especially because in the optimization generic vehicles are designed that represent a market average. The considered key-values are described in the following chapters.

7.2.2 Modularity

In the standardized LCA, the life cycle inventory data is needed for each product for each scenario. Therefore, each alternative scenario needs to be modeled including all the needed processes for the LCA, which leads to a high effort. Instead of modeling all alternatives, it is more efficient to first calculate the LCA results of the individual life cycle stages of a product. The individual life cycle stages can be combined to model and calculate the corresponding scenario. Within the scope of this thesis, a modular CLCA approach is developed to evaluate the dynamic system behavior of a mobility system. To meet the requirements of the goal of this thesis, further adaptations and extensions have to be carried out. Analyzing different scenarios of the mobility system in an automated process leads to the necessity of a modular approach. Due to the complexity of mobility systems with many variables, such as used travel modes, agent behavior, energy chains or infrastructure, the considered modules for the individual emission carriers have to be simplified.

Therefore, the described key-value based approach is considered in this work. I.e. instead of modeling processes for individual modules, these are calculated using CO_{2eq} key-values. This allows to save a lot of computational time, to predict future emissions, to integrate the LCA into the overall methodology and thus to take it into account during the optimization. In addition, forecasts can be derived using the collected key-values. By using individual key-values for the respective life cycle phases of the individual products, the input and output variables as well as the associated system boundaries are clearly defined. In combination with the CLCA approach, allocation is avoided and it can be ensured that there is no double counting of CO_{2eq} emissions. With this approach, emissions are tracked at the point where they occur. A modular CLCA approach with key-values for the modules of each life cycle of each emission source of the mobility system considerably reduces the effort in comparing different scenarios with different improvement measures implemented in the mobility system. In Figure 33 the modular approach to create any number of scenarios is shown. A scenario describes a complete configuration of the mobility system. Here the optimizer can change parameters and add modules within the mobility system to create new scenarios. For example, it is possible to further develop the public transport or change the powertrain portfolio of the considered region.

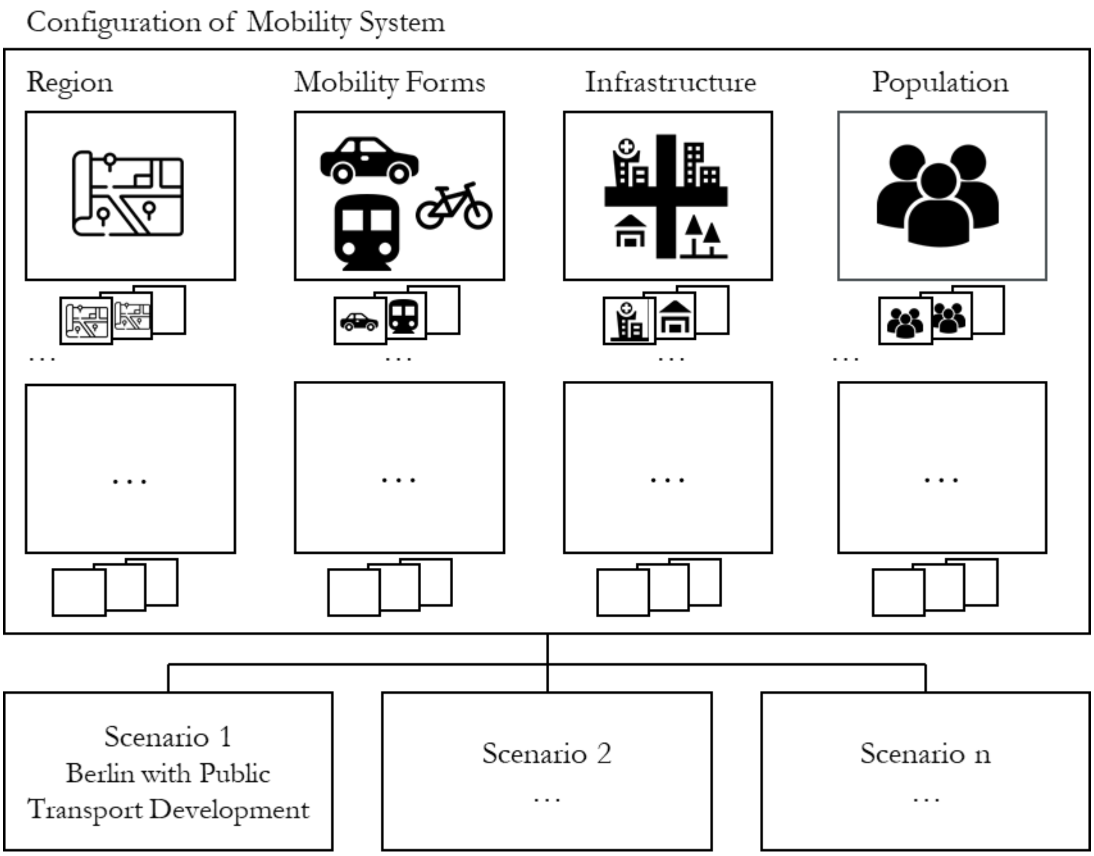

Figure 33: Modular LCA approach

7.2.3 Database for CO_{2eq} key-values

For the chosen LCA approach, key-values for the CO_{2eq} emissions of all emission sources of the mobility system are required. For this purpose, a database is being set up based on the insights in [Schneider 2022] and [Can 2019]. Here the same structure of the database and methodological forecasts approaches are implemented. These are described in the next chapters. To ensure a good quality of results, a large focus is placed on data procurement, preparation as well as derivation of forecasts.

This database is filled with values and insights of publicly available studies, which perform a LCA on the different emission sources of the mobility systems. Additionally, data coming from surveys with experts as well as self-generated key-values with the GaBi LCA software are added into the database. The key-values are presented as a function of the functional unit. For example, the key-value for a battery system per cell chemistry is presented in the form of gram CO_{2eq} per kWh.

The database is subdivided into the categories of cars, other forms of mobility, energy sources and infrastructure. For passenger cars, a further distinction is made between the various powertrain components and the body. For the other forms of mobility, CO_{2eq} values are determined for the production and use phases as a whole and are not analyzed in detail. Here, a distinction is made between public transport, more precisely bus, as well as rail, bicycle and micro mobility. For the energy sources, the electricity mix of the respective regions, the different fossil energy sources as well as hydrogen from different production processes are considered. These include the production emissions as well as the emissions of fossil energy including biofuels sources that occur in the use phase (W2W). In the area of infrastructure, the production emissions of various charging stations as well as hydrogen and gas stations, PV and stationary storage are mapped. In the context of this work, the impact of small parts in cars is neglected. For the necessary road infrastructure it is assumed that this already exists and does not have to be produced, so there are no emissions here either. The structure of the database is shown in Figure 34. The database can modularly be extended with new data as well as new technologies and mobility concepts. For the extension, key-values need to be derived and added in the database. This enables a simple analysis of the impact of new technologies and concepts on the mobility system. In Appendix A.7 the CO_{2eq}-database and all its subcomponents are listed in detail. In addition, the necessary input variables for the calculation of the CO_{2eq} emissions for each emission source of the mobility system are shown in Table 28 in Appendix A.7.

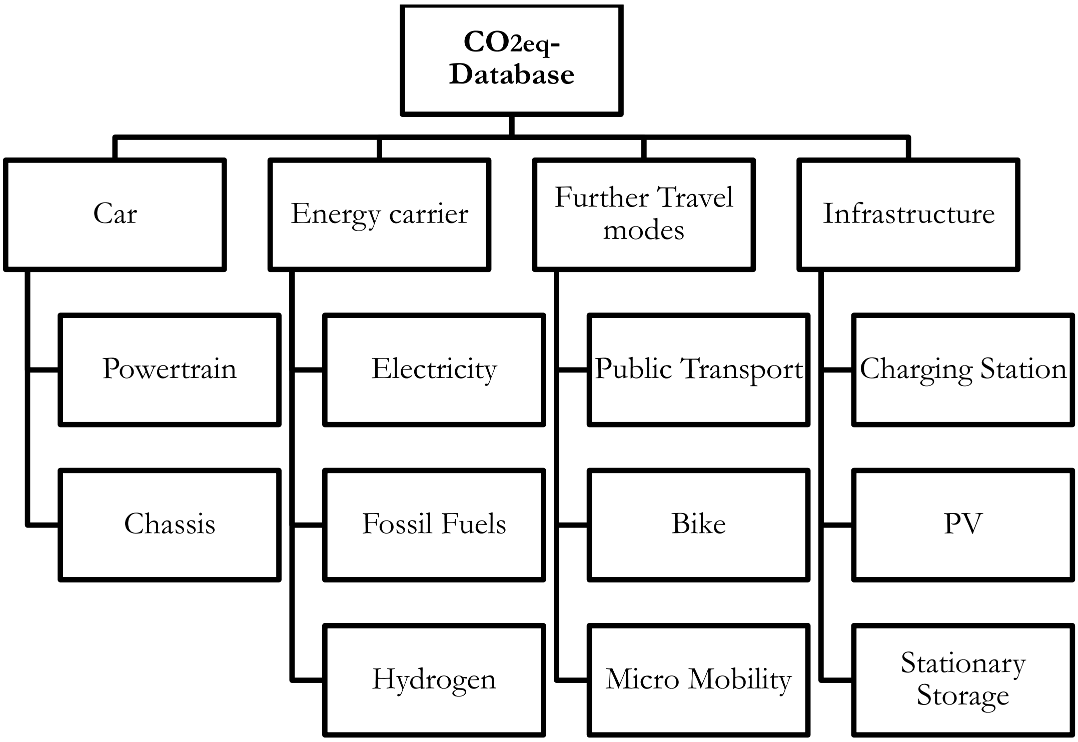

Figure 34: Structure of the CO_{2eq} database

In the following chapters the approach to derive forecasts based on literature research is described. Here, the combination of predictions is explained. Subsequently, meta-analysis is presented as a method for the combination of researched forecasts data. In the next step the identification and evaluation of the forecast data is presented. This includes the research procedure as well as the data analysis. At the end of the chapter results of the research and data analysis are presented. Here data fusion methods are compared, evaluated and suitable methods are then selected.

7.2.4 Forecasts based on literature research

In the context of this work, the goal is to identify, evaluate and then combine forecasts on the defined set of key-values based on literature research. Therefore, findings on predictions based on secondary research are presented below in the form of a combination of predictions and statistical data. The combination of data corresponds to an averaging of independent predictions, e.g. based on different data sources or prediction methods. In this case, the simple average is usually chosen due to reproducibility [Armstrong 2001]. Predictions are affected by a variety of influencing factors. By combining the predictions and data, the error due to wrong assumptions, inappropriate methods or faulty data can be reduced. In [Armstrong 2001], these issues are considered in more detail. It is shown that for 30 studies, on average, a 12.5% lower mean absolute error is achieved compared to the best standalone prediction method. Additionally, in [Lawrence et al. 2006], the combination of different sources of information is cited as a justification for the error reduction. In particular, combining expert opinions with statistical methods provides better results than relying on a single source. On the one hand, expert opinions are complementary information that cannot be modeled, and on the other hand, statistical methods help to identify systematic errors or biases in expert opinions by providing purely objective predictions based on data [Lawrence et al. 2006].

For the increase of the prediction quality the following rules are recommended by [Armstrong 2001]. The data should be as independent of each other as possible. This can be achieved with data from different prediction methods and a different database. This data should also include already combined forecasts, which lead to more accurate forecasts compared to single forecasts. Filtering out outliers improves the prediction accuracy [Armstrong 2001]. Combining predictions is particularly advised if there is uncertainty about the accuracy of the individual methods. In addition, the combining approach is suitable for predictions over long periods of time, because as time increases, the prediction error increases and so does the deviation between prediction methods [Armstrong 2001].

In order to make the resulting prediction data more accurate, a weighting of the data can be carried out. One possible criterion for weighting the predictions is the actuality, allowing to favor new insights. It is recommended to limit prediction data to recent data to avoid errors from older data. However, if only a few predictions are available for a certain time period, it is recommended to include older data in order to be able to perform a combination of predictions. Therefore, a compromise is usually sought between the most recent data possible and a sufficient number of data [Brown 1991]. Due to the exponentially increasing number of scientific publications over the years, a systematic search procedure for finding suitable predictions is required. Therefore, efficient search strategies are required to find as many sources as possible on the searched topic. This has the advantage that the number of sources and thus the number of data increases and inconsistencies in the individual studies can be detected more easily [Ressing et al. 2009].

In the following chapters the methodological approach is described in detail. In the first step, a search strategy is developed to locate a comprehensive and appropriate selection of scientific publications on the topic sought. The search strategy is described by a search string specifying the database and search engine used. The next step is to establish inclusion criteria to filter out unsuitable sources. Once the sources are available, the data are uniformly recorded according to an extraction template. In this process, forecast data are identified according to a uniform measure. In addition to the forecast data, source information and the method used to determine the forecast are documented [Randolph 2009]. The data are then analyzed and compared.

For the representation of the results bubble charts are used [Can 2019]. Figure 35 shows an example of a bubble chart, being able to catch the exact values as well as often used confidence intervals. This confidence interval can also be used as a criterion for weighting the forecast data. The larger the confidence interval, the higher the uncertainty of the available forecast and the lower the influence in the combined mean. The weighting is represented by the size of the bubbles [Randolph 2009]. For the bubble charts used in this thesis, the individual forecast values of a source are represented uniformly by bubbles of different colors.

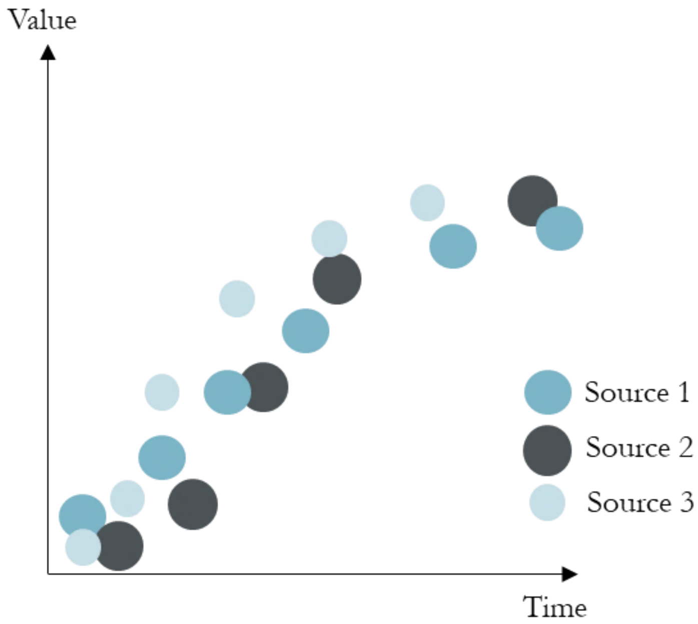

Figure 35: Bubble diagram as a form of representation of the determined forecasts based on [Nykvist et al. 2015]

7.2.5 Determination and evaluation of forecast data

This chapter describes the applied determination and evaluation of the forecast data according to [Hennings 2017]. First, the search procedure for determining the forecast data is described. The search procedure includes the search process and the data collection. In the search procedure, the search string is explained. During data acquisition, the extraction template used is described first, followed by the method used to compare the data, and finally the plausibility check of the forecast data. In the next step, the evaluation of the forecast data for a subsequent weighting of the data is described. For this purpose, a point system with evaluation criteria is extended. Finally, exemplary results of the search are shown in the form of bubble charts.

Search process

The goal of the search is to determine a large number of suitable sources for the sought topic as efficiently as possible. To achieve this goal, a search string is used to narrow down the search area. Here, the search string is composed of three aspects: time, methodology, and application [Hennings 2017]. With the time aspect, the given time range of the predictions in the sources is described. In this context, qualitative search terms such as "future" are used in addition to exact years, such as from 2020 to 2050. The methodology aspect restricts to sources where the methods of prediction are used, such as extrapolation.

The application aspect narrows the search scope, such as sources that deal with LCA in the field of vehicle technology in this case. Figure 36 shows the three aspects with their respective search terms.

English search terms are used to identify as many sources as possible, as German sources usually use English keywords as well. The individual search terms are linked by the OR operators. With the AND operators the three aspects are linked and bundled to a search string. In addition, the AND NOT operator is used to filter out sources that deal with topics that are not relevant to the search. In this way, all sources are covered by the search string that have at least one term from each of the three aspects and do not include a term from the exclusion criteria [McDowall et al. 2006].

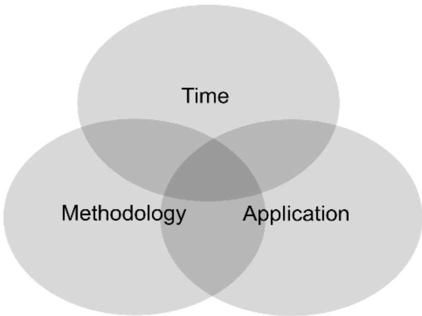

Time
Goal: Limitation to the future development
Terms: tomorrow OR future OR „short term" OR "long term" OR 202? OR 203? OR 204? OR 205?

Methodology
Goal: Restriction to methods of predictions
Terms: perspective OR perspectives OR roadmap* OR scenario OR scenarios OR generation OR outlook OR forecast* OR projection OR projections OR trend OR trends OR prospect OR prospects OR "time series"

Application
Goal: Restriction to mobility applications and LCA
Terms: mobility system OR vehicle OR vehicles OR car OR cars OR public transport OR bike OR micromobility OR powertrain OR powertrains OR HEV OR BEV OR EV OR PHEV OR FCEV OR zEV OR REEV OR "fuel cell" OR "Plug-in Hybrid" AND (LCA OR CO2 emission)

Exclusion Criteria
Goal: Filtering out future, but not relevant topics
Terms: automated OR connected OR control OR autonomous OR "energy management"

Figure 36: Structure of the search string based on [Hennings 2017]

The next step is to use the search string in a search engine. One possible search engine is, for example, the Hannover Technical Information Library (www.tib.eu), which supports the logical operators in the search string. The terms of the search string are matched with the title, abstract and listed keywords of the sources during the search. Other possible search engines are Google Scholar or Google itself.

Data acquisition

Data collection is based on an extraction template following [McDowall 2006]. The following information is manually extracted from the sources considered [Hennings 2017]:

- Title
- Date of publication
- Client / Author
- Number of citations (data from Google Scholar)
- Publishing journal with h5 index (data from Google Scholar).
- Country of origin
- Description of the prediction method used
- Indication of maturity level (research or production status)
- Consideration of uncertainty, value ranges or scenarios

In addition to these details, the following supplementary characteristics or framework conditions are also recorded, which is used to determine the prediction [Hennings 2017]:

- Technological implementation (for example, lithium-ion or lithium-air battery).
- Assumed number of units / market shares
- Scenario (pessimistic, realistic, optimistic).
- System limits (for example, are ancillary components of the component also considered)
- Component dimensioning (for example, power rating, battery capacity)
- Powertrain topology
- Unit and reference year (for costs, the reference year is considered to account for inflation).

A separate column is created for each of these specifications and characteristics. Then, the respective data for the forecast under consideration is entered into these columns. This has the advantage that the data can be filtered and thus better compared for subsequent analysis. Table 3 shows an example of a section of such an extraction table. Here, for example, the data can be filtered by title, year of publication, author or technological implementation.

Table 3: Example of the extraction table

Title	Publication Year	Client / Author	Technological implementation
Source 1	2018	Author 1	Li-Ion Battery
Source 1	2018	Author 1	Fuel Cell System (SOFC)
Source 2	2017	Author 2	Cryotank

The respective forecast values are only included if the associated forecast years have also been specified. In case the forecast values are given in value ranges, the mean values are entered. To ensure comparability of the values, the values are stored in the form of gCO_{2eq} per functional unit. For example, the functional unit for a battery is kWh. The costs are converted into US dollars at the given reference year. The averaged conversion rates for the respective year are used for the conversion [Federal Reserve Bank of St. Louis 2022]. In addition, an inflationary adjustment is also taken into account. Here, costs are converted to 2021 using the "Implicit Price Deflator for gross Domestic Product." This value is a factor proportional to gross domestic product (GDP). If no reference year is provided, the publication year can be used as the reference year [Environmental Protection Agency 2016]. Table 4 shows an example of an extract of the conversion factors for the last ten years. The use of the extraction template and conversion of units ensures reproducibility as well as comparability of the forecast data.

Table 4: Excerpt from Inflation Adjustment Conversion Factor Table, Source: [Federal Reserve Bank of St. Louis 2022]

Year	2014	2015	2016	2017	2018	2019	2020	2021
Implicit Price Deflator for GDP	100.00	105.15	106.72	108.82	110.65	112.98	114.44	121.14
Factor for conversion to $2021	1.211	1.152	1.135	1.113	1.095	1.072	1.059	1.000

Current LCA data and costs are used to check the plausibility of the forecast data. When comparing the forecast data with current LCA data, statements can be made via the difference in values as to whether the forecast values are too optimistic or too pessimistic. Further comparative values are provided by government targets. Governments define target values for certain properties of emission limits, for example, to meet climate protection goals. By comparing the target values with the forecast data, it can be determined whether the government targets represent a suitable upper limit for certain emissions of the respective components. In addition to the two plausibility data mentioned above, technological upper limits can be used. A technological upper limit is a natural (physical or chemical) limit that cannot be exceeded, such as the Carnot efficiency in the internal combustion engine. The plausibility check of the forecast data ensures that strong outliers and incorrect forecast data are not considered [Can 2019].

Weighting criteria

For the evaluation and weighting of the sources, criteria must first be defined. The actuality of the source and the evaluation of the prediction method used in the source are suitable for this purpose. The actuality of the source can be determined based on the publication date. Due to the lower number of historical data, the prediction accuracy decreases with increasing age of the source. The higher the prediction accuracy of a source, the narrower the confidence interval. Figure 37 shows an example of the influence of actuality on prediction accuracy and confidence interval.

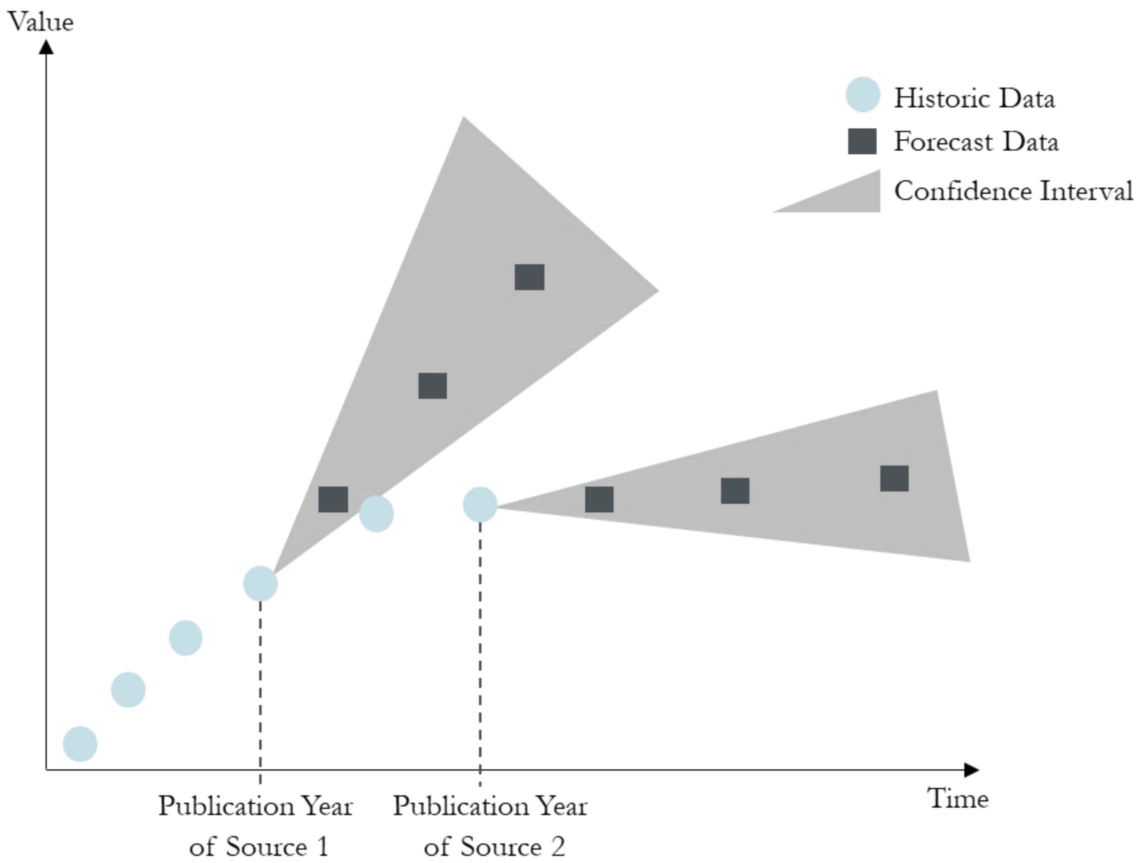

Figure 37: Influence of source actuality on prediction accuracy and confidence interval based on [Hennings 2017]

The evaluation of actuality is based on a linear system. With a linear evaluation, a compromise is made between as much data as possible and the sole focus on current sources [Can 2019]. A degressive evaluation has the disadvantage that the focus would be too much on the most current sources and thus the amount of data is reduced. In linear scoring, sources from 2022 are given ten points and sources from 2013 are given one point. As the year increases, the number of points increases. Sources from the last ten years are considered. The mathematical relationship for calculating the evaluation points of timeliness is presented in the following formula. In it, b_{akt} is the evaluation point of the actuality and x_{ver} is the publication year of the source:

$$b_{akt} = x_{ver} - 2012 \quad \text{(eq. 20)}$$

Another weighting criteria is the evaluation of the used forecast method in the sources. These are evaluated based on the procedure for determining the forecast values. In addition to the description of the forecast method used, it is examined whether different methods have been combined or compared with each other. The use, respectively the comparison of different methods, leads to a larger amount of data and thus to a higher prediction accuracy. As already described in [Armstrong 2001], the combination of predictions has a positive influence on the prediction accuracy.

In [Hennings 2017] a five-point system is developed to evaluate the forecasting method, which is used here as well. However, the evaluation holds some uncertainty, because often the methodological procedure for determining the forecast values is not documented in literature. This occurs especially with forecasts from consulting firms. The consulting firms work with OEMs and suppliers and accordingly use data from these firms. For reasons of confidentiality, these data are not released, but only the forecasts derived from them are published. In addition, the procedure for determining the forecast represents the expertise of the consulting firms, which is also not released. Nevertheless, this forecast data is important, because it incorporates technical know-how from the companies as well as concrete technological roadmaps. In order to continue to consider these types of sources, they are given a three-point rating and are used as a reference for other sources. Sources that perform a combination of multiple prediction methods are awarded an additional point. Furthermore, one point is awarded if a critical review of the own results is performed, and the own results are compared with external results. Sources that only conduct a literature search on forecast data and do not extend the forecasts with their own determined forecasts will have one point deducted. Additionally, one point is deducted if no external comparison of results is performed. This evaluation scheme results in a small evaluation difference between the forecasts. However, this approach has the advantage that the important forecast values of the consulting firms are evaluated neutrally and forecasts with a comprehensive or insufficient approach are highlighted [Hennings 2017]. Table 5 shows the evaluation scheme for the criterion of the forecast method used.

Table 5: Evaluation scheme for the criterion of the prediction method used based on [Hennings 2017]

Points	**1**	**2**	**3**	**4**	**5**
Applied Forecast Method	No independent prediction method **AND** No external reconciliation of results	No independent prediction methodology **OR** No external reconciliation of results	Reference methodology evaluation (sources from consulting firms)	Combination of several forecasting methods **OR** External reconciliation of the results	Combination of several forecasting methods **AND** External reconciliation of the results

Weighting of the forecast data

The weighting of the forecast data is done with the help of the two evaluation criteria mentioned above. For better comparability between the criteria, the evaluation scheme of the forecast method used is normalized to a ten-point system. The weighting represents the ratio of the sum of the evaluation points of a source to all considered sources. The number of considered sources varies depending on the filtering of the data. The mathematical relationship of the weighting is shown in the following formula [Can 2019]:

$$w_i = \frac{a_i + b_i}{\sum_{j=1}^{n} a_j + \sum_{j=1}^{n} b_j} \quad \text{(eq. 21)}$$

In it, w_i is the weighting factor of source i, a_i is the weighting value of the timeliness of source i, and b_i is the weighting value of the forecast method used for source i. In addition to determining the weighting, weighted averages of all forecasts for the respective year under consideration are also formed. Here, forecast data from the years 2010 to 2050 are considered, and the results are presented in a five-year cycle (2010, 2015, 2020, ...). In case no forecast data is available for these points in time, the values are interpolated if the forecast horizon extends beyond the respective points in time. For example, if forecast data is available for 2018 and 2022, the value for 2020 is interpolated. The weighted average is formed from the ratio of the weighted forecast data to the sum of the weights of all forecast data. The weighted averages help to make the forecast data more plausible, as the progression is shown. The forecasts consider the technological performance of various components, so declining trajectories are implausible except for the cost and emission data. In this way, implausible forecast data can be determined. However, no technology leaps can be represented here, such as a strong improvement with the help of a new technology. These new technologies are considered separately and represent a new component. With the help of the following formula and Table 6, the calculation of the weighted mean values is illustrated by means of an example:

$$\bar{y}_{2020} = \frac{w_A * y_{A,2020} + w_B * y_{B,2020}}{w_A + w_B} = \frac{\frac{11}{45} * 180 + \frac{15}{45} * 200}{\frac{11}{45} + \frac{15}{45}} \approx 192 \quad \text{(eq. 22)}$$

In this, $\bar{y}_{2020}$ is the weighted average for the year 2020, $w_{A/B}$ is the weighting factor of source A/B, and $y_{A/B}$ is the forecast value of source A/B.

Table 6: Example values for the calculation of weighted averages

	Actua-lity	Forecast Method	Weighting	Source	Component	2015	2020	2025
	5	6	11/45	A	Battery	160	180	205
	7	8	15/45	B	Battery	180	200	210
	10	9	19/45	C	Battery	170		
Sum	22	23	1	**Weighted Average Value**		171	192	208

Presentation of the forecast data

In this chapter, exemplary results of the research are presented. In total, the forecast database contains over 100 sources with associated data series for the emission sources of the mobility system. The bubble chart form is chosen as the presentation format. Here, the emissions are shown over the forecasted years. The data series of a source is represented by a color. The size of the bubbles is determined by the weighting factors. In contrast to the individual data series, the weighted averages are highlighted by bubbles with a black border. Figure 38 shows the degression of production emissions of the lithium-ion battery with a NMC cell chemistry over the years. The data represents expected values without using optimistic or pessimistic assumptions at the system level. In addition, it is clear that predominantly current and historical data is used, as no forecasts are derived in the area of LCA. In the next step a trend curve needs to be derived. The determination of this trend curve is described in the following chapters.

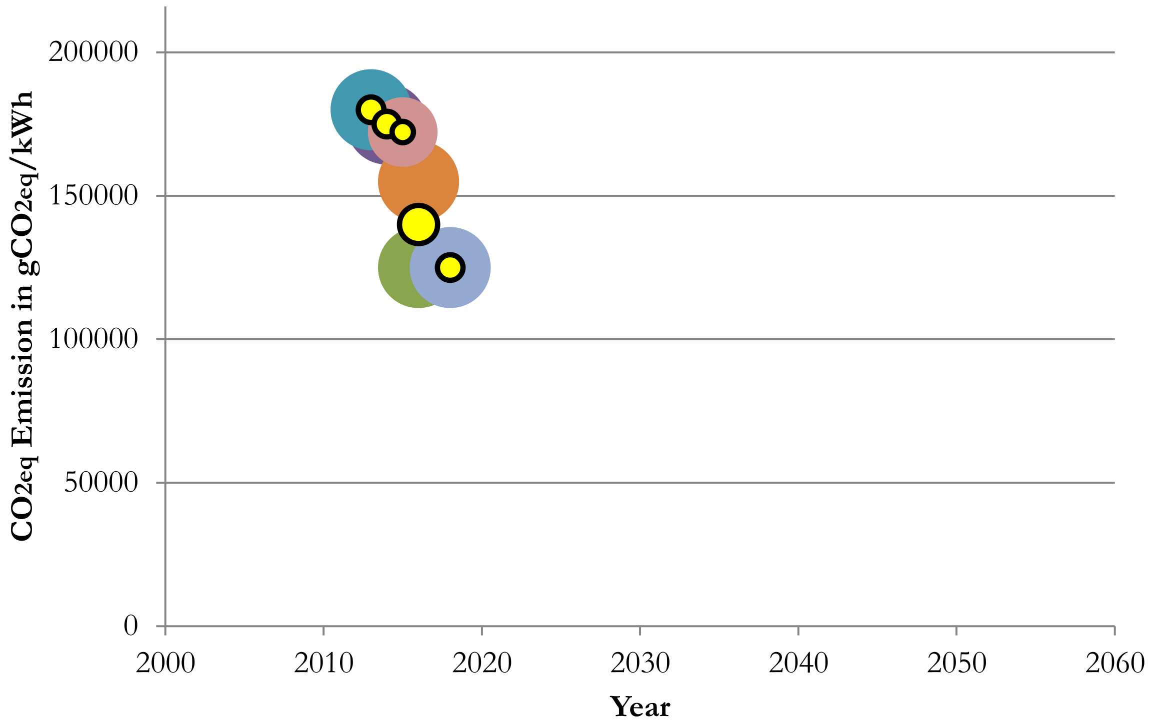

Figure 38: Example results of the research for the lithium-ion battery (NMC)

The cost database is set up in an analogous manner, and in chapter 8 the costs key-values and forecasts are discussed in more detail.

7.2.6 Analysis of suitable methods for data fusion

Since the future course of CO_{2eq} emissions is unknown, various types of curves are analyzed below. Typical curve types for the derivation of trend curves are "growth curves", "learning curves" and "polynomial regression". Therefore, in this chapter, these three curve approaches are examined for suitability for determining trend curves of the CO_{2eq} emission forecast data. Evaluation criteria are established for this purpose. Based on these criteria, the curve approaches are compared with each other. Once suitable methods for the CO_{2eq} emissions are found, the curve fitting to the forecast data is described. In the next step, the methods are compared and evaluated so that a selection can be made afterwards. For the evaluation of the curve approaches, the following criteria are considered based on [Can 2019]:

- Minimization of error squares: the curve must be as close as possible to the collected data. Here the CO_{2eq} emissions for the production of the lithium-ion battery are exemplary analyzed.
- Course of the curve: the CO_{2eq} emissions represent a special case. In order to reduce the impact of climate change the goal should be to reduce the emissions in the future, as described in different policies and statements of OEMs. Therefore, the course of the curve needs to decrease over the forecast years.

The mathematical description of the curve fitting to the forecast data for the three curve approaches growth curves, learning curves and polynomial regression is developed in [Can 2019] and described in appendix A.8.

7.2.7 Selection of suitable methods for data fusion

In this chapter, the three curve approaches are examined regarding the evaluation criteria and compared with each other. Suitable methods are then selected.

Analysis of the minimization of the error squares

In the case of the fitting quality of the curve, the sum of the squares of errors is considered. Table 7 shows the mean square error of the three curve approaches for the consideration of the CO_{2eq} production emissions of lithium-ion battery with a NMC cell chemistry. Due to the analytical determination of the coefficients, the polynomial regression shows low errors. Regarding the CO_{2eq} emissions, the polynomial regression has the lowest error. The growth curve has low fitting quality when considering CO_{2eq} emissions. The quality of the learning curve is suitable for the CO_{2eq} emissions. Based on these values, it can be stated here that growth curves are unsuitable when considering CO_{2eq} emissions. This is also obvious, since the goal is that emissions decrease. However, this must always be checked for plausibility as there may be cases in the future where CO_{2eq} emissions rise again. For example, in the case of energy shortage, where fossil fuels need to be used.

Due to the analytical determination of the coefficients and variation of the degree of the polynomial, curves can be fitted well to the forecast data using polynomial regression. However, the danger of overfitting i.e. an overfitting of the curve to the forecast data must be considered. This results in the curve corresponding too closely to a particular data set. Accordingly, further data sets may not be well represented, and future observations may not be reliably predicted [Leinweber 2007].

Table 7: Fitting quality of the different curve approaches

	Polynomial Regression	Growth Curve	Learning Curve
Mean Square Error regarding CO_{2eq} Production Emissions of lithium-ion battery with a NMC cell chemistry	**80.8**	407.2	396.9

Figure 39 shows the CO2eq emissions of the lithium-ion battery with NMC chemistry at the system level including the three curve fitting approaches. Here it is clear that the polynomial regression and learning curves run closest to the data. This is also reflected in the good fitting quality. In contrast, the growth curve is steadily increasing and therefore it does not match the data well. The best fitting curve coming from the polynomial regression is a linear curve. This would mean, that the emission decrease to zero and below in a short amount of time, which is not realistic. The learning curve shows the expected degression of the CO2eq emissions over the years.

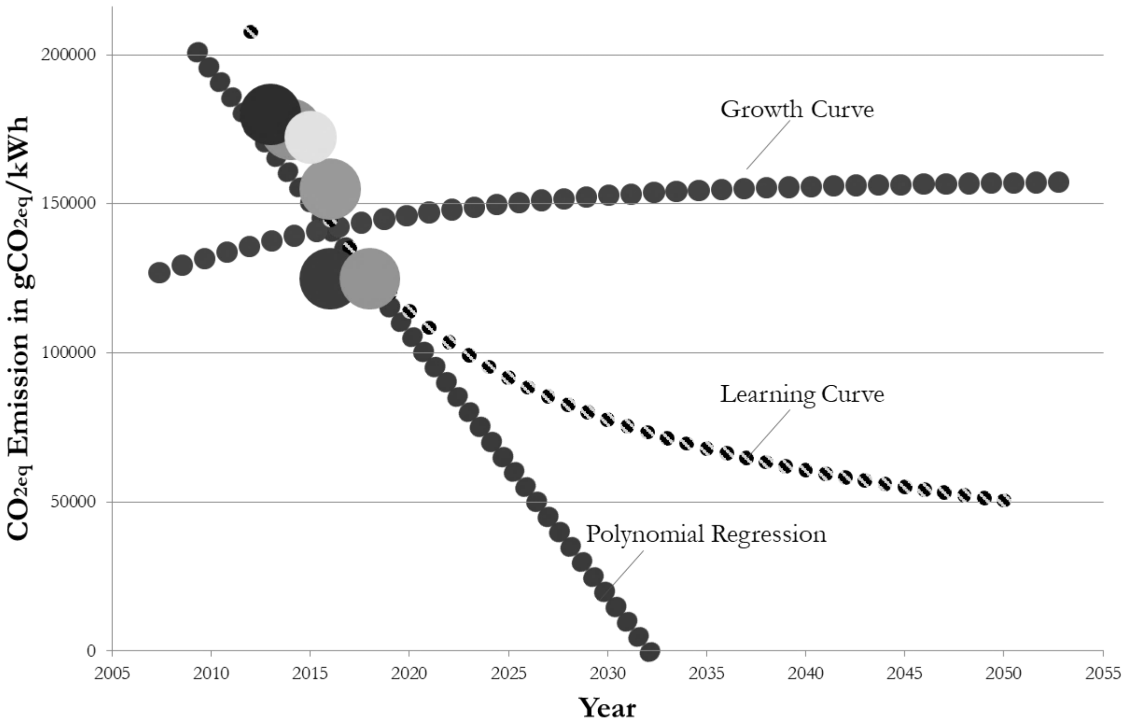

Figure 39: Curve approaches when considering lithium-ion battery CO2eq emissions at the system level

Selection of suitable methods

In addition to the quality, the curves course must also be taken into account. In polynomial regression, the curve is fitted as closely as possible to the forecast data. However, if the forecast data is too spread out, the curve may fall off or oscillation at a higher degree of polynomial can occur. In polynomial regression, no limit value is defined, so that the curve theoretically rises or falls steadily. The growth curve has a continuously rising course instead. In addition, a limit value is implemented for the growth curve.

The course of the $CO2_{eq}$ emissions represents a special case. The goal is to reduce the $CO2_{eq}$ emissions of a component over the years. This course is also reflected in the forecast data. Therefore, a decreasing course of the curve is necessary for the consideration of the $CO2_{eq}$ emissions. Here the growth curves with their constantly rising course are unsuitable. The polynomial regression can be adapted to the forecast data in such a way that it has a decreasing course. However, it can happen that the curve becomes negative or rises again. The learning curves represent the course of $CO2_{eq}$ emissions very well. In case of the $CO2_{eq}$ emissions it should be noted here that most of the data comes from current LCA and that there are not many forecast data available. This can lead to errors due to missing data. The analysis of the existing data shows that the learning curve seems to be the most suitable approach to derive the trend curves of $CO2_{eq}$ emissions. This also makes sense since economies of scale can be used analogously to costs and the goal is to reduce $CO2_{eq}$ emissions.

Given the summary of the curve approaches in Table 8, the following can be stated. The polynomial regression exhibits low errors, which are reflected in the good fit of the curve to the forecast data. However, no limit values are considered. This has the consequence that the curve can rise or fall arbitrarily and results in negative emissions, for example, which should not be possible, since technology evolutions are considered in the forecast and not revolutions. In addition, in polynomial regression, the curve parameters are calculated on a mathematical level. Other influencing factors are not included in the calculation of the curve parameters. This eliminates the learning effects over the years. For these reasons, polynomial regression is unsuitable as a trend curve for forecast data. The growth curve has low errors for technological properties such as gravimetric energy density as shown in [Can 2019]. In contrast, the curve approach is unsuitable for $CO2_{eq}$ emissions, due to the steady rising of the curve.

The learning curve has low errors when considering $CO2_{eq}$ emissions. The course of the learning curve corresponds to the expected course of the $CO2_{eq}$ emissions over the years. The goal of the companies and policy makers is to reduce the $CO2_{eq}$ emissions to be competitive and reduce the impact of climate change. This downward progression is very well represented by the learning curve. In addition, various influencing factors in the form of scale and non-scale effects are also taken into account in the learning curves. For these reasons, the learning curve is used as a trend curve for the consideration of $CO2_{eq}$ emissions in the context of this work. This shows that the goal of zero $CO2_{eq}$ emissions can only be achieved with the support of negative emission technologies.

Table 8: Summary of the evaluation of the curve approaches

	Polynomial Regression	**Growth Curve**	**Learning Curve**
	$CO2_{eq}$ emissions	$CO2_{eq}$ emissions	$CO2_{eq}$ emissions
Minimization of the error squares	++	-	+
Course of the curve	-	-	++

++ : very well suitable

+ : well suitable

- : unsuitable

7.3 Investigation of the different ways of calculating $CO2_{eq}$ emissions

With the help of the derived approach, there are different possibilities to calculate the $CO2_{eq}$ emissions of the mobility system. In the following, four cases are described and compared to show the influence of the different approaches on the resulting total emissions. In the first case, the standardized LCA is considered when calculating the $CO2_{eq}$ emissions. Here, a static system is evaluated, where the boundary conditions and the scenario are defined at the beginning and kept constant. This means, that the initial configuration of the mobility system including the mobility behavior and used transport modes of the agents do not change over time. Additionally, $CO2_{eq}$ key-values, such as the electricity mix or emissions for the production of components are defined for the initial year and remain constant. In the second case, compared to the first case, time-dependent variables, such as a changing electricity mix, are introduced. Here for example the $CO2_{eq}$ key-values for the electricity mix change over the years according to the derived predictions. In the third case, the derived enhanced LCA is applied. This includes the time-dependent variables as well as a dynamic system behavior, in which agents can change their vehicles or travel mode. Furthermore, the realistic market behavior is considered. In the fourth case, an additional condition to the enhanced LCA is introduced, that existing components of the mobility system do not generate production emissions because they have already been produced in the past.

The region under consideration is the Berlin scenario derived in Chapter 5. The network, the infrastructure and a synthetic population including plans are therefore available here. The mobility behavior is determined with the help of the mobility simulation. With the approach presented in Chapter 6 for evaluating the used travel modes, the next step is to evaluate the mobility system concerning CO_{2eq} emissions. Here, the four cases are configured and calculated. In addition to the four cases, two scenarios are calculated. In the first scenario the actual state of the mobility system is modeled based on statistical data. This is the reference scenario and compared to the second scenario, which is a 100% BEV scenario. For all four cases the calculated driven distances in MATSim are used. For the electricity mix the German electricity mix is considered. The starting year is 2021. A period of 14 years is considered. The reason is that in standardized and public studies on LCAs of vehicles, a typical mileage of 200,000 km as well as 15,000 km per year is given, which results in the 13-14 years.

The results are shown in Figure 40. Here it can be seen that the calculated emissions for the two scenarios vary depending on the way CO_{2eq} emissions are calculated. In case one, the standardized LCA is applied. A static consideration of the system leads to no further production emissions over the considered time frame since no changes occur and all production emissions occur at the beginning of the calculation. The impact of the use-phase increases with the progression of the considered time frame. Therefore, here the use-phase has a higher impact overall. This can also be seen in the results. In scenario one, the highest CO_{2eq} emissions are calculated. This is due to the fact, that in the current state of the mobility system mainly ICEVs are used in the private owned sector. Since the use-phase has a high impact, this leads to overall high emissions. In scenario two the CO_{2eq} emissions are 32% lower compared to scenario one, since only BEVs are deployed here. BEVs are overall more energy efficient and with the considered German electricity mix the impact is lower. In case two, time-dependent variables are applied. Here the used CO_{2eq} key-values change over time. Comparing the results of case one and two, it can be seen that time-dependent variables have only a small influence with regard to the overall system. This is especially evident in the second scenario. Due to the steadily decreasing emissions in the electricity mix, the emissions in the use-phase also decrease slightly in 100% BEV scenario. In scenario one the changes are negligible.

The calculation of CO_{2eq} emissions with the developed enhanced LCA approach in case three has a much larger impact. The dynamic consideration of the mobility behavior as well as the change of vehicles results in overall higher CO_{2eq} emissions in the first and second scenario. The consideration of the vehicle change in the enhanced LCA approach also leads to the fact, that new vehicles must be produced and thus further production emissions are considered in the course of time. This gives the production phase of the vehicles a higher weighting and has a greater influence on the result. This leads to much higher production emissions in the second scenario, where only BEVs are deployed, which have higher production emissions compared to other powertrains such as ICEVs or PHEVs.

In the fourth case, emissions decrease compared to the enhanced LCA approach in case three. This is because the emissions of the components of the mobility system that have already been produced are not taken into account. The approach on how $CO2_{eq}$ emissions are calculated has a large impact, when it comes to optimizing mobility systems. One example can be the optimization of the powertrain portfolio. The impact on the optimization is discussed in more detail in chapter 9. Here it can be summarized that the developed enhanced LCA approach offers the possibility to calculate $CO2_{eq}$ emissions in different ways, whereas more realistic emissions of future mobility systems can be analyzed and evaluated.

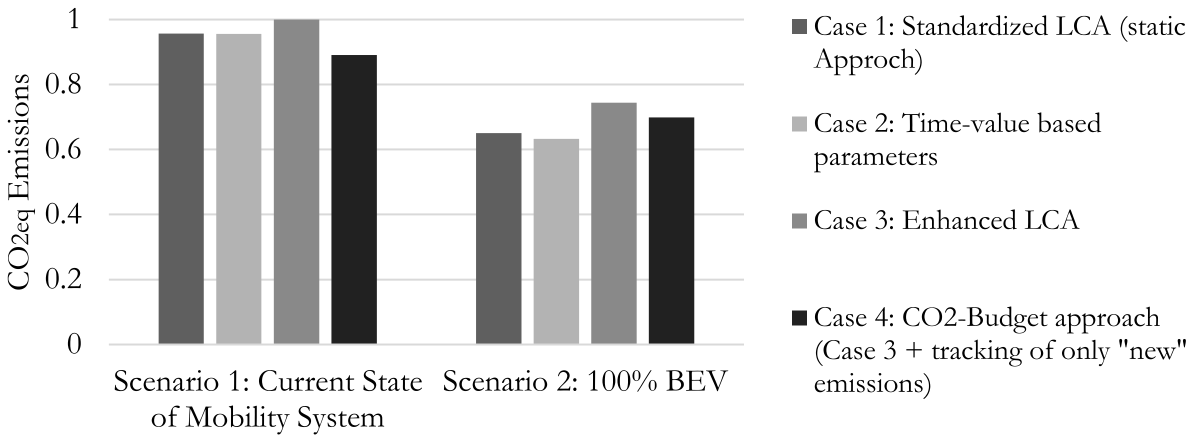

Figure 40: $CO2_{eq}$ emission for the four cases and two scenarios

8 Cost analysis

The costs in perspective of this work are differentiated between the costs for mobility from the customer's point of view and investment costs such as the development of the infrastructure or public transport, as shown in Figure 41. In this thesis the focus lies on the cost from the customer's point of view and is described in detail. The cost parameters, required for all developed models, are collected and treated with the described database and forecast approach based on [Schneider 2022] and [Can 2019]. In the following, the individual cost models are described.

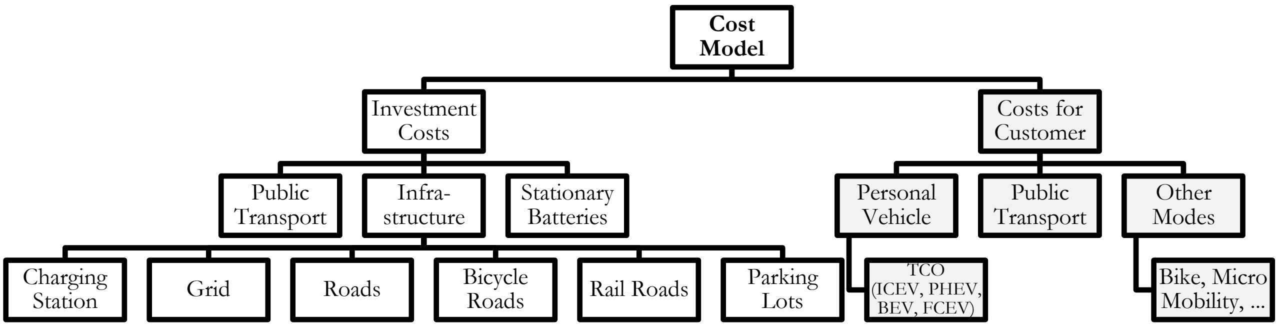

Figure 41: Structure of cost database

8.1 TCO model for private owned vehicle

A TCO model based on [Propfe 2016] is implemented to estimate the total costs of ownership for passenger cars. Figure 42 shows the cost structure. The total costs result from the operating costs and the loss in value that occurs over the years. The operating costs result from costs for the maintenance of the vehicle, vehicle taxes, insurance, subsidies as well as the costs for the energy sources depending on the consumption. The value loss represents the difference between the list price and the resale value. The resale value depends on the list price, the vehicle type, the powertrain type and the mileage driven. The list price is derived from the manufacturing costs, which can be calculated with the help of the powertrain simulation, the profit margin, which is added on, the value-added tax and a factor for premium vehicles. The TCO per month as well as per km can be calculated depending on the usage time and the resulting annual mileage of each agent. However, an uncertainty arises when using cost parameters, such as the maintenance costs in € per km, which are determined for a fixed annual mileage. In this case, it is an average value of different driving profiles reaching from 1.000 to 60.000 km [Propfe 2016]. Varying mileage can lead to distorting the calculated maintenance costs. Therefore, in this work, for each agent when calculating the TCO a usage time of 5 years with 15.000 km driven distances per year are assumed to achieve consistency and comparability. Once this is proven, these assumed premises do not apply in the application of the method. Here the TCO cost factor per month and km are derived for each individual agent in dependence of their actual mobility behavior and used vehicle, which are calculated in the mobility simulation as well as powertrain simulation.

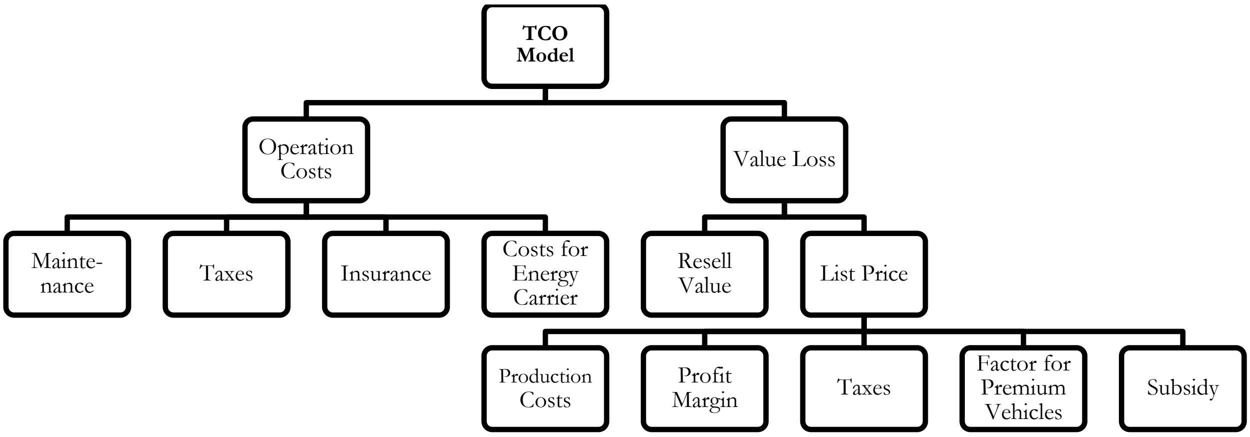

Figure 42: TCO Model for private owned vehicles based on [Propfe 2016]

As described, the operating costs consist of maintenance of the vehicle, vehicle taxes, insurance, subsidies as well as the costs for the energy sources depending on the consumption. The maintenance costs are analyzed in detail in [Propfe 2016]. Here, the maintenance costs per km for the considered component groups are derived for different powertrain types and vehicle segments. In Figure 43, the maintenance cost values are presented. In dependence on the driven distances, the total maintenance costs can be calculated. The driven distances result from the mobility simulation for each agent and can be used to calculate the total maintenance costs. In Figure 43 the maintenance costs according to the defined premise of 5 years with 15.000 km driven each year are calculated.

$$k_{maintenance} = c_{maintenance} * distance \qquad \text{(eq. 23)}$$

- $k_{maintenance}$: Total costs for maintenance
- $c_{maintenance}$: Maintenance cost value
- $distance$: Driven distance

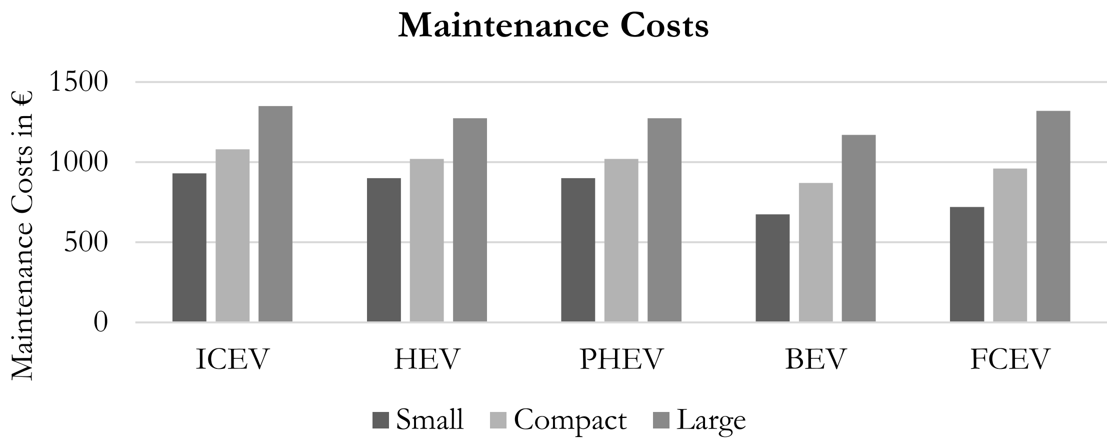

Figure 43: Maintenance costs for the considered vehicle segments and powertrain types for a mileage of 75.000 km based on [Propfe 2016]

In the next step, the taxes for the designed vehicle are calculated. Since the focus of this work is on the Berlin region, the taxes from Germany are used. However, it is possible to extend the model as needed and consider other countries. Electric vehicles remain tax-exempt for 10 years from initial registration or until 2030 at the most [Bundesregierung 2020]. After the tax exemption, the following formula applies according to [Uhlig 2021]:

$$k_{tax} = 0{,}5 * \left(11{,}25\,€ * ceil\left(\frac{min(m_{car},\ 2000kg)}{200\,kg}\right) + 12{,}02\,€ * ceil\left(max(\frac{(min(m_{car},\ 3000kg) - 2000\,kg)}{200\,kg}, 0)\right) + 12{,}78\,€ * ceil\left(max(\frac{(m_{car} - 3000\,kg)}{200\,kg}, 0)\right)\right) * t_{years} \quad \text{(eq. 24)}$$

The taxes of ICEVs and PHEVs are calculated as follows [FinanceScout24 2022]:

$$k_{tax} = \left(2 * \left(CO_{2,T2W} - 95\right) + V_{H,ICEV} * x_{Gasolin,Diesel}\right) * t_{years} \quad \text{(eq. 25)}$$

- k_{tax}: Total taxes
- m_{car}: Vehicle weight
- $CO_{2,T2W}$: CO2eq emissions from tank to wheel
- $V_{H,ICEV}$: Engine displacement
- $x_{Gasolin}$: Factor of 20 € per liter engine displacement
- x_{Diesel}: Factor of 95 € per liter engine displacement

For insurance costs, mean values are derived for the respective vehicle segments using the data from [ADAC 2021a]. In addition, subsidies for e-cars are taken into account. E-cars up to a list price of 40,000€ can be subsidized with 9,000€. E-cars up to a list price of 65,000€ can be subsidized with 7,500€. For PHEVs, a subsidy of 6750€ applies up to a list price of 40,000€ and a subsidy of 5625€ applies up to a list price of 65,000€. These subsidies are expected to be valid until 2025 and reduce the overall list price by these amounts [Kroher et al. 2022].

In the last step of the operating cost calculation, the costs for the consumed energy carriers are calculated. Depending on the powertrain type, these are gasoline or diesel fuel, hydrogen or electricity. The costs for the consumed energy result from the costs for the energy carriers that are stored in the cost database as well as the consumption of the vehicle and the distance traveled. The consumptions are calculated with the described powertrain simulation (see chapter 6), in which the WLTC is assumed for the drive cycle. For hybrid vehicles both energy carrier need to be considered separately and summed up. The norm values are assumed:

$$k_{energy} = c_{energy} * consumption * distance \quad \text{(eq. 26)}$$

- k_{energy}: Total energy costs
- c_{energy}: Key-value for costs of energy carrier
- $consumption$: Consumption of vehicle
- $distance$: Driven distance

The total cost of ownership results from the sum of the individual costs:

$$k_{operation} = k_{maintenance} + k_{tax} + k_{insurance} - k_{subsidies} + k_{energy} \qquad \text{(eq. 27)}$$

- $k_{operation}$: Operation costs
- $k_{maintenance}$: Total costs for maintenance
- k_{tax}: Total taxes
- $k_{insurance}$: Total insurance costs
- $k_{subsidies}$: Total subsidies
- k_{energy}: Total energy costs

The value loss is calculated with the difference between the list price and the resale value. The calculation of the list price is shown in the following. Here the production costs for each component including chassis of each designed vehicle are calculated with the help of the derived cost database based on [Schneider 2022] and [Can 2019]. For every relevant powertrain component of ICEVs, PHEVs, BEVs and FCEVs, key-values for the production costs including forecasts are available in the cost database. This is illustrated using the example of a PEM fuel cell in Figure 44. In [Can 2019] it is shown, that learning curves are suitable for the derivation of the trend curve of cost values. The reason for this is that the increasing technological maturity as well as the expansion of mass production reduce the manufacturing costs. Such learning effects, which take place over the years, are usually represented by learning curves. This curve is also shown by the weighted mean values. It is noticeable that the confidence interval becomes narrower as the forecast year increases. This is mainly due to the defined target values of the governments. These target values are defined by the various sources as limits for the learning curves. In Figure 44 the researched cost values including forecast are shown as well as the derived trend curve in form of a learn curve. The forecast values are expected values without using optimistic or pessimistic assumptions at the system level. The time-based key-values for the cost parameters are taken from the derived trend curve.

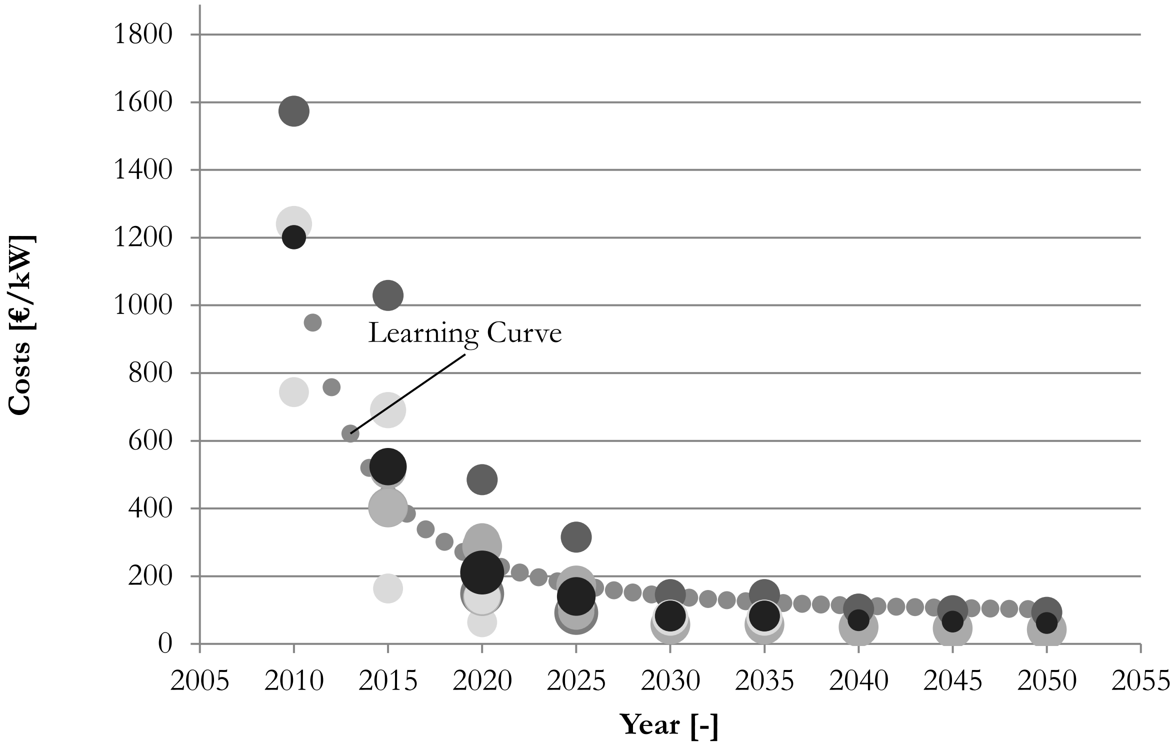

Figure 44: Cost key-values and trend curve for the PEM fuel cell [Can 2019]

In equation 28 the calculation of the production cost for the considered component in the considered year is shown:

$$k_{prod,component}(x_{time}) = c_{component}(x_{time}) * x_{component} \quad \text{(eq. 28)}$$

- $k_{prod,component}(x_{time})$: Production cost for considered component in the considered year
- $c_{component}$: Key-value for costs per functional unit for considered component. For example, the key-value for the battery is given in € per kWh.
- $x_{component}$: Functional unit of component coming from powertrain simulation. For example, the functional unit of the battery is the capacity in kWh.
- x_{time}: Considered year, in which the vehicle is produced

In the next step the list price can be calculated. The list price contains the production costs as well as the profit margin, the value-added tax and a factor for premium vehicles. Assumptions are made for the profit margin in dependence of the vehicle segment based on [Bay 2019]. The factor for premium vehicles is also considered in the profit margin.

The mathematical relationship is shown in the following:

$$k_{list}(x_{time}) = k_{prod,component}(x_{time}) * c_{profit} * c_{valueTax} \quad \text{(eq. 29)}$$

- $k_{list}(x_{time})$: List price in the considered year
- $k_{prod,component}(x_{time})$: Production cost for considered component in the considered year
- c_{profit}: Profit margin in dependence of vehicle segment
- $c_{valueTax}$: Value added tax for Germany

The value loss is described by the difference between the list price and the resale value:

$$k_{valueLoss} = k_{list}(x_{time}) - k_{resaleValue} \quad \text{(eq. 30)}$$

- $k_{valueLoss}$: Value loss
- $k_{list}(x_{time})$: List price in the considered year
- $k_{resaleValue}$: Resale value

The resale value depends on the list price, the vehicle type, the powertrain type and the mileage driven. In [Propfe 2016] regression curves are derived for different vehicle types of the ICEV to calculate the resale value based on historical data on resell platforms. These regression curves are then also applied to other powertrain types. In addition to the regression curves it is assumed that the resale value of PHEVs is 10 % higher than of ICEVs and the resale value of BEVs is 20 % lower than of ICEVs [Propfe 2016]. These regression curves and assumption are also used here to calculate the resale value of each vehicle. With the known value loss the TCO can be calculated with the following formula:

$$k_{TCO}(x_{time}) = k_{operation} + k_{valueLoss} \quad \text{(eq. 31)}$$

- $k_{TCO}(x_{time})$: Total cost of ownership
- $k_{operation}$: Operation costs
- $k_{valueLoss}$: Value loss

In the following, exemplary calculations of the total cost of ownership of agents with a BEV, ICEV and PHEV in the year 2021 is performed and compared to the results of [ADAC 2021a] for the VW ID.4 Performance with 150 kW, VW Polo with 70 kW and VW Golf GTE with 180 kW. To enable a comparability the same premises as in [ADAC 2021a] are assumed. Here a usage time of 5 years and 15.000 km driven distance per year are assumed. In the first step the VW ID.4 is compared. With the help of the powertrain simulation a consumption of 19 kWh/100km is calculated with an average cost for electricity of 19 ct€/kWh. In [ADAC 2021b] monthly costs of 838 € and 67 ct€/km are calculated. It is not stated if subsidies are considered in the TCO calculation. With the described TCO model the following costs are calculated for a 5 year time frame and 15.000 km driven distance per year, as shown in Table 9. As a result a TCO per month of 770 € and 61 ct€/km is calculated.

Compared to the results of [ADAC 2021b] these values are lower. One reason could be the consideration of subsidies in the amount of 9000 €. Without subsidies the TCO per month results in 830 € and 66 ct€/km, which almost equals to the values of [ADAC 2021b]. If the TCO calculation is applied in the context of this work, the real driven distances as well as usage time of the vehicle are considered. Therefore, the calculation is performed again for an exemplary agent who owns an ID.4 and uses it for almost 14 years and 200,000 km. This results in a TCO per month of 377 € and 32 ct€/km including subsidies, which corresponds to the typical mileage allowance.

Table 9: Cost calculation for the VW ID.4

Cost Description	**Costs Values**
Maintenance	5850 €
Insurance	5500 €
Tax	0 €
Subsidies	-7500 €
Operation Costs	2700 €
List Price	61580 €
Resell Value	20800 €
Value Lost	31780 €
TCO per Month	770 €/month
TCO per Kilometer	61 ct€/km

In the second example the VW Polo with 70 kW is compared. With the help of the powertrain simulation a consumption of 4.8 l/100km is calculated with an average cost for gasoline of 1.53 €/l. In [ADAC 2021a] monthly costs of 499 € and 39.9 ct€/km are calculated. With the described TCO model the following costs are calculated for a 5 year time frame and 15.000 km driven distance per year, as shown in Table 10. Here a TCO per month of 490 € and 39 ct€/km is calculated. Here the calculated values are overall similar to the reported values in [ADAC 2021a]. For an agent who owns a VW Polo and uses it for almost 14 years and 200,000 km, this results in a TCO per month of 274 € and 24 ct€/km.

Table 10: Cost calculation for the VW Polo

Cost Description	**Costs Values**
Maintenance	4725 €
Insurance	3400 €
Tax	342 €
Subsidies	0 €
Operation Costs	5300 €
List Price	21850 €
Resell Value	6300 €
Value Lost	15550 €
TCO per Month	490 €/month
TCO per Kilometer	39 ct€/km

In the third example the VW Golf GTE with 180 kW is compared. With the help of the powertrain simulation a combined consumption of 1.0 l/100km is calculated with an average cost for gasoline of 1.53 €/l and an average cost for electricity of 19 ct€/kWh. In [ADAC 2021a] monthly costs of 664 € and 53.1 ct€/km are calculated. In this report high value losses are calculated. With the described TCO model the following costs are calculated for a 5 year time frame and 15.000 km driven distance per year, as shown in Table 11. Here a TCO per month of 409 € and 33 ct€/km is calculated. The difference is mainly due to the fact, that subsidies of 6750 € as well as higher resell values are assumed in the presented TCO model. Without subsidies and an assumption of 10% lower resale values compared to ICEVs, a new TCO per month of 590 € and 48 ct€/km is calculated, which comes nearer to the reported values in [ADAC 2021a]. In addition, the calculated list price is lower compared to the 41940 € list price used in [ADAC 2021a]. Considering the difference in list price adds up to a calculated TCO per month of 649 € and 52.7 ct€/km. For an agent who owns a VW Golf GTE and uses it for almost 14 years and 200,000 km, this results in a TCO per month of 225 € and 20 ct€/km including subsidies and the assumption of higher resell values. Due to the assumed combined consumption of the PHEV, the operation cost is low compared to e.g. an ICEV. Considering longer usage times, this leads to overall lower TCO per month and km.

Table 11: Cost calculation for the VW Golf GTE

Cost Description	Costs Values
Maintenance	5100 €
Insurance	4000 €
Tax	150 €
Subsidies	-6750 €
Operation Costs	2815 €
List Price	38414 €
Resell Value	21460 €
Value Lost	10204 €
TCO per Month	409 €/month
TCO per Kilometer	33 ct€/km

Overall, these examples show, that the calculated TCO for private owned vehicles with the shown approach reaches a sufficient quality. In addition, it is possible to predict future costs by including forecasts and to analyze future mobility systems with this approach.

8.2 Cost analysis of additional transport modes

Key-value based models are implemented to calculate the mobility costs of additional transport modes such as public transport or micro-mobility. The required key-values are determined with the help of a literature research and stored in the cost database. The key-value based model consists of characteristic values that are represented in the form of costs per passenger kilometer. Depending on the distance traveled, the costs incurred are calculated, as shown in the following formula:

$$k_{transport} = c_{transport} * distance \qquad \text{(eq. 32)}$$

- $k_{transport}$: Total costs for considered transport modes
- $c_{transport}$: Cost key-value per person kilometer for the considered transport mode
- $distance$: Driven distance

In the context of this work the public transport, bicycle, walking and micro mobility are considered as additional transport modes in the mobility system, whereas walking generates no costs. In Table 12 the cost key-values for Germany are shown. It is assumed that these costs are valid for all regions in Germany and therefore are also used in the Berlin scenario.

Table 12: Cost key-values for additional transport modes

Transport Mode	**Cost Values**
Public Transport	1.5 € + 25 ct€/km [Kowalewsky 2021]
Micro Mobility	1€ + 20 ct€/km [Imhof et al. 2021]
Bicycle	6 to 10 ct€/km [Hamburger Verkehrsverbund 2019], [Dambeck 2011]

9 Optimization methods

After introducing the metrics for the target values CO_{2eq} emissions, costs and energy demand, the goal is to enable the mobility system to be optimized with respect to these target criteria. One challenge in determining optimal mobility systems including optimal powertrains and agent behavior is the huge number of parameters that need to be defined and lead to a significant number of possible configurations. In addition, trade-offs between target criteria need to be made such as finding solutions in which emissions are reduced, but the costs for the customer are not increasing that much. Because these cannot all be examined with regard to the target variables, a random or well understood and known start selection must be made over the entire search space. To carry out this selection in a targeted manner and thus reduce the overall required computational effort, an optimization algorithm is used in this thesis. One task of the algorithm is to control the selection of the configurations to be examined in the optimization process in such a way that in its course an improvement of the target variables takes place. The following approach to find a fitting optimization method is based on [Weiß 2018].

In chapter 9.1 the basics of optimization are presented. Subsequently, the requirements for the optimizer are presented in chapter 9.2. Chapter 9.3 analyzes the different optimization approaches. The focus here lies on meta models and the genetic algorithm. In Chapter 9.4 the possibilities to reduce computation times are analyzed.

9.1 Basics of optimization

In the field of optimization, a distinction can be made between static and dynamic optimization. The dynamic optimization differs from the static optimization, that instead of optimal input variables a time-dependent function is sought which minimizes an objective function. For a detailed description of the dynamic optimization, please refer to [Papageorigou 2012]. The objective of the optimization corresponds to a typical static optimization problem. According to [Koziel et al. 2011], a static global optimization is characterized by a function which is to be minimized. The input variables of this function can be continuous as well as discrete or mixed values. The search space is constrained by the lower and upper bounds and includes the range of values for the input variables, in which the optimal parameter set is searched [Weiß 2018]. The following definition of terms is used:

- **Search Space**: Multi-dimensional space defined by the possible parameter sets and limited by lower and upper boundaries
- **Optimization Parameter**: Input parameter set of the objective function
- **Objective Function**: Function describing the target criteria depending on the input parameters, that needs to be minimized

The goal of the optimization is to find a global optimum. A fundamental goal of global optimization algorithms is the balance between exploration and convergence behavior. The convergence behavior describes the speed with which possible optima can be identified. These can be suboptimal, local optima or the global optimum. It is controlled by the ability of algorithms to use known solutions, i.e. to combine and improve them. Exploratory behavior refers to the ability to find previously unknown regions of the search space. This should leave the local optimum and determine the global optimum [Chiong 2009].

Multi-dimensional problems can be optimized by minimizing several functions describing different target criteria [Koziel et al. 2011]. Due to conflicting objectives, it is usually not possible to find an optimal input parameter set which minimizes all objective functions. For this reason, Pareto optimal solutions are sought for multi-objective optimization problems. All solutions together result in the Pareto optimal solution shown in Figure 45, which represents a boundary or an edge region of the solution space and is therefore called the Pareto front [Weiß 2018]. In this thesis, a multi-objective optimization is performed, whereas cost over benefit is optimized, as shown in Figure 45. However, because optimization algorithms always minimize the objective variables, the axis with the benefit, which needs to be maximized, must be transformed according to [Siebertz et al. 2010]. Costs and benefits are obtained by normalizing and weighting the optimization parameters, which include, for example, the powertrain portfolio and powertrain design. The methods for modeling and calculating these criteria thus represent parts of the objective functions. Furthermore, the search space is limited by minimum requirements for the mobility system as well as the possibilities the considered region offers. The optimal input parameter sets identified with the help of an optimization algorithm thus result in the characteristics of the optimal mobility systems. In the next chapter, the requirements toward the optimization algorithm are described.

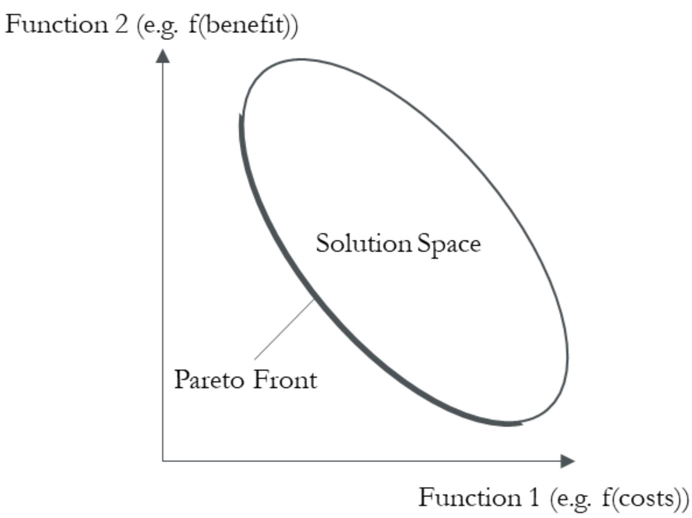

Figure 45: General representation of a pareto front based on [Weiß 2018]

9.2 Requirements towards the optimization algorithm

The requirements for the optimization algorithm to be selected are essentially derived from the properties of the optimization problem. In the context of this work, different approaches are investigated to determine a suitable optimization method for the given problem. Due to the very large data space caused by the combination of individual data-intensive models, such as mobility simulation and LCA, the computation time plays a very important role to enable optimization. In addition to computation time, the problems to be investigated with the methodology are static optimization problems, since mobility systems are analyzed in discrete time points and therefore no time-dependent optimal input parameters are sought, but optimal input parameters at discrete time points. Furthermore, the characteristic of the resulting solution space is not known in advance and can have both local and global extrema comparable to Figure 46. The goal is always to find the global optimum of each target variable, but since the system is very complex it is possible that only local optima are found. Since several target variables are to be optimized, the algorithm must allow for multi-objective optimization. Following requirements need to be considered:

- Various constraints have to be considered, such as customer requirements and constraints in terms of renewable energy, resources, cost and comfort to limit the search space.
- Continuous input parameters such as varying characteristics of powertrain components or plans of agents and discrete input parameters such as transport modes, powertrain types or component types should be considered.
- Numerical map-based simulations are used to calculate the target parameters. Therefore, a derivation-free algorithm is needed since a direct calculation of derivatives is not possible.
- The ability to compute in parallel is also considered a prerequisite. However due to the complexity of the system, the exploration and evolution need to be limited and this can lead to a local optimum instead of a global optimum.
- The objective of the optimization corresponds to a typical static optimization problem.
- Multi-objective optimization considering CO_{2eq} emissions, costs and energy demand is performed.

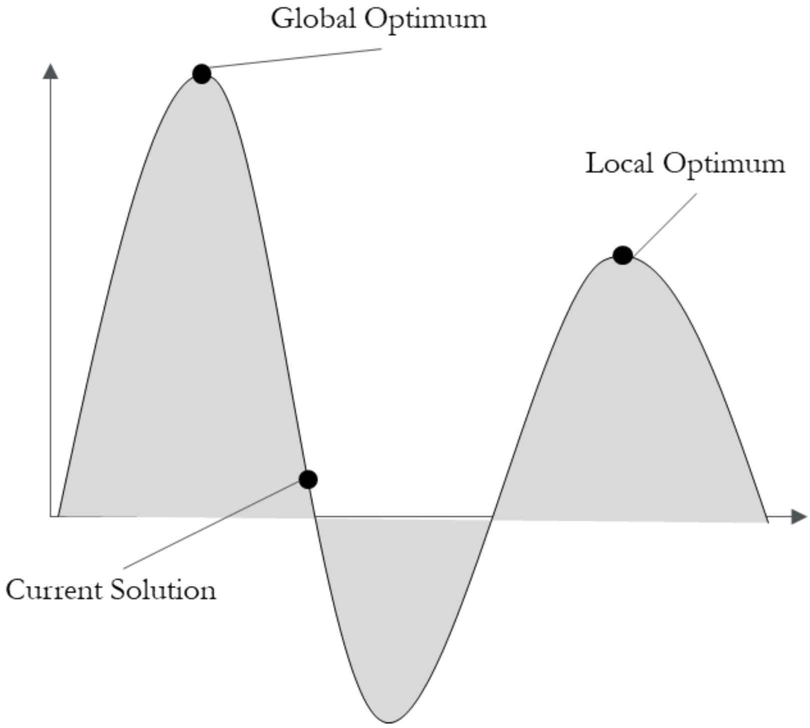

Figure 46: Presentation of local and global optima in an exemplary search space based on [Weiß 2018]

9.3 Investigation of different optimization approaches

A large number of optimization algorithms are described in the literature, each suitable for a specific application area. Some of these create good results for a variety of different problems, while other highly specialized algorithms are only suitable for specific problems but are significantly faster and more efficient. This also means, that there is no general algorithm that is better and more efficient than all the other existing algorithms [Weise 2009]. In this thesis, different objective functions are to be optimized. These differ with respect to the number of input parameters, which in turn can be varied discretely or continuously.

Optimization algorithms can be classified by distinguishing between static and dynamic problems and the methods that can be used in each case. Algorithms for solving static optimization problems are divided into derivative-based and derivative-free methods. A typical algorithm that uses the first derivative of the objective function is the Gauss-Newton method, while for example the Nelder-Mead method only uses the function value. According to Figure 47, the optimization methods can be further classified into deterministic and stochastic processes. Deterministic means that the optimization process is based on strict non-random rules. Therefore, under the same starting conditions, these algorithms always provide the same solution. On the other hand, stochastic methods use random components, which means that the optimization process and possible outcomes are different for each run. The simplest random part can involve choosing a random starting point. Another possibility is to implement random parts in various components of the algorithm [Koziel et al. 2011].

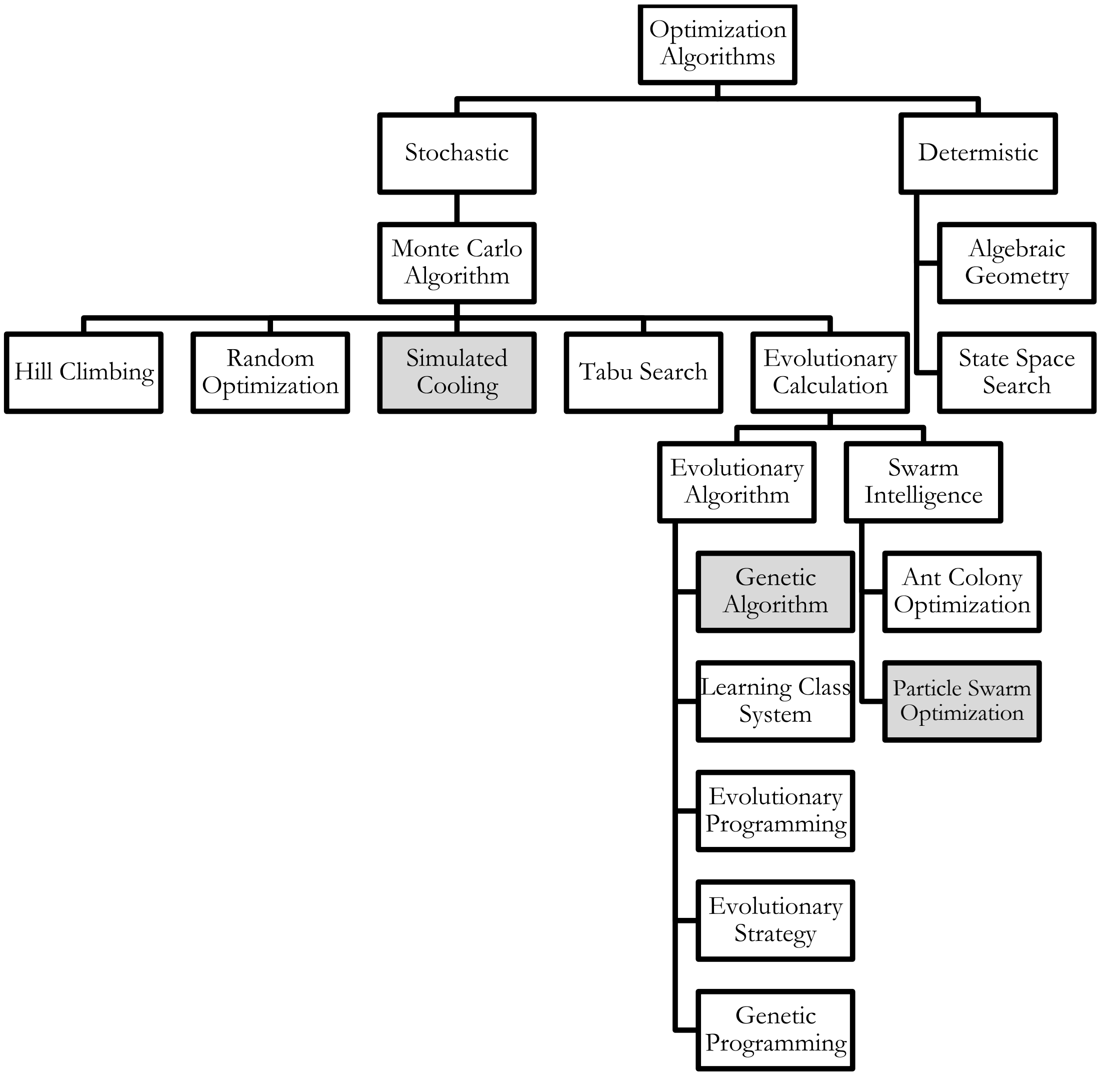

Figure 47: Classification of optimization algorithms based on [Weiß 2018] based on [Weise 2009]

Another aspect of classifying optimization algorithms is the ability to search for global optima. Local optimization methods fundamentally lack the ability to further explore once a local minimum is reached, as they are usually based on deterministic rules. The basic global optimization capability is achieved through a random component. Therefore, local optimization methods can be extended to global optimization methods by adding random starting points, but may not be efficient and successful [Koziel et al. 2011].

An optimization run can require many thousands of calls to the objective functions, which means that the computation time for the entire optimization can be long despite the short computation time of a single call. One way to solve this problem is to use a metamodel. With such a model, complex simulation models are approximated by simplified models with significantly reduced computation time [Siebertz et al. 2010]. This can be achieved by, for example, ignoring physical relationships of a complex model. Here the simplified model only describes direct dependencies between input parameters and target variables. As shown in Figure 48, the objective function is first reduced to a metamodel and then used for optimization to determine the target value. Compared to the original objective function, the number of input parameters of the metamodel is reduced, whereas the rest of the input parameters remain constant during the optimization [Weiß 2018].

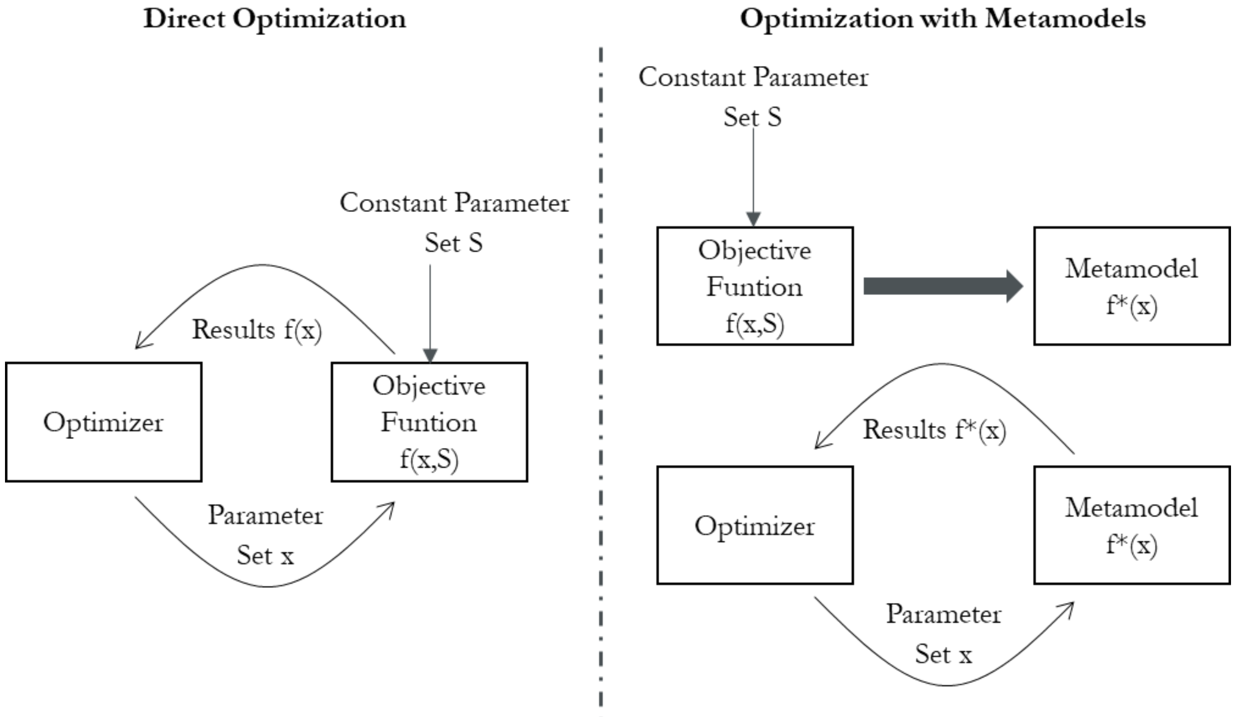

Figure 48: Optimizing with metamodels [Weiß 2018]

A big disadvantage of the metamodels approach is the uncertainty regarding the approximation error with the resulting reduction of the result quality. Another problem with metamodel generation is the loss of information. For example, the generation of simplifications of the mobility simulation leads to information loss because information is summarized, such as traffic flows, and thus no optimizations can be performed at the agent level, which is again a requirement for the optimizer. Therefore, the metamodel approach is not suitable for the optimization of the holistic mobility system.

To optimize such large and complex mobility systems a simplification is needed at some point such as to downscale the population shown in the following chapters. In order to do that, DoE is used to derive metamodels describing recommended scaling factors. To maintain a good model quality and to reduce computation time, additional methods are applied. The optimization time can be reduced by restricting the search space, by parallelizing computations and unacceptable areas can be identified and avoided. The parallelization of the calculation is a programming-technical aspect for the reduction of the calculation time. Thereby calculations independent of each other are executed in parallel. Thus, the entire computing capacity is better used and the computation time is reduced. The extent to which processes and algorithms can be parallelized depends to a large extent on the optimization algorithm and is therefore taken into account in the selection of an algorithm suitable for the use case shown here analogue to [Weiß 2018]. Based on the requirements for the optimization algorithm the simulated cooling, genetic algorithms as well as the particle swarm optimization are fitting. Therefore, in the following chapter these are analyzed and a suitable optimization approach is chosen.

9.3.1 Genetic algorithm

Due to the formulated requirements on the optimization algorithm, only derivative-free methods can be considered and due to the complexity of the holistic mobility system, stochastic methods are best suited to identify the global optimum. [Weiß 2018] describes that according to this categorization for the optimization algorithm, three variants have prevailed in the context of powertrain optimization. These are the simulated cooling, the genetic algorithms as well as the particle swarm optimization, as shown in Figure 47. The genetic algorithms (GA) and the particle swarm optimization are particularly well suited for parallelization because they are population-based algorithms in which independent computations are performed in each generation. In [Moses 2014], [Jain et al. 2009] and [Desai et al. 2010], a variant of the genetic algorithm, NSGA-II was found to be particularly suitable for the multi-objective optimizations. This is selected as method and adapted for the powertrain optimization problem there. Due to the very similar requirements for the optimization algorithm, the genetic algorithm with the NSGA-II variant is also chosen in this work, extended and applied for the considered optimization problem, namely the optimization of a holistic mobility system. In the following, the basics as well as the application of the genetic algorithm developed in [Weiß 2018], based on the work in [Moses 2014], are described.

9.3.2 Basics of genetic algorithm

Genetic algorithms were first introduced in the early 1960s by John Holland and his collaborators at the University of Michigan [Holland 1975] and have been further developed over time by various authors for different applications. They are based on insights from biological genetics and abstract Darwin's evolution of biological systems. The genetic algorithm enables the following points:

- Possibility to optimize complex problems
- Parallelizability
- Adaptability for special application areas

In Figure 49 the generalized flow of a typical genetic algorithm is shown. First, a starting population with a defined number of individuals, each with different characteristics, is selected. Using the objective functions as well as further procedures, a fit value is assigned to the individuals, on the basis of which a particularly fit parent generation is selected from the original population. The reproduction takes place by recombination (or crossing) of different parent pairs, whereby the characteristics of the parents pass directly into the characteristics of the children. Besides crossbreeding, mutation takes place with a certain probability. Thereby individual characteristics are modified independently of the parents. This ensures that the entire search space can be investigated and that the algorithm does not remain in a local minimum. Subsequently, a new generation is formed from parents and children and the entire process starts again. This is done until a maximum number of iterations or a tolerance limit regarding the change of the optimum is reached [Siebertz et al. 2010].

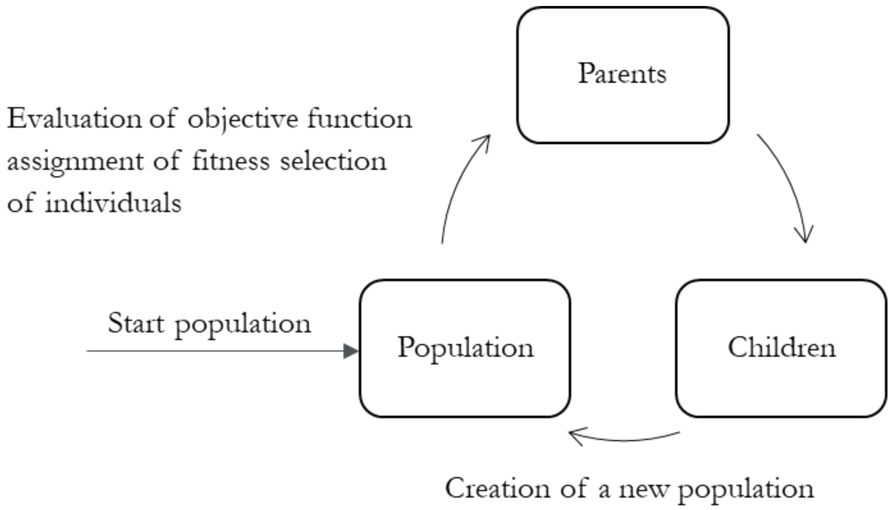

Figure 49: Generalized flow of genetic algorithm based on [Weiß 2018]

The basic terms of GA originate from evolutionary biology and thus differ from the typical terms of optimization. These include the individual, gene, allele, genotype, phenotype, population, and fitness and are described in the following [Weiß 2018]:

Individual: An individual in the biological sense is a living organism whose genetic information is stored in a set of chromosomes. In the context of genetic algorithms, however, the terms individual and chromosome are usually equated. It describes a possible solution or point in the search space of the problem to be optimized. It is defined by a certain number of genes and represents a mobility system in the context of the developed methodology.

Gene: A particular site or sequence of a chromosome is referred to as a gene. Genes store the input parameters of an individual. This is normally done in an encoded fashion. For example, an input parameter that can only take two values is encoded by the binary form 0 and 1. There are however also procedures, which make the coding by floating-point numbers possible, in order not to limit the search area. A single input parameter does not necessarily have to be represented by one gene, since it is possible to combine input parameters as well as to encode one input parameter by several genes. The genes represent the variation parameters of the mobility system optimization.

Allele: The specific expression of a gene is called an allele. If the gene is understood as a variable, the allele is the value of the variable. In the binary case these are the values 0 and 1.

Genotype: The genotype is the encoded vector of the input parameters. It generally determines which coding method is chosen.

Phenotype: The phenotype is the decoded vector of the input parameters. Its expression depends on the genotype and the chosen decoding method.

Population: A set of structurally similar individuals of a certain genus is called a population. When new creatures of this genus are born or others die, the size of the population inevitably changes. If one considers the populations of a genus over several points in time, one speaks of generations of the living beings. By the population concept the search space is examined at several places at the same time and the probability of finding the global optimum is increased.

Fitness: The fitness describes the quality of an individual and thus the probability of being reproduced. It is calculated from the results of the objective function and is the decisive criterion for the selection of the parent generation.

9.3.3 Application of the genetic algorithm

In the following, the flow of the genetic algorithm for the optimization of holistic mobility systems is described. The flow of the optimization is shown in Figure 50:

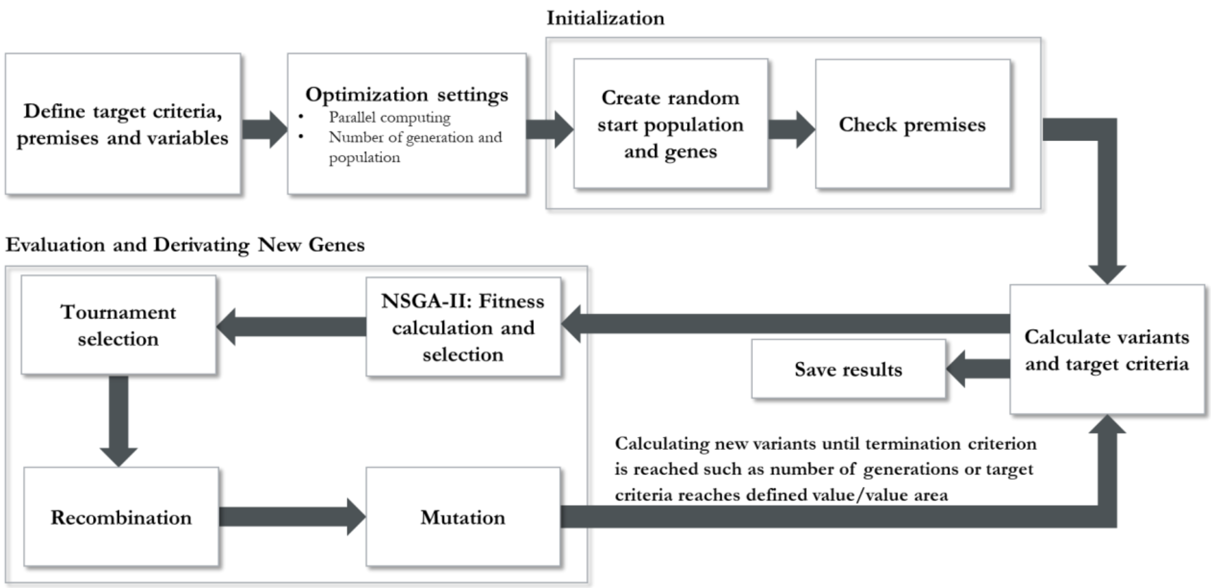

Figure 50: Sequence of the genetic algorithm based on [Weiß 2018]

Before the initialization takes place in the first step, the target criteria, premises, variables and optimization settings must be defined. Then, the initialization starts and a starting population and genes are generated randomly distributed in the search space. By using a random seed it is possible to reproduce an optimization process. If prior knowledge exists or similar optimizations have been performed, this knowledge can be incorporated into the selection of the start population. The closer these are already to the optimum, the faster the optimization algorithm is able to identify the Pareto front. Subsequently it needs to be checked, if the start population and genes fulfill all premises.

In the next step, the different variants of the mobility system are calculated. Then the fitness calculation and selection is performed according to the NSGA-II approach [Deb et al. 2002]. According to [Weiß 2018], [Moses 2014], [Jain et al. 2009] and [Desai et al. 2010] the NSGA-II has been shown to be particularly suitable for multi-objective optimization and is therefore selected in this thesis as well.

It describes the rules by which the best individuals of a population are selected for the parent generation. Unlike single-objective optimizations, it is not possible here to rank individuals based on the calculated objective, since two or more objectives have to be weighed against each other. Nevertheless, in order to obtain a meaningful ranking of the individuals and thus be able to make a comparison, the NSGA-II determines the rank and crowding distance (CDT) for each individual. The rank results from the classification of all individuals into non-dominated fronts. Accordingly, the first rank includes all individuals that lie on the Pareto front of the current generation, since these are not dominated by any others, for example there is no individual in the current population that performs better in all target variables. In the next step, the individuals of rank one are removed, resulting in a new Pareto front to which rank two is assigned. This is continued until all individuals are assigned a rank as shown in Figure 51 [Deb et al. 2002].

A comparison of all individuals based solely on their rank is not possible, as any number of individuals can be assigned a rank and thus cannot be compared with each other. Therefore, the CDT is calculated to further rank individuals of the same rank. It indicates the distance between an individual and his immediate neighbors on the same front. The aim here is to identify a front that is as wide and evenly distributed as possible and avoids dense accumulations. To this end, the two outer individuals are assigned the highest CDT value, while a value proportional to the sum of the distances of the two neighbors applies to all other individuals. With the help of these two metrics, an almost unambiguous assignment of ranking and fitness is possible. This is primarily based on ranking, and secondarily on CDT. Tournament selection is used to select the parent. It involves running several tournaments among a few individuals chosen at random from the population. The winners, i.e. the ones with the best fitness are selected. For each parent individual, a defined number, which is the tournament size, of random individuals are selected and the one with the best fitness is used as parent individual. The larger the tournament size, the higher the selection pressure and the less likely it is that individuals with a low fitness will also be reproduced. However, this is sometimes necessary in order to reach new regions of the search space. This increases the probability of identifying the global optimum. In NSGA-II, binary tournament selection with two individuals to compare is recommended [Weiß 2018].

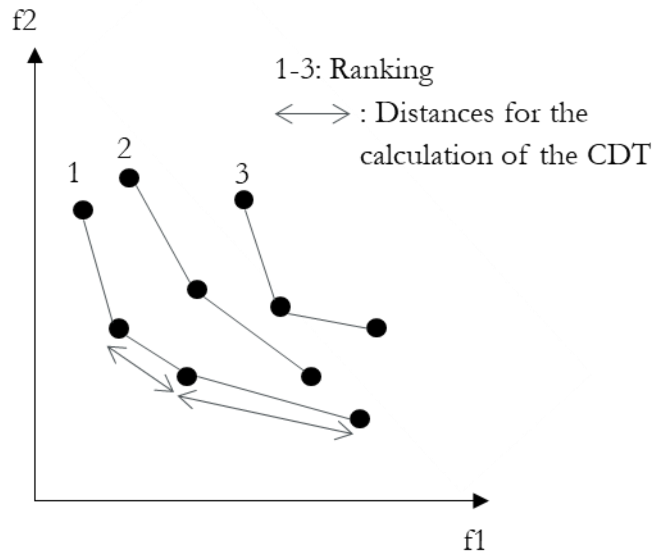

Figure 51: Determination of the rank and crowding distance (CDT) of single individuals of a population according to the NSGA-II based on [Weiß 2018]

In order to consider constraints, which is a requirement for the optimization algorithm, an adaptation of the tournament selection is applied. Variants of solutions that do not meet specific requirements can be excluded from further analysis. Here the constraints are considered in the selection of the parent individuals. If two individuals are compared, one of which violates a constraint, the other one always wins, independent of the other criteria. However, if both violate one or more constraints, the individual that violates the constraints less is selected. For this purpose, the absolute violations within the current population are normalized with respect to the maximum value for each constraint and multiplied for each individual. This results in a measure for the total violation of all constraints [Moses 2014].

In the next step offspring are produced from one pair of parents or from more than two parents by recombination. This is done to some degree of probability by shuffling the genes or by simply copying the parent pairs. The goal here is to reach unknown regions of the search space without losing already identified targetable traits. For recombination of real numbers, the BLX-α according to [Eshelman et al. 1993] is used in this work analogue to [Weiß 2018]. Here, the alleles of a gene from two parents are used to generate a child whose allele lies in a range around the expressions of the parent genes defined according to equation 33, where the adjustment parameter α specifies the size of this range. A random value in this range is used as shown in Figure 52. The whole procedure is repeated until the desired number of offspring has been generated [Weiß 2018].

$$[min(A_1, A_2) - \alpha|A_1 - A_2|, \max(A_1, A_2) + \alpha|A_1 - A_2|] \quad \text{(eq. 33)}$$

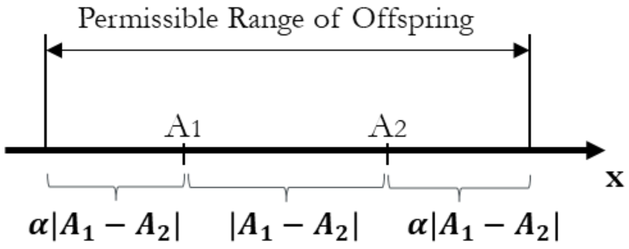

Figure 52: Permissible range of children in the recombination of a parent pair according to the BLX- α method based on [Weiß 2018] based on [Siebertz et al. 2010]

After recombination, a mutation is carried out with a certain probability. With this mutation probability, which should be significantly lower than the recombination probability and is applied to each gene individually, a random variation of the respective value takes place. This can produce offspring that cannot result from recombination of the parental genes, improve the exploration behavior and allow leaving local minima once reached. Mutation can occur by choosing a purely random value from the entire definition range as well as by using a probability function, in which a value in the same definition range is calculated [Siebertz et al. 2010]. In the last step of the optimization cycle, a new population is generated. For this purpose, all individuals of the last generation are again compared with the offspring on the basis of fitness, i.e. rank and CDT. The best individuals from this set form the new generation. This procedure ensures that already identified very fitting individuals are not lost in the next generation [Weiß 2018].

9.3.4 Settings of the genetic algorithm

For the performance of the optimization algorithm, it is important to choose the appropriate settings of the genetic operators for the problem. Since mobility systems are to be optimized with varying numbers and types of input parameters, a compromise must be found for all applications considered. The approach to identify the right settings is described in [Weiß 2018] and performed here. For the evaluation of the settings an optimization of the powertrain portfolio of the considered mobility system in Berlin is performed. To get as close as possible to the complexity of the target application various parameters are chosen. Here the five parameters, which are the shares of the ICEVs with gasoline and diesel, PHEVs, FCEVs, and BEVs and one discrete parameter, which is a measure to reduce the CO_{2eq} emissions by smart charging electric vehicles are varied. As a boundary condition the sum of all shares is defined as 1. In Table 13 the identified right optimization settings based on [Weiß 2018] are listed. The parameter settings are derived one time and it is assumed that these settings are valid for all regions as well as all mobility system configurations.

Table 13: Identified settings of genetic operators based on [Weiß 2018]

Tournament Size	10
Mutation Probability	20 %
Recombination probability	85 %

9.4 Complexity reduction of the mobility system

As described in the previous chapter, the properties of the genetic algorithm have proven to fit the formulated requirements for the objective in this thesis. Due to the complexity of the overall system and the variety of parameters in the simulation as well as in the analysis, as shown in Figure 53, the computation effort of one variant is very high. Therefore, a simplification of the system must be carried out to enable optimization in a reasonable timeframe. To reduce the computation time, the holistic model is considered first and the computation times of the individual submodels are determined. As shown in Figure 16 ("Overall overview of the method") of the objective function of the optimization includes the entire design and evaluation of the mobility system, including mobility simulation, powertrain simulation and the analysis of the target variables. Here, especially the mobility simulation has a large share in the computation time, since a certain number of iterations have to be performed for a converged result and, depending on the size of the considered system, the mobility behavior consists of a large number of single events.

For the Berlin use case scenario, a 10% sample size of the population with over 300.000 agents with a modern CPU (see appendix A.9) results in a computation time of about 6.5 hours for the mobility simulation with 200 iterations and around one day for the subsequent evaluation of the travel modes and analysis of the target variables. Here, only one mobility system configuration is considered. Several hundred configurations are calculated for the optimization. To reduce the computation time, the following considerations are made. On the one hand, the scaling of the population size is considered, with the goal of generating a down-scaled system similar to the reference system based on a sample size of 10 %. A reduced sample size leads to a reduced number of calculations that need to be performed and therefore to reduced computation times. Second, the number of iterations in the mobility simulation necessary to produce a converged result is investigated. Subsequently, the findings are integrated and implemented in the holistic method including optimization.

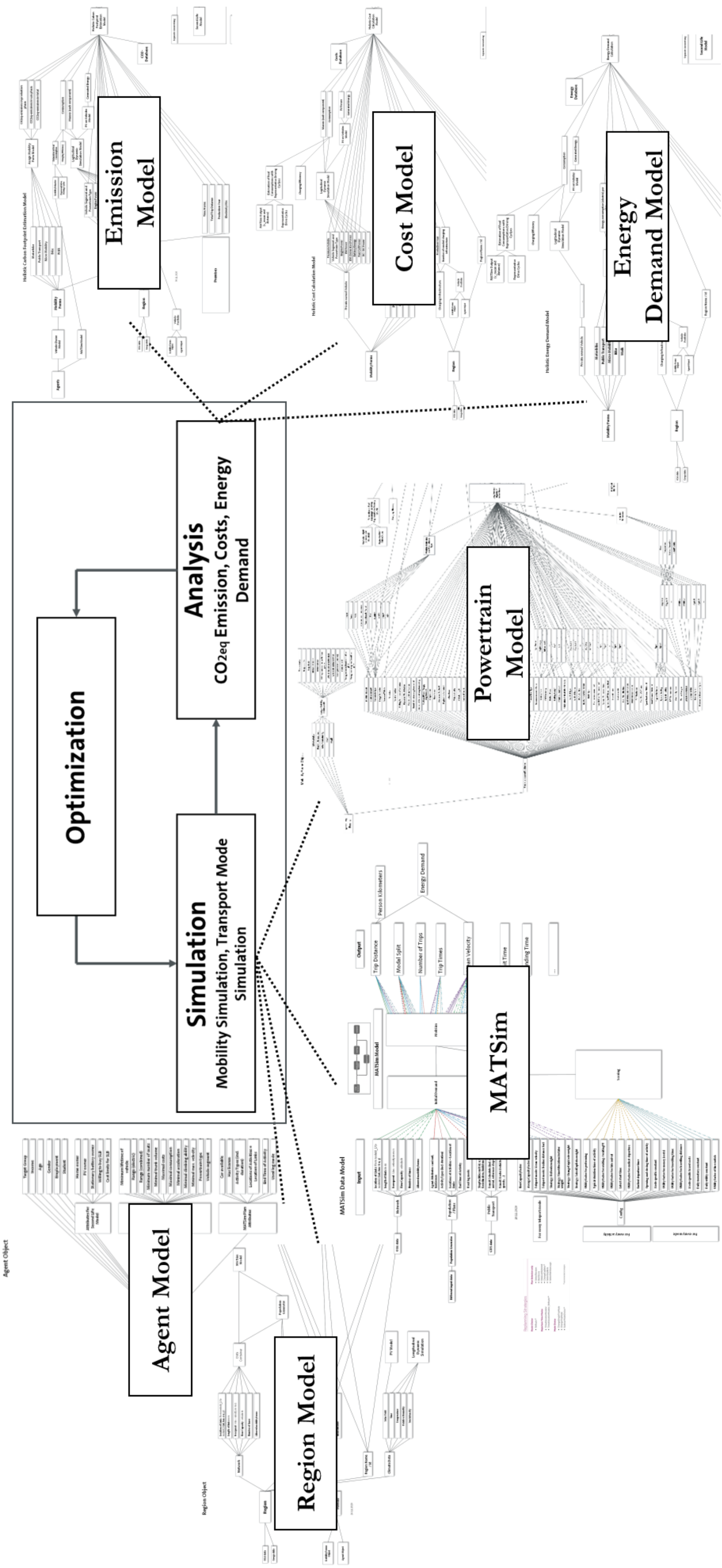

Figure 53: Representation of the system as a data model with the parameter variety

9.4.1 Reduction of sample size of the population

One way to reduce the computation time is to downscale the sample size of the population. With a reduced sample size, the calculation effort is also reduced. However, side effects of scaling have to be taken into account, because scaling affects the mobility behavior of the agents and therefore the results regarding average driven distances, travel times and average speed change. To achieve similar results, the storage and flow capacity of the network needs to be scaled down. The scaling of networks in MATSim is controlled by the flow capacity factor and the storage capacity factor. The flow capacity factor describes how many vehicles can exit the link per hour and the storage capacity factor describes how many vehicles can be stored at the same time in the considered link. With the flow capacity factor, the gap between consecutive vehicles can be increased and with the storage capacity factor the number of stored vehicles can be decreased. The goal of this scaling approach is to achieve a similar mobility behavior with the reduced sample size compared to the reference sample size [Horni et al. 2016]. Here it is assumed that a constant mobility behavior can be achieved with a constant modal split. A similar modal split leads to similar relative amounts of used travel modes and therefore to a similar mobility behavior. This enables an extrapolation of results regarding CO_{2eq} emissions, costs and energy demand. In chapter 10 these effects of scaling on the target criteria are analyzed in detail.

Most studies focus on sample sizes between 1% and 100% such as in [Rieser 2019] and [Llorca et al. 2019]. In [Rieser 2019], recommended values for the factors depending on the sample size in the range of 10% to 50% are suggested. Figure 54 shows the recommended factors. The storage capacity factor is deliberately chosen to be larger. This is because, if the size of the links is decreased too much, it may happen that no vehicles fit on the links. However, an extrapolation of the factors for sample sizes smaller than 1% are not allowed.

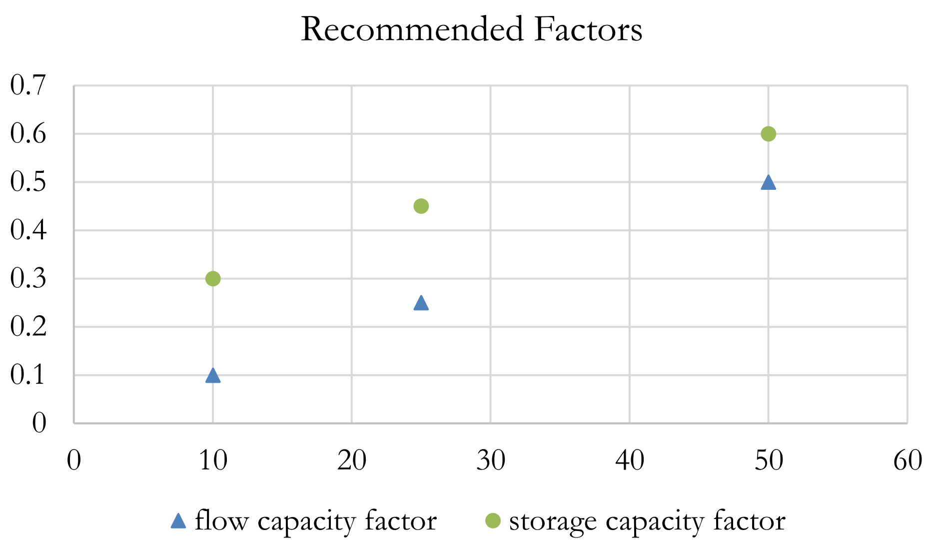

Figure 54: Recommended factors based on [Rieser 2019]

Therefore fitting storage capacity factors and flow capacity factors need to be found to achieve the same mobility behavior of the considered reference scenario. The goal is to find factors with which the modal split of the mobility system remains constant for all considered sample sizes. A constant modal split leads to the same relative usage of the respective transport modes and this leads to a similar mobility behavior of the agents. This approach though can have side effects on the travel times, distances as well as the target criteria $CO2_{eq}$ emissions, costs and energy demand since for example taken routes can change. These side effects need to be analyzed afterwards.

In the following, sample sizes below 1 % are considered and suitable factors are derived for this purpose, in which the mobility behavior of the different sample sizes remains constant. To achieve this goal the design of experiments (DoE) approach is used to find significant factors and derive meta models for the calculation of factors in dependence of the sample size. For the theoretical basis of a statistical experimental design, please refer to [Siebertz et al. 2010]. Subsequently, the target variables in MATSim, the mean distances, travel times and mean speeds for the different sample sizes are examined. The influence of the scaling on the target variables are shown. The whole process is carried out using the Berlin scenario as an example. In addition, it is assumed that the reduction of the sample size is distributed equally over the considered region. An equal distribution can be seen as a clustering of agents and therefore the assumption can be made, that the mobility behavior remains constant. In Figure 55 the distribution of the trip distance for each travel mode is shown for the 0.1% sample size on the left and 10% sample size on the right. Here it can be seen that an equally distribution of the agents on the region has a very small impact on the distances and is therefore a valid assumption.

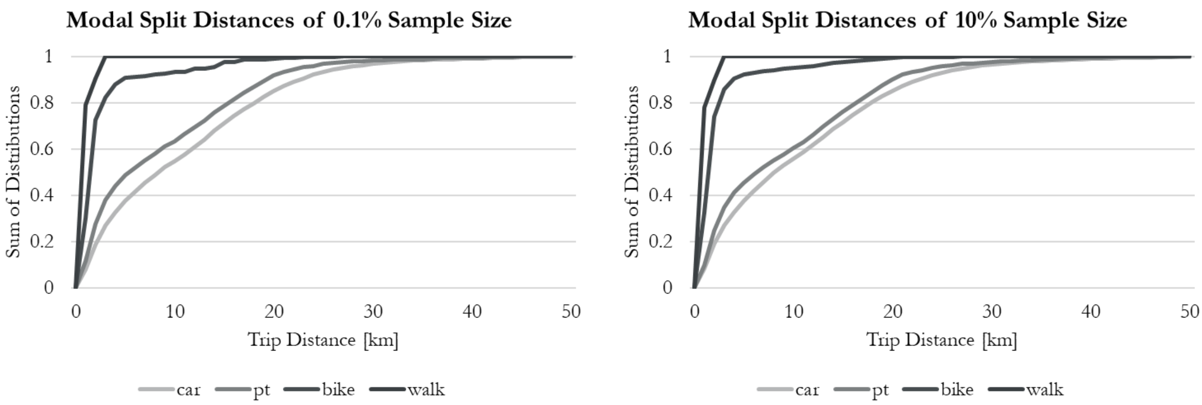

Figure 55: Trip distance distribution for each travel mode in Berlin for a 0.1% and 10% sample size

The DoE is used to identify significant effects of factors in the scaling of the population, and then derive appropriate factors to scale down the system to save computation time. Here, the resulting modal split of the 10% population with a storage capacity factor of 0.3 and flow capacity factor of 0.1 is taken as a reference. The considered travel modes are cars as well as teleported public transport, bike and walk. The factors investigated in the DoE are the sample size (A) with the values 1% as well as 0.1%, the storage capacity factor (B) with the values 0.0005 as well as 0.01 and the flow capacity factor (C) with the values 0.0005 as well as 0.01. In Figure 56 it can be seen that for this experimental design the flow capacity factor has a significant influence and the other factors each have only a slight influence. Here, the effects of the respective travel modes are considered individually.

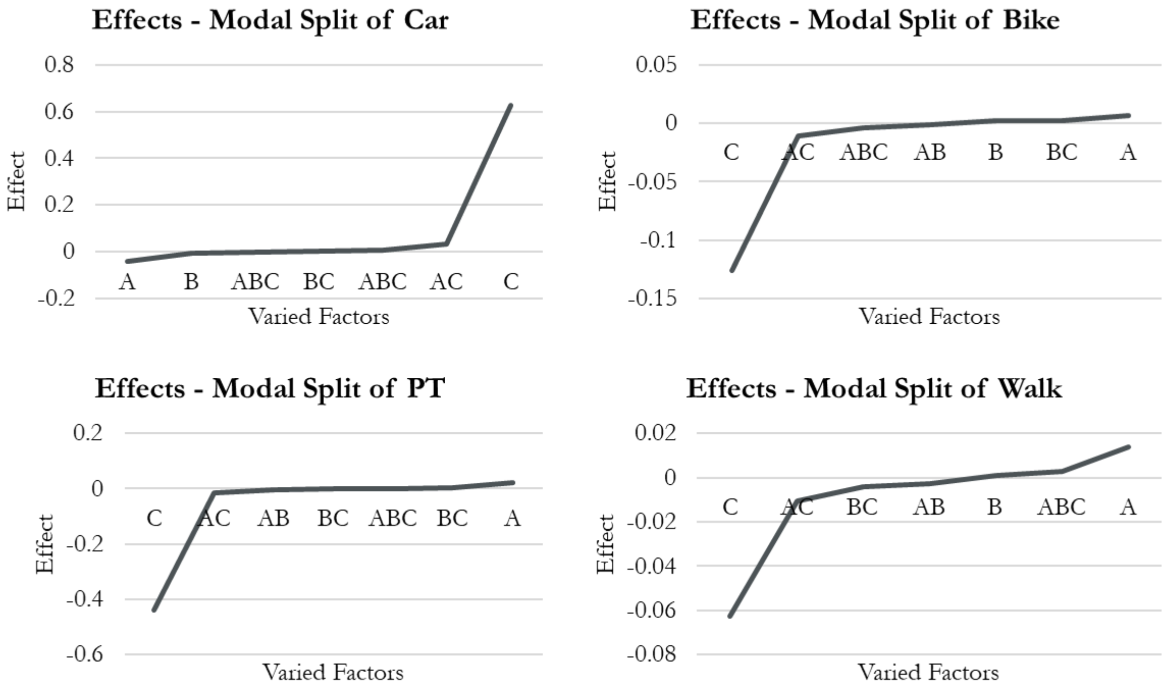

Figure 56: Effects of factors sample size (A), storage capacity factor (B) and flow capacity factor (C) on the modal split of the different transport modes

In the next step, the individual factors are examined in more detail. For this purpose, the storage capacity factor is varied for different sample sizes of 0.1%, 0.5%, 1% and 10% and the change in the modal split compared to the baseline scenario with a sample size of 10%. The flow capacity factor is kept constant and equals the corresponding sample size. For small sample sizes, the storage capacity factor has a very small impact on the modal split. This is because the storage capacity factor must have a minimum value so that at least one vehicle fits on a link. This is done internally by MATSim. For larger sample sizes such as 10% the storage capacity factor has a higher impact on the modal split. Figure 57 shows the results. On the y-axis the modal split is shown and on the x-axis the number of the calculation with the corresponding changed storage capacity factor.

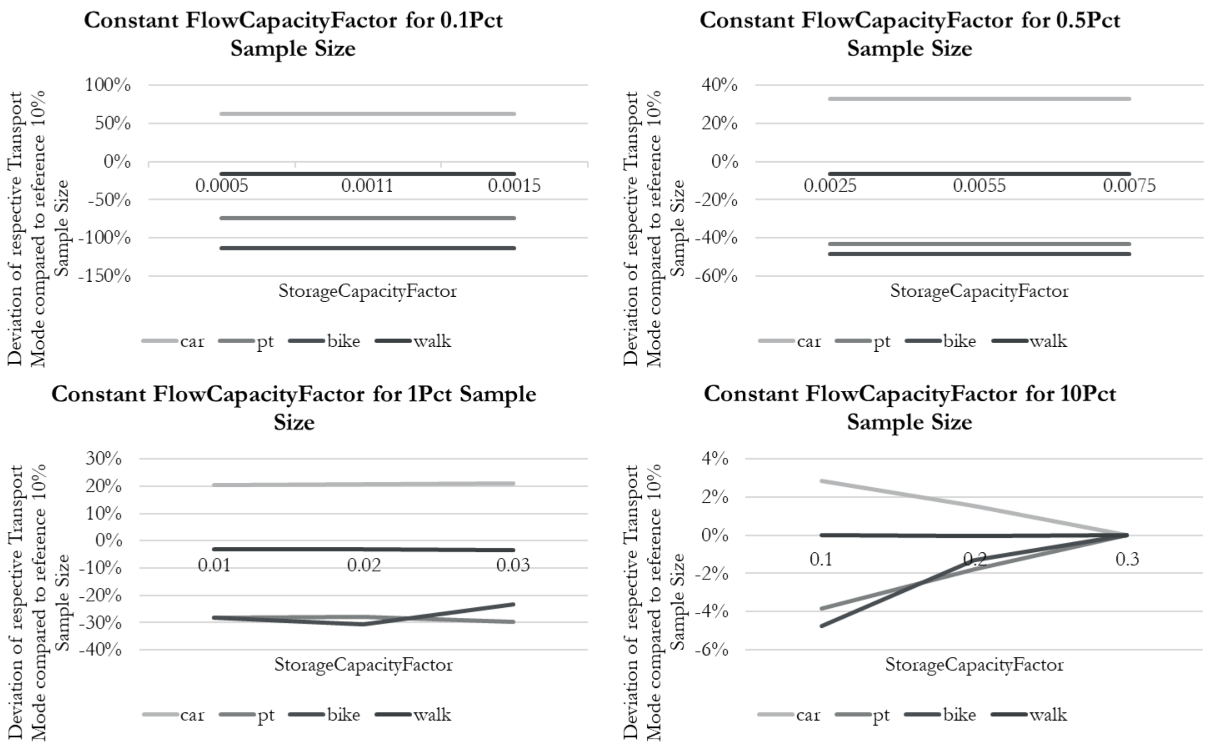

Figure 57: Effect of the storage capacity factor with a constant flow capacity factor on the modal split of different sample sizes

Subsequently the flow capacity factor is varied. Here, the storage capacity factor is kept constant and set equal to the sample size. Figure 58 shows the differences of the respective modal split of the considered travel modes of the 0.1% sample size compared to the modal split of the considered travel modes of the reference scenario, which is the 10% sample size. Here it can be seen that for smaller sample sizes the flow capacity factor has a higher impact on the modal split, as already expected from the DoE, and the modal split changes linear to the increasing of the flow capacity factor. This shows that the modal split of the new scenario can be fitted to the modal split of the reference scenario via the flow capacity factor for sample sizes below 1%.

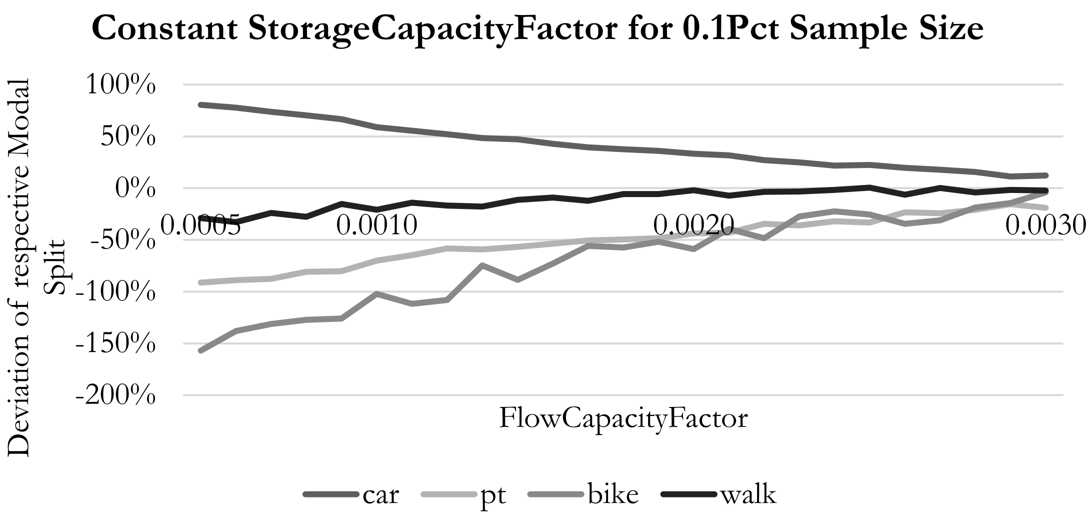

Figure 58: Effect of the flow capacity factor with a constant storage capacity factor on the modal split of the 0.1% sample size

This was repeated for further sample sizes up to 1% and the following recommended key-values for the factors were derived as a function of the sample size, as shown in Figure 59. Here, each travel mode is considered individually and the slope of the linear curve is determined. Additionally, a weighting of the respective travel modes is considered. The cars are analyzed in more detail in the mobility simulation since it is a network mode, i.e. a travel mode that actually moves on the network. Therefore, this mobility mode has a greater impact on the physical effects of the system. To better match the system to the reference scenario, this mobility mode is weighted higher. Then, the values are combined to form a recommended factor. As shown before the storage capacity factor has little impact on the modal split. Therefore, it is set to equal the considered sample size. Equation 34 and 35 show the mathematical relationship of the calculation of the factors. With the help of these factors, it is possible to adjust the downscaled system to the reference scenario of 10% in such a way that a constant mobility behavior exists. This is done for sample sizes in the range 0.1% and 1%.

$$F_{flowCapacity} = \sum_{i=1}^{N_{TransportModes}} w_i * \left(\frac{y_{ref,i} - y_{0,i}}{m_i} * F_{flowCapacity,0}\right) \qquad \text{(eq. 34)}$$

$$F_{storageCapacity} = sampleSize \qquad \text{(eq. 35)}$$

- $F_{flowCapacity}$: Calculated recommended flow capacity factor for the considered sample size
- $N_{TransportModes}$: Number of transport modes
- w_i: Weighting of transport modes. Here the following weights are assumed:
  - w_{cars} = 80%
  - w_{pt} = 10%
  - w_{bike} = 5%
  - w_{walk} = 5%
- y_{ref}: Modal split of the reference scenario for the considered transport mode, which needs to be achieved
- $y_{0,i}$: Modal split of the considered sample size for the point of 0 for the considered transport modes
- m_i: Slope for the considered transport mode
- $F_{flowCapacity,0}$: Flow capacity factor of the considered sample size for the point of 0
- $F_{storageCapacity}$: Calculated recommended storage capacity factor for the considered sample size
- $sampleSize$: Considered sample size

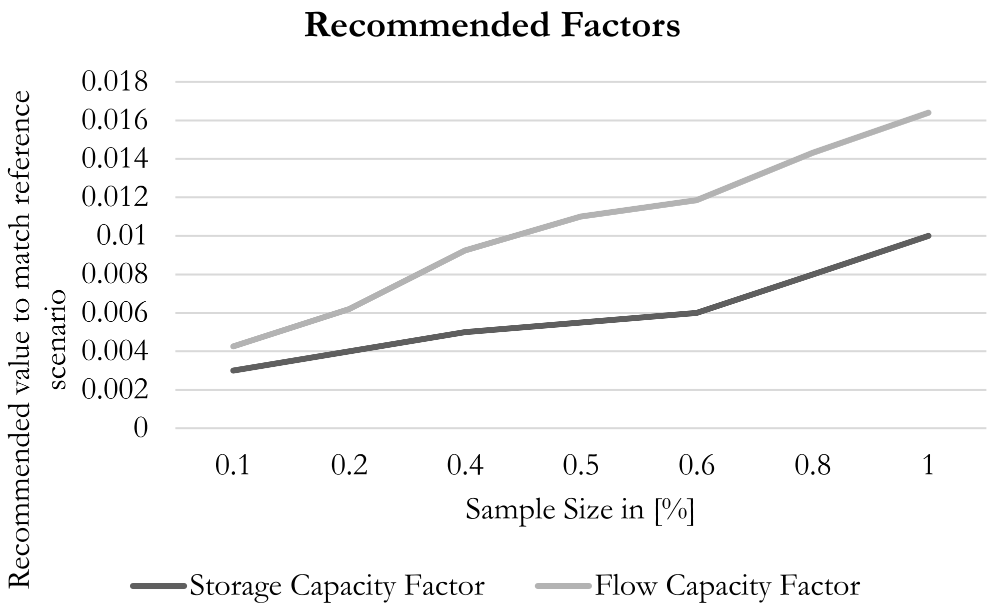

Figure 59: Recommended factors to match the modal split of the reference scenario of 10% sample size

In the next step, the target values are calculated with the recommended factors for the respective sample sizes between 0.1% and 1% and compared with the reference scenario of 10% sample size. For each sample size an own plan with the respective sample size is created and a mobility simulation is performed. First, the modal split is considered as shown in Figure 60. The modal split is very well matched overall. Here it can be seen that the largest deviations for the travel mode *car* are at just under 3% at the sample size of 0.1%. All other sample sizes are very well matched and the deviation is just under ±1%. The situation is similar for *public transport*. Here, the largest deviation is just under -2% for a sample size of 0.1%, whereas the deviations for the other sample sizes are less than ±1%. In the case of *bike*, there are larger deviations in the range of -5% for the 0.1% sample size. This is mainly due to the fact that this travel mode has a smaller share in the modal split. Small absolute changes in the modal split can lead to larger relative changes. In the case of *walk*, it is similar to *bike*. The deviations across all sample sizes are in the range of -9% and 4%. Again, due to the fact that this travel mode has a smaller share in the modal split. Here it can be seen that with smaller sample sizes the deviations increase. This is plausible since with smaller sample sizes less individual agents are considered and smaller changes in the system have a higher influence on the mobility behavior. Overall, it can be stated that the modal split of the reference scenario can be met very well with smaller sample sizes and thus the assumption that the mobility behavior remains constant is fulfilled. This also makes sense, since the factors are derived in dependence of the modal split.

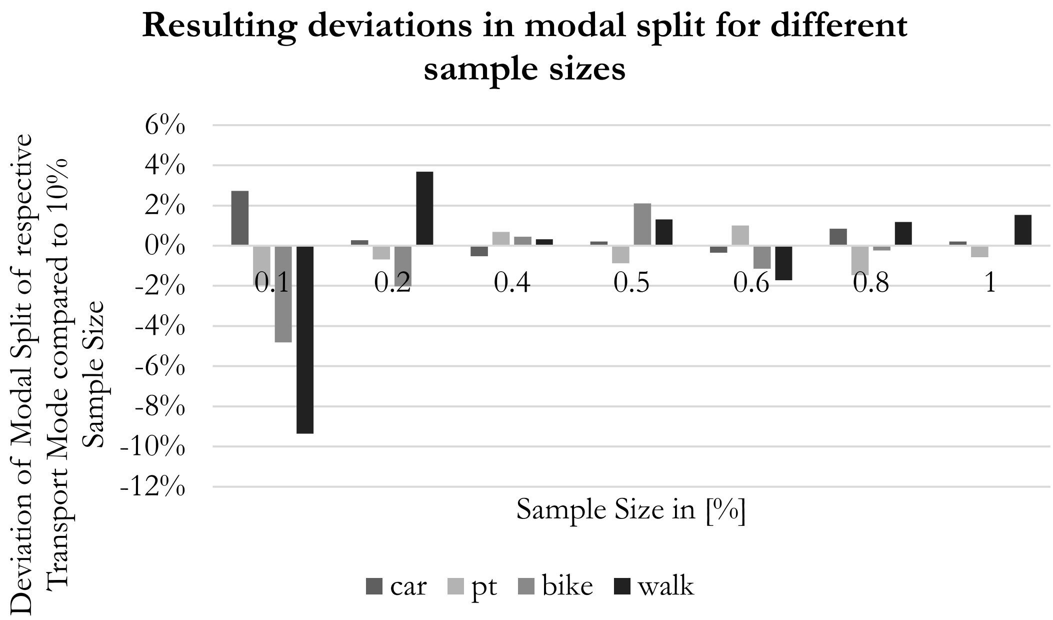

Figure 60: Simulated modal split with derived recommended factors for the sample sizes between 0.1% and 0.5%

In the following, the mean distances, speeds and travel times for sample sizes in the range of 0.1% and 1% are considered and compared with the reference scenario. Figure 61 shows the deviations of the mean distances of the respective travel modes for the respective sample sizes compared to the reference scenario. Here, the larger deviations are noticeable for the travel mode *bike* in the amount of up to 12% and walk in the amount of -9%. This is again due to the fact that the share of *bike* and *walk* in the modal split as well as mean distance driven with the *bike* or *walk* is low compared to the other travel modes. Scaling thus has a greater influence on the results, since small absolute changes lead to large relative deviations. In this specific case, it can happen that when scaling down, mainly bicyclists or walking agents with a larger or smaller distance are taken into account, and it therefore also affects the average distances. For *cars*, the deviations are quite small. Here, the deviations are in the range of under 2%. For *public transport*, the deviations are in the range of -8% to -1%. Overall it can be seen that the deviation increases with smaller sample sizes.

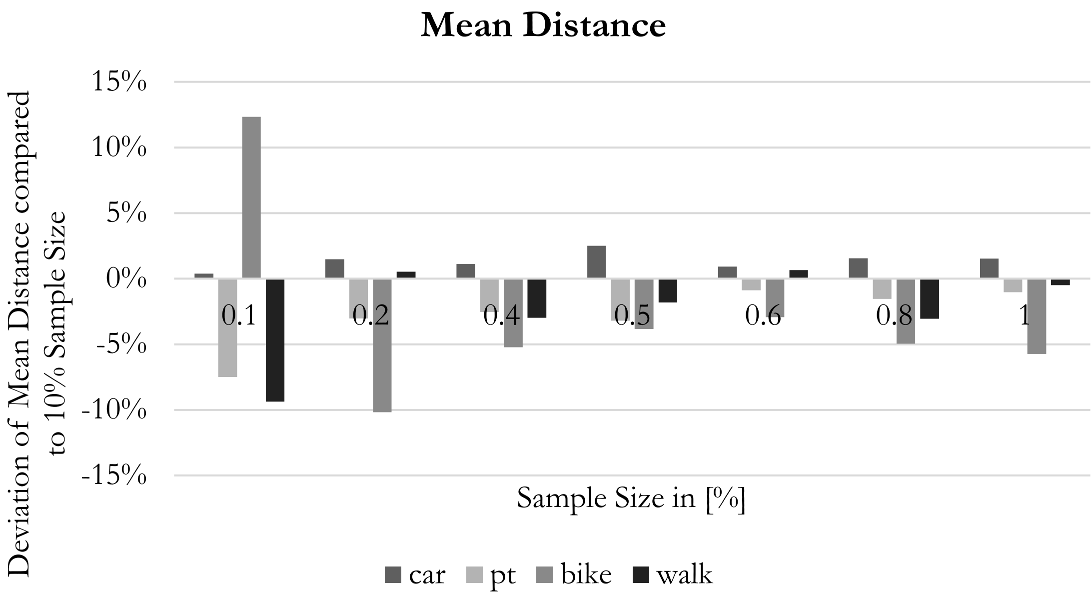

Figure 61: Difference of mean distance between considered sample size and reference scenario

Figure 62 shows the deviations of the average speed for the different travel modes of the respective sample sizes compared to the reference scenario. The mean velocity shows larger deviations for *car* with decreasing sample sizes compared to the reference scenario. This is due to the selected flow capacity factor. Compared to the reference scenario, the flow capacity factor is set relatively higher for smaller sample sizes in order to achieve a constant modal split. An increase of the flow capacity factor means that more vehicles can leave a link in a certain time. This leads to an increase in the average speed compared to the reference scenario of up to 8% in the 0.1% sample size. This linear relationship of the selected factors is also reflected in a linear increase of the mean speeds. The other travel modes show hardly any deviations from the reference scenario. The largest deviation occurs for *walking* which lies in a range of ±2%. This is due to the fact that this form of mobility uses teleported modes and therefore the average speed is predefined.

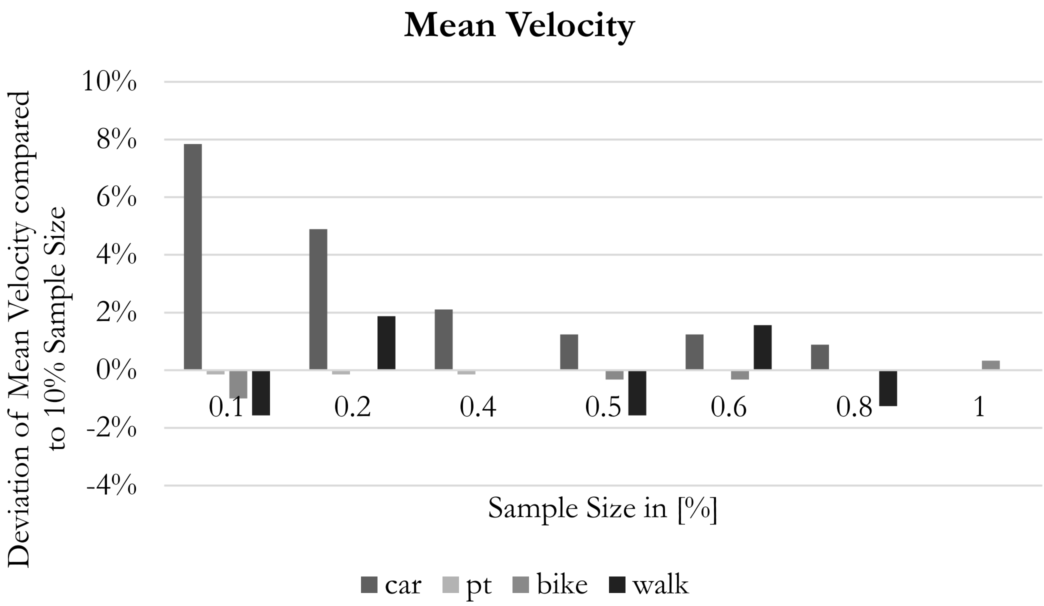

Figure 62: Difference of mean velocity between considered sample size and reference scenario

Figure 63 shows the deviations of the average travel times for the considered travel modes of the respective sample sizes compared to the reference scenario. The average travel times result from the average distance and average speed. This is also reflected in the results. Due to the higher average speed for cars and the slightly higher average distance, travel time savings of up to -5% result for 0.1% sample size. Analogously, it can be seen that for the other travel modes, the change in mean distance is basically equal to the change in mean travel time, since the mean speed remains almost constant.

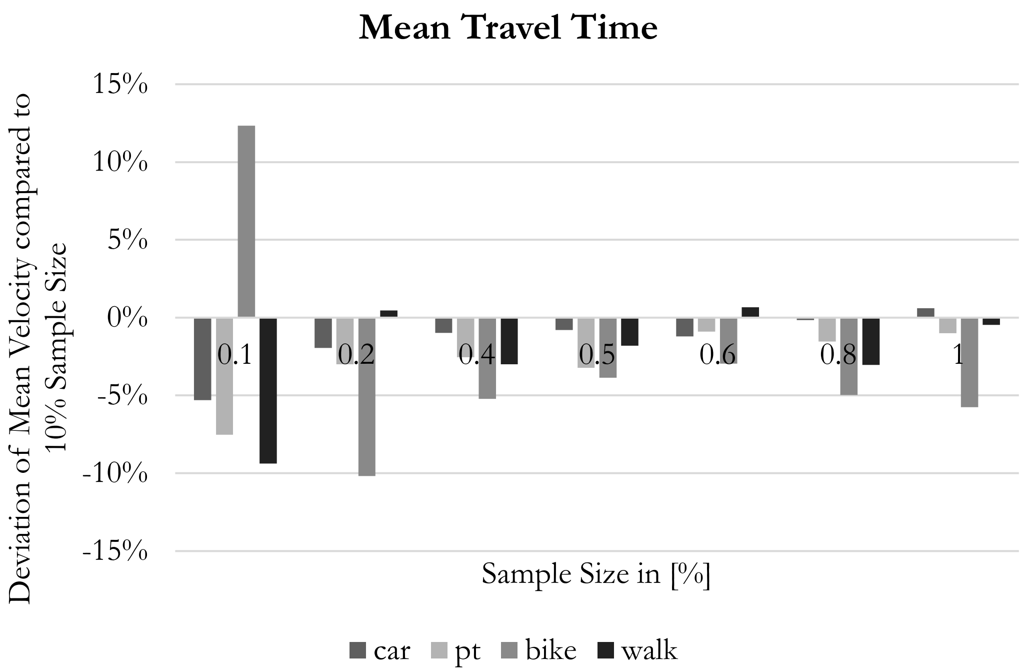

Figure 63: Difference of mean travel times between considered sample size and reference scenario

Figure 64 shows the reduction in computation time compared to the reference scenario. The results show that downscaling the sample size leads to computation time savings of up to 95% at 0.1% sample size compared to the reference scenario. The more the sample size is scaled down, the greater the savings in computing time.

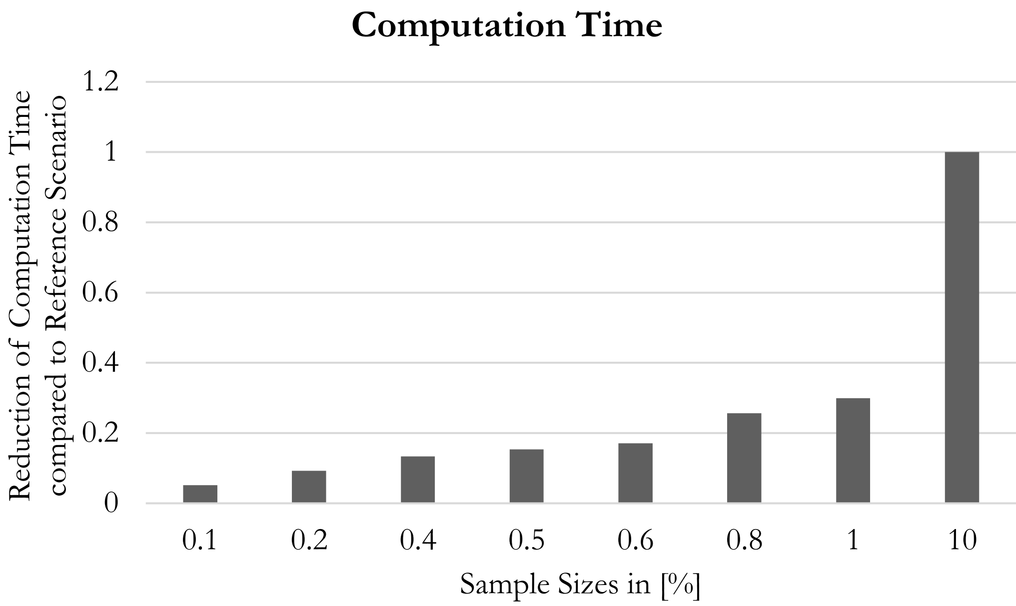

Figure 64: Difference of computation time between considered sample size and reference scenario

Overall, it can be summarized that the modal split can be kept almost constant with small deviations when scaling down the sample size. However, the consideration of the target variables show that the deviations and thus the side effects of the scaling become larger with increasingly smaller sample sizes, as shown in Figure 60. Considering these deviations, it can nevertheless be stated that a downscaling of the sample size generates comparable scenarios with a similar mobility behavior and thus reduces the computation time immensely. Since the goal of the downscaling is to calculate similar $CO2_{eq}$ emissions, costs and energy demand and not the optimization of traffic flows, this approach is valid. In Figure 65 the total $CO2_{eq}$ emission including production emissions for all travel modes per individual agent per year for the two scenarios is shown for the sample sizes of 0.1% and 10%. In the first scenario the current status of the mobility system in Berlin with mainly ICEVs is considered. In the second scenario a 100% BEV setup is considered. Here it can be seen that scaling has a little impact on the emissions for both scenarios. Further analyses are performed in chapter 10.

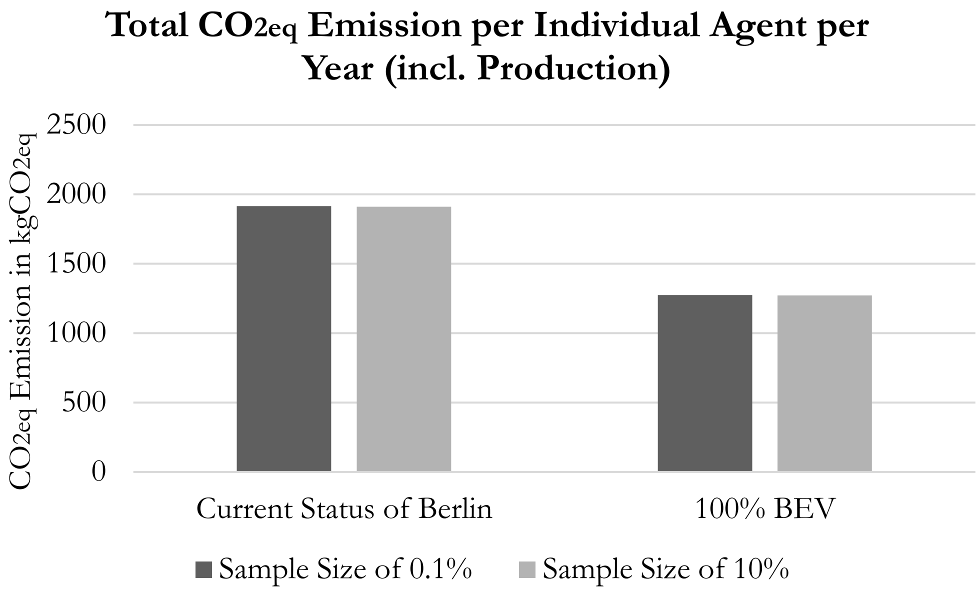

Figure 65: Total CO2eq emissions per individual agent

In addition, it is possible to match the target variables via the freespeed of the links even better. Here, for example, a reduction of the freespeed of all links by 15% with a sample size of 0.1% with the same simulation settings and factors leads to a similar modal split. In addition, the deviation in the average speed of cars is reduced to 4% instead of the 8% as shown in Figure 62. This shows that by iteratively adjusting the freespeed of the links, not only the modal split of the reference scenario with 10% sample size, but also the relevant target variables can be reproduced. However, this approach will not be pursued further in the following since physical changes in the system can generate unintended side effects.

The downscaled mobility system helps to calculate, understand as well as it enables an optimization with regard to the considered target criteria. In this thesis a compromise between results quality and computation time is chosen. Therefore, in the application of the optimization, the converged 0.5% sample size is taken to find optimal parameter settings for the mobility system since the computation time is reduced drastically and all target criteria of the mobility simulation of the 0.5% sample size including the modal split are similar to the reference scenario. Nevertheless, it is important to state that these factors are derived with the scenario, in which cars as network modes and public transport, bike and walk as teleported modes are considered. If new scenarios are analyzed, for example with new travel modes, it needs to be checked if these derived factors are still valid. It is also important to make sure, that these new travel modes are scaled accordingly.

9.4.2 Reduction of number of iterations

In this section, the number of iterations is examined in more detail to see whether it can be reduced. Figure 66 shows the modal split determined for the respective iteration under consideration. This shows that a reduction in the number of iterations does not make sense, due to the change of the modal split over the different iterations. Due to the co-evolutionary approach in MATSim, a certain number of iterations must be calculated until the results settle and converge. However, not only the modal split needs to converge, but also the routing of the vehicles becomes stable only after many iterations. Experience during this thesis has shown that this is achieved after about 200 iterations.

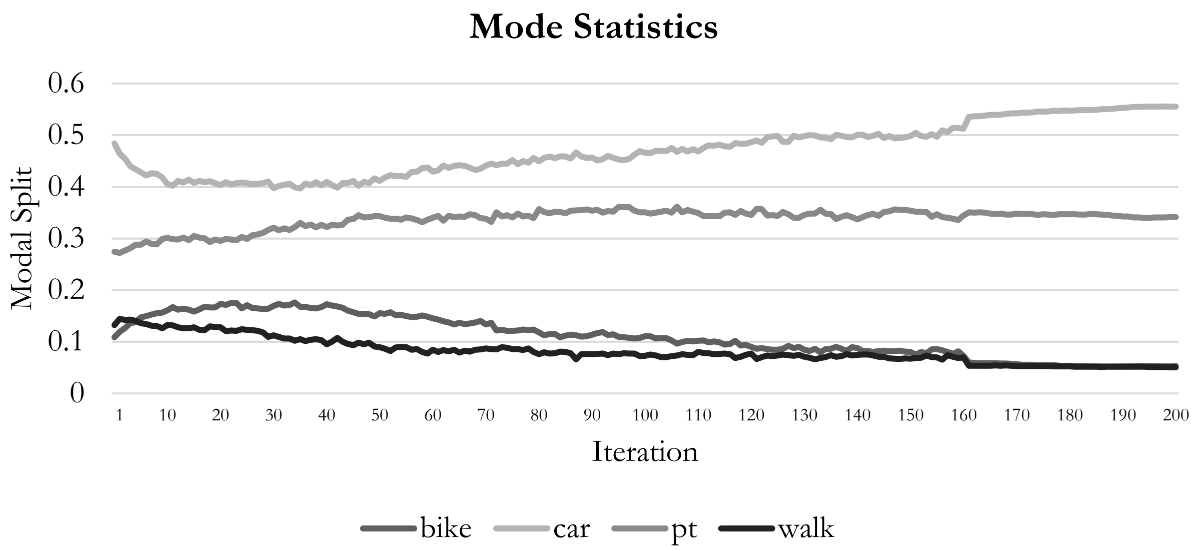

Figure 66: Share of travel modes for all iterations

Another possibility that exists is the generation of an iterated scenario that can subsequently be used as a baseline plan. For this purpose, a converged plan with 200 iterations is generated in a pre-process as a base plan for the optimization. Subsequently, further iterations are calculated with this base plan. Figure 67 shows the results of the modal split of the further iterations. The results show that the modal split remains almost constant for a converged plan. Thus, the assumption can be made that a converged plan leads to a representative mobility behavior and that only a few iterations are sufficient. A reduction in the number of iterations within the optimization loop can be achieved under certain premises such as the same mobility system configuration. This includes the transport mode offer as well as the calibration of the transport modes and activities in the configuration.

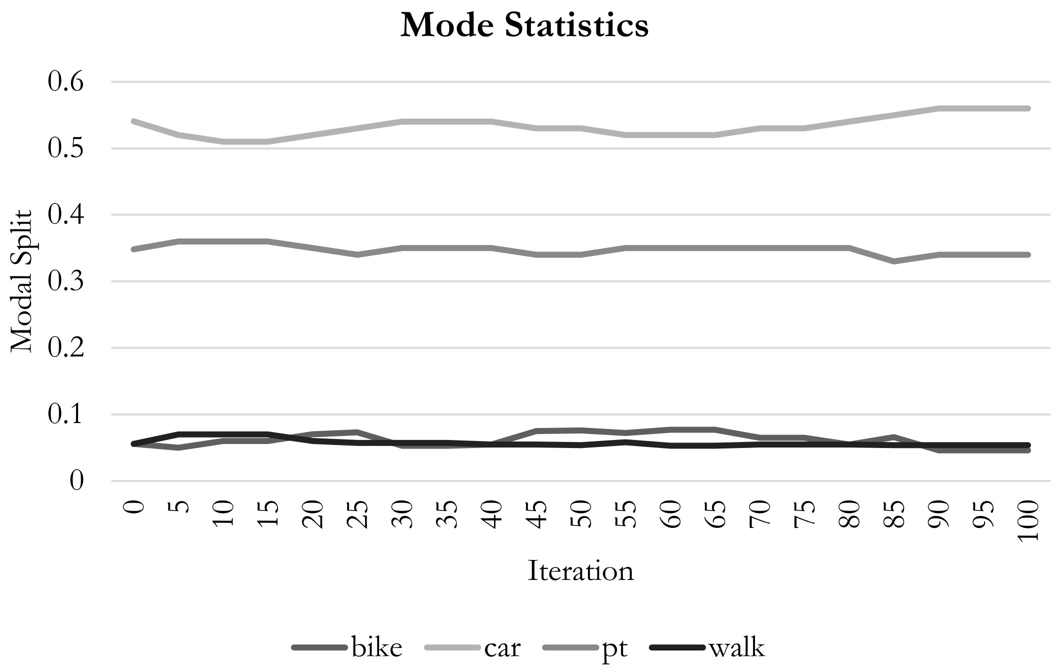

Figure 67: Share of travel modes for additional 100 iterations

However, if changes are made in the mobility system such as adding new travel modes, it needs to be checked, if these assumptions are still valid. For this consideration, the following calculations are performed. A converged plan is taken as the base plan for further calculations. Subsequently, micro mobility is offered as another mobility type. Here, the number of iterations per mobility simulation is increased. The same calculated storage and flow capacity factor in dependence of the sample size is used. The results are shown in Figure 68. Looking at the overall mobility system it can be seen that the influence of the new travel mode, in this case micro mobility, has no large impact on the overall modal split.

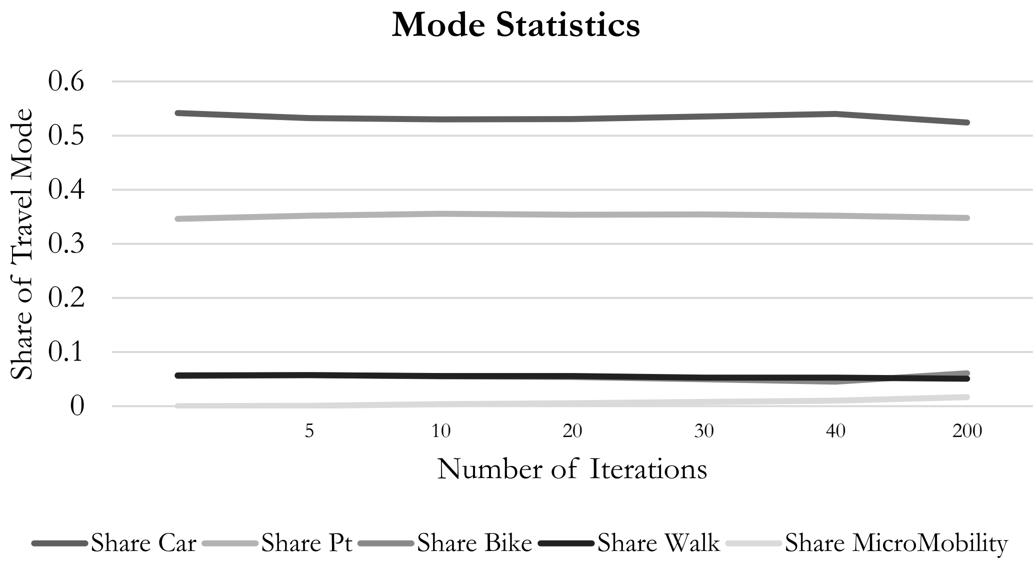

Figure 68: Share of travel modes for additional 100 iterations

In Figure 69 the share of micro mobility is shown over the different number of iterations considered in the mobility simulation. Here it can be seen that the assumption made previously, that for additional iterations the mobility behavior remains constant, no longer applies, since the share of micro mobility increases steadily with the number of iterations up to a share of 1.8%, while other travel modes such as cars or public transport decrease. This shows that the agents' plans have not yet converged with a lower number of iterations. In order to evaluate new mobility concepts and their predicted impact on the future mobility system a converged plan is needed. These results show, that if big changes are made in the mobility system, such as adding new travel modes, a new base plan needs to be calculated. In this case, before evaluating the new system with micro mobility, a new base plan with 200 Iterations including micro mobility should be calculated. Then the number of iterations within the optimization loop can be reduced again. In addition, it can be seen that the calculated storage and flow capacity factor are still valid. The mobility behavior remains constant for different sample sizes with the recommended factors compared to the 10% reference scenario with included micro mobility.

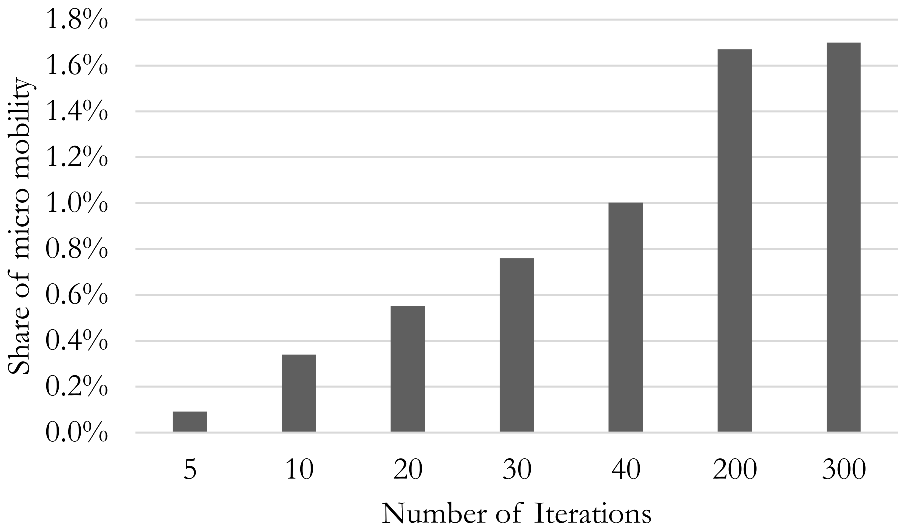

Figure 69: Share of micro mobility for different number of iterations

From this analysis, it can be deduced that due to the software design of MATSim, agents innovate their plans, if changes are made. Therefore, changes in the system require a minimum number of iterations for saturated market penetration of the considered travel modes. In this work, the minimum number of iterations is 200 runs, since here a converged plan in terms of modal split and routing can be achieved as shown in Figure 69. However, with the help of converged plans, it is possible to use them as base plans in the optimization loop and reduce the number of iterations there, since converged plans hardly change and the mobility behavior remains almost constant. Therefore it is recommended to always use converged and routed plans as an inertial plan for the mobility simulation. These findings as well as the insights from the downscaling of the population are implemented in the holistic optimization method in the following.

9.4.3 Holistic optimization approach

The following section describes the holistic optimization approach (Figure 70) with the findings of the previous chapters. In the first step, the reference scenario is defined. In this case, a 10% sample size scenario of the considered Berlin scenario is considered. Subsequently, a comparable downscaled system with a sample size of 0.5% is generated with the premise of a constant mobility behavior. In the next step, the first mobility simulation takes place. The simulation is run until the agents' plans converge. This converged plan describes the actual state and serves as the basis for the optimization as well as the base scenario for the later comparison.

Then the optimization starts. For this, the parameters are first set in the system. In the first optimization loop, these are random start values. If settings in the mobility system are changed that can have a major impact on mobility behavior, such as adding a new travel mode, a new converged plan must first be generated. Here it is assumed that the changes with a 0.5% sample size are representative for the reference sample size of 10%. This assumption is validated at the end of the optimization when the optimal settings are applied to the 10% sample size scenario. Otherwise, this step is skipped. Then, it is checked if a valid scenario is generated. In the following the mobility system is designed and evaluated. This includes the powertrain simulation, evaluation of the other travel modes as well as the evaluation of the infrastructure with respect to the target variables CO_{2eq} emissions, costs and energy demand. Via the genetic algorithm, new parameter settings are determined until the optimal variables are found with respect to the defined optimization target. The deliberate separation of the individual simulation blocks has the additional advantage here that calculations are only performed when they are necessary to save further computation time. In the powertrain simulation, there is also the option of loading a vehicle portfolio from a pre-process to further reduce the computation time. Once the optimization is done and optimal parameter settings are derived, they are applied on the actual reference scenario with the 10% sample size and the results are compared to the base scenario to quantify the impact of the optimization of the mobility system.

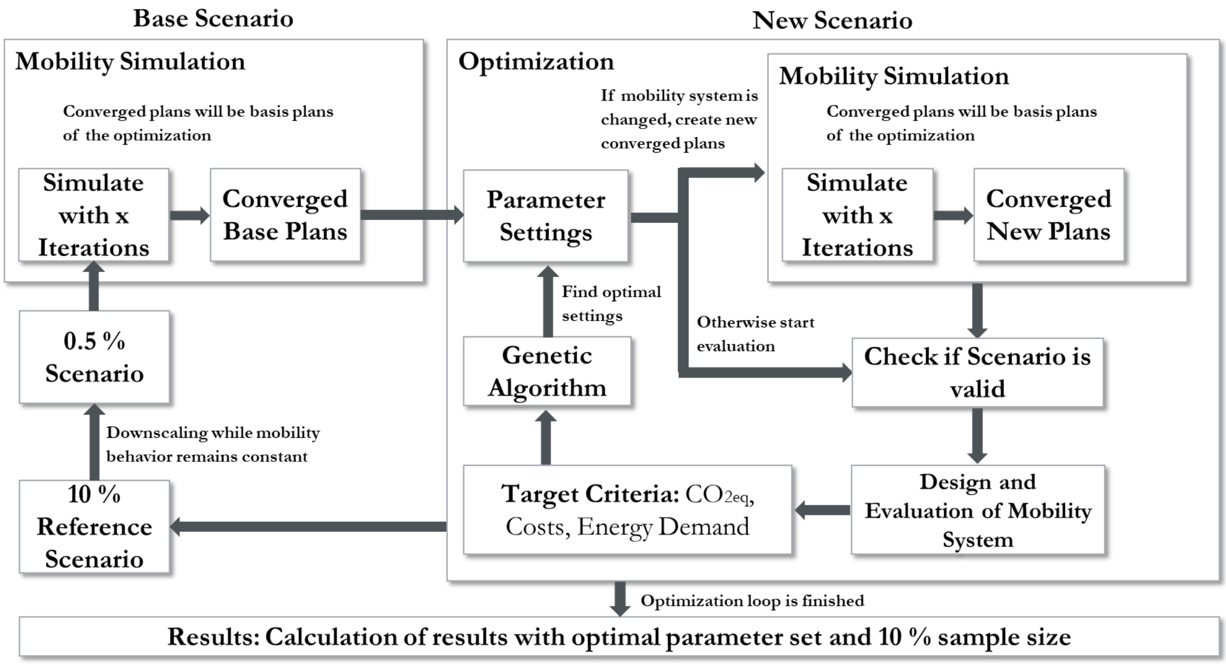

Figure 70: Overview of the holistic optimization process

Overall, it could be shown that the reduction of the sample size is valid for the considered use case and fulfills all requirements regarding similar mobility behavior as well as target values of the mobility simulation. However, it has to be taken into account that for other use cases, e.g. including sharing concepts, new effects may occur that need to be analyzed separately.

9.4.4 Example of powertrain optimization

In the following example the holistic optimization approach is applied on the mobility system of Berlin as described in chapter 5. Here, a multidimensional optimization is carried out in which the powertrain portfolio for the considered region of Berlin is optimized regarding emission and cost reduction. Initially, the actual state of the powertrain portfolio is analyzed based on the statistical data of the Kraftfahrt-Bundesamt [Kraftfahrt-Bundesamt 2022]. Here, the powertrain portfolio consists of 94% ICEVs, 1% BEVs and 5% (P)HEVs. The optimization is performed with a 0.5% sample size of the population. For PHEVs, a realistic charging behavior is assumed as described in Chapter 6. The optimizer varies the proportions of the powertrain types until the objective is achieved. In total, 5 generations with 200 variants each are considered. One variant represents a holistic mobility system. The results of the last generation with all its variants are shown in Figure 71. The consideration of total emissions over costs shows that a Pareto front emerges. A conflict of objectives thus arises in the determination of the optimum powertrain portfolio.

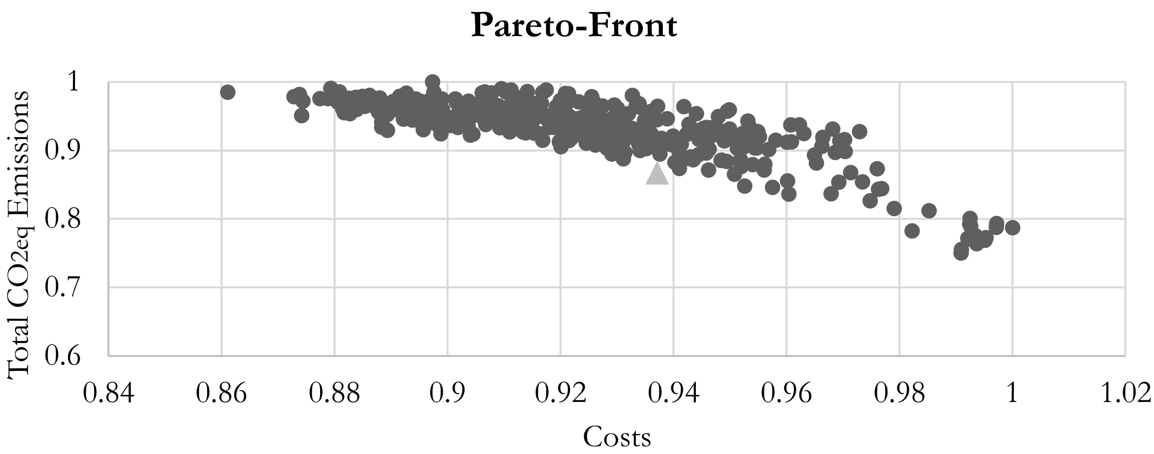

Figure 71: Calculated solutions of powertrain optimization

Since the solutions are determined by means of optimization with a 0.5% sample size, it needs to be shown that these settings also apply to larger sample sizes. In order to show that the optimal settings also apply to larger sample sizes, a parameter set is then selected from the solutions and applied to the two sample sizes of 0.5% and the reference sample size of 10%. For the selected parameter set, shown as a light grey triangle in Figure 71, the powertrain portfolio consists of 33% ICEVs, 37% BEVs, 27% PHEVs and 2% FCEVs. This parameter set is a solution that represents a compromise of cost as well as emission reduction. Figure 72 shows the results of the target parameters of total CO_{2eq} emissions, costs as well as energy demand per agent as well as per year. Compared to the results of the current state of Berlin shown in Figure 65, it can be seen that the emission decreased and that the optimizer has found a valid solution. The results show that with the determined optimal setting of the powertrain portfolio for the 0.5% sample size, similar results are calculated for the 10% sample size as well. This example outlines that optimal settings for larger sample sizes can be determined with a reduced sample size. In the next chapter a sensitivity analysis is performed to examine the influence of different variables in the overall system.

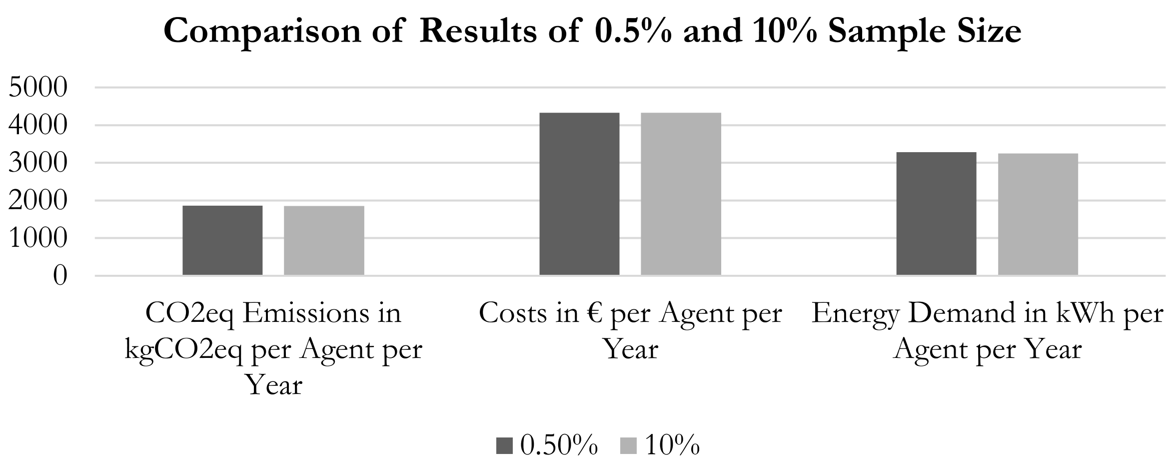

Figure 72: Comparison of results of 0.5% and 10% sample size

10 Sensitivity analysis

In this chapter, the results of a sensitivity analysis are given. For the sensitivity analysis, the described example scenario for Berlin is analyzed. Here, the sample sizes of 0.1% and 10% are considered. The time period set is 14 years. Two scenarios are simulated. In the base scenario, the actual state of the mobility system under consideration is presented. The powertrain portfolio consists mainly of ICEVs: 94% of vehicles are ICEVs, 4.0% are hybrid vehicles, 1.0% are PHEVs and 1.0% are BEVs. Other types of powertrains are neglected here, since their share is very small [Kraftfahrt-Bundesamt 2022]. For a comparison a new single scenario is defined. Here, the same mobility behavior and a 100% BEV scenario is assumed for the powertrain portfolio. In both scenarios, the total $CO2_{eq}$ emissions, costs from the customer's point of view, and the energy demand of the mobility system are calculated for the two sample sizes of 0.1% and 10% and then compared to investigate the influence.

The goal of the sensitivity analysis is to examine the influences of the scaling of the population as well as the influences of the input key-values. Since it must be ensured that the scaling does not have a major influence on the results and thus delivers good result quality with reduced computing power, this will be investigated in detail. In addition, the influence of selected parameters on the target values $CO2_{eq}$ emissions, costs and energy demand will be investigated. The $CO2_{eq}$ key-values for the production of the battery, the internal combustion engine as well as the electricity mix and the tank-to-wheel emissions of the fossil fuels will be analyzed when considering the $CO2_{eq}$ emissions. The tank-to-wheel emissions can be reduced by using renewable energy. Since ICEVs dominate the powertrain portfolio in the first scenario, the focus here is on the internal combustion engine as well as the respective fuel. In the second 100% BEV scenario, the batteries have a large impact during the production phase and here the impact in the holistic system will be investigated. In the use phase, the electricity mix as the main energy source has a large impact when considering BEVs and is therefore examined in more detail. When considering costs, the production costs of the battery and the internal combustion engine as well as electricity and fuel costs are varied. For the energy demand, the charging efficiency of the BEVs is analyzed to estimate the impact of charging losses on the energy demand in the overall system.

10.1 Influence of sample size

In the first step, the influence of the sample size on the target variables is investigated. Figure 73 - Figure 75 show the results of the analysis. Here the deviations between the sample sizes are quantified. For this purpose, the results of the target values of the sample sizes between 0.1% and 1% are compared with the results of the sample size of 10%, taking into account the scaling factor. All the results are extrapolated to 100% sample sizes to achieve a better comparability between the values. Figure 73 shows the CO_{2eq} Emissions per agent per year for cars. The largest deviations in the base scenario are found for the 1% sample size and lie in a range of 2%. The deviations in the new 100% BEV scenario are similar. Here it can be seen that again at the sample size of 1% the biggest deviation with 2% occurs, which is relatively small.

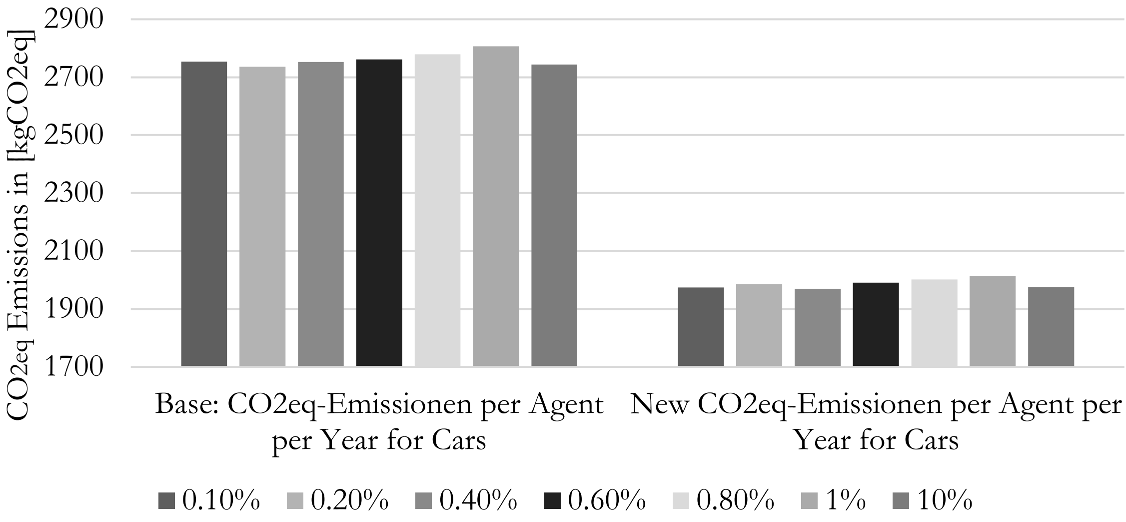

Figure 73: CO2eq emissions per agent per year for cars of considered sample size compared to the results of the 10% sample size

In Figure 74 the deviations for the costs are shown. It can be seen that the largest deviations are found for the 0.2% sample size in the base and new scenario and lie in a range of 2% as well. Overall, the deviations are relatively small. It is evident that with decreasing sample size, the deviations increase, since less individual agents with different paths and user behavior are considered. Nevertheless, these deviations are within a reasonable range.

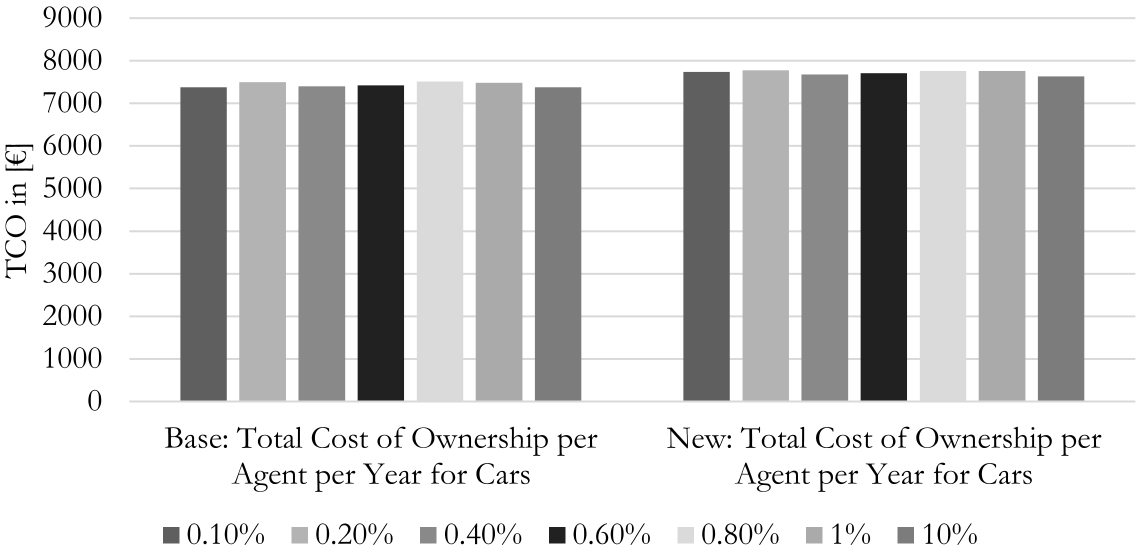

Figure 74: TCO per agent per year for cars of considered sample size compared to the results of the 10% sample size

In Figure 75 the deviations for the energy demand are shown. Here it can be seen that the largest deviations are found for the 0.8% sample size in the base and new scenario and lie in a range of 4%. Overall, the deviations in the base scenario are larger, but still relatively small. In this example it can be seen that the influence of the sample size on the target variables is very small. The ratios are almost equal to the scaling factor. For example, from 0.1% to 0.2% sample size corresponds to a doubling of the population size. This is also reflected in the target variables, i.e. a doubling of emissions, costs as well as energy demand with very little deviation in a range between 1-4% for the different target criteria. This is also true for both scenarios.

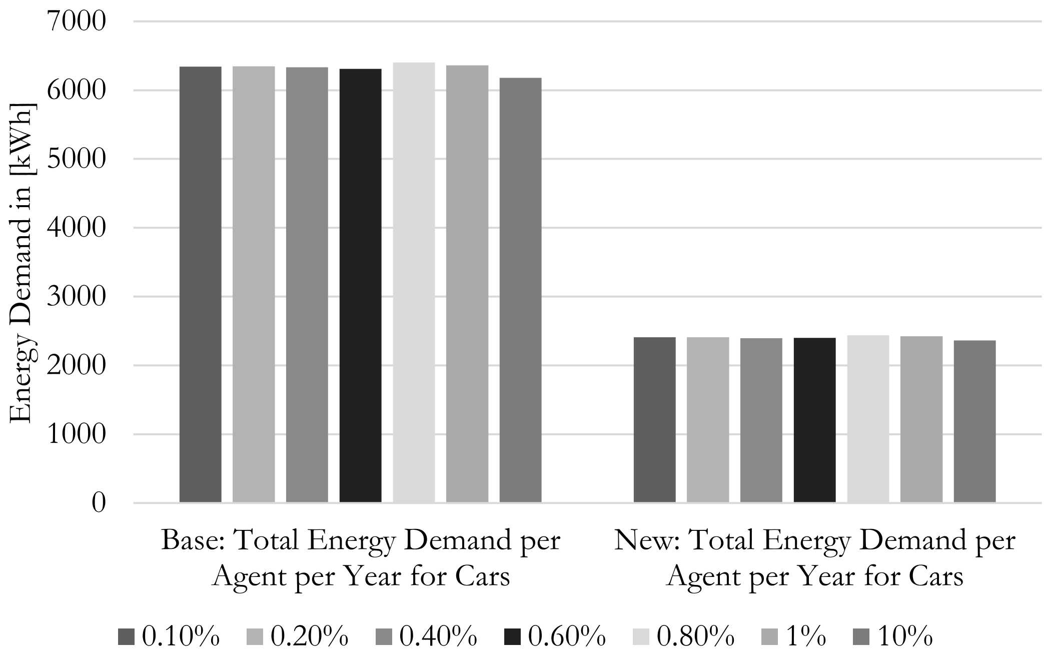

Figure 75: Energy demand per agent per year for cars of considered sample size compared to the results of the 10% sample size

Influence of sample size on optimization results

In the following the influence of the sample sizes on the optimization results is analyzed. The powertrain portfolio of the Berlin scenario under consideration is optimized in terms of $CO2_{eq}$ emissions and costs in the same way as in Chapter 9.4.4. To minimize emissions and costs, the optimizer varies the proportions of the powertrain portfolio. Figure 76 shows the results of the optimization for different sample sizes. A variant represents a scenario with the respective powertrain portfolio. Depending on the powertrain portfolio considered, suitable vehicles are assigned to the agents and the mobility system is considered holistically and evaluated in terms of $CO2_{eq}$ emissions, costs and energy demand. The results are presented in relative terms. The variants with the highest emissions and costs are taken as a reference and all other variants are compared with them. Overall, the result of the optimizations shows that the sample size has only a minor impact on the results. The Pareto front of the different sample sizes indicate a similar trend as well as a similar dispersion. This shows that with smaller sample sizes similar exploration behaviors in the search space can be achieved and thus suitable results for the reference scenario can be determined.

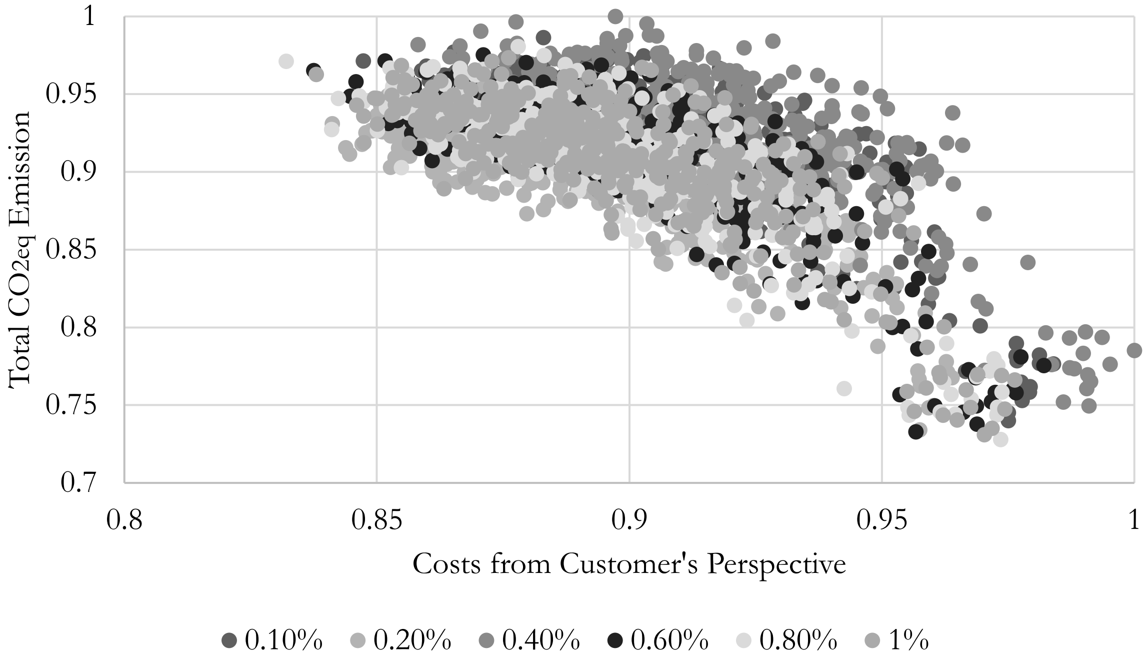

Figure 76: Pareto-Front of optimization results for different sample sizes

10.2 Influence of key-values on CO2eq emissions

In the next step, the influence of the key-values on the target variables is examined. All three target variables are analyzed separately and the 1% sample size is assumed for the population size each. Due to the high impact of cars on the transport sector, the focus in this sensitivity analysis lies therefore on cars. For all parameter settings the enhanced LCA approach is applied, i.e. the dynamic system behavior is considered in the sensitivity analysis. In addition, the derived distances for each agent from the mobility simulation is considered instead of a typical value of 200.000 km valid for all agents. Thus, next to the typical long distance commuter the cases with agents, who drive shorter distances in urban region and their impact on the mobility system are considered here. The yearly driven distances are calculated as described in chapter 5.2.

In terms of the CO2eq emissions, the CO2eq parameters for the production of batteries and combustion engines as well as the electricity mix for the charging of BEVs and the well-to-tank emissions of fossil fuels are varied. The parameter settings for the sensitivity analysis are shown in Table 14. The values in the first row are the reference values. The results of the other parameter settings are compared with these reference values.

Table 14: Parameter settings for the sensitivity analysis of the CO_{2eq} emissions

Parameter settings number	CO_{2eq} key-values for batteries in [$kgCO_{2eq}$/kWh]	CO_{2eq} key-values for electricity mix in [$kgCO_{2eq}$/kWh]	CO_{2eq} key-values for combustion engine in [$kgCO_{2eq}$/kW]	Well-to-Tank emissions in [gCO_{2eq}/kWh]
Reference values	75	0.331	3.05	58
1	60	0.331	3.05	58
2	90	0.331	3.05	58
3	75	0.300	3.05	58
4	75	0.360	3.05	58
5	75	0.331	2.7	58
6	75	0.331	3.4	58
7	75	0.331	3.05	52
8	75	0.331	3.05	64

The two scenarios are analyzed separately here. In the first scenario, the current state of the powertrain portfolio in Berlin is described. The powertrain portfolio consists of >94% ICEVs, ~5% (P)HEVs and 1% BEVs [Kraftfahrt-Bundesamt 2022]. In the first four parameter settings, the emission parameters for the production of the battery as well as the electricity mix and the resulting emissions are varied. Due to the very high proportion of ICEVs in this scenario, the variation of these parameters has hardly any influence and can therefore be neglected with regard to the overall system, as can be seen in Figure 77. In the other parameter settings 5-8, the emission key-values for the production of the combustion engine and the well-to-tank emissions of fossil fuels, in this case gasoline, are varied. For these boundaries, the influence of the parameter variation in the range of +-10% is also small and the results vary in the range of +-0.2% to +-0.5% compared to the reference parameter settings, as can be seen in Figure 77. Overall, it can be stated that the potential for ICEVs seems to have been exhausted with regard to these variables and improvements can only be achieved with great effort.

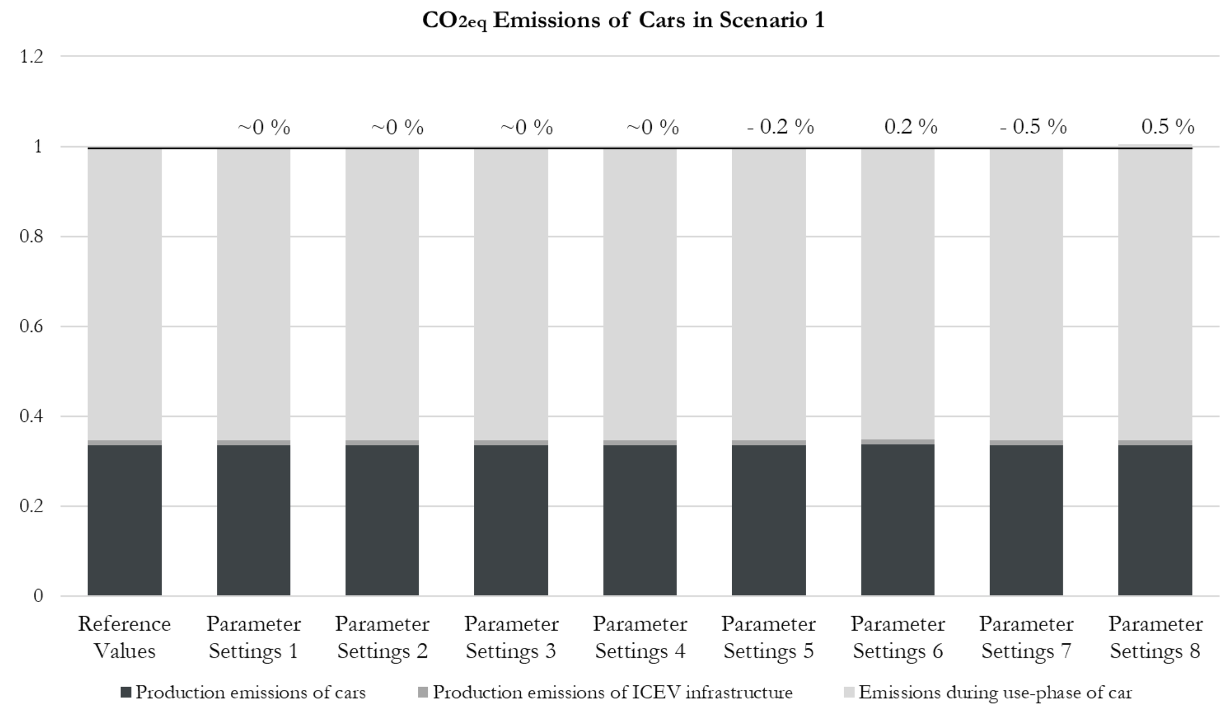

Figure 77: Influence of various parameter settings on total CO_{2eq} emissions of cars in scenario 1

In the second scenario a 100% BEV scenario is assumed and calculated. Overall, there is greater potential here, as can be seen in Figure 78 when considering the first four parameter settings. The battery production emissions are varied between 60 and 90 $kgCO_{2eq}/kWh$ and this leads to a change in CO_{2eq} emissions in the overall system of ±3.5% compared to the reference parameter settings. It can also be stated, that the battery emissions have a high influence on the overall emissions of the mobility systems. This also shows the high impact of the production emissions in the mobility system. The influence of the electricity mix is high as well. In the simulation with the reference values, the stored electricity mix curve is considered, which decreases dynamically over the years. The average value over the 14 years is 331 gCO_{2eq}/kWh. For the sensitivity analysis these values are increased and decreased by 10%. With that, the average electricity mixes with an emission value of 300 gCO_{2eq}/kWh and 360 gCO_{2eq}/kWh are now assumed here. Reducing the average electricity mix to 300 gCO_{2eq}/kWh leads to a 3.5% reduction in total emissions and increasing emissions to 360gCO_{2eq}/kWh leads to a 3.5% increase in emissions compared to the reference parameter settings. It can be seen that the electricity mix has a big influence, if it comes to emission reduction in the overall mobility system. In this example, only changes in emissions in the electricity mix in the range ±10% are considered. However, there are solutions that enable far greater savings, such as charging with green electricity with almost zero emissions. Overall, this shows that very high reductions in emissions during the use phase of electrified vehicles can be achieved with simple means, which also have a very large impact on overall emissions. A change in the production emissions of combustion engines and fossil fuels have no impact on BEVs, as can be seen in parameter Settings 5-8, as shown in Figure 78. The results show that the

BEVs seem to have a very large potential that can be achieved with relatively little effort compared to the first scenario.

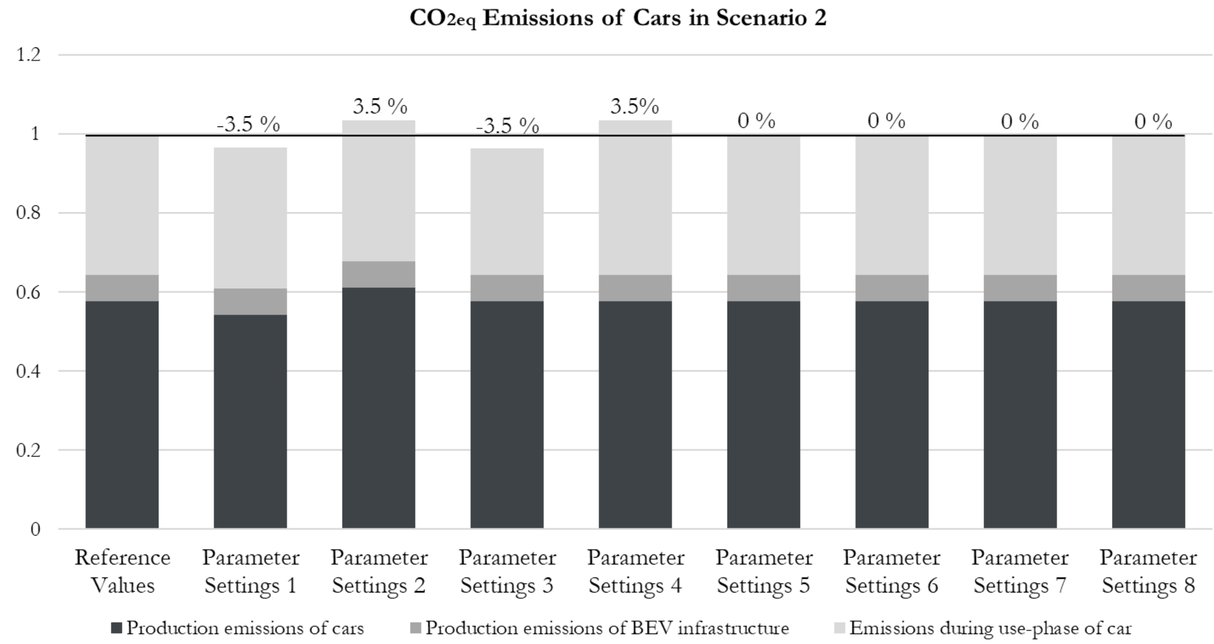

Figure 78: Influence of various parameter settings on total CO_{2eq} emissions of cars in scenario 2

In the following, the influence of the key-values on the individual forms of mobility and thus on the overall system is examined for scenario 1. Figure 79 shows the emissions of the various forms of mobility. The production emissions of passenger cars, public transport, bicycles, the required infrastructure for ICEVs and the emissions in the use phase of passenger cars and public transport are shown. The emissions of the public transport are determined with the help of key-values depending on the passenger kilometers. Here, a value of 37 gCO_{2eq}/km is assumed for the production emissions and a value of 62 gCO_{2eq}/km for the emissions in the use phase based on [Merchan et al. 2017]. Electrically powered public transport vehicles are assumed for the operation of the public transport. This leads to the fact that a change in the electricity mix also has an impact on the emissions in the use phase. It is assumed that the emissions in the use phase change proportionally to the changes in the electricity mix. In the first scenario, a similar pattern as in Figure 77 emerges. Since there are hardly any BEVs in the powertrain portfolio in the first scenario, a change in production emissions of batteries has no effect. In this scenario, a change in the electricity mix has an impact on emissions in the use phase of public transport. Here, it can be seen that a ±10% change in electricity mix results in a ±1% change in total emissions. Furthermore, it can be seen in Figure 79 that a change in the production emissions of the internal combustion engines has hardly any impact in the holistic system. Whereas a ±10% change in well-to-tank emissions cause a ±0.4% change of the emissions in the overall system. This is mainly due to the fact that the use phase of passenger cars, especially ICEVs has the largest impact on the total emissions in the mobility system.

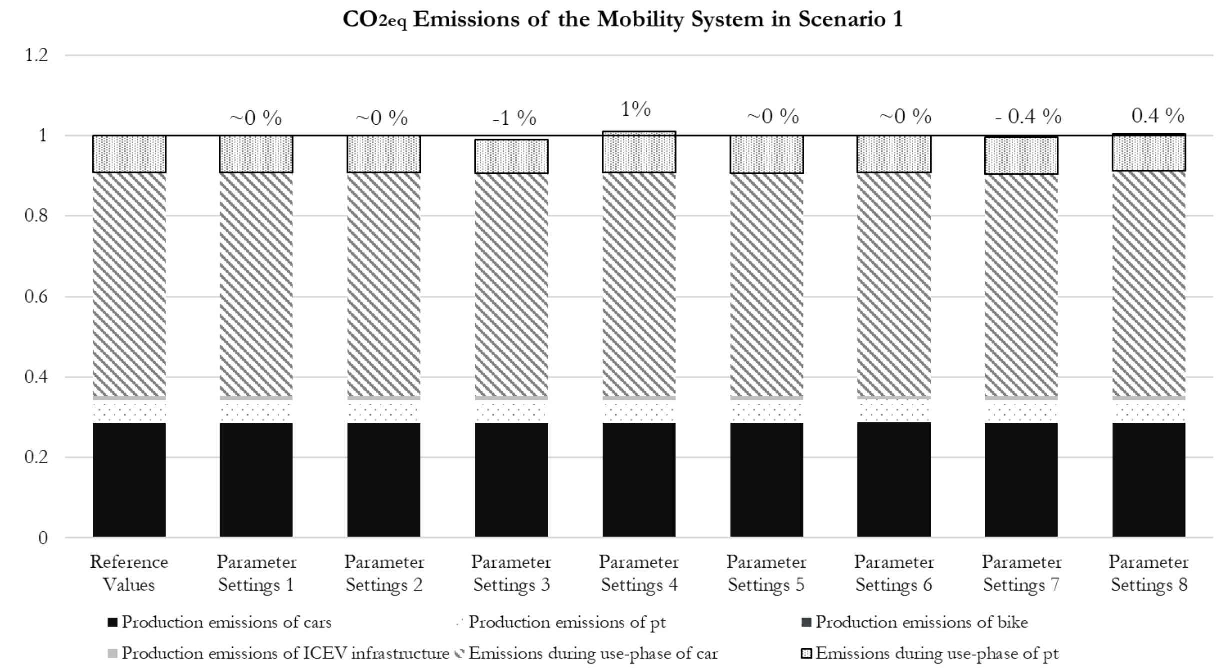

Figure 79: Influence of various parameter settings on total CO_{2eq} emissions of the mobility system in scenario 1

In Figure 80 the influence of the key-values on the individual forms of mobility and thus on the overall system is examined for scenario 2. Again, it can be concluded that vehicles have the largest impact on CO_{2eq} emissions in the mobility system. A ±10% change in vehicle battery production emissions results in a ±3% change in emissions across the system, as seen in parameter settings 1 and 2. This shows the large impact of the passenger cars and in this case specifically the large impact of the production emissions of BEVs. In parameter Setting 3 and 4, the emissions in the electricity mix are varied by ±10% and this leads to a ±4% in the emissions in the whole system. Again, this shows the large influence of the electricity mix in an electrified mobility system including BEVs and electrically powered public transport. Emissions in the use phase account for almost 40% of the total emissions in the mobility system, as can be seen in Figure 80, which can be saved by means of renewable energy. Since there are no ICEVs in the second scenario a change in the production emissions of the combustion engine as well as the well-to-tank emissions of fossil fuels have no influence on the emissions of the overall mobility system, as can be seen for the parameter setting 5 to 8.

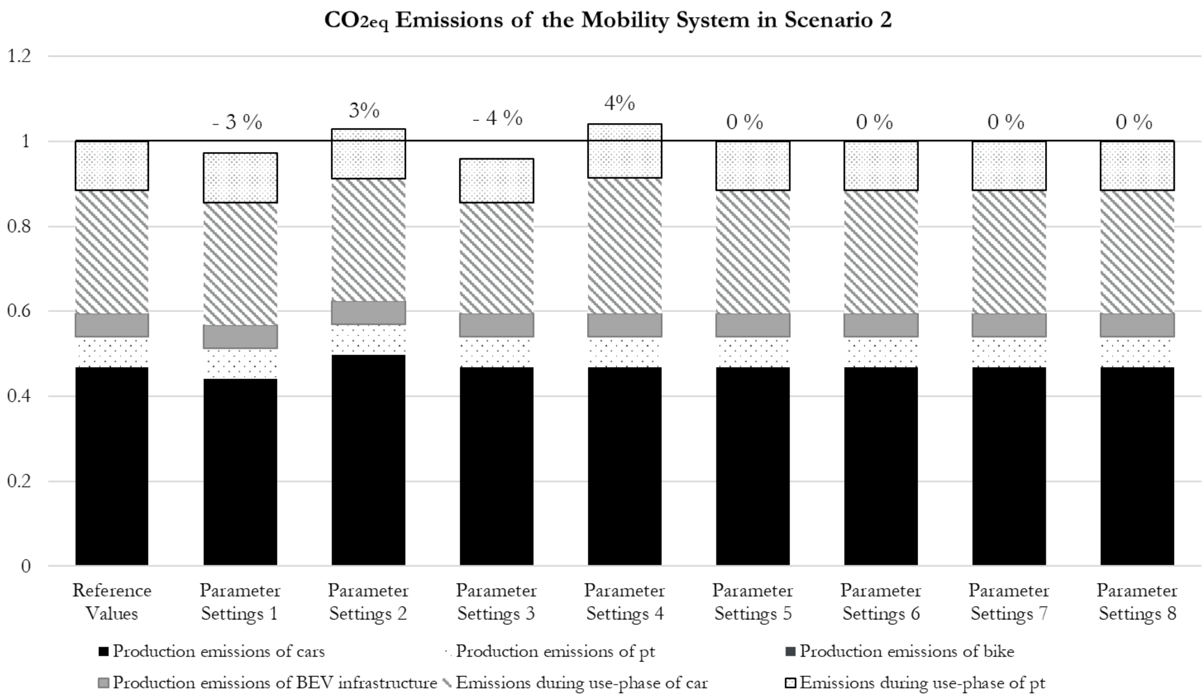

Figure 80: Influence of various parameter settings on total CO_{2eq} emissions of the mobility system in scenario 2

10.3 **Influence of key-values on costs**

When considering the costs, the cost parameters for the battery and combustion engine production as well as the electricity and fossil fuel costs are varied. The parameter settings of the sensitivity analysis are shown in Table 15. The values in the first row are the reference values. The results of the further tests are compared with the reference values.

Table 15: Parameter settings for the sensitivity analysis of the costs

Parameter settings number	**Production costs of batteries in €/kWh**	**Electricity costs in ct€/kWh**	**Production costs of combustion engine in €/kW**	**Fossil fuel costs in €/l**
Reference values	268	22	72	1.5
1	230	22	72	1.5
2	300	22	72	1.5
3	268	20	72	1.5
4	268	24	72	1.5
5	268	22	65	1.5
6	268	22	79	1.5
7	268	22	72	1
8	268	22	72	2

The two scenarios are analyzed separately. In Figure 81 the mobility costs for the first scenario for the used travel modes is shown. In the first four parameter settings the production costs key-values for the battery and the electricity costs are varied. Since the first scenario mainly consists of ICEVs, this has a very little impact on the overall system. In the parameter setting 5-8 the productions of the combustion engine as well as the fossil fuel costs, in this case gasoline, are varied. Here it can be seen that a variation of the production costs of the combustion engine in a range of ±10% lead to a change in the mobility costs in the overall mobility system of ±0.4%. The variation of the fossil fuel costs from 1.5 €/l to 1 €/l as well as 2€/l lead to overall change of the mobility costs in the mobility system of ±2%. The operation costs have a higher influence on the mobility costs than the single production costs.

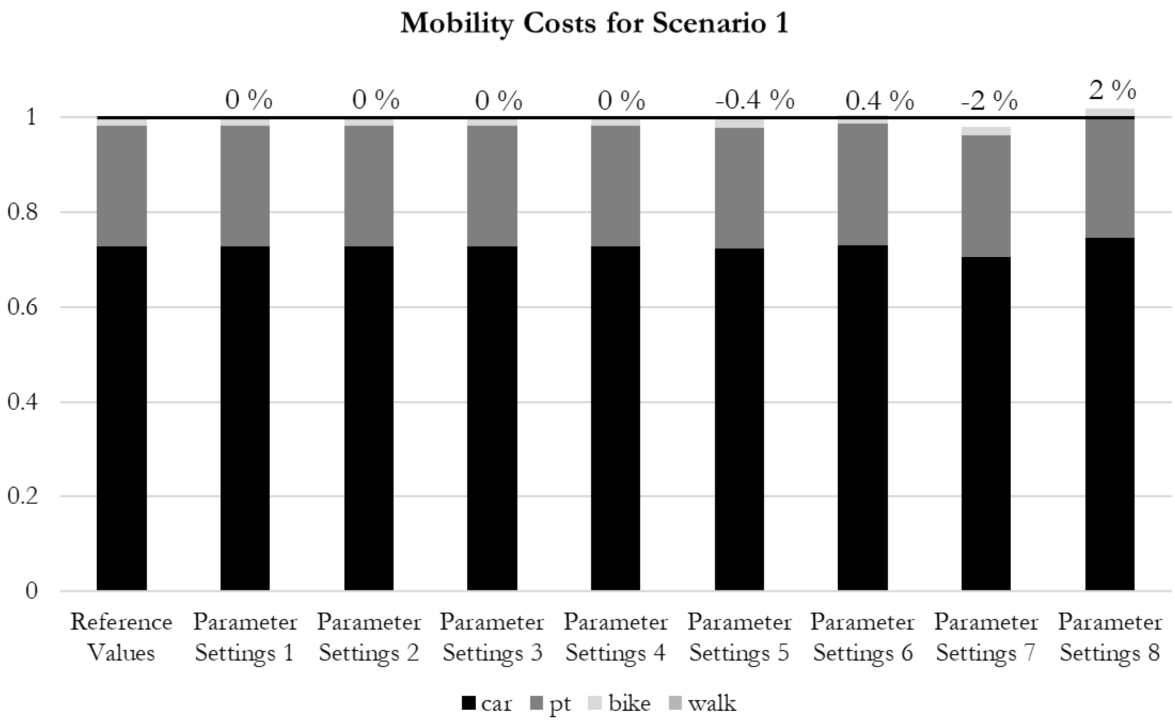

Figure 81: Influence of various parameter settings on mobility costs per travel mode in scenario 1

In Figure 82 the mobility costs for the second scenario are shown. In the first two parameter settings the production costs of batteries are decreased to 230 €/kWh as well as increased to 300 €/kWh. This leads to a total increase of the mobility costs in the mobility system of ±2%. In the parameter setting 3 and 4 the electricity costs for charging are decreased to 20 ct€/kWh and increased to 24 ct€/kWh. In this case it is assumed that these costs apply to every form of charging. These changes lead to an overall change of the mobility costs in the mobility system in a range of ±0.3%. The variation of the production costs of combustion engines as well as fossil fuel costs have no effect on the 100% BEV scenario, as shown in Figure 82. Here it can be seen that the production costs of batteries have a higher impact on the total mobility costs. This reflects the greater leverage of the production phase with regard to costs due to the dynamic system behavior and relatively frequent change of vehicles of the agents over the years.

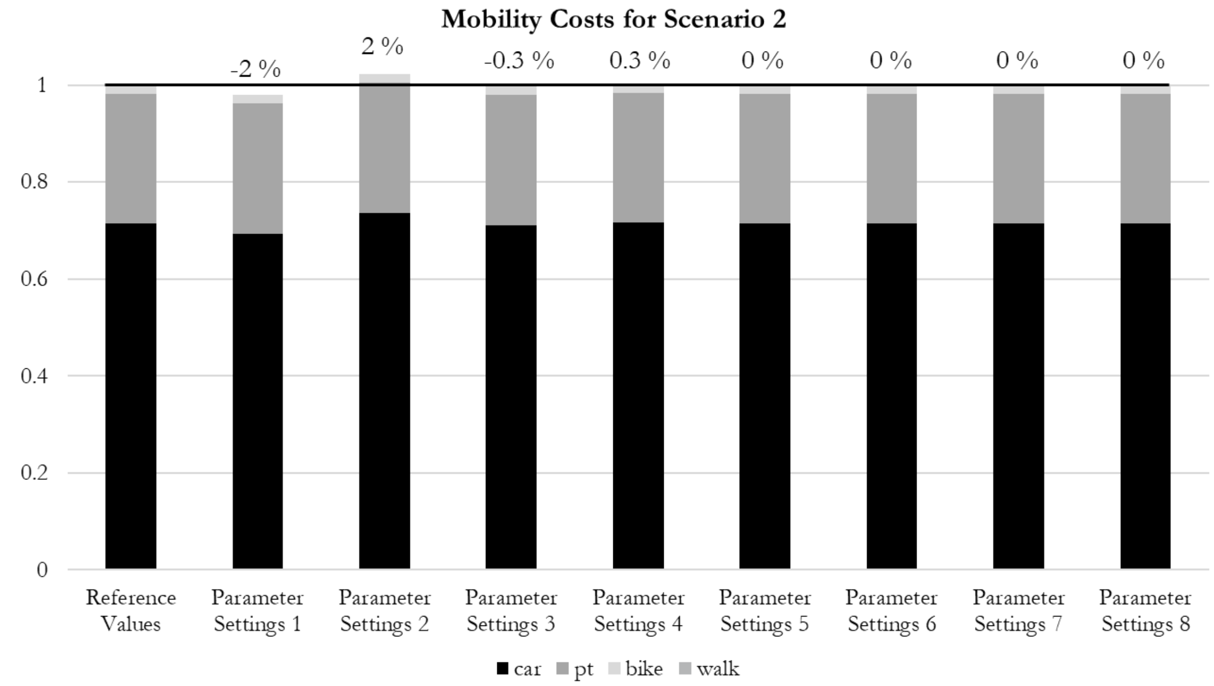

Figure 82: Influence of various parameter settings on mobility costs per travel mode in scenario 2

10.4 Influence of key-values on energy demand

When considering the energy demand, the charging efficiency of the charging station is varied. The parameter settings of the sensitivity analysis are shown in Table 16. The values in the first row are the reference values. The results of the further tests are compared with the reference values.

Table 16: Parameter settings for the sensitivity analysis of the energy demand

Parameter settings number	**Efficiency of charging station**
Reference values	0.89
1	0.83
2	0.95

Figure 83 shows the relative changes in the calculated energy demand due to the change in the charging efficiencies for both scenarios. In the first parameter setting, the charging efficiency is lowered to 0.83. In the first scenario, this again has a very small impact due to the very high proportion of ICEVs in the powertrain portfolio, as shown in Figure 83 on the left side. In the second scenario, a deterioration of the efficiency leads to an increase of the energy demand by 1%, as shown in Figure 83 on the right side. In the second parameter setting, the charging efficiency is raised to 0.95. Again, this has hardly any impact on the first scenario and in the new scenario it leads to a reduction of the energy demand by 1%, as depicted in Figure 83 on the right side.

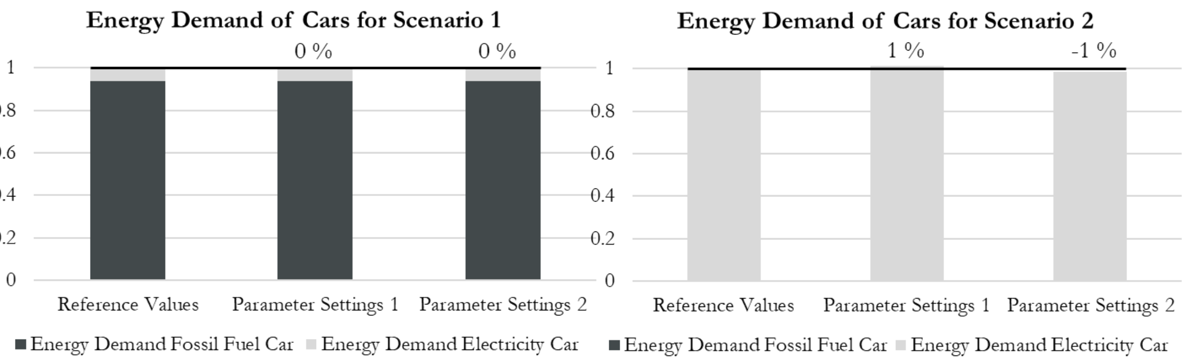

Figure 83: Influence of various parameter settings on energy demand of cars in scenario 1 and 2

Overall, the results show that the individual parameters have a relatively small influence on the costs and energy demand. From this, it can be concluded that the uncertainty of the results is low and thus, overall, a sufficient quality of results is achieved, which was initially defined as a requirement for the methodology. With regard to emissions, it can be seen that especially for BEVs there are potentials in order to reduce the overall CO_{2eq} emissions with relatively small effort, such as by producing green batteries or using clean energy for driving.

11 Application of the method

In this chapter, the method is applied exemplarily for the region of Berlin for different use cases in order to validate the methodology. In the first step, the scenario analysis is described. Subsequently, the actual state of the Berlin region is presented based on statistical data and this represents the reference scenario. In the next step, two use cases are calculated. On the one hand, a powertrain optimization of the vehicle portfolio with respect to CO_{2eq} emissions is performed for the mobility system. Then, a multidimensional powertrain optimization of the vehicle portfolio with respect to CO_{2eq} emissions and costs is performed for the mobility system.

11.1 Scenario analysis

A comparative analysis is used to quantify the influences of the decarbonization strategies on the target values. In the first step, a reference scenario is defined. This can be, for example, the actual state of the region under consideration based on statistical data such as census data and traffic data that area. A new scenario is then designed, evaluated and optimized. By comparing it to the reference scenario, the impact of the changes in the new scenario can be quantified. This is exactly what is described in this chapter.

The comparison of the two scenarios is done on different levels. Starting at the agent level, the agent under consideration is compared in the two scenarios with respect to the target criteria, CO_{2eq} emissions, costs and energy demand. On the next level, the results are summarized on the respective life stage and compared with each other. Then the results are summarized per used travel modes. At the highest level, the mobility system is considered holistically and the target variables are compared with each other. The different levels are shown in Figure 84.

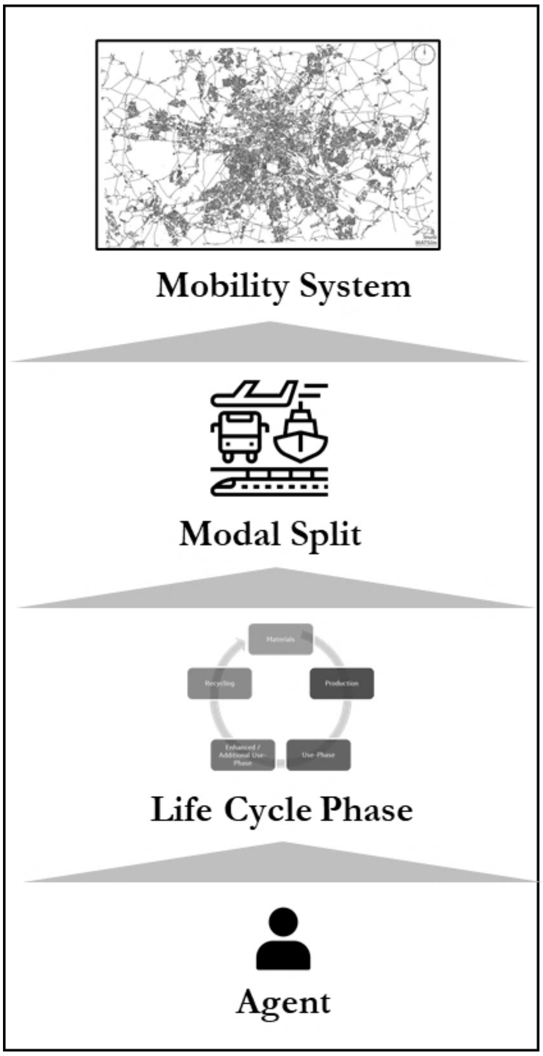

Figure 84: Comparison of scenarios on different levels

11.2 Reference scenario

In the following application example, the Berlin region is considered based on statistical and map data and used as the reference scenario. Figure 85 shows a section of the road network. The scenario is parameterized using fully automatable processes. For this purpose, a section of the Berlin region is extracted from OpenStreetMap and converted into a network for MATSim. Subsequently, relevant locations are extracted from the same OSM dataset and classified into different categories. In the next step, a synthetic population is generated based on statistical data, such as [Statistik Berlin-Brandenburg 2021]. Here, a sample size of 10% is chosen. In total, four mobility types are available to the agents. These are private cars, public transport, bicycles and walking. The subsequent analysis is carried out over a period of 14 years, which is based on typical observation horizons of LCAs.

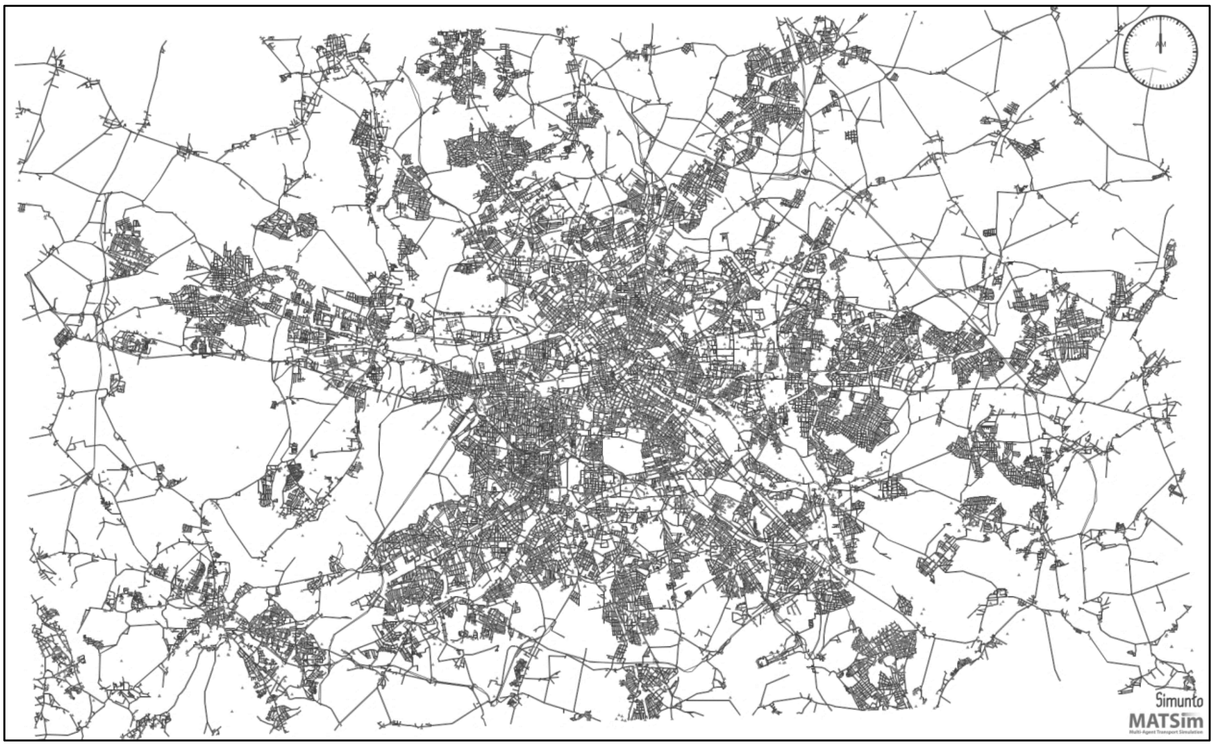

Figure 85: Considered area of Berlin for the mobility simulation

In this section, the results of the mobility simulation are compared with available public data on the Berlin region to validate the mobility behavior and results in the reference scenario.

Modal split

Figure 86 shows the resulting modal split by person-kilometers per day for the region of Berlin. The simulation results are compared to the statistical data of [Gerike et al. 2019]. Here it can be seen that the resulting person-kilometers per day for public transport and bike fits very well to the data of [Gerike et al. 2019]. For cars it can be seen that the resulting person-kilometers per day are higher than the values of [Gerike et al. 2019]. This could be related to the fact that a larger area around Berlin is considered in this simulation compared to [Gerike et al. 2019] and thus longer distances are taken into account in the simulation. In connection with this, fewer pedestrians or pedestrians with shorter distances are considered here. Therefore the simulated person-kilometers per day for walking is lower. Overall, it can be seen that the simulation results match the statistical data very well and therefore represent the current state of the modal split in Berlin.

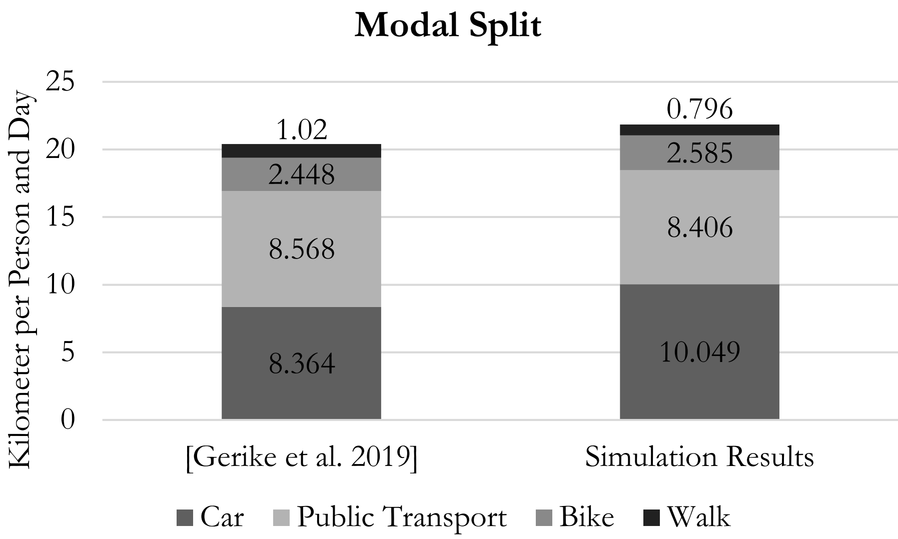

Figure 86: Resulting modal split compared with publicly available data

Number of trips

Figure 87 shows the resulting number of trips per age group per day for the region of Berlin. Here it can be seen that the simulated values fit very well to the statistical data. This is due to the fact that the statistical data is used as an input value to determine the number of activities of each agent. It can be concluded that these statistical distributions are still valid for the simulated scenario.

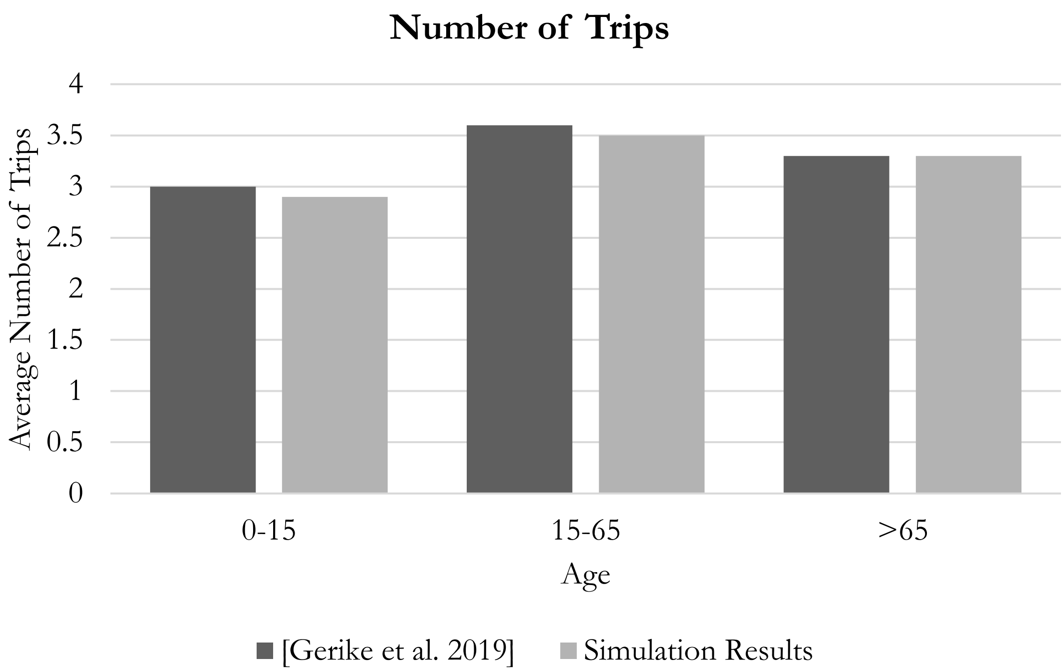

Figure 87: Resulting number of trips compared with publicly available data

Distribution by distance classes

Figure 88 shows the distribution by distance class and travel mode as a dotted curve compared to publicly available data [Gerike et al. 2019]. In general, it can be stated that the distribution of distance classes by travel mode fits well. The focus for walk and bike is on shorter distances, whereas for car and public transport the focus is on longer distances for the simulation as well as the collected data. For public transport the share of smaller trips is a little bit higher and for cars the share of longer distances is higher. The reason could be the considered area of Berlin in the simulation compared to the area of [Gerike et al. 2019]. Depending on the analyzed area as well as the available public transport in the considered area the distances can vary. However, as mentioned before, the distributions represent the collected data very well. The distribution of the trip purpose shown in Figure 20 for Berlin is an input value.

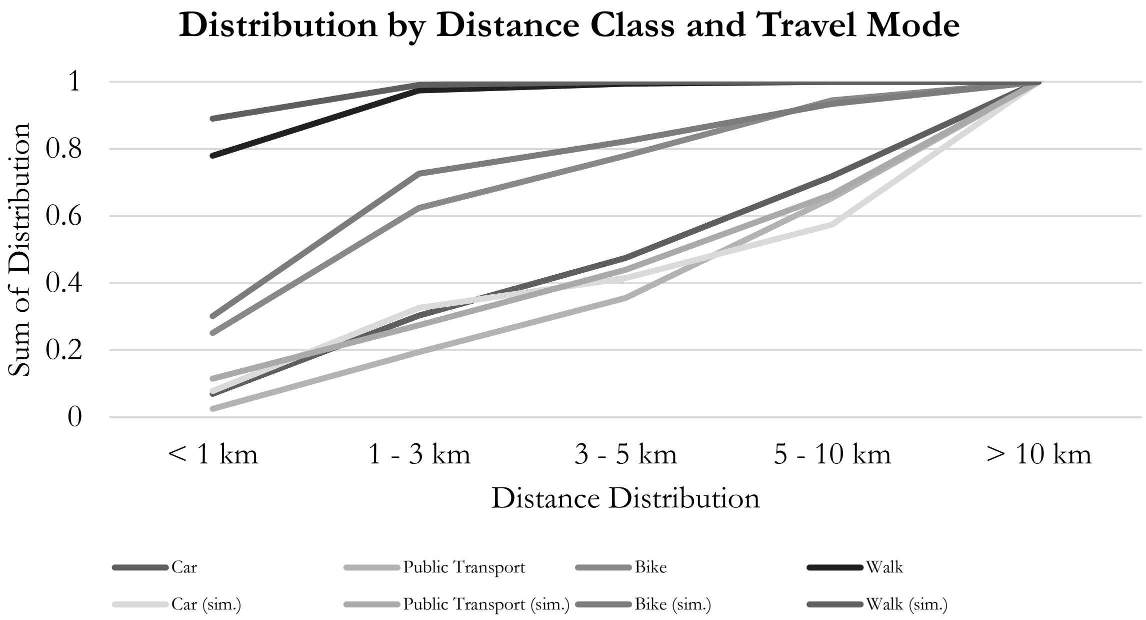

Figure 88: Resulting distribution by distance class and travel mode compared to publicly available data

Vehicle fleet

The distribution of the vehicle fleet of the current state in Berlin is an input value. In Figure 89 the distribution of powertrain types in Berlin based on [Kraftfahrt-Bundesamt 2022] is shown. In 2021 the powertrain portfolio in Berlin consists of 94% ICEVs, 4% HEVs, 1% PHEVs and 1% BEVs.

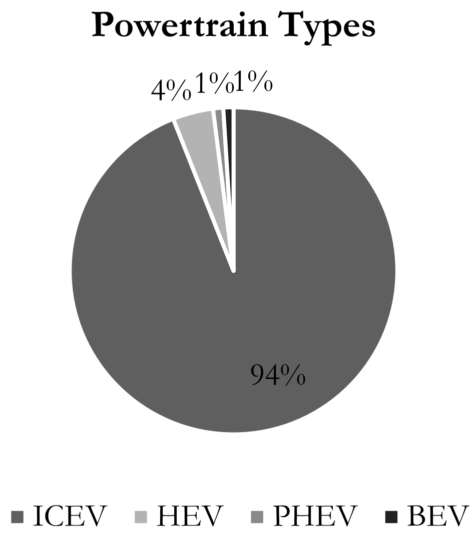

Figure 89: Distribution of powertrain types in Berlin based on [Kraftfahrt-Bundesamt 2022]

In Figure 90 the distribution of vehicle segments in Berlin based on [Kraftfahrt-Bundesamt 2022] is represented. In 2021 the vehicle fleet in Berlin consists of 20% small vehicles, 38% compact vehicles and 42% large vehicles. The resulting assigned simulated vehicle portfolio for the reference scenario in Berlin is shown in Appendix A.10. For each vehicle in the vehicle portfolio a similar reference vehicle is chosen and adapted to the different requirement classes as described in chapter 6. An equal distribution of the three requirement classes is assumed. This approach enables the possibility to model a realistic vehicle fleet of the current state of the considered region.

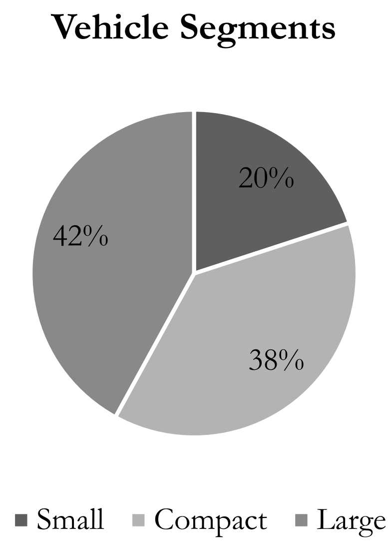

Figure 90: Distribution of vehicle segments in Berlin based on [Kraftfahrt-Bundesamt 2022]

CO_{2eq} emission

In the next step, the emissions for mobility in Berlin are examined. First, the total mobility including vehicles, public transport, bike and walk is considered in the actual state. In the simulation, just under 1.98 tCO_{2eq} per person per year is calculated for this case. According to [VCÖ 2021], 2 tCO_{2eq} are generated per person for mobility in Germany. Here, the results of the simulation and the collected data match very well. If the emissions for cars per person and kilometer are considered separately, the simulation results in just under 156 gCO_{2eq}/km. According to [Umweltbundesamt 2021], passenger cars in Germany emit in the use phase just under 152 gCO_{2eq}/km. The emissions in the simulation are slightly higher overall. This is due to the setup of the vehicle fleet in Berlin compared to the fleet in Germany. Compared to Germany, in Berlin there is a larger share of SUVs and compact vehicles compared to small vehicles. This then leads to higher total emissions. Overall, the simulation results appear plausible.

Costs

The second analyzed target values are the costs for mobility from the customers perspective. The TCO analysis and validation for cars as well as the costs analysis of public transport and bike is shown in chapter 8. In chapter 8 the used cost factors are described. Therefore, reference is made to chapter 8.

Energy demand

In the last step of the analysis of the reference scenario in Berlin, the energy demand is examined in more detail. Here, the focus lies on cars, since a constant value of 12 kWh/100km per person [Mitusch 2019] is assumed for public transport and the energy demand for bike and walk is neglected. In [Schmidt 2018], the energy demand for an assumed 100% BEV scenario in Germany is investigated. Here, an energy demand of just under 129 TWh is calculated for 46.5 million cars with an average consumption of 20 kWh/100km and an annual mileage of 13,922 km. In order to generate comparable results, a 100% BEV scenario is also simulated in this case. Here, comparable BEV vehicles are assigned to all agents in the simulation. The vehicle stock in Berlin with 1.24 million vehicles represents just under 2.7% of the total vehicle fleet in Germany [Kraftfahrt-Bundesamt 2022]. Therefore, the calculated energy demand is scaled up and an energy demand of 142 TWh follows. Due to the assumed vehicle portfolio based on the current state, there is a high share of SUVs and compact vehicles and the average consumption here is 22 kWh/100km. The resulting annual mileage per agent is just under 13,200 km. Overall, the simulation results show that valid values are calculated.

11.3 **Use-cases**

For the validation of the method, two use cases are considered in the following. Since the focus of the work is on cars, in the first use case a powertrain optimization is performed about minimizing the emissions of the Berlin scenario considered. In addition, a second optimization for a future scenario in 2030 is performed to also analyze the impact of the technology forecasts included in the method. In the second use case, a multidimensional powertrain optimization with respect to emissions and costs is performed to additionally consider the influence of costs. With the help of the two use cases, the entire methodology is applied and the results can thus be validated. Using the agent-based mobility simulation, a realistic mobility behavior of the considered region Berlin is generated. The integrated powertrain simulation allows to evaluate the agents' vehicles in detail. Subsequently, the emissions, the energy demand as well as the costs for mobility are evaluated using the developed and implemented methods. The determination of the optimal powertrain portfolio is then determined with the integrated optimizer. By applying these use cases, the developed methodology can be applied step by step and thus validated.

11.3.1 Powertrain optimization regarding emissions

The application example shown here illustrates the influence of a technology forecast in 2030 compared to the current status for four different scenarios of the powertrain portfolio. For the two periods considered, the electricity mix of the respective years is assumed and changes dynamically over the years. Here, the CO_{2eq} emissions for the electricity mix starting in 2021 show an average value of 331 gCO_{2eq}/kWh [Bundesministerium für Umwelt 2021] and starting in 2030 an average value of 96 gCO_{2eq}/kWh [IEA 2019]. In addition, the mobility behavior is kept constant across the different scenarios in order to evaluate the impact of the powertrain type. That is, changes in the system do not affect the mode choice. An agent who uses a passenger car in the reference scenario will accordingly also use a passenger car in the new scenarios. The only manipulated variable in this application example is the powertrain portfolio of the region under consideration with the goal of minimizing CO_{2eq} emissions. Analogous to the reference scenario, a 10% sample size of the population is again considered. For the mileage of the mobility type used, the realistic mileage resulting from the mobility simulation is taken. For cars, for example, the average mileage is just under 13,200 km per year. In addition, a dynamic system with realistic market behavior including vehicle changes is considered in the LCA calculation. As a result, the influence of production emissions increases and thus has a stronger impact on the powertrain portfolio selection.

Powertrain portfolio optimization

The results are described below. Figure 91 as well as Figure 92 show the normalized influence of the technology forecasts on CO_{2eq} emissions and mobility costs from the customer's perspective starting in 2021 as well as 2030. Four scenarios are shown for both cases. The first scenario is the reference scenario, which is based on statistical data and described in chapter 11.2. Here, the powertrain portfolio consists of just under 94% ICEVs and 5% (P)HEVs and 1% BEVs. All other scenarios are compared to Scenario 1 from the respective production year, as shown in Figure 91 and Figure 92. Scenario 2 represents a 100% BEV scenario. In Scenario 3 and 4, optimization is performed. The optimizer varies the powertrain portfolio with the goal of minimizing CO_{2eq} emissions. The difference between Scenario 3 and 4 lies in the assumption of how PHEVs are charged. In scenario 3, an optimal PHEV charging behavior is assumed. This leads to a higher share of electric trips when an agent is assigned a PHEV, which in turn leads to a higher share of PHEVs in the powertrain portfolio, as shown in Figure 93. This is mainly due to the fact that PHEVs produce comparatively low CO_{2eq} emissions in production compared to BEVs, while at the same time producing low emissions due to optimal charging behavior in the use phase. This leads to lower emissions overall, as shown in Figure 91 and Figure 92. In Scenario 4, on the other hand, a more realistic charging behavior depending on a random energy content of the battery is assumed, which leads to a lower share of electric trips. This increases emissions in the use phase, which in turn leads to a decrease in the share of PHEVs in the powertrain portfolio, as shown in Figure 93.

Figure 91 shows the results for the case starting in 2021. It can be seen that a 100 % BEV scenario reduces total emissions by 20 %. By means of the optimization in scenario 3, it is shown that there is still further potential under the given boundary conditions. In scenario 3, for example, emissions are reduced by 34%. In scenario 3, as described, there is a high proportion of PHEVs. The assumed optimal operation of the PHEVs in combination with the low production emissions lead to higher potential savings in emissions. In scenario 4, the more realistic operation of PHEVs leads to a 100% BEV scenario. The decreasing shares of electric driving lead to higher emissions in the use phase, so that BEVs again represent the lower CO_{2eq} powertrain types, resulting in a pure BEV powertrain portfolio again. Here, it can additionally be seen that an electrification of the vehicle fleet slightly increases the costs from the customer's point of view.

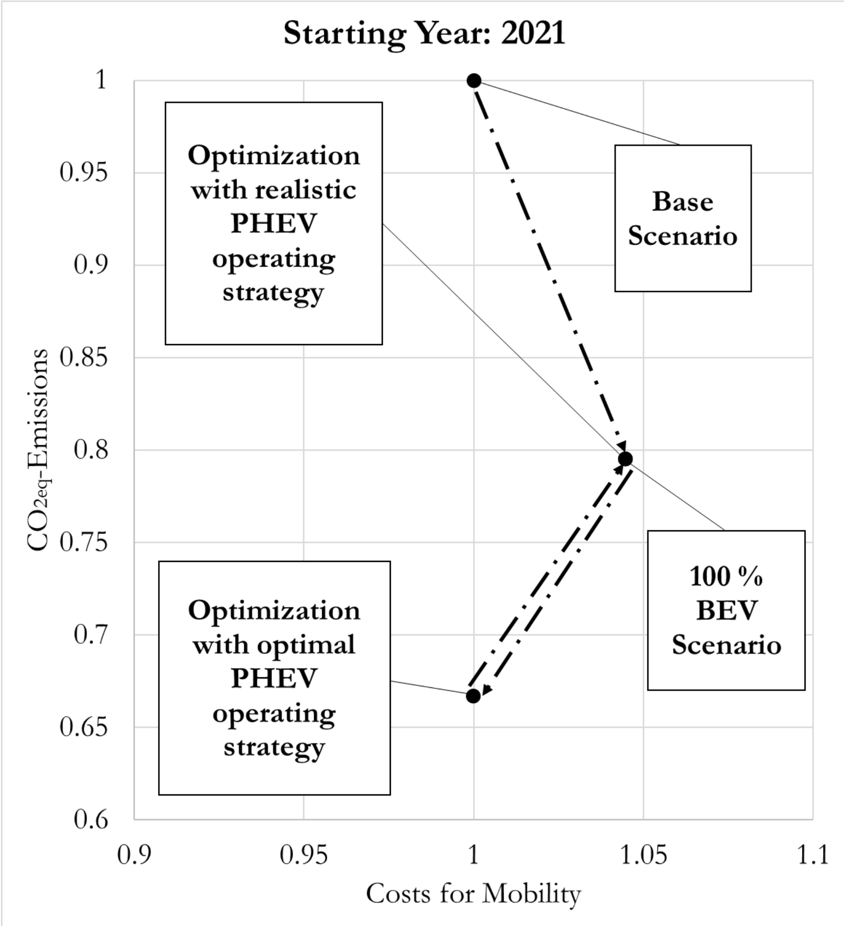

Figure 91: CO_{2eq} emissions for the whole mobility system for the four scenarios in 2021

Compared to the case starting in 2021, the case starting in 2030 shows that the overall savings are greater. This is mainly due to the positive development of technological powertrain components in the mobility system and the lower projected CO_{2eq} emissions in the electricity mix and in the production of the components. Here, the savings in scenarios 2 and 4 are 37.5%. In scenario 4, a 100% BEV scenario is analyzed. In scenario 3, the powertrain portfolio was optimized to such an extent that a saving of 45% is achieved. In contrast to the first case, the costs for electrified mobility decrease, as can be seen in the 100% BEV scenario in scenario 2 and 4. In scenario 3, PHEVs dominate the powertrain portfolio again and here the cost savings are lower.

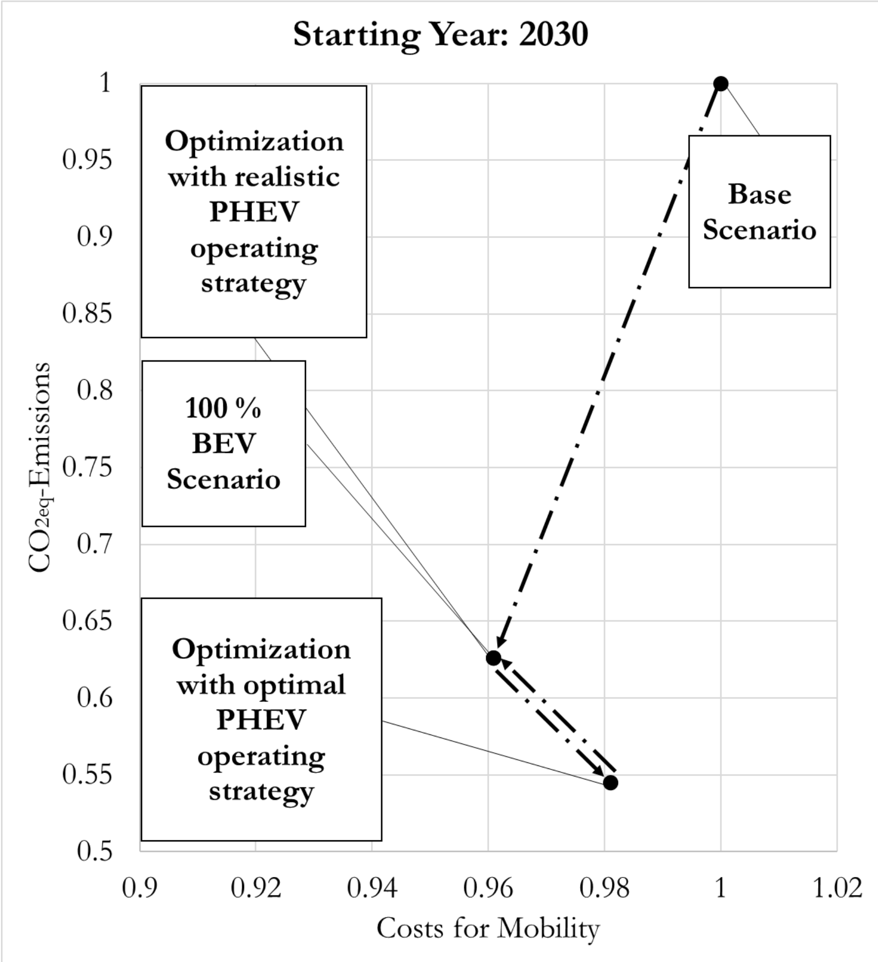

Figure 92: CO_{2eq} emissions for the whole mobility system for the four scenarios in 2030

Figure 93 visualizes the resulting powertrain portfolios for the case starting in 2021. It shows on the y-axis the shares of the respective powertrain types for the four scenarios considered. In scenario 1 as well as scenario 2, the powertrain portfolio is an input variable. In Scenario 3 and 4, the powertrain portfolio results from optimization. In scenario 1, the powertrain portfolio consists of 94% ICEVs, 5% (P)HEVs, and 1% BEVs. In scenario 2, the powertrain portfolio consists of 100% BEVs. For the case starting in 2021 in scenario 3, the powertrain portfolio consists of 75% PHEVs and 25% BEVs. This result is due to the low CO_{2eq} emissions of the PHEVs compared to BEVs in the production phase and the low emissions in the use phase due to the optimal charging behavior, which leads to a high share of electric driving. Since all agents are considered individually, there are many agents which achieve lower CO_{2eq} emissions with BEVs than even an optimal charged PHEV. Scenario 4 results in a 100% BEV scenario referring to the more realistic consideration of the PHEV. Due to the increased emissions in the use phase, the BEV is best in terms of emission reductions.

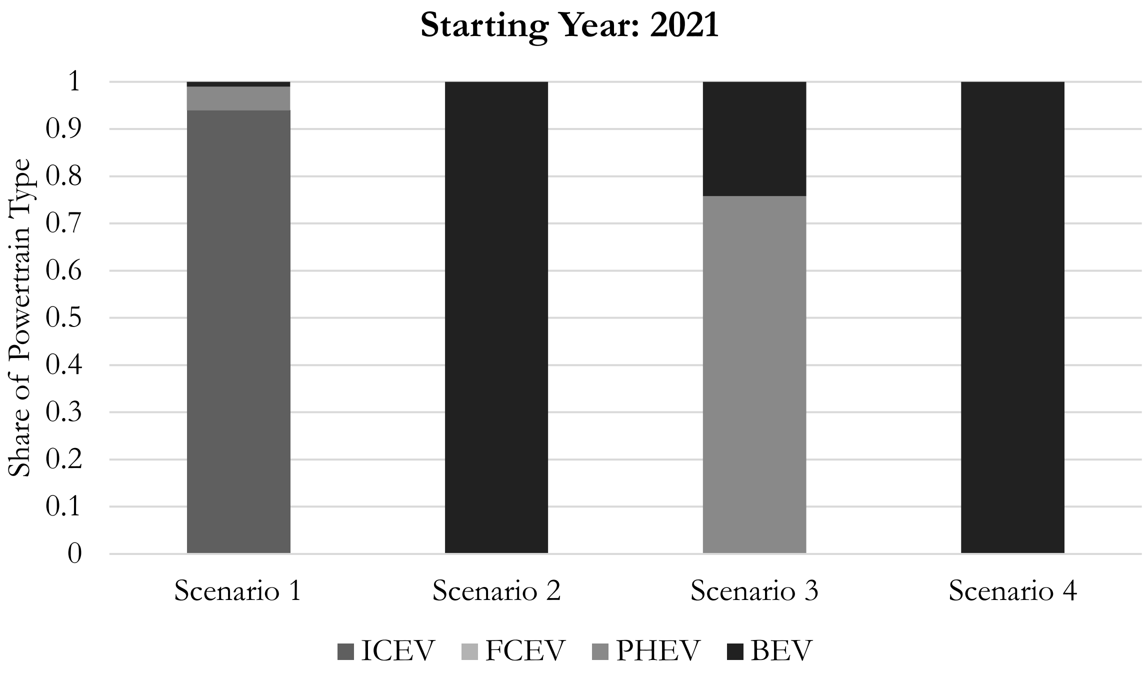

Figure 93: Shares of the powertrain types in the powertrain portfolio across the four scenarios for the case starting from 2021

Figure 94 shows the resulting powertrain portfolios for the case starting in 2030. The figure indicates on the y-axis the shares of the respective powertrain types for the four scenarios considered. For the case starting in 2030, Scenario 1 and 2 look the same as the case starting in 2021 because the powertrain portfolio is an input variable. In scenario 3 and 4, the powertrain portfolio results from optimization. Analogous to the case starting from 2021, there is a large share of PHEVs in scenario 3. However, the share has decreased and the share of BEVs has increased. This is mainly due to the positive development of the powertrain components as well as the lower CO_{2eq} emissions in the use phase, which are included in the calculation here. For scenario 4, the results are similar for both cases. Here, there is also a 100% BEV scenario, since due to the realistic charging behavior, the emissions in the use phase increase due to the lower electric driving share. This leads to BEVs being the lower CO_{2eq} powertrain types overall.

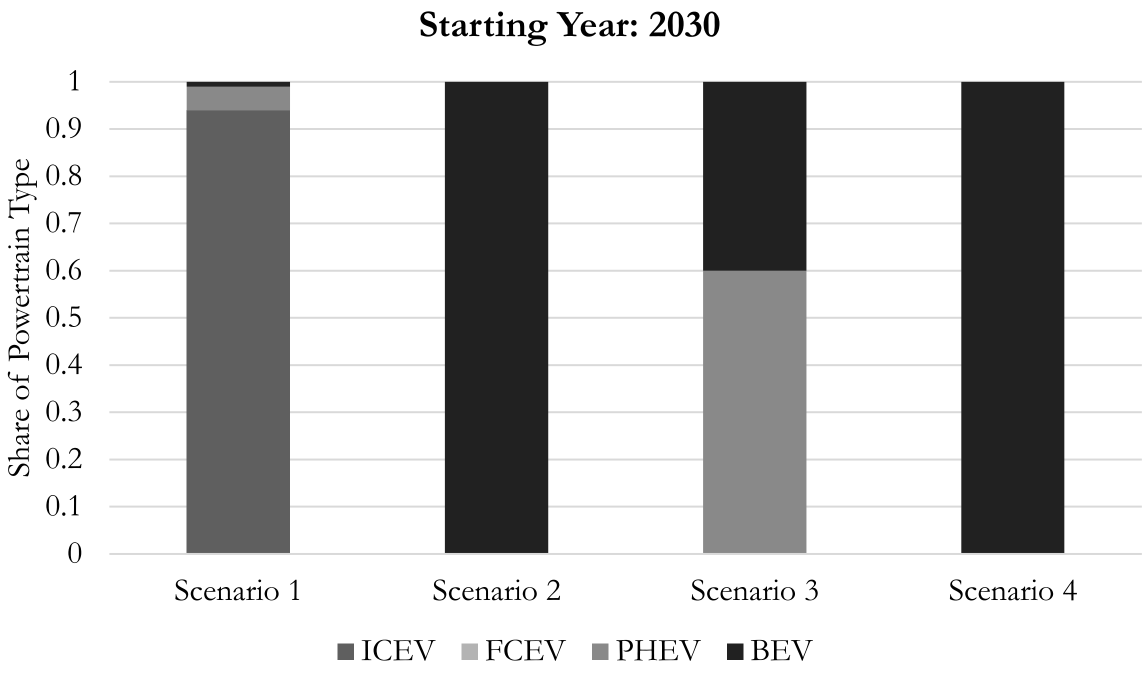

Figure 94: Shares of the powertrain types in the powertrain portfolio across the four scenarios for the case starting from 2030

Similar to CO_{2eq} emissions, the same considerations are made for the energy demand. Here, it can be seen that electrification of the vehicle fleet leads to more energy-efficient mobility systems. Furthermore, Figure 95 shows that the 100% BEV scenario represents the most energy efficient mobility system. This is also plausible, since the BEV is the most energy-efficient powertrain system among the powertrain systems considered here. For the case starting in 2021, the energy demand is reduced by 56% in scenarios 2 and 4 and by 50% in scenario 3.

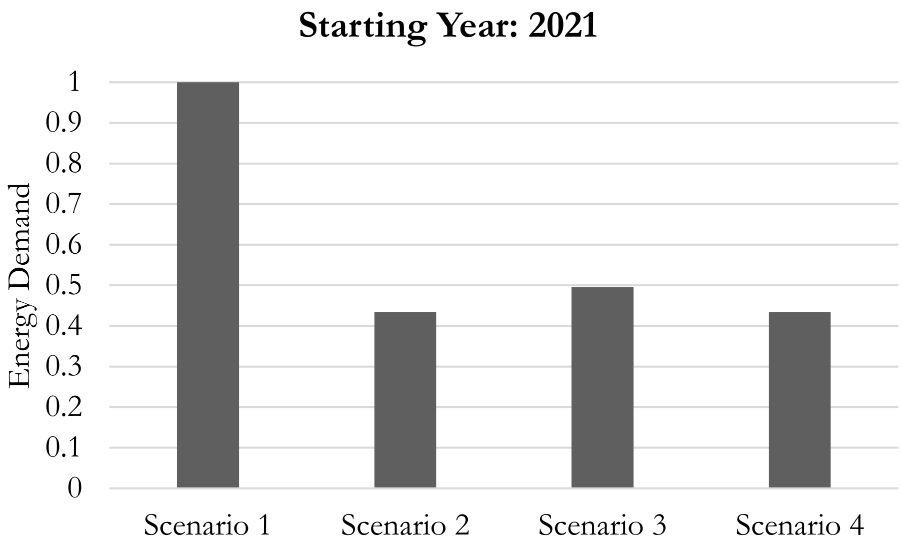

Figure 95: Energy demand for the four scenarios for the case starting from 2021

Compared to the case starting in 2021, the energy demand for the case starting in 2030 is further reduced due to the efficiency increase considered in the forecasts for the powertrain components. For the case starting in 2030, the energy demand in scenario 1 reduces by 1% compared to the first scenario starting in 2021 due to efficiency improvements in ICEVs. In scenarios 2 and 4, the energy demand is reduced by 57% and in scenario 3 by 51%. In Figure 96 the results are shown.

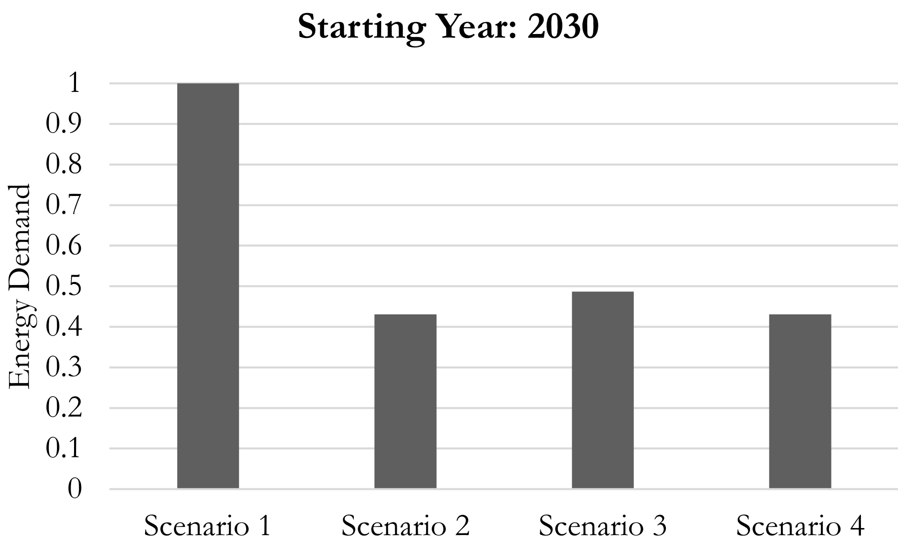

Figure 96: Energy demand for the four scenarios for the case starting from 2030

11.3.2 Powertrain optimization regarding emissions and costs

The application example shown here illustrates the influence of a multidimensional optimization of the powertrain portfolio regarding emissions and costs for the same four scenarios as in the application in 11.3.1. The electricity mix of the respective year is assumed and it changes dynamically over the years. Here, the CO_{2eq} emissions for the electricity mix starting in 2021 shows an average value of 331 gCO_{2eq}/kWh [Bundesministerium für Umwelt 2021]. In addition, the mobility behavior is kept constant across the different scenarios in order to evaluate the impact of the powertrain type. Again, changes in the system do not affect the mode choice. An agent who uses a passenger car in the reference scenario will accordingly also use a passenger car in the new scenarios. The only manipulated variable in this application example is the powertrain portfolio of the region under consideration with the goal of minimizing CO_{2eq} emissions and costs. Analogous to the reference scenario, a 10% sample size of the population is again considered. For the mileage of the mobility type used, the realistic mileage resulting from the mobility simulation is taken. For cars, for example, the average mileage is just under 13,200 km per year. In addition, a dynamic system with realistic market behavior including vehicle changes is considered in the LCA and costs calculation. As a result, the influence of production emissions and costs becomes greater and thus has a stronger impact on the powertrain portfolio selection.

Powertrain portfolio optimization

In Figure 97 the different variant solutions of the optimization of scenario 3 and 4 are shown. Each variant represents a different powertrain portfolio. All four scenarios are also depicted here. The powertrain portfolio of scenario 1 is shown as a big square. The first scenario is the reference scenario, which is based on statistical data and described in chapter 11.2. Here, the powertrain portfolio consists of just under 94% ICEVs and 5% (P)HEVs and 1% BEVs. The second 100% BEV scenario is shown as a big triangle. The optimization results of scenario 3 are visualized as grey bubbles and of scenario 4 are shown as black bubbles.

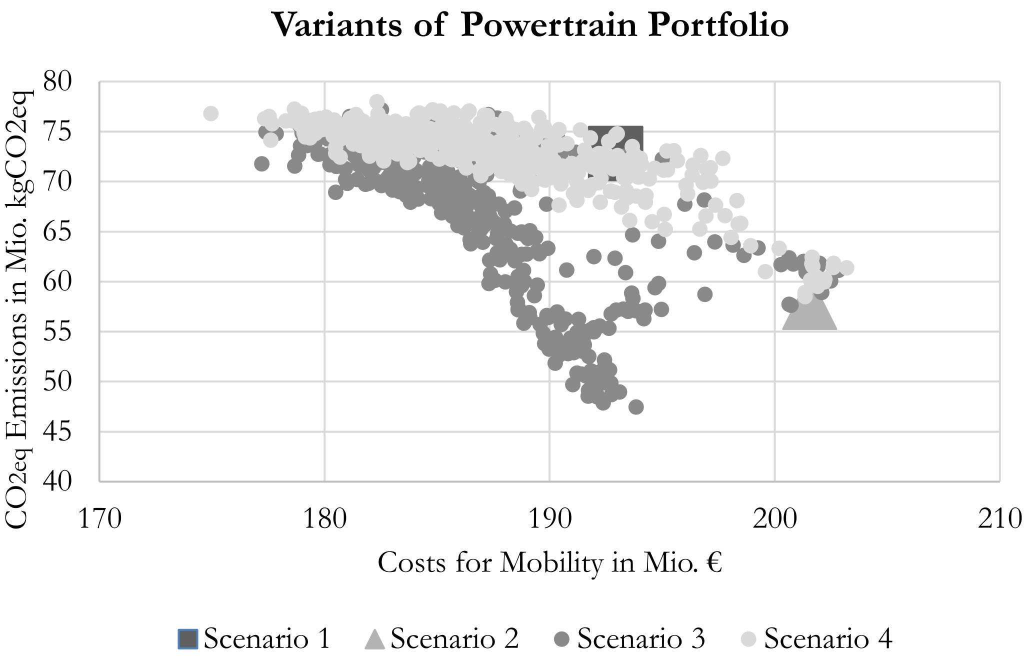

Figure 97: Variants of powertrain portfolios for the four scenarios

Figure 98 shows the normalized influence of the multidimensional optimization of the powertrain portfolio on CO_{2eq} emissions and mobility costs from the customer's perspective starting in 2021. Four scenarios are shown here. All other scenarios are compared to Scenario 1 from the respective production year, as shown in Figure 98. Here the results differ more than for the first use case. Scenario 2 represents a 100% BEV scenario. The results are equal to the first use case. A 100% BEV powertrain portfolio reduces the CO_{2eq} emissions by around 20% but the costs from the customers perspective increase slightly for the case starting from 2021. In Scenario 3 and 4, a multidimensional optimization is performed. The optimizer varies the powertrain portfolio with the goal of minimizing CO_{2eq} emissions and costs from the customers perspective, since costs are a main driver for the buying decision of customers. Here again, the difference between scenario 3 and 4 lies in the assumption of how PHEVs are charged. In scenario 3, an optimal PHEV charging behavior is assumed. This leads to a higher share of electric trips when an agent is assigned a PHEV. In scenario 4, on the other hand, a more realistic charging behavior depending on a random energy content of the battery is assumed, which leads to a lower share of electric trips. The optimal powertrain portfolio in scenario 3 chosen by the optimizer consists of 80% PHEVs, 17% BEVs and 3% FCEVs. This is mainly due to the fact, that optimal charged PHEVs produce overall low CO_{2eq} emission compared to other powertrain types and are also slightly more cheap than comparable ICEVs. FCEVs are also taken into account here, as they bring cost advantages, especially for large vehicles, and emissions are not much higher than for comparable vehicles. Overall, in scenario 3 an emission reduction by 8% and a cost reduction by 1.5% can be achieved. The optimal powertrain portfolio in scenario 4 chosen by the optimizer consists of 33% ICEVs, 12% PHEVs, 47% BEVs and 8% FCEVs. The realistic charging behavior leads to higher emissions in the use phase, which then leads to a higher share of ICEVs in the powertrain portfolio due to the higher potential of cost reductions. The emissions increase by 1% and the costs are reduced by nearly 10%. With the help of the optimization results for the different cases, it is now possible to determine optimal powertrain portfolios regarding cost reduction, emission reduction or a compromise of both target variables.

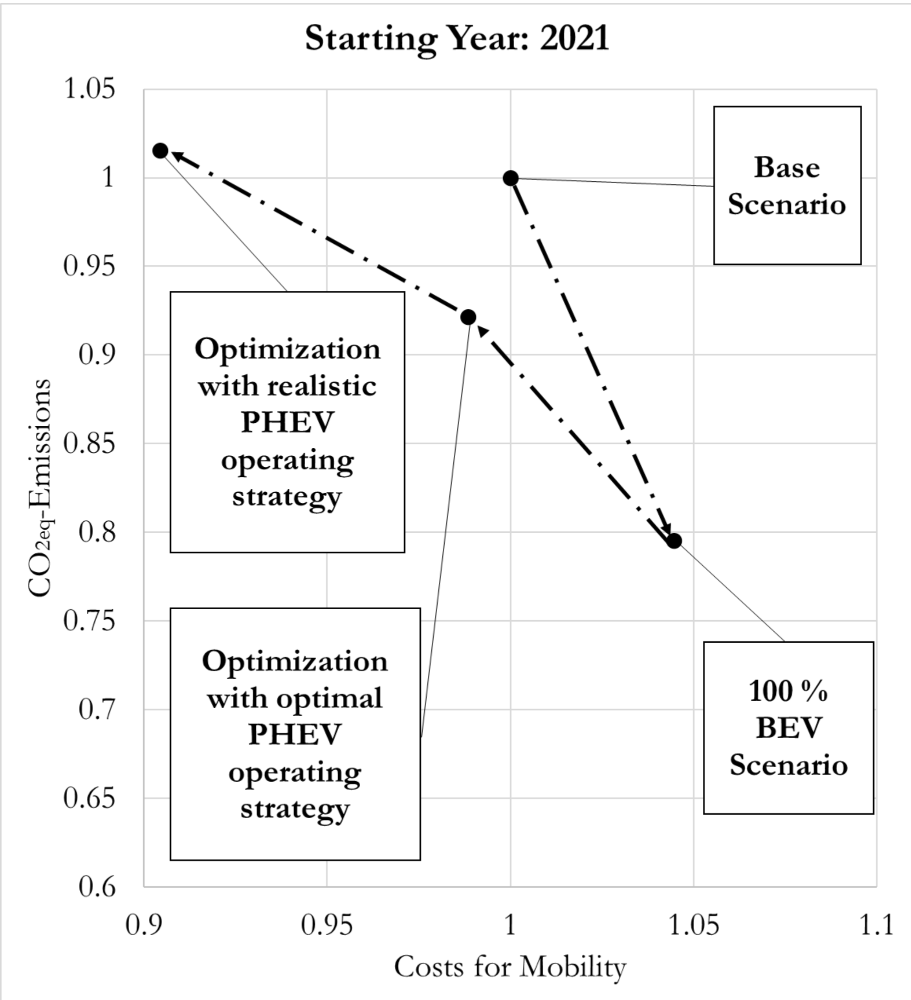

Figure 98: CO_{2eq} emissions for the whole mobility system for the four scenarios in 2021

Figure 99 shows the resulting powertrain portfolios for the case starting in 2021. The figure shows on the y-axis the shares of the respective powertrain types for the four scenarios considered. In scenario 1 as well as scenario 2, the powertrain portfolio is an input variable. In Scenario 3 and 4, the powertrain portfolio results from the multidimensional optimization. In scenario 1, the powertrain portfolio consists of 94% ICEVs, 5% (P)HEVs, and 1% BEVs. In scenario 2, the powertrain portfolio consists of 100% BEVs. For the case starting in 2021 in scenario 3, the powertrain portfolio consists of 80% PHEVs, 17% BEVs and 3% FCEVs. This result is due to the low CO_{2eq} emissions of the PHEVs compared to BEVs in the production phase and the low emissions in the use phase due to the optimal charging behavior, which leads to a high share of electric driving. Combined with similar costs compared to ICEVs, there is a high share of PHEVs here. Since all agents are considered individually, there are many agents which achieve even lower CO_{2eq} emission with BEVs than an optimal charged PHEV, whereas the costs are not much higher. Therefore, there is still a big share of BEVs. In scenario 4 the powertrain portfolio consists of 33% ICEVs, 12% PHEVs, 47% BEVs and 8% FCEVs. As a more realistic PHEV charging behavior is assumed, ICEVs are preferred by the optimizer due to cost reduction. Thus, the share of PHEVs is lower and the share of ICEVs is higher. Larger FCEVs can be cheaper than comparable vehicles and the overall emissions are just slightly higher than those of BEVs, which is why there is also a higher share of FCEVs. The shown powertrain portfolios for scenario 3 and 4 are just one example of the pareto front of the different variants, which can be chosen from depending on the weighting of the target variables.

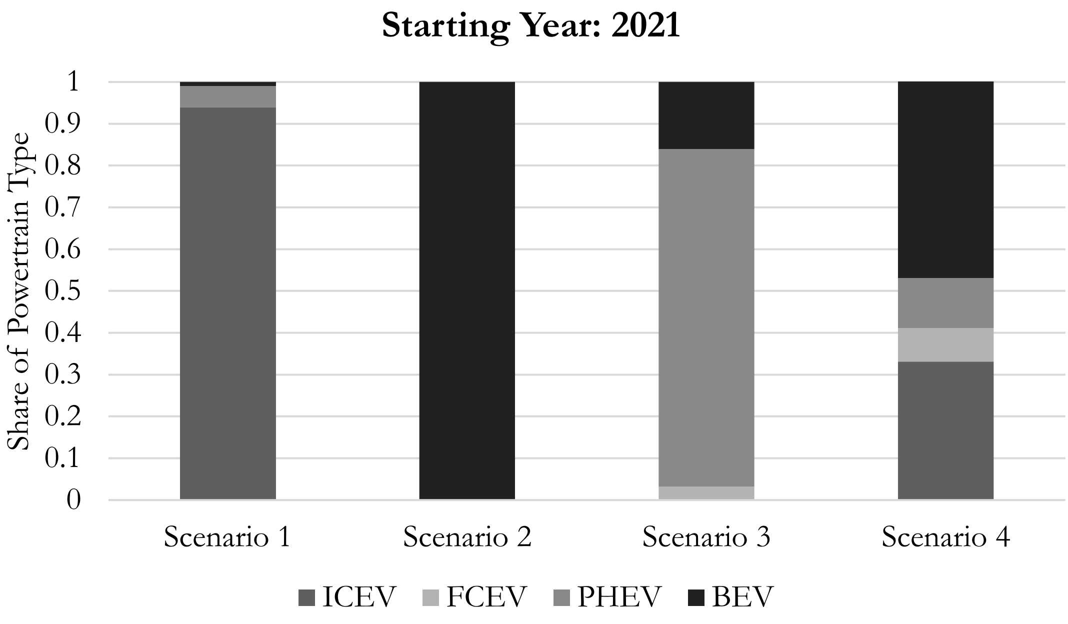

Figure 99: Shares of the powertrain types in the powertrain portfolio across the four scenarios for the case starting from 2021 with the multidimensional optimization

In Figure 100 the energy demand for mobility for the four scenarios is shown. Here, it can be seen that electrification of the vehicle fleet leads to more energy-efficient mobility systems, as shown in scenario 2. Furthermore, Figure 100 shows that the 100% BEV scenario represents the most energy efficient mobility system. This is also plausible, since the BEV is the most energy-efficient powertrain system among the powertrain systems considered here. With the optimal powertrain portfolios determined for scenario 3 and 4, the energy demand for mobility is also reduced. In scenario 3, the energy demand is reduced by 52% and in scenario 4 by 13%. Here it can be seen that if costs are also considered in the determination of the optimal powertrain portfolio there can be differences and that solutions such as subsidies are needed to promote energy efficient and low emission solutions such as BEV. In the next chapter a critical discussion of the overall method is performed and analyzed if the set goals are achieved

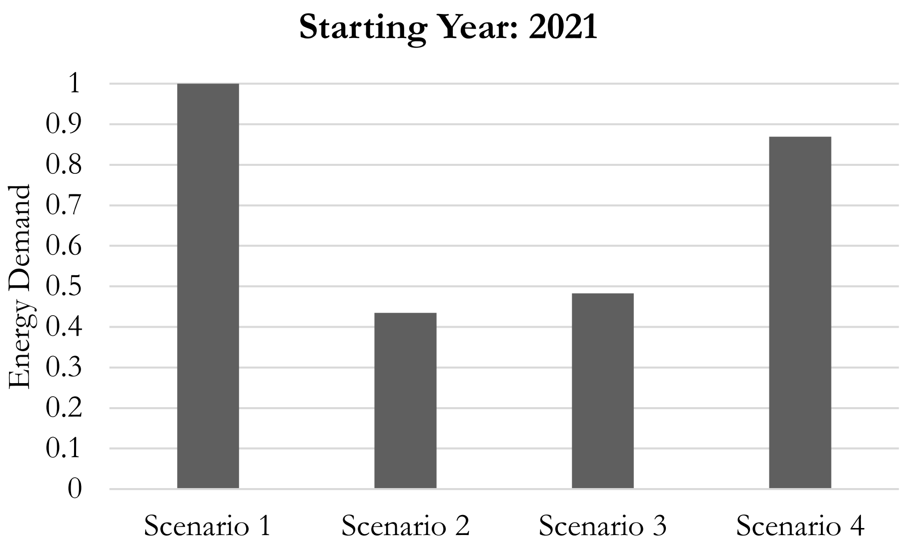

Figure 100: Energy demand for the four scenarios for the case starting from 2021

12 Critical discussion of the overall method

The following chapter is divided into the following subchapters according to the sub-targets developed: 12.1 Development of a modular method framework to evaluate and optimize holistic mobility systems, 12.2 Integration of MATSim, 12.3 Integration of powertrain simulation, 12.4 Development of a new and enhanced LCA, 12.5 Combination of individual methods and integrating optimization approach, 12.6 Performing a sensitivity analysis, 12.7 Validation of the method. For each subchapter the derived problem is briefly outlined and the achieved results are presented. The limitations of the investigations and possible improvements are outlined in detail.

12.1 Development of a modular method framework to evaluate and optimize holistic mobility systems

In order to be able to evaluate mobility systems holistically and thus make more precise statements about the impact of decarbonization measures, a method is needed that takes more into account than conventional LCA do. For this purpose, a modular method framework is created in this sub-target, which enables a holistic view of the mobility system. For the modeling of the region as well as the mobility behavior that takes place there, an agent-based mobility simulation is implemented. Here MATSim is used as a tool. In the next step, the mobility forms are modeled and evaluated with respect to the target criteria. In this work, the focus is placed on passenger cars, since they currently have the greatest impact in terms of CO_{2eq} emissions. Therefore, passenger cars are considered in detail with a powertrain simulation, while other forms of mobility are considered in a simplified, key-value based manner. For the evaluation of the target criteria CO_{2eq} emissions, costs as well as energy demand, analysis methods are integrated into the method framework. For the calculation of CO_{2eq} emissions, a new extended LCA approach is developed and integrated. This is described again in sub-target 4. For the calculation of costs, a TCO approach is integrated. The energy demand is calculated with the help of the determined consumptions as well as the mobility behavior of the individual agents. In the first step, a simulation environment with the respective interfaces is created, whereby the individual methods can be integrated. This sub-target is fully achieved and a modular method framework is developed which integrates an agent-based mobility simulation, a powertrain simulation as well as LCA and cost models.

12.2 Integration of MATSim

An agent-based mobility simulation is needed to investigate the influences on the person level and their mobility behavior. For the generation of the mobility behavior, a region has to be modeled so that a mobility simulation can be performed afterwards. Here, publicly available data are used. In this work, the Berlin region is chosen as an example region, since a good data basis is available. For meaningful results, the data basis plays an important role. The more data is available on the population, mobility behavior and the region itself, the more accurately the region can be mapped and analyzed. However, it must be taken into account that the larger the sample size of the population considered, the longer the calculation times will be, making a scenario analysis with many different scenarios more difficult. In this case, it is possible to limit the analysis to the relevant areas of the mobility system. A smaller sample size can be chosen or non-relevant mobility forms can be teleported instead of being simulated in detail. For the modeling of the Berlin region, census data, mobility surveys and map data from e.g. Open-Street-Map are used in this work. The tool deployed here is MATSim, which is open-source and is further advanced by an active community. In addition, it is possible to look at different forms of mobility, as defined in the sub-target. MATSim already contains mobility forms such as cars, public transport, bicycles and walking, but also new mobility forms such as DRTs. Completely new mobility forms or concepts can be programmed. For this, the events associated with the new mobility form must be defined. For example, reservation, ride or pick-up events in the case of robo-taxis. With the help of agent-based mobility simulation, customer behavior and their mobility behavior can be modeled and analyzed in detail. Additionally, it can be analyzed why agents choose certain mobility forms based on the stored scoring function. Furthermore, it can be analyzed how the respective mobility forms are used by the respective agents in detail. This enables the optimization of the holistic mobility behavior, but also the optimization of the operation of the respective mobility forms. For example, it can be determined how many vehicles are needed in a mobility fleet. By integrating MATSim into the simulation framework the goals of this sub-target are achieved.

12.3 Integration of powertrain simulation

Now that the mobility behavior of the region under consideration is known, the next step is to evaluate the forms of mobility. The focus in this work is on individual transport, since it has the largest share in the generated $CO2_{eq}$ emissions in road transport. For this reason, the powertrain simulation of [Weiß 2018] as well as the technology forecasts for the design and evaluation of future powertrains of [Schneider 2022] are integrated into the method. With the help of this approach, optimal powertrain portfolios of the considered region are to be determined. Other forms of mobility, such as public transport or bicycles, are modeled using a key-value based approach.

With the integrated approach it is possible to model vehicle portfolios in detail. In this work, a vehicle portfolio with 72 vehicles is modeled, which makes it possible to model an entire market. This offers the possibility to determine optimal portfolios with respect to target criteria such as CO_{2eq} emissions or costs from the customers perspective. In addition, customer preferences can be taken into account when designing the portfolios in order to achieve more realistic savings in emissions, since an optimum in theory often does not correspond to the optimum in reality. For example, an optimization of the powertrain portfolio in terms of CO_{2eq} emissions could determine a portfolio with predominantly small vehicles and a BEV powertrain. In reality, however, the distribution looks different, as many customers prefer SUVs in particular.

The integrated approach is also extended with the modeling of a realistic market behavior. Here, the status quo based on statistical data is taken as a starting point and the preferences of customers are determined. Based on these preferences, agents are assigned suitable vehicles accordingly in the powertrain portfolio optimization. In addition, a longer period of time is considered, whereby agents can dynamically change their vehicles and, for example, also buy used cars. The switching is based on probabilities. The consideration of realistic market behavior is limited to the considered region, since otherwise uncertainties arise and allocation takes place at larger system boundaries, which should be avoided. This sub-target is partially achieved. The powertrain simulation enables the detail analysis of vehicles, however other forms of mobility such as public transport cannot be modeled and simplified key-value based models are used. Since the focus of this thesis is on passenger cars, this simplified approach can be carried out.

12.4 **Development of a new and enhanced LCA**

With standardized LCAs as well as known detailed LCA software, the analysis and assessment of holistic mobility systems is more difficult and is better suited for a detailed assessment of individual vehicles. Therefore, a new and extended LCA is needed that allows the assessment of whole vehicle fleets, new decarbonization measures that would be possible with an electrified fleet, and the consideration of the mobility behavior of each individual in the mobility system under consideration. In this work, a new method is developed that includes the following points:

- Dynamic balance and envelope
- Holistic mobility systems analysis
- Predictability of future scenarios
- Integrability into an optimization loop

In order to implement these points, a key-value based approach is taken here, which is also modular. The key-value based approach is a simplified approach and in this work the focus lies on CO_{2eq} emissions. This approach allows a dynamic assessment of the mobility system with changes over time.

It allows the assessment of holistic mobility systems and the integration of LCA into the overall methodology, so that optimizations with respect to CO_{2eq} emissions can also be performed. The key-values for all relevant components of the mobility system are determined with the help of a literature research on LCA studies as well as self-modeled LCA models in the LCA software "GaBi". These key-values are collected in a forecast database and trend curves are derived. Learning curves are suitable for this purpose, which can be used to derive forecasts for the individual components of the mobility system. A lot of data is needed to perform the LCA and depending on where the key-values come from, uncertainties may arise. However, it is shown in this work that good results can be obtained with the key-value based approach. Here, a comparison of the results from the key-value based approach for an ID.3 with published values from a detailed LCA for the ID.3 is carried out, where the differences are minor. In this sub-target, a modular and dynamic LCA approach is developed. This is fully achieved with the key value-based approach, which also enables the derivation of forecast data.

12.5 Combination of individual methods and integration of a fitting optimization approach

A coherent combined methodology is needed to holistically evaluate and optimize mobility systems. Here, a suitable optimization algorithm must be found, and the analysis shows that the genetic algorithm is suitable. In order to evaluate mobility systems holistically, the individual methods are combined into a single methodology. However, since the programming languages differ as well as the programming effort for this work is very high, this work proceeds as follows. The agent-based mobility simulation MATSim is written in Java. The powertrain simulation as well as the evaluation of CO_{2eq} emissions using the new extended LCA, costs as well as energy demand is written in MATLAB, due to the continuation of the tool chain of [Weiß 2018] and [Schneider 2022]. To nevertheless connect the tools interfaces are defined. For example, the agent-based mobility simulation automatically generates an evaluated table containing the mobility behavior of the considered region for each agent. This serves as input for the further tools and the further evaluations are performed automatically. In addition, a call script is written in Java within the scope of this work, which automatically calls all individual tools in the correct order and forwards the necessary data. This also enables a holistic optimization of the entire chain. Since the combined methodology is a very large method and requires a lot of computing time, investigations are carried out to reduce the computing time while maintaining the same quality of results. For this purpose, for example, the sample size as well as the number of iterations in the mobility simulation are considered in more detail. In addition, the modular structure of the simulation environment offers the option of keeping certain modules constant. For example, if the powertrain portfolio is optimized, the mobility behavior can initially be assumed to be constant and thus no mobility simulation is performed during the optimization saving computation time. This sub-target is partially achieved. Since the different toolchains such as MATSim or the powertrain simulation are complex and written in different programming languages interfaces are developed to combine them. However, for future work, it is be more beneficial to develop the entire tool chain in the same programming language and integrate it into an overall tool, so that the interaction between the methods can take place more easily.

12.6 Performing a sensitivity analysis

The combined methodology is a very large and data-intensive method that also requires a lot of computing time. In order to make holistic evaluations and optimizations of considered regions feasible, simplifications have to be made, such as the reduction of the sample size and the use of a key-value based approach for the evaluation of the target variables. The sensitivity analysis is used to analyze their influence. It shows that in the context of this work the influence of the sample size is relatively small and therefore small scenarios can be considered in order to determine optimal parameters for the original scenarios. When considering specific parameters of vehicles such as production emissions of batteries of combustion engines or values for the electricity mix, it can be seen that depending on the scenarios, certain parameters have a greater influence, such as battery parameters for an electrified fleet. However, these are expected influences and therefore do not represent uncertainties. This sub-target is achieved and the sensitivity analysis shows the great potential of electric fleet if it comes to reduction of emissions in mobility systems.

12.7 Validation of the method

In the last step, the method must be validated. For this purpose, the region of Berlin is taken. The region is modeled and the actual state is depicted. For this purpose, the simulated actual state is compared with the respective known, public data. The results show that good results are achieved. With the help of this method it is possible to model, evaluate and optimize the mobility behavior of a considered region. During optimization, different decarbonization strategies can be modeled and analyzed. In addition to CO_{2eq} emissions, the costs from the customer's point of view as well as the energy demand for mobility can be considered in detail. Overall, it can be shown that the defined goals could be implemented to a certain extent. The biggest limitation in this work is the computation time due to the very large computational models and the large data requirements. Nevertheless, the goal of designing and evaluating holistic sustainable mobility systems can be fulfilled and statements can be made about the modeled regions and measures.

13 Summary and outlook

A method for the design, analysis and optimization of sustainable mobility systems is presented. With the objective of a holistic approach including system dynamic effects and the predictability of a more distant future, this method combines an agent-based mobility simulation with a powertrain simulation as well as LCA and cost models and supplements them with an optimization algorithm. The agent-based mobility simulation is used to model the population in the form of agents, the various forms of mobility, and the region itself, i.e. infrastructure and charging infrastructure, and thus describes mobility behavior. The powertrain simulation provides insights into energy consumption and vehicle-specific $CO2_{eq}$ emissions. For the subsequent analysis with regard to the target criteria, an LCA method is developed that extends the guidelines of ISO 14040/14044 to include dynamic considerations. With a view on predictability and system optimization using genetic algorithms, indicator-based models are developed. The same applies to mobility and infrastructure costs. A modular structure of the methodology guarantees the extensibility by further submodels, the integration of a new state of the art as well as the connectivity to detailed methods. With the combined methodology, it is possible to optimize different parameters of the mobility system in a theoretical analysis, such as the powertrain portfolio. The observations show that this approach can be used to optimize various parameters of the mobility system and to identify potentials. In the examples considered here, the powertrain portfolio of the Berlin region is first optimized in terms of emissions and then multidimensionally in terms of emissions and costs. In the first example, $CO2_{eq}$ savings of 34% starting in 2021 and 45% starting in 2030 compared to the base scenario in 2021 can be achieved for the underlying premises by optimizing the powertrain portfolio. At the same time, it is shown that the energy demand can be reduced by 57%. In the second example, the influence of the costs for mobility from the customer's point of view is also taken into account in the optimization. Here, new compositions of the powertrain portfolio result, in which savings can still be achieved, but these are no longer as significant, since in part emission-reduced mobility is more expensive. Depending on the selected variant from the Pareto solution space, savings in $CO2_{eq}$ emissions of 1.5 - 8% result here. Cost savings of 1.5 - 10% can be achieved and at the same time, it is shown that the energy demand can be reduced by 13 - 52%.

Outlook

The holistic view of mobility systems presented makes it possible to map new decarbonization strategies in the transport sector and to evaluate the interplay of measures with regard to ecological, economic and social targets. The evaluation of measures is not limited to vehicle-specific scopes but extends to the diverse components of the entire mobility system. As an obvious step after a broad electrification, for example, an intelligent and, if necessary, bidirectional charging of electric vehicles can be analyzed and optimized regarding the influences on the target variables. In addition, the modular structure of the method enables further studies on new data, vehicle concepts, mobility concepts and services. This concerns, for example, driving bans or autonomous cab services, which are being discussed in many places. In addition, the influence of the expansion of public transport could be investigated and evaluated. Overall, the method thus makes an important contribution to the derivation of target-oriented, cross-sector decarbonization strategies and the understanding of interactions of ecological, economic and social target criteria. In this thesis the region Berlin is used to apply and validate this approach. However, this method can be applied to other regions as well as. For further studies, the following research points are conceivable. In this work, a powertrain optimization with respect to emission reduction as well as a multidimensional optimization of cost and emission reduction is performed. Further optimizations of the mobility system could be, for example, benefits over costs, where surveys and expert interviews have to be conducted to weight the benefits. Additionally, benefits need to be defined. For example, emission reduction can be considered in addition to comfort and travel time. Also, the mode choice can be analyzed further. It would be possible to extend the mode choice of the agents by further criteria, such as the influence of environmental criteria. For this, value studies and surveys have to be conducted in order to be able to weight these new criteria in the decision-making process. Analogous to the detailed consideration of passenger cars, it is possible to add detailed models of other forms of mobility to perform an interpretation in a holistic context. In this paper, the focus is on passenger transport. Besides passenger transport, it is also possible to look at freight transport in detail and evaluate it with respect to different criteria. To show the influence of market behavior even more realistically, it is possible to add detailed market models to the overall methodology. To avoid allocation, a simplified model is used in this work. However, with allocation it would be possible to model a realistic second-hand market for Germany or also the surrounding markets, so that vehicles leave the system under consideration and vehicles outside the system can be included in the system boundaries. Additionally, the mode-choice behavior of the agents can be extended, since used cars represent low-cost forms of mobility and thus can influence the mobility behavior of the agents. In this thesis, the focus is on the cost of mobility from the customer's perspective. For further considerations, investment costs as well as costs from the operator's point of view can be added. The costs for the mobility forms are already deposited. The further considerations enable the evaluation of business cases and can show potentials. The scaling methods and factors shown are determined for the example shown here. For new scenarios that include sharing concepts, for example, the methods must be performed again and the factors determined anew. In addition, it is necessary to see if the methods are valid for these new scenarios. As an alternative to scaling, other approaches can be taken. For example, availability constraints can be neglected for sharing concepts and it can be assumed that shared vehicles are always available, even if this is not realistic. However, this can answer questions such as the impact of the use of shared vehicles on $CO2_{eq}$ emissions. But other questions cannot be answered, such as factors for availability or how the sharing fleet should best be operated or located. Furthermore, dynamic changes of the mobility offer as well as the mobility choice by the agents can be implemented by adding new vehicle services over time and analyzing their impact.

References

ADAC (2021a): Alle Autokosten von A bis Z. Online verfügbar unter: https://www.adac.de/rund-ums-fahrzeug/auto-kaufen-verkaufen/autokosten/uebersicht/; zuletzt geprüft am 17.02.2022.

ADAC (2021b): VW ID.4 Pro Performance. Online verfügbar unter: https://www.adac.de/rund-ums-fahrzeug/autokatalog/marken-modelle/vw/id4/1generation/318521/#kosten; zuletzt geprüft am 19.03.022.

Ahmadi, L.; Yip, A.; Fowler, M.; Young, S.; Fraser, R. (2014): Environmental feasibility of re-use of electric vehicle batteries; Sustainable Energy Technologies and Assessments. 6. 64–74. 10.1016/j.seta.2014.01.006.

Armstrong, J.S. (2001): Principles of forecasting. A handbook for researchers and practitioners. Bosten: Kluwer Academic.

Balmer, M.; Rieser, M.; Meister, K.; Charypar, D.; Lefebvre, N.; Nagel, K.; Axhausen, K.W. (2008): MATSim-T: Architektur und Rechenzeiten.

Baustert, P; Benetto, E. (2017): Uncertainty analysis in agent-based modelling and consequential life cycle 835 assessment coupled models: A critical review', Journal of Cleaner Production, vol.156, pp.378-394.

Baustert, P.; Navarrete Gutiérrez, T.; Gibon, T.; Chion, L.; Ma, T.-Y.; Mariante, G.L.; Klein, S. (2019); Gerber, P.; Benetto, E. Coupling Activity-Based Modeling and Life Cycle Assessment—A Proof-of-Concept Study on Cross-Border Commuting in Luxembourg. Sustainability 2019, 11, 4067.

Bay, L. (2019): Rentabelsten Autohersteller der Welt. Online verfügbar unter: https://www.handelsblatt.com/unternehmen/industrie/autoindustrie-vw-vorne-daimler-stuerzt-ab-das-sind-die-rentabelsten-autohersteller-der-welt/24468460.html?ticket=ST-14554610-zU2FXVe5eMMlUfL9wlzJ-ap6; zuletzt geprüft am 17.02.2022.

Birke, P.; Schiemann, M. (2013): Akkumulatoren. Vergangenheit, Gegenwart und Zukunft elektrochemischer Energiespeicher. München: Herbert Utz Verlag GmbH.

Bischoff,J; Márquez-Fernández, F.J.; Domingues-Olavarría, G.; Maciejewski, M.; Nagel, K. (2019): Impacts of vehicle fleet electrification in Sweden – a simulation-based assessment of long-distance trips, 2019 6th International Conference on Models and Technologies for Intelligent Transportation Systems (MT-ITS), Cracow, Poland, 2019, pp. 1-7, doi: 10.1109/MTITS.2019.8883384.

Blasinski, B. (2008): Optimierung und Integration der Betriebsstrategie eines Kraftfahrzeugs mit parallelhybridem Antriebsstrang. Ingolstadt: Diplomarbeit.

Bobba, S.; Mathieux, F.; Ardente, F.; Blengini, G.; Cusenza, M. A.; Podias, A.; Pfrang, A. (2018): Life Cycle Assessment of repurposed electric vehicle batteries: an adapted method based on modelling energy flows; The Journal of Energy Storage. 19. 213-225. 10.1016/j.est.2018.07.008.

Bothe, B.; Steinfort, T. (2020): Cradle-to-Grave-Lebenszyklusanalyse im Mobilitätssektor Metastudie zur CO2-Bilanz alternativer Fahrzeugantriebe; Forschungsvereinigung Verbrennungskraftmaschinen e.V.; Frankfurt am Main.

Brander, M.; Tipper, R.; Hutchison, C.; Davis, G. (2009): Consequential and Attributional Approaches to LCA: A Guide to Policy Makers with Specific Reference to Greenhouse Gas LCA of Biofuels. Ecometrica. Technical Paper TP090403A. 44.

Brandão, M.; Levasseur, A.; Kirschbaum, M.U.F. et al. (2013): Key issues and options in accounting for carbon sequestration and temporary storage in life cycle assessment and carbon footprinting. Int J Life Cycle Assess 18, 230–240 (2013). https://doi.org/10.1007/s11367-012-0451-6.

Brown, L. D. (1991): Forecast selection when all forecasts are not equally recent. In: International Journal of Forecasting, 7, S. 349–356.

Bundesministerium für Umwelt, Naturschutz und nukleare Sicherheit (BMU) (2019): Klimaschutz in Zahlen. Fakten, Trends und Impulse deutscher Klimapolitik. Online verfügbar unter: https://www.bmu.de/fileadmin/Daten_BMU/Pools/Broschueren/klimaschutz_zahlen_2019_broschuere_bf.pdf; zuletzt geprüft am 31.12.2020.

Bundesministerium für Umwelt, Naturschutz und nukleare Sicherheit (BMU) (2021): Strom- und Wärmeversorgung in Zahlen; Entwicklung der spezifischen Kohlendioxid-Emissionen des deutschen Strommix 1990-2020. Online verfügbar unter: https://www.umweltbundesamt.de/themen/klima-energie/energieversorgung/strom-waermeversorgung-in-zahlen#Strommix; zuletzt geprüft am 20.11.2021.

Bundesregierung (2020): Klimafreundliche, bezahlbare Mobilität. Online verfügbar unter https://www.bundesregierung.de/breg-de/suche/kfz-steuer-1759368#:~:text=E%2DAutos%20bleiben%20steuerfrei,von%20der%20Kfz%20%2DSteuer%20befreit; zuletzt geprüft am 17.02.2022.

Burchart-Korol, D.; Folega, P. (2019): Comparative Life Cycle Impact Assessment of Chosen Passenger Cars with Internal Combustion Engines; Transp. Probl. 14, 69–76.

Can, B. (2019): Simulationsbasierte Analyse der zukünftigen Entwicklung von Fahrzeugantriebstechnologien und –konzepten; Masterarbeit; RWTH Aachen University, Aachen.

Castellani V.; Fantoni M.; Cristobal J.; Zampori L.; Sala S. (2017): Consumer Footprint - Basket of Products indicator on Mobility, EUR 28763 EN, Publications Office of the European Union, Luxembourg, ISBN 978-92-79-73191-4, doi:10.2760/539712, JRC107954.

Chiong, R. (2009): Nature-Inspired Algorithms for Optimisation. Studies in Computational Intelligence. Springer.

Cluzel, C.; Douglas, C. (2012): Cost and performance of EV batteries. Cambridge: Final report for The Committee on Climate Change.

Consequential-LCA (2015). The ISO 14040 standards for consequential LCA. Last updated: 2015-10-27. Online verfügbar unter: www.consequential-lca.org; zuletzt geprüft am 31.12.2020.

Dai, Q.; Kelly, J.C.; Gaines, L.; Wang, M. (2019): Life Cycle Analysis of Lithium-Ion Batteries for Automotive Applications; Batteries, 5, 48.

Dambeck, H. (2011): Kostenvergleich Rad gegen Auto. Online verfügbar unter: https://www.spiegel.de/auto/aktuell/kostenvergleich-rad-gegen-auto-das-velo-ist-sieger-der-herzen-a-753206.html; zuletzt geprüft am 19.03.2022.

Deb, K.; A. Pratap; S. Agarwal; T. Meyarivan (2002): A fast and elitist multiobjective genetic algorithm: NSGA-II. In: Evolutionary Computation, IEEE Transactions on 6.2, S. 182–197.

Dér, A.; Erkisi-Arici, S.; Stachura, M.; Cerdas, F.; Böhme, S.; Herrmann, C. (2018): Life Cycle Assessment of Electric Vehicles in Fleet Applications; In Fleets Go Green; Herrmann, C., Mennenga, M.S., Böhme, S., Eds.; Springer: Berlin/Heidelberg, Germany.

Desai, C.; Berthold, F.; Williamson, S.S. (2010): “Optimal drivetrain component sizing for a Plug-in Hybrid Electric transit bus using Multi-Objective Genetic Algorithm”. In: Electric Power and Energy Conference (EPEC). 2010, S. 1–5.

DieselNet: Emission Test Cycles. Worldwide Harmonized Light Vehicles Test Cycle (WLTC). Online verfügbar unter: https://dieselnet.com/standards/cycles/wltp.php; zuletzt geprüft am 09.03.2022.

Ding, N.; Pan, J.; Zhang, Z.; Yang, J. (2019): Life cycle assessment of car sharing models and the effect on GWP of urban transportation: A case study of Beijing; Sci. Total Environ.; 688, 1137–1144.

Dunn, J.; Gaines, L.; Sullivan, J.; Wang, M. (2012): The Impact of Recycling on Cradle-to-Gate Energy Consumption and Greenhouse Gas Emissions of Automotive Lithium-Ion Batteries; Environmental science & technology. 46. 10.1021/es302420z.

Dunn, J.; Gaines, L.; Kelly, J.; James, C.; Gallagher, K. (2014): The significance of Li-ion batteries in electric vehicle life-cycle energy and emissions and recycling's role in its reduction; Energy Environ. Sci.. 8. 10.1039/C4EE03029J.

Eckstein, L. (2015): Alternative und elektrifizierte Fahrzeugantriebe. Aachen: fka Forschungsgesellschaft Kraftfahrwesen mbH Aachen.

Environmental Protection Agency (EPA); Carlifornia Air Resources Board; National Highway Traffic and Safety Administration (2016): Midterm Evaluation of Light-Duty Vehicle Greenhouse Gas Emission Standards and Corporate Average Fuel Economy Standards for Model Years 2022-2025. Draft Technical Assessment Report. Washington, DC.

Eshelman, L. J.; Schaffer, J. D. (1993): Real–Coded Genetic Algorithms and Interval-Schemata. In: Foundation of Genetic Algorithms 2. Hrsg. von Morgan Kaufmann. San Mateo, S. 187–202.

Estep, D. (2005): Angewandte Analysis in einer Unbekannten. Berlin-Heidelberg: Springer.

European Commission - Joint Research Centre - Institute for Environment and Sustainability (2010): International Reference Life Cycle Data System (ILCD) Handbook - General guide for Life Cycle Assessment - Detailed guidance. First edition March 2010. EUR 24708 EN. Luxembourg. Publications Office of the European Union.

Faria, R.; Marques, P.; Garcia, R.; Moura, P.; Freire, F.; Delgado, J.; de Almeida, A. (2014): Primary and secondary use of electric mobility batteries from a life cycle perspective; Journal of Power Sources. 262. 169–177. 10.1016/j.jpowsour.2014.03.092.

Federal Reserve Bank of St. Louis (2022): Historische Wechselkurse. Online verfügbar unter: https://www.federalreserve.gov/releases/h10/hist/default.htm; zuletzt geprüft am 14.02.2022.

FinanceScout24 (2022): Kfz-Steuer: Rechner und Infos. Online verfügbar unter: https://www.financescout24.de/wissen/ratgeber/kfz-steuer-rechner; zuletzt geprüft am 17.02.2022.

Fink, H.; Fetzer, J. (2015): 2. Generation Li-Ionen-Batteriesysteme. Techniktrends und KPIs. In: Hiebl, J. (Hrsg.): Der Antrieb von morgen 2015. Wiesbaden: Springer.

Francesco, D.P.; Delogu, M.; Pierini, M. (2018): Life Cycle Assessment in the automotive sector: a comparative case study of Internal Combustion Engine (ICE) and electric car. Procedia Structural Integrity. 12. 521-537. 10.1016/j.prostr.2018.11.066.

Friedrich, H.E.; Schmid, S.A. (2011): Strukturanalyse von Automobilkomponenten für zukünftige elektrifizierte Fahrzeugantriebe. Stuttgart: Endbericht.

Fröberg, A.(2008): "Efficient Simulation and Optimal Control for Vehicle Propulsion". Dissertation. Universität Linköping, Department of Electrical Engineering, Schweden.

Gerike, R.; Hubrich, S.; Ließke, F.; Wittig, S.; Wittwer, R. (2019): Mobilitätssteckbrief für Berlin. Technische Universität Dresden.

Girardi, P.; Gargiulo, A.; Brambilla, P.C. (2015): A comparative LCA of an electric vehicle and an internal combustion engine vehicle using the appropriate power mix: The Italian case study; Int. J. Life Cycle Assess; 20,1127–1142.

Göhlich, D.; Nagel, K.; Syré, A.; Grahle, A.; Martins-Turner, K.; Ewert, R.; Jahn, R.; Jefferies, D. (2020): Integrated Approach for the Assessment of Strategies for the Decarbonization of Urban Traffic; 10.20944/preprints202012.0121.v1.

Guzella, L.; Sciarretta A. (2013): Vehicle Propulsion Systems. Introduction to Modeling and Optimization. Heidelberg: Springer.

Hamburger Verkehrsverbund (2019): Mobilität A-Z: Kosten der Mobilität. Online verfügbar unter: https://www.hvv-schulprojekte.de/unterrichtsmaterialien/kosten-mobilitaet/; zuletzt geprüft am 19.03.2022.

Hawkins, T.R.; Singh, B.; Majeau-Bettez, G.; Strømman, A.H. (2013): Comparative Environmental Life Cycle Assessment of Conventional and Electric Vehicles; J. Ind. Ecol. 17, 53–64.

Hennings, J. (2017): Prognoseanalyse der zukünftigen Entwicklung von Fahrzeugantriebstechnologien. Masterarbeit; Otto-von-Guericke-Universität Magdeburg; Magdeburg.

Herdt, I. (2005): Proseminar „Algorithmen der Verkehrssimulation“ - Makroskopische Verkehrssimulation als ein Mittel der Verkehrsplanung. Online verfügbar unter: https://www5.in.tum.de/lehre/seminare/verkehr/WS05/materialien/thema02_handout.pdf; zuletzt geprüft am 02.02.2022.

Hofmann, P. (2014): Hybridfahrzeuge. Ein alternatives Antriebssystem für die Zukunft. Wien: Springer.

Holland, J. (1975): Adaptation in Natural and Artificial Systems; The University of Michigan Press.

Horni, A.; Nagel, K.; Axhausen, K.W. (eds.) (2016): The Multi-Agent Transport Simulation MATSim. London: Ubiquity Press. DOI: http://dx.doi.org/10.5334/baw.

Hörl, S.; Balac, M. (2020): Open data travel demand synthesis for agent-based transport simulation: A case study of Paris and Île-de-France. 10.3929/ethz-b-000412979. 2020.

Huss, A.; Maas H.; Hass, H. (2013): Well-to-Wheel Analysis of Future Automotive Fuels and Powertrains in the European Context. Luxemburg: Publications Office of the European Union.

IEA (2019): World Energy Outlook 2019; IEA; Paris. Online verfügbar unter: https://www.iea.org/reports/world-energy-outlook-2019; zuletzt geprüft am 20.11.2021.

Imhof, S; Schulz, S. (2021): Lime, Circ, Bird, Voi, Tier, Uber Jump im Test: Die besten E-Scooter-Sharingdienste (2021). Online verfügbar unter: https://www.chip.de/artikel/Lime-Circ-Bird-Voi-Tier-Uber-Jump-im-Test-Die-besten-E-Scooter-Sharingdienste_170385530.html; zuletzt geprüft am 19.03.2022.

ISO 14044 (2006): Environmental management – Life cycle assessment – Requirements and guidelines (ISO 14044:2006); German and English version EN ISO 14044:2006.

James, G.; Witten, D.; Hastie, T.; Tibshirani, R. (2015): An Introduction to Statistical Learning. New York: Springer.

Jain, M.; Desai, C.; Williamson, S.S. (2009): "Genetic algorithm based optimal powertrain component sizing and control strategy design for a fuel cell hybrid electric bus". In: Vehicle Power and Propulsion Conference, 2009. VPPC '09. IEEE. 2009, S. 980–985.

Kowalewsky, R. (2021): ÖPNV in NRW: Tarifrevolution mit Abrechnung nur nach Strecke – Eezy. Online verfügbar unter: https://rp-online.de/wirtschaft/oepnv-in-nrw-tarifrevolution-mit-abrechnung-nur-nach-strecke-eezy_aid-64370711; zuletzt geprüft am 19.03.2022.

Koziel, S.; Yang, X.-S. (2011): Computational Optimization, Methods and Algorithms. Bd. 356. Studies in Computational Intelligence. Berlin und Heidelberg: Springer-Verlag.

Kraftfahrt-Bundesamt (2020): Neuzulassungen. Online verfügbar unter: https://www.kba.de/DE/Statistik/Fahrzeuge/Neuzulassungen/Zulassungsbezirke/n_zulassungsbezirke_node.html; zuletzt geprüft am 29.04.2022; Datenlizenz by-2-0.

Kraftfahrt-Bundesamt (2021): Zahlen, Daten, Fakten - Fahrzeugalter 2021. https://www.kba.de/DE/Statistik/Fahrzeuge/Bestand/Fahrzeugalter/fahrzeugalter_node.html; zuletzt geprüft am 16.02.2022; Datenlizenz by-2-0.

Kraftfahrt-Bundesamt (2022): Umwelt 2022. https://www.kba.de/DE/Statistik/Fahrzeuge/Bestand/bestand_node.html; zuletzt abgerufen am 31.03.2022; Datenlizenz by-2-0.

Kroher, T.; Paulsen, T. (2022): Förderung für Elektroautos. Online vergübar unter: https://www.adac.de/rund-ums-fahrzeug/elektromobilitaet/kaufen/foerderung-elektroautos/#umweltbonus-und-innovationspraemie; zuletzt geprüft am 17.02.2022.

Kunze, K.; Kircher, O. (2012): Cyro-Compressed Hydrogen Storage. Oxford: Vortrag für Cryogenic Cluster Day.

Lajunen, A.; Kivekäs, K.; Vepsäläinen, J.; Tammi, K. (2020): Influence of Increasing Electrification of Passenger Vehicle Fleet on Carbon Dioxide Emissions in Finland; Sustainability, 12, 5032.

Lawrence, M.; Goodwin, P.; O'Connor M.; Önkal, D. (2006): Judgmental forecasting. A review of progress over the last 25 years. In: International Journal of Forecasting, 22, S. 493–518.

Leinweber, D. J. (2007): "Stupid data miner tricks". In: The Journal of Investing, 16, S. 15–22.

Llorca, C.; Moeckel, R. (2019): Effects of scaling down the population for agent-based traffic simulations. Procedia Computer Science. 151. 782-787. 10.1016/j.procs.2019.04.106.

Lunze, J. (2012): Automatisierungstechnik: Methoden für die Überwachung und Steuerung kontinuierlicher und ereignisdiskreter Systeme. Oldenbourg Wissenschaftsverlag.

MATSim Javadoc (2022): MATSim Dokumentation. Online verfügbar unter: https://matsim.org/javadoc; zuletzt geprüft am 03.04.2022.

McDowall, W.; Eames, M. (2006): Forecasts, scenarios, visions, backcasts and roadmaps to the hydrogen economy. A review of the hydrogen futures literature. In: Energy Policy, 34, S. 1236–1250.

Merchan, A.; Belboom, S.; Léonard, A. (2017): Life Cycle Assessment of freight transport in Belgium.

Mitusch, K. (2019): Daten und Fakten zum Energieverbrauch des Schienenverkehrs. Online verfügbar unter: https://www.forschungsinformationssystem.de/servlet/is/342234/; zuletzt geprüft am 24.05.2022.

Moses, S. (2014): "Optimierungsstrategien für die Auslegung und Bewertung energieoptimaler Fahrzeugkonzepte". Dissertation. Technische Universität Berlin.

Nykvist, B.; Nilsson, M. (2015): Rapidly falling costs of battery packs for electric vehicles. In: Nature Climate Change, 5, S. 329–332.

Ortúzar, J.d.D.; Willumsen, L.G (2011): Modelling Transport, 4th ed.; Wiley, Hoboken.

Osborne, M.J; Rubinstein, A. (1994): "A Course in Game Theory," MIT Press Books, The MIT Press, edition 1, volume 1, number 0262650401, December.

Papageorgiou, M. (2012): Optimierung: Statische, Dynamische, Stochastische Verfahren. Springer London, Limited.

Paschotta R. (2020): Artikel 'Luftwiderstand' im RP-Energie-Lexikon. Online verfügbar unter: https://www.energie-lexikon.info/luftwiderstand.html; zuletzt geprüft am 09.03.2022.

Peters, J.F.; Baumann, M.; Zimmermann, B.; Braun, J.; Weil, M. (2017): The environmental impact of Li-Ion batteries and the role of key parameters - A review; Renew Sustain. Energy Rev; 67, 491–506.

Pischinger , S. (2016): Alternative und elektrifizierte Fahrzeugantriebe. Aachen: Selbstverlag des Lehrstuhls für Verbrennungskraftmaschinen.

Propfe, B. (2016): Marktpotentiale elektrifizierter Fahrzeugkonzepte unter Berücksichtigung von technischen, politischen und ökonomischen Randbedingungen; Dissertation; Universität Stuttgart.

Querini, F.; Benetto, E. (2014): Agent-based modelling for assessing hybrid and electric cars deployment policies in Luxembourg and Lorraine. Transportation Research Part A: Policy and Practice. 70. 149-161. 10.1016/j.tra.2014.10.017, 2014.

Querini, F.; Benetto, E. (2017): Combining Agent-Based Modeling and Life Cycle Assessment for the Evaluation of Mobility Policies. Environmental Science & Technology. 51. 10.1021/acs.est.7b00079.

Randolph, J. J. (2009): A Guide to Writing the Dissertation Literature Review. In: Practical Assessment Research & Evaluation, 14.

Raugei, M.; Winfield, P. (2018): Prospective LCA of the production and EoL recycling of a novel type of Li-ion battery for electric vehicles; Journal of Cleaner Production. 213. 10.1016/j.jclepro. 2018.12.237.

Reid, G.; Julve, J. (2016): Second Life-Batteries As Flexible Storage For Renewables Energies; Berlin.

Reif, K. (2011): Bosch Grundlagen Fahrzeug- und Motorentechnik. Konventioneller Antrieb, Hybridantriebe, Bremsen, Elektronik. Wiesbaden: Vieweg+Teubner Verlag.

Reif, K.; Noreikat, K.E.; Borgeest, K. (2012): Kraftfahrzeughybridantriebe. Grundlagen, Komponenten, Systeme, Anwendungen. Wiesbaden: Springer Vieweg.

Ressing, M.; Blettner, M.; Klug, S. J. (2009): Systematic literature reviews and meta-analyses. part 6 of a series on evaluation of scientific publications. In: Deutsches Ärzteblatt international, 106, S. 456–463.

Rieser, M. (2019): MATSim Tutorial, European Institute for Energy Research, July 22 – 25. Online verfügbar unter: https://www.simunto.com/matsim/tutorials/eifer2019/slides_day1.pdf; zuletzt geprüft am 24.02.2022.

Schmidt, R. (2018): So viel Strom bräuchte ein vollständig elektrischer Straßenverkehr. Online verfügbar unter: https://edison.media/erklaeren/so-viel-strom-braeuchte-ein-vollstaendig-elektrischer-strassenverkehr/23204256.html#:~:text=Kombiniert%20man%20die%20unterschiedlichen%20Verbrauchswerte,Strombedarf%20von%20knapp%20177%20Terawattstunden; zuletzt geprüft am 24.05.2022.

Schmuck, S.; Mietzel, T. (2010): Ökobilanzielle Bewertung von Maßnahmen der Niederschlagswasserbehandlung. Online verfügbar unter: https://docplayer.org/77551563-Oekobilanzielle-bewertung-von-massnahmen-der-niederschlagswasserbehandlung.html; zuletzt geprüft am 20.10.2022.

Schneider, D. (2022): Methodik für die Analyse zukünftiger technologischer Potenziale von Fahrzeugantriebskonzepten; Dissertation; Technische Universität Chemnitz.

Siebertz, K.; van Bebber, D.; Hochkirchen, T. (2010): Statistische Versuchsplanung. VDI-Buch. Springer.

Sperka, F. (2022): 'Charging' for phase-out Why public chargers won't be a block on EU's combustion car phase-out; Transport & Environment.

Statistik Berlin-Brandenburg (2021): Überblick Zensus. Online verfügbar unter: https://www.statistik-berlin-brandenburg.de/bevoelkerung/zensus; zuletzt geprüft am 26.11.2021.

Steinhilper, W.; Sauer, B. (2012): Konstruktionselemente des Maschinenbaues 2. Grundlagen von Maschinenelementen für Antriebsaufgaben. Berlin-Heidelberg: Springer-Verlag.

Steinmeyer, I.; Manuel Herrmann-Fiechtner, M. (2017): Mobilität der Stadt - Berliner Verkehr in Zahlen 2017. Senatsverwaltung für Umwelt, Verkehr und Klimaschutz. Abteilung Verkehr.

Steubing, B.; Mutel, C.; Suter, F.; Hellweg S. (2016): Streamlining scenario analysis and optimization of key choices in value chains using a modular LCA approach. Int J Life Cycle Assess 21, 510–522 (2016). https://doi.org/10.1007/s11367-015-1015-3.

Syré, A.M.; Heining, F.; Göhlich, D. (2020): Method for a Multi-Vehicle, Simulation-Based Life Cycle Assessment and Application to Berlin's Motorized Individual Transport; Sustainability 2020, 12, 7302.

Töpler, J.; Lehmann, J. (2017): Wasserstoff und Brennstoffzelle. Technologien und Marktperspektiven. Heidelberg: Springer Vieweg.

Uhlig, J. (2021): E-Auto: Kfz-Steuer, steuerfrei. Online verfügbar unter: https://www.autobild.de/artikel/e-auto-kfz-steuer-steuerfrei-2021-3689537.html; zuletzt geprüft am 17.02.2022.

Umweltbundesamt - TREMOD 6.21 (11/2021) (2021): „Vergleich der durchschnittlichen Emissionen einzelner Verkehrsmittel im Personenverkehr in Deutschland". Online verfügbar unter: https://www.umweltbundesamt.de/sites/default/files/medien/366/bilder/dateien/uba_emissionstabelle_personenverkehr_2020.pdf; zuletzt geprüft am 24.05.2022.

Unterreiner, L.; Jülch, V.; Reith, S. (2016): Recycling of Battery Technologies – Ecological Impact Analysis Using Life Cycle Assessment (LCA); Energy Procedia. 99. 229-234. 10.1016/j.egypro.2016.10.113.

VCÖ (2021): „Österreichs Verkehr hat zweithöchsten Pro-Kopf CO2-Ausstoß der EU“. Online verfügbar unter: https://www.vcoe.at/presse/presseaussendungen/detail/vcoe-oesterreichs-verkehr-hat-zweithoechsten-pro-kopf-co2-ausstoss-der-eu; zuletzt geprüft am 24.05.2022.

Volkswagen AG (2021): Die CO_2-Bilanz des Elektro-Fahrzeugs. Online verfügbar unter: https://www.volkswagenag.com/de/news/stories/2021/02/e-mobility-is-already-this-much-more-climate-neutral-today.html; zuletzt geprüft am 14.03.2022.

Weise, T. (2009): Global Optimization Algorithms - Theory and Application. Online verfügbar unter: http://www.it-weise.de/projects/book.pdf; zuletzt geprüft am 17.02.2022.

Weiß, F. (2018): Methodik zur optimalen Konzeptauslegung elektrifizierter Fahrzeugantriebsstränge; Dissertation; Technische Universität Chemnitz; Springer Fachmedien; Wiesbaden.

Wolf, J.; Schönfelder, S.; Samaga U.; Oliveira M.; Axhausen K. W. (2004): Eighty weeks of Global Positioning System traces, Transportation Research Record, 1870, 46–54.

Zhao, Y.; Tatari, O. (2015): A hybrid life cycle assessment of the vehicle-to-grid application in light duty commercial fleet. Energy. 93. 1277-1286. 10.1016/j.energy.2015.10.019.

Ziemke, D.; Kaddoura, I.; Nagel, K. (2019): The MATSim Open Berlin Scenario: A multimodal agent-based transport simulation scenario based on synthetic demand modeling and open data; Procedia Computer Science. 151. 870-877. 10.1016/j.procs.2019.04.120.

Appendix

A.1 Event sequences in MATSim

For the translation of the events, sequences of the considered travel modes need to be defined. In general each travel mode can be analyzed as long as the event sequence is described. In the following the typical MATSim travel modes car, public transport and teleported travel modes are described. For private owned vehicles the event sequences for the agents starts with the end of the current activity, for example leaving its home. Then the agents starts to depart and enters the vehicle. In the next event the vehicle enters the corresponding link. While driving, the vehicle leaves the current link and enters the next link until the destination is reached. At the destination the vehicle leaves the traffic. The agent leaves the car and arrives at the activity location where the activity starts. This sequence is shown in Figure 101.

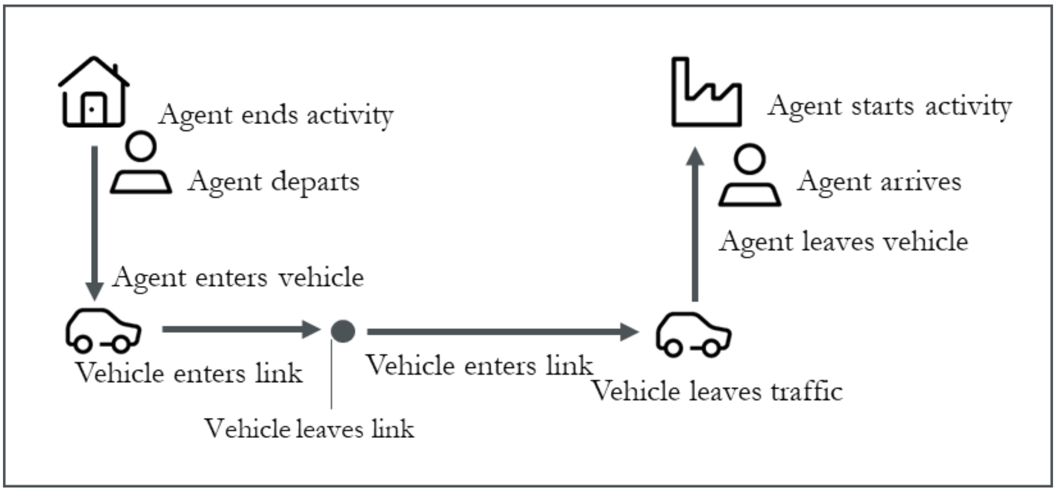

Figure 101: Event sequence for private owned vehicles based on [Rieser 2019]

Another considered travel mode is the public transport. Here the agent ends his current activity and departs from his current location. Then the agent walks to the public transport stop. When arrived, the agent waits to interact with the public transport. Meanwhile the public transport arrives at the stop. The agent interacts with the public transport and enters the vehicle. Afterwards the vehicle departs and drives to the next stop. When the agent reaches his destination, the agent leaves the car. Then the agent walks to the activity location to perform his activity. Meanwhile the public transport departs for the next stop. This sequence is shown in Figure 102.

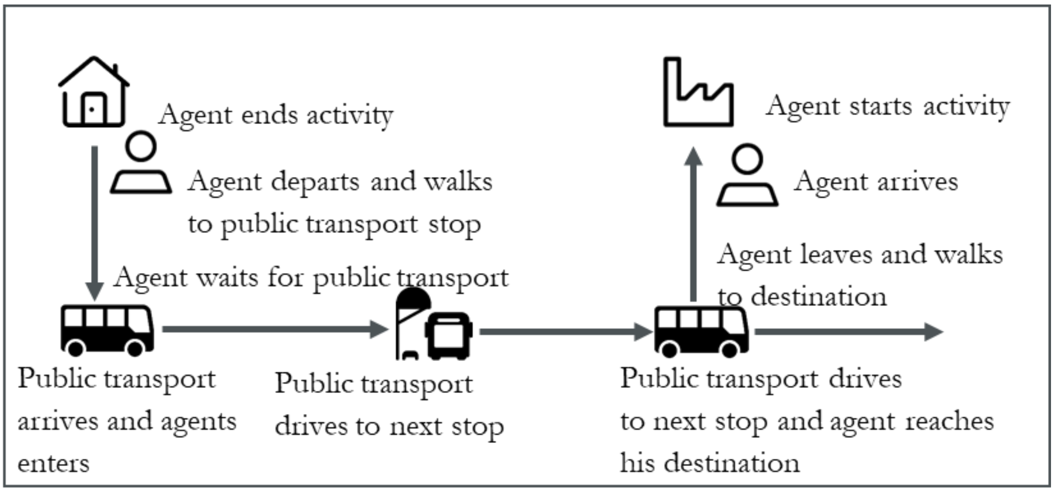

Figure 102: Event sequence for public transport based on [Rieser 2019]

If the events of a certain travel mode is not defined, it is possible to model them as teleported travel modes. This is a simplified approach, where the travel mode is mostly defined by its average speed and beeline distance factor, which estimates the actually traveled distances. In the following the event sequence for teleported modes is described. At the beginning the agent ends his current activity, departs and disappears from the network. Then the travel time is estimated with the average speed of the travel mode as well as the distance from the starting location to the destination. As soon as the travel time has been reached, the agent will reappear at his destination and start his activity. This sequence is shown in Figure 103.

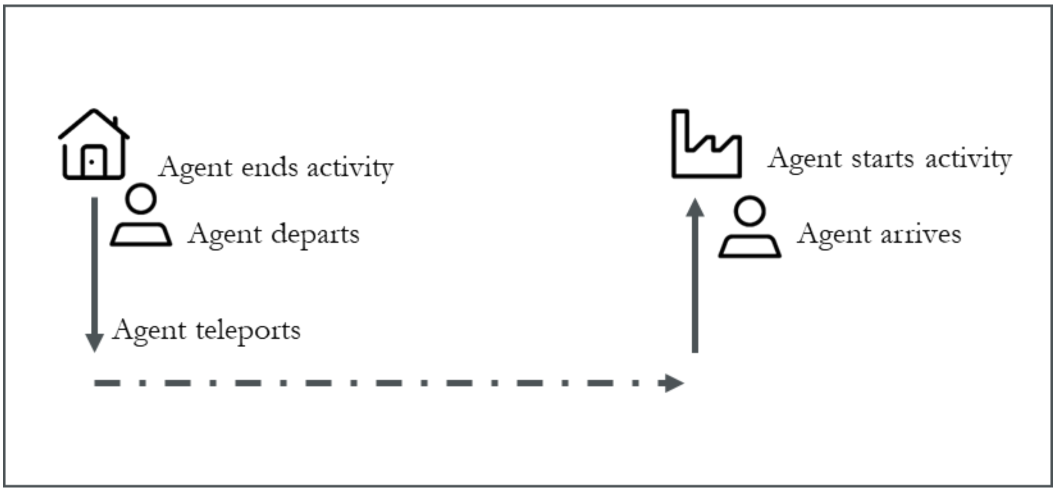

Figure 103: Event sequence for teleported modes based on [Rieser 2019]

Furthermore the event sequence of demand response transport (DRT) for mobility on demand concepts is added and can be analyzed. The event sequence is described in the following. The agent ends his current activity and departs from the current activity location. Then the agent requests a DRT. The passengers request is scheduled. A DRT, which is nearby and reaches the agents as fast as possible is assigned to this agent. The vehicle drives to the agent. The agent waits until the vehicle arrives and enters the vehicle once the vehicle has arrived. The vehicle drives to the destination and the agent leaves the vehicle once the destination has been reached. Afterwards the agents starts his activity. Meanwhile the vehicle is assigned to new customers. In Figure 104 the event sequence is shown. For the DRTs a separate trip table is generated to also evaluate the impact of the DRTs. To avoid double counting, the impact is assigned to the DRTs and not to the agents.

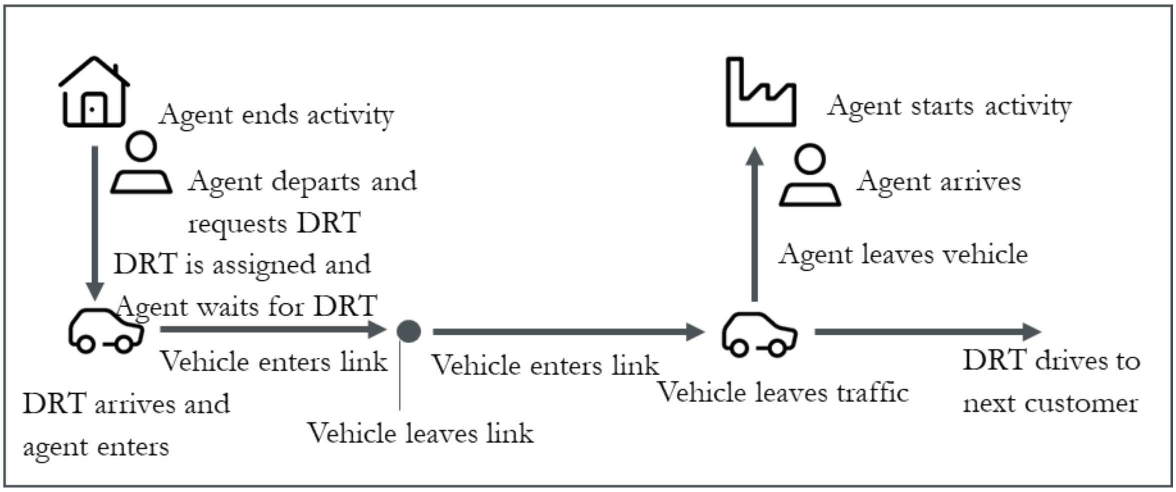

Figure 104: Event sequence for demand response transport

A.2 Berlin parameterization

Table 17: Attributes for the region of Berlin

Variable	**Unit**	**Region**
Id	-	1
Region	-	Berlin
Population	-	3644826
Population density	Residents/km²	4090
Average disposable income	€	20330
Share of male residents	-	0.492
Share of female residents	-	0.508
Share of professionals in the total population	-	0.46
Share of unemployed persons of working age	-	0.091
Share of pupils and students	-	0.232
Share of small cars	-	0.267
Share of compact cars	-	0.397
Share of small SUV	-	0.34
Share gasoline	-	0.991
Share diesel	-	0
Share HEV	-	0
Share PHEV	-	0.0086
Share BEV	-	0.002
Share FCEV	-	0
Share public transport (W)	-	0.15
Share private car (W)	-	0.677
Share motorbike (W)	-	0
Share bike (W)	-	0.090
Share walking (W)	-	0.082
Share micro mobility (W)	-	0
Share of distance under 5 km (W)	-	0.279
Share of distance 5 to 10 km (W)	-	0.199
Share of distance 10 to 25 km (W)	-	0.2750
Share of distance 25 to 50 km (W)	-	0.1310
Share of distance more than 50 km (W)	-	0.077
Share of Home Office (W)	-	0.039
Homeowner (W)	-	0.391
Share public transport (Edu)	-	0.474
Share private car (Edu)	-	0.178
Share motorbike (Edu)	-	0

Share bike (Edu)	-	0.135
Share walking (Edu)	-	0.212
Share micro mobility (Edu)	-	0
Share of distance under 5 km (Edu)	-	0.4950
Share of distance 5 to 10 km (Edu)	-	0.209
Share of distance 10 to 25 km (Edu)	-	0.181
Share of distance 25 to 50 km (Edu)	-	0.072
Share of distance more than 50 km (Edu)	-	0.041
Share public transport (Other)	-	0.474
Share private car (Other)	-	0.178
Share motorbike (Other)	-	0
Share bike (Other)	-	0.135
Share walking (Other)	-	0.212
Share micro mobility (Other)	-	0
Share of distance under 5 km (Other)	-	0.4950
Share of distance 5 to 10 km (Other)	-	0.209
Share of distance 10 to 25 km (Other)	-	0.181
Share of distance 25 to 50 km (Other)	-	0.072
Share of distance more than 50 km (Other)	-	0.041

A.3 Assumption for mean velocity of used travel modes

Table 18: Assumed mean velocity of used travel modes

Variable	**Value in km/h**
Car	90 (for distance over 10 km), 40 (for rest)
Public transport	30
Bike	15
Walk	3
Micro mobility	20

A.4 Attributes of additional travel modes

Table 19: Attributes of bicycle

Attributes	**Unit**
Max. Velocity	30 km/h
Range (electric / fossil)	- km
Number of seats	1
Trunk volume	0 – 50 l
CO_{2eq} emissions in the production phase	8 gCO_{2eq}/km
CO_{2eq} emissions in the use phase	0
CO_{2eq} emissions in total	8 gCO_{2eq}/km * distance
Costs (per month and pkm)	0.1 €/pkm
Total costs	0.1 €/pkm * distance
Investment costs for development of pt, charging infrastructure, …	-
Energy demand (electric / fossil)	0

Table 20: Attributes of walking

Attributes	**Unit**
Max. Velocity	10 km/h
Range (electric / fossil)	- km
Number of seats	-
Trunk volume	-
CO_{2eq} emissions in the production phase	0
CO_{2eq} emissions in the use phase	0
CO_{2eq} emissions in total	0
Costs (per month and pkm)	0
Total costs	0
Investment costs for development of pt, charging infrastructure, …	-
Energy demand (electric / fossil)	0

Table 21: Attributes of public transport (train)

Attributes	**Unit**
Max. Velocity	35 km/h
Range (electric / fossil)	- km
Number of seats	200
Trunk volume	0 – 50 l
CO_{2eq} emissions in the production phase	37 gCO_{2eq}/km
CO_{2eq} emissions in the use phase	64 gCO_{2eq}/km
CO_{2eq} emissions in total	(37 + 64) gCO_{2eq}/km * distance
Costs (per month and pkm)	0.25 €/pkm + 1.5 €/trip
Total costs	0.25 €/pkm * distance + 1.5€/trip * number_of_trips
Investment costs for development of pt, charging infrastructure, …	0.4 €/pkm
Energy demand (electric / fossil)	12.1 kWh/100pkm (electric)

Table 22: Attributes of public transport (bus)

Attributes	**Unit**
Max. Velocity	50 km/h
Range (electric / fossil)	- km
Number of seats	50
Trunk volume	0 – 50 l
CO_{2eq} emissions in the production phase	9 gCO_{2eq}/km
CO_{2eq} emissions in the use phase	85 gCO_{2eq}/km
CO_{2eq} emissions in total	(9 + 85) gCO_{2eq}/km * distance
Costs (per month and pkm)	0.25 €/pkm + 1.5 €/trip
Total costs	0.25 €/pkm * distance + 1.5€/trip * number_of_trips
Investment costs for development of pt, charging infrastructure, …	0.17 €/pkm
Energy demand (electric / fossil)	12.1 kWh/100pkm (electric)

Table 23: Attributes of micro mobility

Attributes	Unit
Max. Velocity	20 km/h
Range (electric / fossil)	30 km
Number of seats	-
Trunk volume	-
$CO2_{eq}$ emissions in the production phase	-
$CO2_{eq}$ emissions in the use phase	-
$CO2_{eq}$ emissions in total	119 $gCO2_{eq}$/km * distance
Costs (per month and pkm)	0.2 €/pkm + 1 €/trip
Total costs	0.2 €/pkm * distance + 1€/trip * number_of_trips
Investment costs for development of pt, charging infrastructure, …	-
Energy demand (electric / fossil)	1.5 kWh/100km (electric)

A.5 Requirement classes

In the following the assumption for the requirement classes for each powertrain type, vehicle type and vehicle segment is described in detail in Table 24, Table 25 and Table 26.

Table 24: Requirement Class Definition for Small Cars (A00 and A0 Segment – One Wheel Drive)

Requirement class	Low	Medium	High
BEV	[200, 140, 14]	[250, 150, 12]	[350, 160, 10]
FCEV	[200, 140, 14]	[250, 150, 12]	[350, 160, 10]
ICEV (PHEV)	[60, 160, 12] 140 km/h purely electric	[80, 170, 11] 140 km/h purely electric	[100, 180, 9] 140 km/h purely electric
ICEV (incl. mHEV)	[40l Tank, 160, 12]	[40l Tank, 170, 11]	[40l Tank, 180, 9]

Format: [range (zero emission), max. velocity, acc.]

Flat: Polo, eUp

Base mass: 700 kg
Cw*A: 0.32 * 2.05 m²
Rolling resistance factor f_R: 0.006
P_N: 300 W
P_N_Performance: 800 W

SUV: T-Roc

Base mass: 800 kg
Cw*A: 0.35 * 2.2 m²
Rolling resistance factor f_R: 0.006
P_N: 300 W
P_N_Performance: 800 W

Table 25: Requirement Class Definition for Compact Cars (A and B Segment – One Wheel Drive)

Requirement class	Low	Medium	High
BEV	[250, 150, 10]	[350, 160, 9]	[500, 180, 7.5]
FCEV	[250, 150, 10]	[350, 160, 9]	[500, 180, 7.5]
ICEV (PHEV)	[60, 180, 10] 140 km/h purely electric	[80, 190, 9] 140 km/h purely electric	[100, 220, 7.5] 140 km/h purely electric
ICEV (incl. mHEV)	[50l Tank, 180, 10]	[50l Tank, 190, 9]	[50l Tank, 220, 7.5]

Format: [range (zero emission), max. velocity, acc.]

Flat: Golf, ID.3

Base mass: 900 kg
Cw*A: 0.3 * 2.2 m²
Rolling resistance factor f_R: 0.006
P_N: 300 W
P_N_Performance: 1 kW

SUV: Tiguan, ID.4

Base mass: 1050 kg
Cw*A: 0.32 * 2.5 m²
Rolling resistance factor f_R: 0.006
P_N: 300 W
P_N_Performance: 1 kW

Table 26: Requirement Class Definition for Large Cars (C and D Segment – AWD)

Requirement class	Low	Medium	High
BEV	[400, 170, 8]	[500, 180, 7]	[750, 200, 5]
FCEV	[400, 170, 8]	[500, 180, 7]	[750, 200, 5]
ICEV (PHEV)	[80, 200, 8] 140 km/h purely electric	[100, 220, 7] 140 km/h purely electric	[150, 250, 5] 140 km/h purely electric
ICEV (incl. mHEV)	[70l Tank, 200, 8]	[70l Tank, 220, 7]	[70l Tank, 250, 5]

Format: [range (zero emission), max. velocity, acc.]

Flat: A6, Tesla Model S

Base mass: 1300 kg
Cw*A: 0.27 * 2.4 m²
Rolling resistance factor f_R: 0.007
P_N: 300 W
P_N_Performance: 1,5 kW

SUV: Q7, eTron

Base mass: 1700 kg
Cw*A: 0.31 * 2.9 m²
Rolling resistance factor f_R: 0.007
P_N: 300 W
P_N_Performance: 1,5 kW

A.6 Parameter set for vehicle simulation

Table 27: Parameter set for vehicles

Parameter Settings	
Vehicle ID	Motor type
Vehicle Name	Engine Power
Production Year	Engine Displacement
Vehicle Type	Transmission Type
Powertrain Type	Transmission Axle Ratio
Requirement Class	E-Motor Type
Premium Vehicle	E-Motor Power
Drag Coefficient	E-Motor Type (Generator)
Cross-Sectional Area	E-Motor Power (Generator)
Rolling Resistance Coefficient	Battery Type
Dynamic Wheel Radius	Cell Chemistry
Weight Share Front Axle	Battery Power
On-Board Power Supply (Electric Vehicle)	Battery Energy
On-Board Power Supply (Hybrid Vehicle)	Fuel Cell Type
Empty Mass	Fuel Cell Power
Base Mass	Type of DC/DC
Maximum Payload	Total DC/DC Power
Wheelbase	Fuel Type
Vehicle Width	Fuel Volume Conventional Tank
Vehicle Height	Specific Fuel Mass Conventional Tank
Center of Gravity Height	Specific Fuel Volume Conventional Tank
Number of Seats	System Mass Conventional Tank
Trunk Volume	Type of Hydrogen Tank
Coefficient of Friction	Fuel Mass of Hydrogen
Type of HV-Drive	Hydrogen Tank Mass
Cooling Type	Specific Fuel Mass Hydrogen Tank
Heating Type	Specific Fuel Volume Hydrogen Tank
PTC Power	Type of CNG Tank
Charger	Fuel Mass CNG
Climate Reference	CNG Tank Mass
Driving Profile	Specific Fuel Mass CNG Tank
Driving Cycles	Specific Fuel Volume CNG Tank

A.7 CO_{2eq} database

Structure of CO_{2eq} database

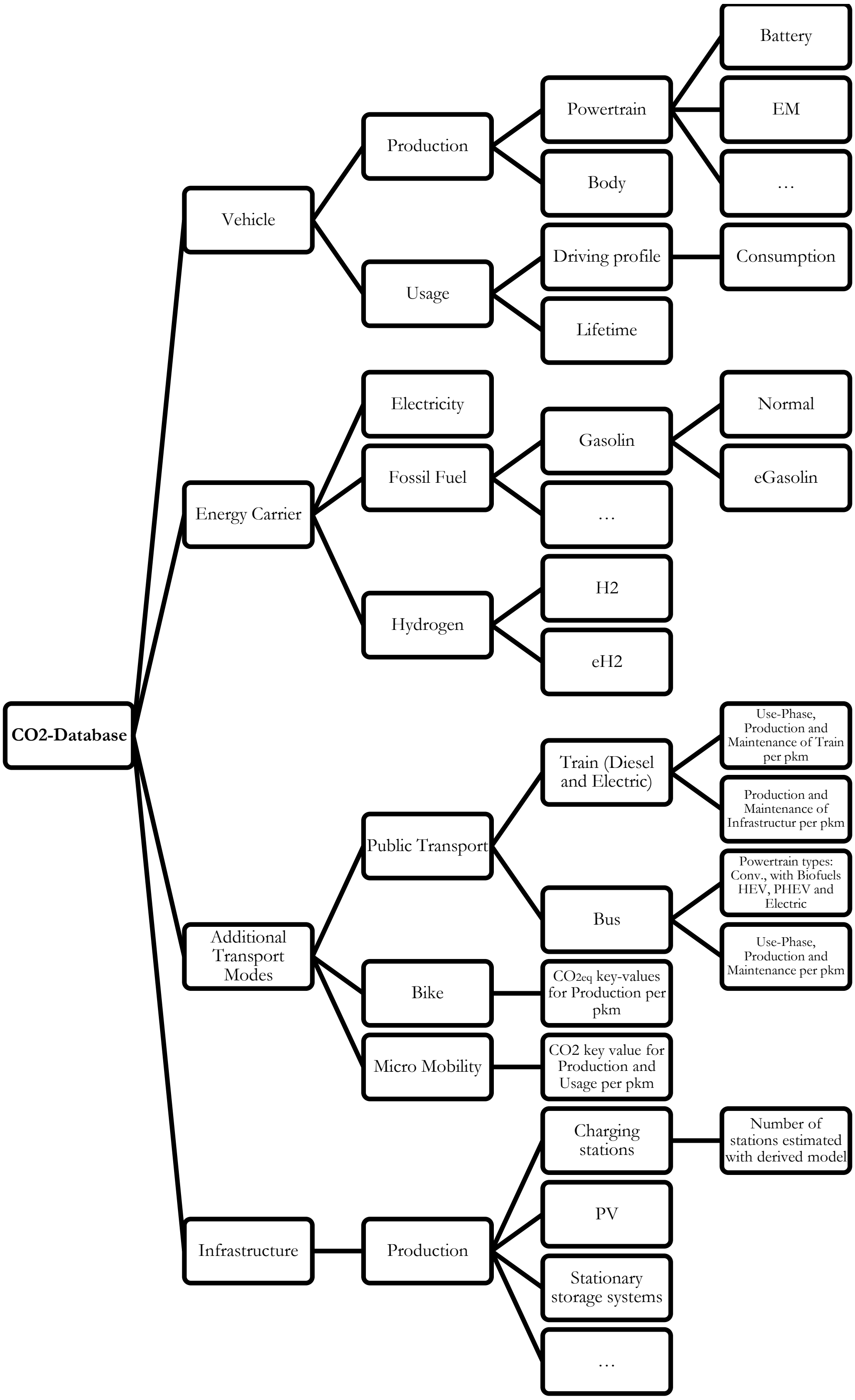

Figure 105: Structure of CO_{2eq} database

Calculation of CO_{2eq} emissions and the necessary input values

Table 28: Calculation of CO_{2eq} emissions and the necessary input values

Component	Source of Input Variable	Input Variable	Key-Value	Comment
Chassis	Powertrain Simulation	Chassis Weight	$kgCO_{2eq}/kg$	Differentiation between vehicle segment and powertrain type
Drivetrain	Mobility Simulation/Powertrain Simulation	Powertrain Type	$kgCO_{2eq}$	Differentiation between powertrain type
Battery	Powertrain Simulation	Battery Size	$kgCO_{2eq}/kWh$	Differentiation between cell chemistry
E-Motor	Powertrain Simulation	E-Motor Power	$kgCO_{2eq}/kW$	Differentiation between e-motor type
Power Electronics	Powertrain Simulation	Power Electronics Weight	$kgCO_{2eq}/kg$	
Fuel Cell	Powertrain Simulation	Fuel Cell Weight	$kgCO_{2eq}/kg$	
Internal Combustion Engine (ICE)	Powertrain Simulation	ICE Power	$kgCO_{2eq}/kW$	
Transmission	Powertrain Simulation	Transmission Torque	$kgCO_{2eq}/Nm$	
Tank	Powertrain Simulation	Tank Content	$kgCO_{2eq}/kg$ Fuel	Differentiation between fossil fuels, CNG and Hydrogen
Production of energy carrier (W2T)	Powertrain Simulation	Driven Distance and Consumption	gCO_{2eq}/km or gCO_{2eq}/kWh (electricity)	Differentiation between Gasoline, e-Gasoline, CNG, e-CNG, Hydrogen (CA, US, German electricity mix), green Hydrogen, Hydrogen based on Natural Gas, Diesel, e-Diesel, Biodiesel, E85, E85 based on Biomass, Ethanol, Electricity mix (depending on region)

A.8 Curve fitting to the forecast data

Curve fitting to the forecast data

One criterion considered is the minimization of the error squares. Before the quality of a curve is determined using the sum of the error squares, the curve under consideration must first be approximated to the forecast data. This means that the parameters of the curve must be selected in such a way that the curve runs as close as possible to the forecast data. Therefore, the respective methods for fitting the different curve approaches are described below.

Curve fitting of polynomial regression

In polynomial regression, systems of linear equations are solved so that the coefficients β_i of the initial function can be determined analytically using the method of least squares. First, the residual is formed. The residual r_i is the difference between the observed point $\mathrm{y_i}$ and the calculated point $f(x_i)$ at time x_i [James et al. 2015]:

$$r_i(x_i) = \mathrm{y_i} - f(x_i) \tag{eq. 36}$$

Hereby the following formula applies depending on the degree of the polynomial [James et al. 2015]:

$$f(x_i) = \beta_0 + \beta_1 x_i + \beta_2 x_i^2 + \cdots + \beta_m {x_i}^m \tag{eq. 37}$$

Here β_i are the coefficients of the curve function and m is the degree of the polynomial. The goal is to minimize the sum of the residuals, analogous to the least squares method. Here, the sum of the squares of the errors is considered [James et al. 2015]:

$$r(x) = \sum_{i=0}^{n} r_i(x_i)^2 = \sum_{i=0}^{n} \left(y_i - f(x_i)\right)^2 \tag{eq. 38}$$

$r(x)$ is the sum of the residuals and n is the number of forecast years. To determine the minimum, the first derivative is set equal to zero. The partial derivatives must be determined for all coefficients [James et al. 2015]:

$$\frac{\partial r}{\partial \beta_0} = 0;\ \frac{\partial r}{\partial \beta_1} = 0;\ \ldots;\ \frac{\partial r}{\partial \beta_m} = 0 \tag{eq. 39}$$

After deriving and ordering the equations, the following system of linear equations can be set up [James et al. 2015]:

$$\begin{bmatrix} n & \sum_{i=0}^{n} x_i & \sum_{i=0}^{n} {x_i}^2 & \cdots & \sum_{i=0}^{n} {x_i}^m \\ \sum_{i=0}^{n} x_i & \sum_{i=0}^{n} {x_i}^2 & \sum_{i=0}^{n} {x_i}^3 & \cdots & \sum_{i=0}^{n} {x_i}^{m+1} \\ \sum_{i=0}^{n} {x_i}^2 & \sum_{i=0}^{n} {x_i}^3 & \sum_{i=0}^{n} {x_i}^4 & \cdots & \sum_{i=0}^{n} {x_i}^{m+2} \\ \vdots & \vdots & \vdots & \ddots & \vdots \\ \sum_{i=0}^{n} {x_i}^m & \sum_{i=0}^{n} {x_i}^{m+1} & \sum_{i=0}^{n} {x_i}^{m+2} & \cdots & \sum_{i=0}^{n} {x_i}^{2m} \end{bmatrix} \begin{bmatrix} \beta_0 \\ \beta_1 \\ \beta_2 \\ \vdots \\ \beta_m \end{bmatrix} = \begin{bmatrix} \sum_{i=0}^{n} y_i \\ \sum_{i=0}^{n} x_i * y_i \\ \sum_{i=0}^{n} {x_i}^2 * y_i \\ \vdots \\ \sum_{i=0}^{n} {x_i}^m * y_i \end{bmatrix} \tag{eq. 40}$$

In the context of this work, weighting factors are considered for the forecasts. The linear equation system can be extended by these factors [James et al. 2015]:

$$\begin{bmatrix} w_i * n & \sum_{i=0}^{n} w_i * x_i & \sum_{i=0}^{n} w_i * {x_i}^2 & \cdots & \sum_{i=0}^{n} w_i * {x_i}^m \\ \sum_{i=0}^{n} w_i * x_i & \sum_{i=0}^{n} w_i * {x_i}^2 & \sum_{i=0}^{n} w_i * {x_i}^3 & \cdots & \sum_{i=0}^{n} w_i * {x_i}^{m+1} \\ \sum_{i=0}^{n} w_i * {x_i}^2 & \sum_{i=0}^{n} w_i * {x_i}^3 & \sum_{i=0}^{n} w_i * {x_i}^4 & \cdots & \sum_{i=0}^{n} w_i * {x_i}^{m+2} \\ \vdots & \vdots & \vdots & \ddots & \vdots \\ \sum_{i=0}^{n} w_i * {x_i}^m & \sum_{i=0}^{n} w_i * {x_i}^{m+1} & \sum_{i=0}^{n} w_i * {x_i}^{m+2} & \cdots & \sum_{i=0}^{n} w_i * {x_i}^{2m} \end{bmatrix} \begin{bmatrix} \beta_0 \\ \beta_1 \\ \beta_2 \\ \vdots \\ \beta_m \end{bmatrix} = \begin{bmatrix} \sum_{i=0}^{n} w_i * y_i \\ \sum_{i=0}^{n} w_i * x_i * y_i \\ \sum_{i=0}^{n} w_i * {x_i}^2 * y_i \\ \vdots \\ \sum_{i=0}^{n} w_i * {x_i}^m * y_i \end{bmatrix} \quad \text{(eq. 41)}$$

w_i are the weighting factors. This system of equations is of the form:

$$A * x = b \quad \text{(eq. 42)}$$

The matrix A and the vector b are known, so that the system of equations can be solved via the inverse of the matrix A. Here x represents the solution with the searched coefficients:

$$x = A^{-1} * b \quad \text{(eq. 43)}$$

For the minimization of the error squares the degree of the polynomial is varied.

Curve fitting of the growth and learning curve

In contrast to polynomial regression, no analytical solution approaches exist for the growth curves and learning curves. Optimization methods must be used here to calculate the variables. In this chapter, the bisection method is used to describe an optimization method for determining the curve parameters. The bisection method is used because it is a simple and computationally efficient optimization method for determining the curve parameters. In the bisection method, also called interval bisection method, the considered search space is bisected or divided into n-size pieces. The search space is the area spanned by the parameter support points [Can 2019].

In the context of this work, modified forms of the growth and learning curve are considered. The following applies to the growth curve:

$$y(x) = \frac{b_{growth} * G}{b_{growth} + (G - b_{growth}) * e^{-a_{growth}(x - x_0)}} \quad \text{(eq. 44)}$$

Here G is the upper limit, a_{growth} is the slope of the curve, b_{growth} is a constant parameter, x is the run variable time (forecast year) and x_0 is the time of the inflection point. The additional parameter b_{growth} allows the curve to better fit the forecast data. The bisection procedure is used to optimize the variables G, a_{growth}, b_{growth} and x_0. In case the values are known, it is possible to specify the upper limit value G and the time of the inflection point x_0. Otherwise, these values are derived from the historical data.

For the modified form of the learning curve applies:

$$y(x) = a_{learn} + b_{learn} * (x - x_{0,learn})^{-q} \quad \text{(eq. 45)}$$

Here, $a_{learn}$is the lower limit, b_{learn} is a constant parameter, x is the run variable time (forecast year), $x_{0,learn}$ is the start time of the technology and q is the learning rate. When considering the learning curve, in contrast to the classical approach, the running variable x is not the cumulative production quantity, but the respective forecast year. In addition, the variable $x_{0,learn}$ is used to determine the start time of the technology. Since the forecast data only start from the year 2010, this is necessary for a meaningful progression of the learning curve. The variables a_{learn}, b_{learn}, $x_{0,learn}$ and q are optimized with the bisection procedure. Analogous to the growth curve, the lower limit value a_{learn} as well as the starting time $x_{0,learn}$ can be specified.

A.9 Computer configuration

Laptop:

- Windows 10
- Processor: Intel i5 8365U 1.6 GHz (4 Cores, 8 Threads)
- RAM: 8 GB

Workstation:

- Linux
- Processer: 2x Intel Xeon 6234 3.3 GHz (8 Cores, 16 Threads each)
- RAM: 384 GB

A.10 Vehicle fleet of current state of Berlin

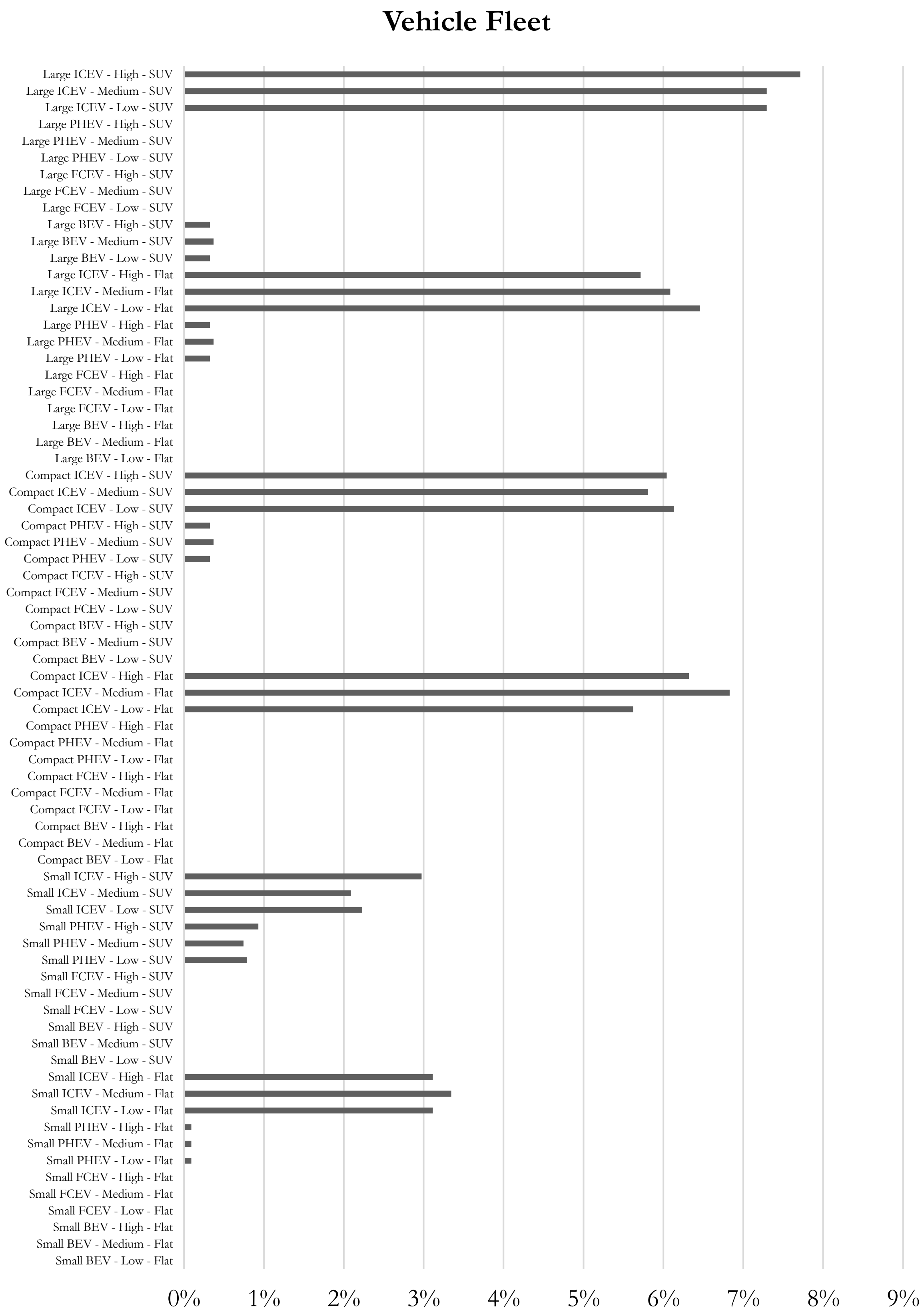

Figure 106: Vehicle fleet of current state of Berlin

Lebenslauf

Aus Datenschutzgründen ist der Lebenslauf in der elektronischen Version nicht enthalten.

PRODUKT
SICHERHEIT
QUALITÄT

BERGISCHE
UNIVERSITÄT
WUPPERTAL